Tampere University

MIKAEL RITAMÄKI

Steering Capacitor Film Development with Methods for Correct and Adequate Dielectric Performance Assessment

Tampere University Dissertations 98

Tampere University Dissertations 98

MIKAEL RITAMÄKI

Steering Capacitor Film Development with Methods for Correct and Adequate Dielectric Performance Assessment

ACADEMIC DISSERTATION
To be presented, with the permission of
the Faculty of Information Technology and Communication Sciences
of Tampere University,
for public discussion in the auditorium TB109
of Tietotalo, Korkeakoulunkatu 1, Tampere,
on 13th September 2019, at 12 o'clock.

ACADEMIC DISSERTATION
Tampere University, Faculty of Information Technology and Communication Sciences
Finland

Responsible supervisor and Custos	Adjunct Professor Kari Lahti Tampere University Finland	
Pre-examiners	Professor Hans Edin KTH Royal Institute of Technology Sweden	Associate Professor Davide Fabiani University of Bologna Italy
Opponents	Associate Professor Davide Fabiani University of Bologna Italy	PhD Sari Laihonen ABB Corp. Research Sweden

Cover design: Roihu Inc.

ISBN 978-952-03-1175-9 (print)
ISBN 978-952-03-1176-6 (pdf)
ISSN 2489-9860 (print)
ISSN 2490-0028 (pdf)
http://urn.fi/URN:ISBN:978-952-03-1176-6

PunaMusta Oy – Yliopistopaino
Tampere 2019

Abstract

The transition of electric power systems towards renewable generation has created an increasing market for power electronics using film capacitors as one of their key components. Size, weight, and cost reduction can be achieved with better capacitors – an objective achievable with advanced dielectric films. The current state-of-the-art biaxially oriented polypropylene (BOPP) films are already operated close to their fundamental limits, causing a growing demand for next-generation technologies. To perform well when used in a capacitor, a film needs to have a wide range of fundamental and applied properties, all of which should be evaluated during film development to ensure there are no unwanted trade-offs. Power capacitors are used in applications with high downtime costs, e.g. HVDC, thus especially the reliability aspects must be given scrutiny. This thesis work was inspired by the lack of knowledge of the long-term performance of next generation dielectrics, e.g. polymer nanocomposites. Equally important was to fill the gaps in published knowledge of measurement methods to evaluate long-term properties, voltage endurance, and surprisingly, also the dielectric permittivity of thin ($\approx$10 µm) low-loss films. In this thesis, a suitable measurement for each three is presented along with examples of their capability and an approach to applying them to steer film development.

The large-area multi-breakdown method developed in our research group is extended to measurements at realistic operating temperatures, and industrial BOPP films are shown to exhibit an 11–20 % decrease in the DC breakdown strength between room temperature and 100 °C. The results align with literature, which supports the validity of the approach. BOPP films made of base materials varying in terms of molecular weight are measured: these films exhibit similar short-term breakdown performance at room temperature, yet at 100 °C differences emerge. The difference did not correlate with the reduction of breakdown performance after DC electro-thermal aging, demonstrating the necessity of long-term tests.

Electron beam evaporation in high vacuum (P<10^{-6} mbar) is established as

a repeatable and suitable method to metallize electrodes on ultra low-loss BOPP films, solving earlier issues of abnormally high dielectric losses or unrealistically low real permittivity. Metallization process is identified as the crucial factor: no pre- or post-treatments are required, and valid results are obtainable with various electrode metals. The method was demonstrated by measuring true "literature value" dielectric permittivity of commercial BOPP films: $\epsilon \approx 2.25$ and $tan\delta \approx 10^{-4}$. The importance of successful metallization process for measuring the intrinsic losses is demonstrated: samples with sputter deposited electrodes exhibited abnormally high dielectric losses, as also did samples metallized using another e-beam evaporator.

The multi-breakdown approach is also extended to times-to-breakdown tests, and accelerated ageing tests are conducted on an industrial BOPP film. High-field degradation and drastically reduced insulation life are observed. Analysis of the Weibull failure rate supports the notion that at current design stresses, BOPP is already operated close to the fundamental material limits, and also that the life in operating conditions cannot be determined by simple inverse power law extrapolation of accelerated rapid ageing data. Again, long-term ageing testing is advocated. Space charge measurements on "classic" BOPP films reveal charge accumulation at high fields, as expected. Interestingly, no space charge accumulation is detected in a novel nanostructured material under similar conditions, demonstrating the potentiality of nanofilled DC insulation.

A DC electro-thermal ageing test method is presented to investigate long-term phenomena in realistic operating conditions. Two 1000 h DC electro-thermal ageing tests associate ageing with the formation of electrically weak points. Large-area breakdown behavior, being sensitive to local changes, is established as a recommended ageing indicator. Material characterization does not reveal ageing-induced changes in bulk properties, supporting the literature-backed conclusion that early ageing progresses by localized degradation. A trial with eight pilot-scale materials demonstrate that weak point formation may be inhibited in nanostructured materials, but also that material-specific optimization of film processing is required to reach optimal dielectric performance.

Ultimately, the methods developed are fused into one resource-efficient approach to capacitor film development, in which the short-, mid-, and long-term properties are evaluated in three overlapping phases. Reliance on individual performance metrics to steer film development is discouraged: all properties need to be at an appropriate level for a film to perform in application, and there are trade-offs to be managed.

Preface

This dissertation work was carried out at Tampere University of Technology (TUT) during the years 2015 – 2018. In year 2019 TUT merged with University of Tampere and this thesis was finalized in the new Tampere University. The research was conducted under various projects in co-operation with VTT Technical Research Centre of Finland, Borealis AG, Optoelectronics Research Centre (ORC) of TUT, DuPont Teijin Films, Terichem Tervakoski, Alstrom Grid Oy and GE Grid Solutions Oy, to name a few. I wish to express my gratitude for this collaboration. Funding from EU Horizon 2020 programme, Walter Ahlström Foundation and Finnish Foundation for Technology Promotion is also greatly appreciated.

I have been fortunate to work with outstanding people whose contribution made this thesis possible. First of all I wish to express my sincere gratitude to my supervisor Kari Lahti, for providing me the opportunity to work with this interesting topic, for all the guidance during these years and also for giving me the opportunity to participate in research services. I am also grateful to all the members of the high voltage research group during my years at the University: Ilkka Rytöluoto, Minna Niittymäki, Hannes Ranta, Juha Alhainen, Aleksi Eilo, Eerik Järvinen, Juuso Kukkaro, Otto Rantanen, Nida Riaz and Daiana da Silva. I learned a lot from you, and the knowledge that I would meet you again motivated me to get up and go to work every morning. I am also grateful to all new and future members of the research group for continuing the quest to unravel the mysteries of solid dielectrics. I wish that in the future I can look back and see this dissertation as a piece of a puzzle nearing completion.

I also wish to express my gratitude to the pre-examiners, Davide Fabiani and Hans Edin, for agreeing to review my work and for your comments. I am equally grateful to my opponents for committing yourselves to the task. I also also grateful to Gian Carlo Montanari, Paolo Seri, and everybody I made acquaintance of during my research exchange in the University of Bologna. It was a good time. I would also like

to thank everybody from the TUT workshop: Pentti Kivinen, Hannu Nieminen, Pekka Nousiainen, Lasse Söderlund and others; the things you made were extraordinary and I learned a lot from you. I am also grateful to Bengt-Olof Holmström, Jukka Kaipainen, Taru Karhula, Mervi Koskinen, Nitta Laitinen and Terhi Salminen from TUT. I also wish to express my gratitude to Timo Flyktman, Mikko Karttunen, Mika Paajanen and Satu Pasanen from VTT, Antonis Gitsas and Torvald Vestberg from Borealis AG, Lucien Schosseler from Dupont Teijin Films, Jari Kotiniitty from GE Grid Solutions and to all the wonderful people of the GRIDABLE consortium.

I am grateful to all my colleagues for the positive atmosphere, to the teaching personnel for all the interesting courses and to the administration and other personnel for keeping the university running. I was fortunate to participate in the DEIS Summer School in Bertinoro in 2015, I would like to thank its organizers and IEEE DEIS for making it possible. In the summer school I met many great people, our discussions had invaluable contribution to this thesis. Thanks to my supervisor Kari Lahti I could participate in several outstanding international conferences, I am grateful to everybody who shared their time with me in these, with special thanks to Janet Ho for sharing your thoughts about capacitor films. I am also grateful to the Doctoral Programme in Electrical Energy Engineering (DPEEE) for supporting my participation in the EES-UETP HVDC course in Belgium in 2018 and for organizing the DPEEE summer conferences. I also wish to express my gratitude to the editorial staff and to all the reviewers of IEEE TDEI for the important work you are doing.

Special thanks belong also to my friends and family and everybody who provided me company for lunch or coffee. Thanks also to everybody from the TUT Radio Club. Ultimately however I have to admit the futility of trying to include everybody who contributed to the thesis in a two-page preface, thus I wish to express my sincerest gratitude to all those, who contributed, but who were not mentioned here.

Tampere, May 2019

Mikael Ritamäki

This project has received funding from the European Union's Horizon 2020 research and innovation programme under grant agreement No 720858.

Contents

Acronyms

2-p	2-parameter
AC	alternating current
ADC	analog to digital converter
BOPP	biaxially oriented polypropylene
CSC	current source converter
DC	direct current
DFT	density functional theory (a modeling method)
DSC	differential scanning calorimetry
DUT	device under test
FACTS	flexible AC transmission systems
FEM	finite element method (a modeling method)
GPC	gel permeation chromatography
HVDC	high voltage direct current
IPL	inverse power law
iPP	isotactic polypropylene
KP	polypropylene film (type of capacitor)
MD	molecular dynamics (a modeling method)
MKP	metallized polypropylene film (type of capacitor)
MOS	metal-oxide-semiconductor
PD	partial discharge
PDIV	partial discharge inception voltage
PEA	pulsed electro-acoustic (a space charge measurement method)
PID	Proportional-integral-derivative (a controller type)
PNC	polymer nanocomposite
PTFE	polytetrafluoroethylene
PVD	physical vapor deposition

PVDF	polyvinylidene fluoride
R&D	research & development
RMS	root mean square
SA	small area (type of breakdown measurement)
SPICE	Simulation Program with Integrated Circuit Emphasis (electronic circuit simulator)
STATCOM	static synchronous compensator
TSDC	thermally stimulated depolarization current
UHVDC	ultra high voltage direct current
VEC	voltage endurance coefficient
VSC	voltage source converter
WAXS	wide angle x-ray scattering

List of publications

[P1] M. Ritamäki, I. Rytöluoto, K. Lahti, and M. Karttunen, "Effects of thermal aging on the characteristic breakdown behavior of Nano-SiO_2-BOPP and BOPP films," in *2015 IEEE 11th International Conference on the Properties and Applications of Dielectric Materials (ICPADM)*, pp. 400–403, 2015. 10.1109/ICPADM.2015.7295293

[P2] M. Ritamäki, I. Rytöluoto and K. Lahti, "Temperature Effect on Breakdown Performance of Insulating Polymer Thin Films," in *24th Nordic Insulation Symposium on Materials, Components and Diagnostics (NORD-IS 15)*, pp. 75–79, 2015.

[P3] M. Ritamäki, I. Rytöluoto, M. Niittymäki and K. Lahti, "Differences in AC and DC large-area breakdown behavior of polymer thin film," in *2016 IEEE International Conference on Dielectrics (ICD)*, pp. 1011–1014, 2016. 10.1109/ICD.2016.7547789

[P4] M. Ritamäki, I. Rytöluoto, K. Lahti, T. Vestberg, S. Pasanen, and T. Flyktman, "Large-area Approach to Evaluate DC Electro-thermal Ageing Behavior of BOPP Thin Films for Capacitor Insulation Systems," in *IEEE Transactions on Dielectrics and Electrical Insulation*, vol. 24, no. 2, pp. 826–836, 2018. 10.1109/TDEI.2017.006405

[P5] M. Ritamäki, I. Rytöluoto and K. Lahti, "High Temperature and Ageing Test Methods to Characterize the Dielectric Properties of BOPP Capacitor Films," in *2017 IEEE Conference on Electrical Insulation and Dielectric Phenomenon (CEIDP)*, pp. 266–269, 2017. 10.1109/CEIDP.2017.8257518

[P6] G.C. Montanari, P. Seri, M. Ritamäki, K. Lahti, I. Rytöluoto and M. Paajanen, "Performance of Nanoparticles in the Electrical Behavior of DC Capacitor Films," in *2018 IEEE 12th International Conference on the Properties and Applications of Dielectric Materials (ICPADM)*, pp. 41–44, 2018. 10.1109/ICPADM.2018.8401024

[P7] M. Ritamäki, I. Rytöluoto and K. Lahti, "DC Voltage Endurance of Capacitor BOPP Films at High Temperature," in *2018 IEEE International Conference on Dielectrics (ICD)*, pp. 1–4, 2018. 10.1109/ICD.2018.8514598

[P8] M. Ritamäki, I. Rytöluoto and K. Lahti, "Performance Metrics for a Modern BOPP Capacitor Film," in *IEEE Transactions on Dielectrics and Electrical Insulation* (In press)

Chapter 1

Introduction

High energy density capacitive energy storage brings forth space, weight and thus cost savings: lighter offshore HVDC converter platforms on lighter foundations and compact STATCOM installations requiring less land area and easily located indoors away from public opposition. In both applications a major portion of the total size and weight comes from capacitors. The largest and heaviest part of a film capacitor is its primary insulation, and with a better insulation material both the size and weight is reduced. The trend towards lighter and smaller has existed since the early years of commercial capacitor technology, and next generation insulation materials are a part of this megatrend. Such materials are developed in the High Voltage Engineering research group of Tampere University of Technology (TUT).

One of the latest advances in this field is the European Horizon 2020 project GRIDABLE, with a budget of 8.32 M€ and eight participating organizations around Europe. One of the main objectives of this project is to increase capacitor energy density with a next-generation nanostructured primary insulation material. In this project, TUT is responsible for determining the electrical performance or "goodness" of prototype materials manufactured by VTT, and provides vital information on the short- and long-term dielectric and material properties of industrial prototype films. Having this prominent role was enabled by vast experience in dielectric measurement, acquired in two TEKES-funded projects, NANOPOWER (1.4 M€) and NANOCOM (1 M€). Nevertheless, the responsibilities in the GRIDABLE project required major advances in the art of dielectric characterization, including metrology, sample preparation and the knowledge how to implement comprehensive testing programs in a resource-efficient way. Many of these advances are documented in this thesis.

Film-type power capacitors are used in grid-connected power electronic appli-

cations e.g. HVDC and STATCOM that are indispensable in integrating renewable power generation into electrical grids. These capacitors use biaxially oriented polypropylene (BOPP) film as the primary insulation, and metallized or nowadays less often foil electrodes. Operating temperature range, physical size and service life are their key performance metrics that depend on the quality of this film: to perform it must maintain its high electric strength, low dielectric and conduction losses and demonstrate adequate voltage endurance up to the maximum operating temperatures. In the development of next generation capacitor dielectrics it is necessary to monitor these fundamental properties to verify all of them remain at adequate level and there are no unpredicted trade-offs among them. Broad characterization is required since these properties may not be deductible from each other, for example higher electric strength might come together with inferior voltage endurance [1]. Standardized performance and reliability testing can be done for capacitors, their elements and film rolls, but only at a late stage of development when film production is upscaled to the industrial level. At this time, the cost of correcting an error in base material selection or processing has escalated substantially and resources have been wasted. As tempting it might be, early reliance on an insufficient set of performance metrics must be avoided. A common difficulty with early testing is that it needs to be done using small laboratory-stretched film samples. For them only the dielectric strength measurement can be regarded as relatively well-established. There is no generally accepted test procedure for the long-term endurance of such small samples and no information about its correlation with film performance in capacitors. The bulk of scientific literature on the ageing of capacitors films is from the 90s or earlier, and its relevance today is questioned by the advances of capacitor film technology evident as new product launches. Finally, also the publicly available information on preparing low-loss thin films for the basic dielectric measurements of permittivity and conduction is conflicting and ambiguous.

Thus, the objectives of this thesis work were to develop the necessary methods to properly and adequately assess the dielectric quality of capacitor films, and to design an approach to capacitor film development using these methods. The principles of this approach were “least effort” resource optimization and applicability as early as possible during film development, viz. all measurements should be realizable with laboratory-scale oriented films. These methods are then to be demonstrated in steering the development of nanostructured materials in e.g. project GRIDABLE. This thesis draws from the work of D.Sc. (Tech.) Rytöluoto of the TUT High Voltage Engineering research group in determining the relation of film processing

and structure on the short-term DC breakdown strength at room temperature [2, 3]. However, this thesis was founded on the recognition that once the short-term, room temperature breakdown strength is at an adequate level, as the situation was after several years of TEKES-funded projects when this thesis work began, it is necessary to expand the measurement spectrum to dielectric spectroscopy, high temperature, and long-term properties. That is because these are the properties that should ultimately determine the film performance when it is used in its application in power capacitors, where the electric stress is only a fraction of the short-term breakdown strength.

1.1 Objectives of the Thesis

The objectives of the thesis raise from the existing research gap in efficient dielectric quality assessment of capacitor films already at an early R&D phase, as described in the previous section. The specific objectives are:

- To develop methods and to conduct DC electro-thermal ageing tests and voltage endurance tests on dielectric films.
- To identify the most suitable method(s) for evaluating ageing progression in commercial and laboratory-scale films.
- To discover a repeatable method to prepare low loss thin film samples for the measurement of complex dielectric permittivity.
- To develop a streamlined approach for the development of capacitor films by using key measurements to verify early, when only laboratory-scale oriented films are available, that all dielectric properties are at an acceptable level.

1.2 Author Contributions

The author was the main author in associated publications [P1, P2, P3, P4, P5, P7], had equal contribution to [P8] with Dr. Rytöluoto and had notable contributions to [P6]. Detailed author contributions are listed next.

- In [P1] the main results and methods from the author's master of science thesis [4] were refined and presented. The author had been responsible for the thermal ageing experiment and associated data analysis. The pilot-scale materials studied were from an earlier project which did not involve author contribution.

The test hardware was constructed at what was then the workshop of the department of electrical engineering.

- In [P2] the author was responsible for expanding the breakdown test methodology to elevated temperatures, conducting the measurements, and analyzing the results. The breakdown data processing toolkit had been developed earlier by Dr. Rytöluoto.

- In [P3] the author was responsible for the development of the AC large-area multiple breakdown measurement and the associated data analysis.

- In [P4] the author was responsible for developing and conducting the electrothermal ageing tests, all the permittivity measurements, associated sample preparation and the breakdown strength measurements of aged samples. Room temperature breakdown strength measurements on the materials were largely done by Dr. Rytöluoto. Laboratory-scale film manufacturing and electron microscopy was done at VTT Technical Research Centre of Finland Ltd. Base PP was provided by Borealis Polymers Oy who also did the DSC and GPC measurements.

- In [P5] the author was responsible for planning and conducting the ageing test itself and for the high temperature measurements and breakdown measurements on aged samples. The author had been responsible for upgrading the high temperature measurement system originally used for measurements in [P2]. Ageing test hardware was largely the same as in [P4]. Films studied were provided as rolls by a project partner who was also responsible for the WAXS and DSC measurements.

- In [P6] the author was responsible for commissioning a new space charge measurement system for thin films. The author also did certain necessary modifications to the system, and utilized it to conduct the total charge measurements that were reported in this publication. The author also did the space charge measurements on the thick cast films and contributed to the data analysis with G.C. Montanari and P. Seri. The materials were from an earlier project which did not involve author contribution.

- In [P7] the author was responsible for planning and constructing the voltage endurance test setup, conducting the constant voltage tests and 3 out of 4 of the high temperature ramp tests whose results were reported. Author was also

responsible for developing the analysis software for the times-to-breakdown data analysis.

- In [P8] the author was responsible for the voltage endurance tests, space charge measurements, and some of the progressive stress breakdown tests. Permittivity and conductivity measurements, TSDC, DSC, surface roughness measurements and the rest of the progressive stress breakdown tests were done by Dr. Rytöluoto. The manuscript was prepared together.

- The measurement program proposed in Section 3.4 was drafted by the author. It is founded on the author's experience in co-operation projects with industrial partners and research institutions alike, but has not been applied as such in any of the projects with author involvement.

- The commercial capacitor-grade BOPP films studied in several papers were provided by Tervakoski Films Group and GE Grid Solutions Oy (previously Alstrom Grid Oy).

1.3 Structure of the Thesis

This thesis is divided into four parts: introduction, background, experimental and conclusions. In the background chapter the publicly available state-of-the-art of film capacitor technology is reviewed and three currently pursued pathways to reach higher energy density are explained: thinner films, polymer nanocomposites and computation design methods. Two first are integral to this thesis and project GRIDABLE, and the third is included for its prominence is recent literature. The background chapter concludes with an in-depth discussion about nanostructured materials as they were studied in several publications included in this thesis.

In pursuing the thesis objective of comprehensive dielectric characterization, measurements of various time scales were implemented. In Chapter 3, these methods are presented in an ascending order of measurement duration. Chapter 3 begins with short-term fundamental dielectric properties, only after they are at adequate level it is meaningful to R&D progress further. In this thesis *short-term* refers to measurements with a duration of minutes. The exception is DC conductivity that is regarded as a short-term property although a measurement typically takes at least several hours, even at elevated temperatures. A high dielectric breakdown strength at operating temperature is a desirable short-term dielectric feature, a film must exhibit it to be suitable for demanding applications. This topic is discussed in Section 3.1.1.

High temperature breakdown strength measurements were the main topic of [P2] and prominent in [P5, P7, P8].

Low DC conductivity and low AC losses are also desirable features that are directly related to short-term fundamental film properties, they are necessary to limit self-heating. Excess heat generation, in combination with relative low thermal conductivity of polypropylene may accelerate ageing and in the extreme case destroy the capacitor by thermal runaway. The key to successful dielectric permittivity and conductivity measurements is in proper sample preparation – methods suitable for thick millimeter-scale samples yielded unrealistic results on low-loss micrometer-scale thin films. The measurements themselves are implementable using commercial equipment and extensive literature is available to support the analysis of the dielectric spectra. Thus one of the focus areas of the thesis work was the development of a repeatable sample preparation for thin films. A suitable method that was identified and the background work are the topic of Section 3.1.2. Permittivity measurement results are presented in publications [P4, P8].

Voltage endurance testing is closer to realistic operating conditions with electrical stress far below that required to cause a near-instantaneous breakdown in a brief progressive stress test. Voltage endurance is fundamental in reaching a reliable system service life of 30 years or more. In principle once the voltage endurance of a film is known, it is possible to work all the way up to the service life of a capacitor. This of course requires prior knowledge on the stresses, which however can be envisioned to be available from detailed electrical modeling. With proper design over- and under-engineering is avoided and total costs are reduced. DC voltage endurance testing of thin films is the topic of Section 3.2.1, it was the main topic of publication [P7], and these results were also presented and analyzer further in [P8]. The measurement durations varied from minutes to hours and thus they fall midway between short- and long-term properties.

Space charge measurement on thin films is the topic of Section 3.2.2. The advantage of space charge measurements is that a relatively short measurement of a few hours or even less can yield information on long-term behavior: it can detect injected charge that typically reduces the insulation life. Space charge measurement on cables is standardized and well-established [5], but available knowledge on $\lessapprox 10\,\mu m$ thin films is much more limited and the equipment and methods are often highly experimental. It would be advantageous for R&D if the space charge properties of thin biaxially oriented films could be determined by measuring their precursor cast films prior to orientation. Space charge in $<20\,\mu m$ biaxially oriented PP films and

their ≈0.5 mm thick precursor cast films was the topic of publication [P6].

Especially with a new generation of nanostructured capacitor films, but also with BOPP films advanced beyond those studied in the 90s and before, it is essential to study their ageing under stresses comparable to operating conditions. In plastics there may be e.g. morphological changes [6] and antioxidant migration [7] in long-term, but also phenomena of entirely new kind, e.g. interaction between nanofillers and antioxidants and slow antioxidant release may occur in nanostructured materials [8]. Identifying these phenomena is necessary before these materials can be regarded as suitable for use in high reliability applications. Long-term phenomena in capacitors films, in a time scale of a thousand hour, is discussed in Section 3.3. It was the main topic in publications [P4, P5].

Capability to assess both the short and long-term properties of capacitor films is essential for successful product development, but equally important in a world of limited resources and tendency for cost reduction is to know when, and in which order to deploy each measurement. Thus in Section 3.4 an approach to using the methods presented in Chapter 3 is proposed. Finally, conclusions are presented in Chapter 4, along with discussion about future research topics.

Chapter 2

Background – Film Capacitor Trends and the State of the Art

2.1 Film Capacitors State of the Art

Two types of BOPP capacitor technologies are in widespread use: metallized film and film-foil. Both technologies have their benefits and shortcomings, but the myriad of designs allows engineers to select the best capacitor for each applications.

2.1.1 Metallized Polypropylene Film Capacitors

Metallized polypropylene film capacitors (also known as MKP for the German name Metallisierter Kunststoff Polypropylen) are ubiquitous in power electronics where they are used for snubbering, blocking and filtering etc. [9]. Typical applications include power factor compensators [10], motor drives [11], high voltage direct current (HVDC) transmission [12], [13] and flexible AC transmission systems (FACTS). Capacitors are key components in state-of-the-art modular multilevel converters (MMCs) employed in HVDC transmission [13–15]. The myriad of applications and their different demands are catered by a broad selection of capacitors available for the design engineer.

The base material for the thin film insulation used in these capacitors is highly isotactic polypropylene (iPP). High isotacticity is a prerequisite for high crystallinity, which is advocated to reduce dielectric losses and conductivity [16], but highly isotactic material is more difficult to process [17]. Several commercial products are available for producing capacitor films; the different grades can be used to produce films of different crystallinity. These “electrical grades” are of high purity, which can

be realized by washing the polymer after polymerization [18]. Alternative patented approach is to negate the effects of catalyst residues by using single-cite catalysts [19]. High purity and the absence of many additives used in commodity plastics result in small amounts of residue in burn tests, this is advertised as "low ash content" [20, 21]. Purity is generally required for low dielectric losses [22, 23] and improves film performance at high temperatures [24]. PP is sensitive to oxidation because of its tertiary carbon [25] and the commercial granulates in the market are stabilized to protect it during melt processing, usually by adding < 0.5 wt-% hindered phenolic antioxidants such as Irganox 1010 [26].

Based on patent applications capacitor-grade PP may also contain small quantities of acid scavenging additive, such as calcium stearate, to reduce the effect of catalyst residues [27]. Several other patent claims exist on better capacitor films, mentioning methods such as adding beta nucleating additives to improve film performance and processability [17, 28] and mixing linear and branched PP [29]. Their use in commercial products is not known since their recipes are not publicly available.

The PP granulates are hot-melt extruded and biaxially oriented either using tenter or bubble process [30]. Both processes result in different film characteristics [30]; metallized film capacitors mainly use tenter films which are reported to exhibit superior high-field electrical properties [31]. The biaxial orientation improves the mechanical, optical and barrier properties [30], the dielectric strength [3, 22], and in-plane thermal conductivity [32] over bulk PP, the current technology enabling design electric fields as high as 225 [13]–240 V/µm[33]. Typical film thicknesses are in the range of 2 µm to 20 µm and there is a trend towards thinner films, 1.9 µm becoming available recently [34, 35]. Cooling conditions during processing are adjusted to produce either a textured "hazy" or smooth film surface, the first providing wicking action necessary for oil impregnation [22]. Nonetheless also smooth films have minor surface texture [P8].

The oriented film is corona treated to facilitate metallization, and an electrode of few tens of nanometers is metallized on the film surface. The electrode has a free margin on one edge and sometimes a heavy edge on the other. The metal can be zinc [36], aluminum [37] or their alloy [38]. The metallization can be uniform or segmented, the latter offering improved reliability due to fusing action but at the cost of increased dielectric losses [13]. The metallized electrode is self-healing, allowing the capacitor to tolerate multiple breakdowns during service. When the film breaks down, the faulted area is isolated because the metallization evaporates around it. [39] Thin metallization is needed for reliable self-healing [40], and its resistance is

the main cause of losses in metallized film capacitors [41].

Offsetted metallized films are wound, often on a mandrel, and non-metallized films can be placed in between to increase the voltage rating. If mandrel was not used, the winding can be flattened afterwards. End connections to the metallized electrode are made by plasma spraying zinc on them. The resulting bond is incontinuous, non-metallic and has contact resistance, but apart from pulsed power applications, the effect of end-connection losses on capacitor performance are usually negligible [42]. Nevertheless, it is the weak point of metallized film capacitors. [39, 43] A wavy film edge is advertised to improve the end contacts [10, 44]. Weak points are removed during manufacture by self-healing by applying voltage to the winding. Multiple windings can be connected in series or parallel to reach desired capacitance and voltage ratings. [45]

The wound capacitor is potted in a cheap plastic enclosure as-is, or placed inside a metal can, possibly also vacuum dried, and the can is filled with inert gas (e.g. Nitrogen, SF6), oil (e.g. Rapeseed), polyurethane or other resin [10, 13, 33, 46]. Suitable oils do not react with the metallized film and penetrate through the porous end-connections filling any gaps. [45] Oil impregnation is advertised to result in better cooling, being used at least in traction applications [33, 46], while dry designs are advertised to be safer [47]. Partial discharging in the gap between the end-contact and metallized film edge limits the use of dry designs in HV AC applications [45]. Vacuum impregnation and metal casing provides hermetic sealing, greatly increasing resistance to corrosion and PD [10], but is presumably more expensive. Potted general-purpose capacitors are not sealed, and thus susceptible to corrosion and oxidation [46], having limitations related to storage and operation in humid environments [9]. As the self-healing action may fail [48], overpressure disconnector can be fitted to the capacitor enclosure to prevent explosion [10].

The insulation life and thus the maximum permissible operating voltage of metallized film capacitor depend on the voltage waveform and is reduced at high temperatures [49]. For sinusoidal voltage stresses at low frequencies the maximum allowable operating voltage is constant, limited by partial discharges whose inception voltage is largely unaffected by frequency [50]. As frequency is increased the reactive power and -current increase linearly. This results in a rapid increase of metallization I^2R losses and the resulting self-heating begins limiting the operating field. As the frequency is increased further or in pulsed power applications the end contacts become the limiting part. [9, 41, 51]

Partial discharges (PD) are a problem associated with harmonics and voltage

distortion generated by power electronics. Pulse width modulated waveforms can have higher peak voltages than sine wave of equivalent RMS, and since PD inception is strongly influenced by voltage magnitude PD activity may begin, degrading PP and other organic materials rapidly. This is seen as a strong relationship between capacitor life and peak voltage. Fast sub-microsecond rise times accelerate PD degradation further as voltage will increase during the time delay between applied voltage exceeding partial discharge inception voltage (PDIV) and the discharge itself, resulting in more destructive discharges of higher magnitude. [49, 52, 53] Partial discharging may be unavoidable in converter-fed motor winding insulation systems, but can and should be avoided in capacitors by proper design based on the real voltage and current waveforms. It is thus a design issue, and not discussed further in this thesis.

The life of a metallized polypropylene film power capacitor ends when the capacitance has decreased sufficiently due to demetallization. Actual percentages vary but are usually in the few percent range. [39] Gross design errors and events outside human control aside, the life of MKP capacitor is dictated by the temperature, electric field, and moisture [46]. Corrosion of metallization under moisture is well-recognized and studied phenomena [54]. This can corrode the metallized electrode and the end-contacts of non-sealed capacitors [55] but can be avoided by proper drying and hermetic sealing [40, 56]. It is thus a cost optimization issue, and not within the scope of this thesis. Capacitors for demanding high-reliability applications are usually sealed.

In properly designed high-reliability applications, the ageing of metallized film capacitors is thus dictated by temperature and electric field. Early studies using oil-impregnated PP film suggest its life as the function of temperature can be modeled using the Arrhenius relation, and the effects of voltage can be modeled using the inverse power law [57]. As recently reviewed by Gallay [46] using manufacturer given design guidelines these models seem to apply adequately also for modern metallized film capacitors. Worth mentioning is also the failure of end connections under pulsed and high-current excitation, explained by numeric simulation [42] and confirmed by experiments [58]. It becomes a limitation also for power electronic designs if attempts to increase capacitor energy density are successful and if the operating frequencies keep increasing [51].

2.1.2 Polypropylene Film – Foil Capacitors

Polypropylene film-foil capacitors, also known as KP for the German name Kunstoff Polypropylen, are used where the highest voltages or currents, and thus the lowest dielectric losses and inductances are required [39]. Typical application is series compensation in high voltage power transmission grids. The electrodes are thin aluminum foil, and thus the first breakdown is fatal for the element. Several films are stacked as the probability of pinholes or other weak points ending up on top of each other in high-quality films approaches negligible. The capacitors are oil-impregnated and hazy polypropylene film is used to provide the necessary wicking action. Contrary to metallized film capacitors, oils which react with the polypropylene and swell it can be utilized. Epoxide containing oils can be used to suppress PD activity [59]. Film-foil capacitors usually consist of several elements stacked in series and parallel, to increase the voltage rating and to provide defect tolerance should individual elements fail.

The field enhancement at electrode edges is the weak point where overvoltage or improper design may cause partial discharging leading to insulation failure. Various techniques such as folding and laser cutting, all with rather similar performance can be used to lessen the field enhancement at the edges [39]. The edge discharges presumably occur in the oil, its breakdown strength being significantly less than that of the PP film [39, 60], even though the breakdown strength of thin oil layers is increased compared to 2 mm gap used in IEC 156 measurement [61].

2.2 Emerging Technologies for Metallized Film Capacitors

There is a need for capacitors with higher energy density and better thermal properties. Higher energy density enables more compact power electronics, and improved endurance at high temperatures helps in the thermal design and -management of power electronics where space is premium. In power electronic converters capacitors are needed in the vicinity of heat-generating semiconductors. [41] These demands are closely related, since assuming constant loss factor, heat generation increases linearly with capacitor reactive power and unless the cooling performance is correspondingly improved, the capacitor temperature will rise. The I^2R losses caused by metallization resistance increase with current and the dielectric must either tolerate the heat or dissipate it. Metallization resistance cannot be decreased infinitely, since the thicker metallization required would risk the self-healing action. The energy W stored in a

capacitor is a function of capacitance C and applied voltage U and can be increased by increasing either of them:

$$W = \frac{1}{2}CU^2 \tag{2.1}$$

Stored energy and thus the energy density increases rapidly if voltage is increased, but the dielectric must be capable of enduring the increased stresses and careful design is needed to verify PD is not incepted. This approach is not suited for applications where the voltage is fixed (such as low voltage reactive power compensation) or limited by other components such as semiconductors.

Polypropylene being a linear dielectric, the capacitance of a BOPP film capacitor is independent of applied voltage. The capacitance of a film capacitor C can be approximated well using a parallel plate model with electrode area A and thickness d,

$$C = \varepsilon_0 \varepsilon_r \frac{A}{d} \tag{2.2}$$

where ε_0 is the vacuum and ε_r the relative permittivity. BOPP has a low relative permittivity of 2.2 and thus capacitance can be increased by switching to a higher permittivity dielectric such as biaxially oriented polyesters, whose relative permittivity varies from 3.05 to 3.25. Polyesters such as polyethylene naphthalate (PEN) and polyethylene terephthalate (PET) however have a lower dielectric breakdown strength than BOPP, which requires reducing the operating voltage, and while doing so the available energy density decreases in a power of two. Polyesters along with many other high-permittivity dielectrics also suffer from higher dielectric losses that typically increase with relative permittivity. [62] Therefore, polyester capacitors are most suited for low-voltage general-purpose designs where their processability into sub-micron films is a benefit.

2.2.1 Thinner Films

Reducing the dielectric thickness increases the capacitance and stored energy without increasing the applied voltage. This way the energy density is increased without exceeding deleterious partial discharge inception field at the electrode edge, which is especially problematic for film-foil designs [60] but also for dry metallized film capacitors [45]. This of course requires dielectric films capable of sustaining the increased electric fields and the increased heat generation especially at higher frequencies. An issue with thinner BOPP films is that the number of low breakdown voltage weak points increases as film thickness is reduced. This is acknowledged in product brochures [63–65] and supported by literature [2]. This may not be problematic for

metallized film capacitors where weak points can be "burned out" during manufacturing. These weak points nevertheless determine large-area dielectric strength. Weak points appear to be extrinsic of the film, as the thermal breakdown mechanism suggested to hold true for BOPP [66] would result in dielectric strength increasing with reducing thickness [67], which is indeed true for many polymer dielectrics [68] and at least for parylene thin films [69] but appears not to be the case for BOPP [2]. Weibull analysis of breakdown fields measured using large areas places the weak points in a distinct subpopulation, which suggests that they originate from different breakdown mechanism [2, 70], but no thickness dependence is recognized even in the main Weibull population [2]. Thinner BOPP films also expand the market of metallized PP capacitors to low-voltage applications that have been traditionally dominated by polyester.

2.2.2 Polymer Nanocomposites

Polymer nanocomposites (PNCs) are plastics where nanometric particles are contained in a polymer matrix. The particles can be of arbitrary shape, such as spheres, platelets or tubes, but with at least one dimension is in the <100 nm range. Nanometric filler size results in large surface areas where interaction with the surrounding polymer can occur. These interactions may result in properties unlike the base materials. To facilitate interactions between inherently incompatible nanoparticles and the polymer matrix compatibilization is needed. As an example, hydrophobic polypropylene and hydrophilic silica can be mixed if the silica is turned hydrophobic with a proper surface treatment. This is similar to how soap molecules bond to a grease stain and facilitates its dissolution in water. One surface treatment suiting fumed silica is with Hexamethyldisilazane (HMDS), silica with this type of functionalization was used in the PP-silica nanocomposites in e.g. [P1, P3, P4]. [71]

PNCs have demonstrated improved electric properties compared with their base polymers, such as increased resistance to partial discharges and reduced space charge accumulation, the latter explained by modified charge-trapping behavior. Due to these advantages, PNCs are finding use in high voltage insulation other than capacitors, where their unknown long-term and ageing properties have inhibited their proliferation. [71–73] A prime example of the benefits of PNC technology is partial discharge resistant enameled wires used in motor windings [74, 75].

Nevertheless, a few nanostructured materials for dielectric film have been patented. A patent from 2008 [76] presents a film with better temperature stability and presumably also a higher permittivity than BOPP. This film is a dispersion

of polyester and polycarbonate, one in the form of platelets with dimensions preferably less than 1 µm. In 2013 a patent was filed on polymer dielectric materials with inorganic nanoparticles with claims of good high temperature properties above 200 °C [77]. The inventor's publication [78] specify boron nitride nanoparticles in polyimide matrix as a promising combination with significantly reduced ionic space charge and conductivity especially above 150 °C. A recent patent from 2016 presents a modified PET-based film with nanometric silicon dioxide (silica) and boron fiber. This film is claimed to result in less interlayer air and exhibit better high temperature properties and longer life in application. [79]

Nanoparticle agglomeration must be avoided as it results in worse overall properties. The optimal nanoparticle loading in dielectrics is low to avoid percolation failure paths and the purity of the base materials and adequate quality control must be maintained to ensure possible "nano-effects" are not hidden under extrinsic factors such as adsorbed water or contamination from external sources. [72, 73]

2.2.3 Computational Methods

Computational methods are advocated in the design of new high energy density capacitors [41]. Methods can be coarsely divided into two categories, (1) those used to predict the properties of new materials from molecular structure and (2) those used to model the behavior of macroscopic structures, such as actual capacitors. Both are integral parts of current capacitor development state-of-the-art and discussed briefly.

Rational design methods are advocated to enable the identification and selection of the most promising polymers from an almost endless number of possibilities for synthesis and testing. It is much faster to calculate the properties of a dielectric than to synthesize one in the laboratory and measure them. An extensive overview of the available methods was published recently [41], highlighting the present capability of density functional theory (DFT) and molecular dynamics (MD) –computations to calculate several key dielectric properties of small-scale structures. Intrinsic breakdown strength [80] and the real part of permittivity can be calculated with reasonable accuracy, but the effects of complex morphology, the dielectric losses below GHz, and degradation modes cannot yet be calculated [81]. Another approach is to use data-driven methods to interpolate the properties of unknown compounds from large datasets of known dielectrics, but such methods may not reveal, as stated by Huan et al. in [41] any "remarkable "outlier" materials".

As reviewed by Treich et al. in [81], results from the synthesis and characteri-

zation of three generations of polymers based on rational design are available as of 2017. These organometallic polymers and polyimides have demonstrated small-area dielectric strength comparable to BOPP, higher dielectric constant of 3 to 8 and operating temperatures above 200 °C. On the downside, these materials still exhibit relatively high dielectric losses. Initial problems with processability into thin films have been at least partially solved and the aim is towards using commercially available materials for cost reduction. No attempts to upscale the production of rationally designed materials to pilot- or commercial level have been reported so far and the technology appears to be limited to laboratory-scale film production.

Temperature has a significant effect on capacitor life; thermal design and thus the energy density can be improved by numerical simulation. Finite element method (FEM) modeling of capacitors has focused on two topics: the temperature rise and associated failure of metallized film end connections in high current applications [42, 43] and the hot spot location and -temperature during thermal stability tests [13]. Temperature rise in hot spots may ultimately determine the maximum rated operating temperature. Improving the end connections is necessary to achieve increased power densities [51], which can be envisioned to be reachable, for example, by using exact knowledge on hot spot temperature rise to reduce "unnecessarily large" safety margins. In addition to FEM, SPICE simulation originating from early the 70s [82] has been used to study failures of metallized capacitor end-connections [83].

2.3 Nanostructured Materials

Nanostructured dielectric films for capacitors were studied in [P1, P3, P4, P6], thus a more thorough review of this technology and its current state is warranted. As outlined in Section 2.2.2, polymer nanocomposites (PNCs) are materials whose properties are determined at a nanoparticle-polymer matrix interface. As with any other technical materials, proper manufacturing process is needed to achieve the desired performance.

As reviewed by Kumar et al. in [72], in 2018 polymer nanocomposites are already relative well-established technology in several fields, major applications being filled rubber tires and continuous fiber reinforced composites. Improving ordinary materials by nanostructuration began to gather interest in the 90s, but has yet to yield revolutionary advances in any major field. Dielectric polymer nanocomposites are a small subset of nanostructured solids, which have been proposed to improve insulation systems in various applications such as HVDC power transmission and

rotating machines [84]. The focus of this thesis is on capacitor insulation, but cable insulation systems are also reviewed briefly as selected additives are routinely used to improve the latter [85, 86]. Nanoparticles are after all a subtype of additives and thus the literature on cable insulation provides a solid starting point.

Nanometric fillers can be used in HVDC insulation systems to reduce space charge accumulation and conductivity, accelerate charge dissipation during depolarization, and increase the breakdown strength. The current consensus is that the reduced space charge accumulation and higher resistivity of nanostructured materials are caused by increased electron trapping [87], and that the accelerated charge dissipation results from locally increased conductivity. The regions of increased conductivity are truly localized, and thus a nanostructured material can exhibit reduced bulk DC conductivity and accelerated charge decay simultaneously. [88, 88–90]

Space charge accumulation is a problem and a limiting factor for HVDC insulation, as charge injection may cause local field enhancements that drastically reduce the insulation life [91–93]. This injected charge will also increase the risk of breakdown during voltage reversals [94], which are needed to reverse the direction of power flow in current source converter (CSC) -based HVDC. While CSC technology still offers the highest power transmission capacity [95], the technology trend is towards voltage source converter (VSC) -based HVDC that accomplishes power flow control without voltage reversals, thus avoiding this problem [96].

Extremely low conductivity, space charge suppression and increased breakdown strength are among the key requirements for materials to enable ultrahigh DC voltage transmission (UHVDC). Current XLPE-based DC cable insulation materials, usually operated at low fields below 20 V/µm, where space charge accumulation is negligible [97], cannot answer this demand. Proper nanostructuration can improve several of these key properties without degrading others, thus this approach is highly promising, in addition and in combination with elastomeric insulation, that has the additional benefit of recyclability over XLPE. [88, 89, 98] Similar improvements would also enable increasing the operating ratings of capacitor insulation and thus the achieved power density. This would yield VSC units that are more economical, as has been presented in Chapter 1.

Extruded HVDC cable insulation is fertile grounds for nanostructuration as additives are a well-established approach to suppressing space charge and improving other properties such as treeing resistance [67, 85, 86]. Inorganic additives are known to suppress space charge, but agglomerates increase the risk of breakdown [85]. Nanotechnology can be envisioned to provide better ways to compatibilize the filler with

the surrounding polymer and thus by improving dispersion and reducing agglomeration yield an improvement over the current technology. Compared to capacitors, cable insulation is relatively forgiving environment, as it is several millimeters thick and operated at relatively low fields below 20 V/µm [97]. Moreover, other necessary additives cause localized field enhancements [96] which the insulation system has to tolerate. These can be envisioned to be the reasons why even micron-sized agglomeration of nanoparticles was not considered deleterious even in 500 kV XLPE/MgO cable insulation [90]. Indeed the preferred particle size of <15 µm reported by Hanley et al. [85] is reachable even with significant nanoparticle agglomeration. One may imagine that the negative effects of small localized field enhancements are compensated by the overall reduction of space charge in the surroundings. Optimum filler loading for nanodielectrics is in the few percent range, to prevent the formation of percolation-type failure paths [72].

Numerous examples of nanostructured materials claiming improved space charge properties are found in scientific and patent literature. To name a few, in 2011 an extensive characterization of hot-pressed XLPE samples with and without 5 % of nanosilica was published [89]. In this study, the silica nanoparticles reduced the amount of accumulated and residual charge and increased the resistivity. The improvements were greater if the silica was surface functional with a chemical coupling agent to promote its dispersion. Only minor variations in dielectric breakdown strength were reported, and the silica-containing materials exhibited significantly higher dielectric losses. In another study published in 2015 syndiotactic PP (sPP) compounded with 0.5 wt.% to 1 wt.% hydrophobic silica was space charge free at 60 V/µm as opposed to unfilled sPP and XLPE [99], the hindrance of sPP is however its high price [96]. As reviewed in [100] inorganic nanoparticles also reduce the charge accumulated in iPP and EVA (ethylene vinyl acetate) at high fields, but decrease the charge injection threshold, the latter may be avoidable by improving the purity of the fillers [101]. 500 kV nanocomposite HVDC cable with higher resistivity and reduced space charge has been developed with main insulation of XLPE with 1 wt.% of silane-treated nanometric magnesium oxide, compounded using a master batch approach [90]. It is unclear whether this type of cable has been installed somewhere.

Patented nanostructured HVDC cable materials claiming improvement in space charge properties include polyethylene compounded with functionalized inorganic nanoparticles such as silica, titania or magnesium oxide [102], polypropylene and LDPE with either silicon or titanium dioxide or carbon black [103], XLPE with nanodispersed carbon black, iPP compounded with EPDM rubber and surface treated

nano zinc oxide [104] and fullerene [105]. Prysmian [106] has patented a cable with untreated nanofiller having reduced space charge accumulation at 30 V/µm compared to unfilled references. The patents usually mention several other additives besides nanoparticles.

Nanocomposite HVDC cable has been installed at least between Spain and France [72]. It was not known at the time of writing this thesis if other nanocompounds have been commercialized and used in full-scale cables. The lack of knowledge on the ageing and degradation of nanodielectrics is still a recognized issue [72] and can be reasonably assumed to hinder the mainstream adoption of nanomaterials. Moreover, improper manufacturing such as too high nanoparticle loading, improper or only partial surface functionalization or external contamination will lead to various problems masking any possible "nano-effects" [72, 73].

The electric fields in capacitors are decade higher than in cables, yet compared to cable-grade polyethylene [86] BOPP appears to be extremely resistant to space charge accumulation, as little conduction current associated with space charge is measured even at 500 V/µm [97] at room temperature. Nanostructured capacitor films have demonstrated promising short- and long-term properties [107], also with functionalized hydrophobic silica [2], the addition of which improves space charge behavior in cable and bulk insulation. To the authors knowledge literature mentions no attempts to characterize the space charge properties of nanostructured biaxially oriented thin $\lessapprox 20$ µmfilms. It would be extremely interesting to know if these films demonstrate increased resistance to space charge injection as that could translate to longer insulation life or alternatively to higher possible design fields. Nanostructuration has been also used to improve the high temperature properties of polyimide thin films. [78] For capacitors improving the in-plane thermal conductivity would be of interest [108], but no attempts to realize such measurement on nanostructured thin films was found in literature. Measurement would need a full winding of such film, as small-area measurements are complicated [108].

Agglomeration is a challenge in nanostructured capacitor films as contrary to cable insulation even micron-sized agglomerates span considerable portion of the film cross-section, and result in severe field enhancement. Self-healing designs tolerate a few such agglomerates and resulting breakdowns but the amount of any agglomerates should be kept at a very low level. A recent study demonstrated DC ramp-rate dependency in 4.5 wt.% hydrophobic SiO_2–filled BOPP nanocomposite film [109]. Ramp rate dependency in the publication's timescales equals extremely short insulation life under high-field electrical stress. While the general conclusion

drawn of the charge dynamics being the culprit is reasonable justified, it would be interesting to know if root cause for this phenomenon is in the nano-interface or agglomerates inside the material.

Chapter 3

Experimental – Capacitor Films at High Temperature

"In physical science a first essential step in the direction of learning any subject is to find principles of numerical reckoning and methods for practicably measuring some quality connected with it."

— William Thomson, 1st Baron Kelvin, *Electrical Units of Measurement, a Lecture delivered at the Institution of Civil Engineers May 3, 1883*

Regardless of the way better capacitor dielectrics are developed, their electrical properties must be screened sooner or later to ensure no harmful trade-offs are being made. Some commonly cited performance metrics of metallized film capacitors result directly from film properties while others are more determined by design choices. Properties resulting from film properties include the permissible operating and storage temperature and physical size, the corresponding properties being degradation and melting at high temperatures and the maximum tolerated electric field determining the energy density. Properties more related to design choices are the rated voltage and losses, determined by the number of series connected elements, impregnation, hermetical sealing and metallization type and geometry, these are only indirectly related to film properties. Service life depends both on design choices and film properties: hermetic sealing, allowable temperature range, voltage endurance of the insulation and so on.

Electrical and thermal properties of films are directly related, as any increase in the reactive power Q results in an increased power loss $P_{dissipated}$ and self-heating [110]:

$$P_{dissipated} = Q \times \tan \delta \tag{3.1}$$

Metallized film capacitor loss factor $\tan\delta$ cannot be decreased infinitely since the main cause of the losses, the metallization resistance cannot be decreased without risking the self-healing functionality[40]. Metallized film capacitors can be regarded as a relatively mature technology already operable close to the material limits with design fields around 30 % of the short-term small-area breakdown strength [33] and operating temperatures 65 % of the melting point [110]. Therefore, improving the film performance at elevated temperatures or developing films with increased in-plane thermal conductivity are required to develop film capacitors with higher energy density [41]. Thermal conductivity can be easily measured only from capacitor windings, requiring resource intensive industrial film production [108], while measuring the film performance as a function of temperature requires only laboratory-scale oriented films and a broad selection of standardized methods and measuring equipment has been available for decades [111]. Regardless of the way better films are pursued, screening the dielectric properties as a function of temperature is required to ensure all trade-offs are recognized and tolerable. There is some room for trade-offs in film capacitor design, e.g. the dielectric loss of the base film may be increased slightly as long as its contribution to the total loss (and heating) is kept negligible. On the other hand even a moderate increase in accumulated space charge will locally increase the electric field and reduce the insulation life from years to months [92].

Film-foil capacitors have less room for trade-offs, as the foil electrode losses are negligible and the dissipation factor of the film itself has greater impact on the total capacitor losses. Dielectric heating is to be avoided as even a moderate increase in the hot spot temperature can reduce the insulation life significantly. Weak points are also undesirable as single breakdowns decimate whole elements.

While moving from short-term breakdown voltage tests at room temperature to measurements at elevated temperature, then to constant stress times-to-breakdown measurements and finally to long-term and ageing experiments of several thousand hours, the measurements become progressively more time consuming and require more effort. Simultaneously the test conditions become closer and closer to the real use application in capacitors, and the measurements bring forward subtle differences between films.

3.1 Variation of the Fundamental Dielectric Properties with Temperature

3.1.1 Decrease of Breakdown Strength at Elevated Temperature

The short-term DC breakdown strength of BOPP film at room temperature is in the range of 500 V/µm to 800 V/µm, and decreases with increasing temperature and measurement area [66, 112, 113]. In the absence of partial discharge activity and at short measurement times the AC breakdown strength approaches the DC value [114], as also verified in [P3], but may decrease at higher frequencies due to dielectric heating [115]. Ho & Jow reported in 2012 [66] a monotonic 11 % decrease in DC breakdown strength between 25 °C to 100 °C for a 7 µm film, they also propose that the high field breakdowns of BOPP are of thermal nature and influenced by hopping conduction. Sanden & Ildstad reported in 1998 [116] a greater but still monotonic 32 % decrease between 20 °C to 100 °C for a 50 µm stack of two BOPP films. This and any other old BOPP film breakdown data at elevated temperatures should be evaluated carefully as it may be influenced by impurities in the film which reduce the DC breakdown strength above 50 °C to 60 °C [24], but interestingly the high temperature results presented in [116] do not display the abrupt change associated with impurities [24].

In this thesis the large-area multiple breakdown measurement system developed in our research group for studying thin plastic films [2, 117] was upgraded to support measurements at elevated temperature [P2, P5, P7]. The nominal dimensions of the square large-area electrode in these measurements are 90 mm × 90 mm, yielding to an active area of 81 cm^2. A rudimentary form of this method has been used to study thin Metal-Oxide-Semiconductor (MOS) capacitors [118]. The high temperature measurement was realized with a new heat resistant test bench made of PTFE and glass and an 800 W hot plate system to control the temperature of the test bench accurately. The final embodiment of this system with the highest temperature accuracy incorporated a test chamber with forced air circulation, heated with 800 W PID-controlled heaters. The temperature accuracy achieved with with this system was 3 % and the measurements were time-efficient because the temperature stabilization took only approximately 10 min. A transparent glass window enabled real-time observation and video recording (or photographing) the breakdowns and other discharge events. This system is primarily intended for short-term tests in air, but is also suitable for tests in inert gas. Inert atmosphere or other means to prevent

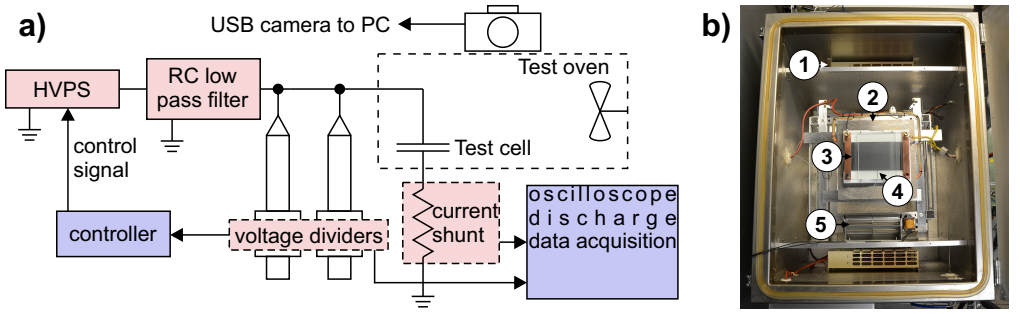

Figure 3.1: Final embodiment of the circuit used for large-area high temperature DC breakdown and voltage endurance measurements. The latter are reviewed in Section 3.2.1. **a)** Schematic diagram of the test setup, from [P7], ©2018 IEEE. **b)** Photo of the test oven, with a sample fastened. Its key components are **1)** two 400 W heaters, **2)** 800 W hot plate, **3)** PTFE sample holder, **4)** thermocouple **5)** cross-flow fan. By changing the sample holder the same setup is used for single-breakdown measurements. Gasifying materials must be excluded from the oven as the fumes may affect the dielectric under test.

oxidation would be required to conduct longer tests for the test conditions should be representative of service conditions in actual capacitors. The high temperature test system is illustrated in Figure 3.1 and the decreasing DC breakdown strength of the various BOPP films studied in publications [P2, P5, P7] is depicted in Figure 3.2.

The system was evaluated by measuring the DC breakdown strength of a commercial smooth 10 µm BOPP film at 100 °C using several ramp rates [P7]. The characteristic 63.2 % short-term large-area breakdown strength decreased from 770 V/µm to 690 V/µm between room temperature and 100 °C and further down to 600 V/µm with slow ramps where breakdown occurred typically after 40 minutes. The 10 % decrease with short measurement times agrees well with the results presented by Ho & Jow in [66]. The results from the slowest ramp should be evaluated cautiously as oxidative degradation may have had time to damage the film.

Measuring the breakdown strength at elevated temperature instead of at room temperature has two advantages: materials performing well at room temperature but not at real operating temperatures are detected and differences between materials are revealed. These benefits were exemplified in [P5], where two industrially produced BOPP films whose highly isotactic base materials were of different molecular weights were compared. In general this type of comparison can be used to e.g. select the most promising base material or to adjust a process parameter. At room temperature these films had displayed similar large-area breakdown performance and high characteristic breakdown strength of 790 V/µm comparable to commercial

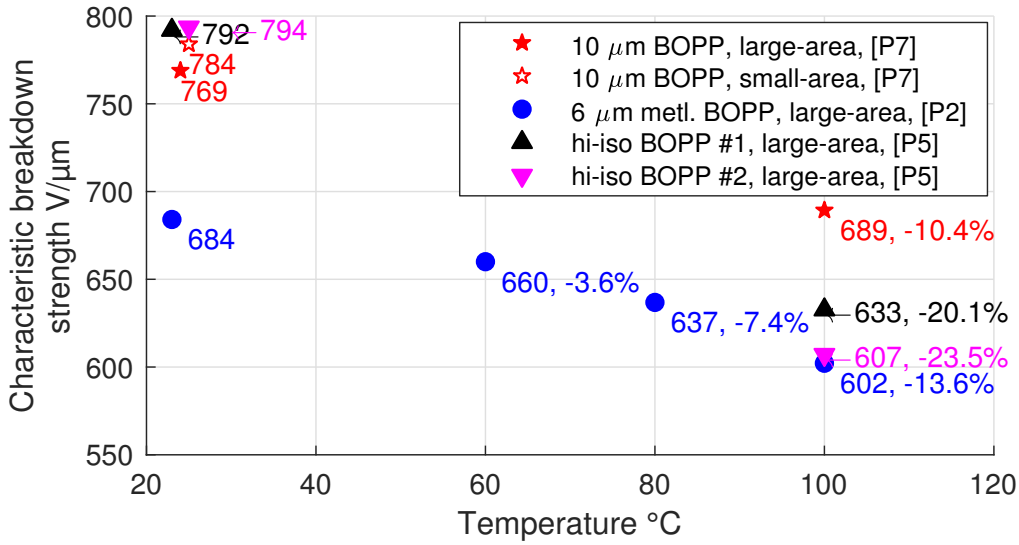

Figure 3.2: The breakdown strength of the 10 µm and 6 µm commercial BOPP films studied decreased by 10 % and 14 % between 23 and 100 °C. The high ≈20 % decrease in two other highly isotactic "hi-iso" BOPP films studied indicates inferior performance at typical operating temperatures which in some applications extend today above 100 °C. High temperature short-term measurements can bring forward such differences between films.

products. At 100 °C however, the breakdown strength of one film had decreased more in the <50 % probability region. This revealed difference is illustrated in Figure 3.3. The characteristic 63.2 % breakdown strength of both films decreased by ≈20 %, which is rather high in comparison with the 10 % to 11 % decrease achievable with commercial capacitor-grade BOPP films [66, P2, P7, P8]. This highlights the potential for improvement of the high temperature performance with these films. Rather unsatisfactory performance at elevated temperature was also evident in subsequent DC electro-thermal ageing tests, where planar test capacitors constructed from these films were rapidly destroyed when subjected to 200 V/µm at 100 °C. Nonetheless, the lack of knowledge on the constituents and processing of these films prevents definite conclusions on this aspect and prohibits root cause analysis. Such analysis was however not within the scope of this thesis, and the results exemplify the potential of high temperature multi-breakdown measurement to reveal differences between films, and aid in steering their development by doing so. More details of the ageing experiment are presented in Section 3.3.

In publication [P2] it was concluded that being briefly subjected to temperatures up to at least 100 °C in atmospheric air does not adversely affect the room temperature,

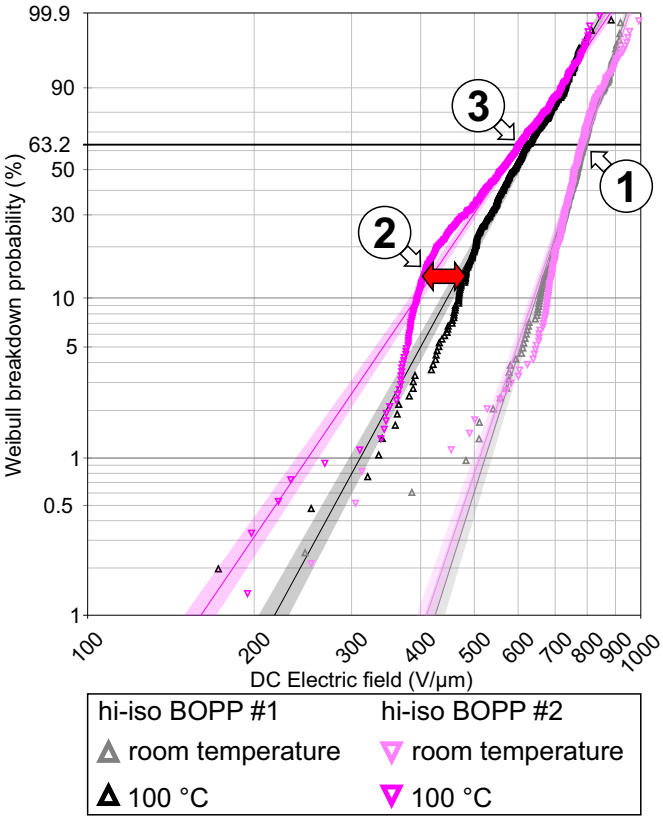

Figure 3.3: The importance of high temperature breakdown strength measurements. Two BOPP films of different base material were compared. **(1)** At room temperature their breakdown strengths were similar, **(2)** but at 100 °C the breakdown strength of the second film decreased more in the <50 % region. This results also exemplifies the importance of gathering tens of breakdown data points: because the characteristic 63.2 % breakdown strength **(3)** is similar at 100 °C, the difference might not have been visible if only the IEC 62539 recommended minimum of 10 breakdowns were measured.

large-area DC breakdown behavior of commercial capacitor-grade BOPP film. Large-area DC breakdown behavior is a sensitive indicator of thermally activated permanent changes in the film [4, P1], and as it remains unchanged thermal degradation is highly unlikely. Consequently it was deducted that DC breakdown measurements at least up to 100 °C can be conducted in atmospheric air, as was done in all subsequent progressive stress and voltage endurance tests at elevated temperature.

In publication [P2] thermal degradation caused by brief exposure to elevated temperatures was evaluated by subjecting a commercial, metallized 6 µm BOPP film film to temperatures between 60 °C to 100 °C for durations in the range from

10 min to 20 min and then measuring their large-area DC breakdown behavior after cooling to room temperature. The time range correspond to a typical warm-up and temperature stabilization time in a high temperature breakdown measurement. It is in advance of the application of the electric field. In this study the film was also measured at room temperature, 60 °C, 80 °C and 100 °C. Between room temperature and 100 °C the characteristic breakdown strength decreased by ≈14 %. At some point there were concerns about the temperature accuracy of this early system, but these were alleviated as the results aligned well with successive measurements on commercial film reported in publications [P7, P8]. These latter measurements were done using systems with better temperature monitoring capabilities and forced air circulation.

Omitting the hot oil eliminated hazardous fumes and the risk of swelling. Some dielectric oils swell BOPP films and increase their thickness, which must be taken into account [119]. Ingress of oil also increases the breakdown strength [120] of at least hazy films; measuring the dielectric properties of a swelled PP film does not reveal the film characteristic, but rather those of a film-oil multicomponent insulation system. Earlier it has been established [2] that the DC breakdown strength of ≈10 µm BOPP films at room temperature is not affected by whether the test fixture is immersed in dielectric oil or in ambient air. This is explainable by the slow reaction between the "Shell Diala" oil used and PP at room temperature. Typically the breakdown measurement reported in [2] ended a few minutes after the sample had been subjected to the oil, thus it had had no time to swell. At elevated temperatures, the reactions become near instantaneous, as was verified in an early test trial where BOPP film samples wrinkled instantly when immersed in heated oil of the same type. This was hypothesized to indicate instant a physical change and oil absorption.

Summary: High Temperature Large-Area Multiple Breakdown Measurement

Section 3.1.1 focused on a large-area method to determine the variation of the DC breakdown strength of capacitor films with respect to temperature. This method utilizes 81 cm^2 self-clearing electrodes and highly automated discharge energy and -voltage based data analysis. A photograph of a typical measurement setup is presented in Figure 3.1 b, additional imagery can be found in [2]. Primary purpose of these measurements is to screen capacitors dielectrics based on the decrease of breakdown strength with increasing temperature. Such screening is justified since high breakdown strength at maximum overload temperatures is a fundamental requirement

in practical application, and one of the current research gaps is the lack of proven high temperature capacitor dielectrics. This method enables more rapid acquisition of statistically significant amount of data points than well-established single-breakdown approaches, such as those described in IEC 60243. Usage of square 110 mm × 110 mm samples makes this measurement applicable in all phases of capacitor film development, even prior to large-scale film manufacturing. Based on the experience of the research group with this type of measurements, repeatable results are achieved with four samples, but major deviations are identified with a single measurement. The typical time required for one measurement is 15 minutes, thus one type of film can be characterized at one temperature in approximately one hour. The total time required for associated sample preparation and data analysis depends on the user proficiency and the required level of detail respectively. Usage of e.g. manual thickness correction, as was done in [P4], may increase the time required. The main limitation of this measurement is that if done in air, this approach is best suited for short measurements in the range of a few minutes, at in longer tests film degradation may influence the results.

3.1.2 Measuring the Dielectric Permittivity

Dielectric permittivity ϵ is a material property that defines its capability to store electrical energy. It has a complex value whose real part ϵ' defines the recoverable electrical energy and imaginary part ϵ'' the energy lost as heat. The tangent of the angle between real and imaginary parts is the loss tangent, $tan\delta$. Permittivity is a function of temperature, frequency and field strength [111] and can be measured in a broad frequency range from 10^{-6} Hz to 10^{12} Hz [121]. Electronic and atomic polarization contribute to the permittivity of plastic insulation in power electronics frequencies below 10^{6} Hz, but often more interesting are the effects of orienting permanent dipoles, if present, and charge migration, the latter also explaining DC conductivity. Charge may also accumulate in polymer-electrode interfaces and in internal interfaces of nonuniform systems. Dielectric spectroscopy provides information on this wide range of phenomena and is thus a powerful tool in material development. [121, 122]

To the authors best knowledge there is lack of published information on how to prepare BOPP thin film samples for dielectric spectroscopy, and this prevents dielectric spectroscopy studies of thin BOPP films. That is, despite the availability of measuring equipment [123, 124], application notes [125, 126] and books [111, 121]. The literature focus on the physics of dielectric relaxation and the workings of

measurement devices, but does not explicitly state the key factors for acquiring reliable and repeatable results. In measurement techniques commonly utilized below 10^6 Hz the sample is usually a small capacitor [121], which requires metallized electrodes to make a low-resistance electrical connection with the measuring system and to eliminate air layers between sample surfaces and the electrodes. Importance of adhesion of the metal to the sample surface is recognized in literature, and can be improved with multilayer metallization [127].

Developing a sample preparation procedure for the dielectric spectroscopy of BOPP films was part of the thesis work. Work focused on physical vapor deposition (PVD) methods as conductive silver paint was found unsuitable early on. It did not adhere to the non-polar polypropylene and there were concerns regarding possible interactions with the solvent. PVD encompasses a variety of methods such as sputter deposition and evaporation, where metal is vaporized, transported and deposited on the subrate surface [128]. Literature mentions the use of sputter deposited silver [113] and evaporated aluminum [129], silver [16] and gold [66] electrodes in permittivity and/or DC conduction measurement of BOPP films. Evaporated zinc and/or aluminum is also used in the commercial production of metallized films. Various procedures to condition the metallized samples before measurement are mentioned in literature: Kahouli et al. annealed their silver-evaporated (30 nm) samples short-circuited for 2 h hours at 120 °C [16] or 1 h at 100 °C [130] in nitrogen to ensure the good reproducibility of measurements, which was attributed to removal of space charge and mechanical constraints. The low $tan\delta$ values in the range of 10^{-4} to 10^{-5} presented in both papers agree with typical BOPP film specifications [35, 63]. For similar reasons Ho & Jow [66] conditioned their gold evaporated (100 nm) samples short-circuited at 70 °C for 24 hours before their conduction measurements. In [130] attempts to limit infrared heating during deposition are also mentioned.

A series of test trials was conducted between 2015 to 2017 within the research group using several DC magnetron sputter coaters mainly marketed for electron microscopy sample preparation. Lot of work was done on sputter deposition because of the availability of the equipment, their compact size, and affordability. Adjusting the sputtering parameters yields different metal structures whose properties often differ from bulk metals [128]. Variables in the test trials included, but were not limited to deposited metal (gold-palladium alloy, gold and silver), process time and current, throw distance, pre- and post-treatment using heat and vacuum and constant versus intermittent sputtering in attempt to reduce heating of the plastic sample. Numerous masks made of plastic, sheet metals or tape with different geometries were

also tested.

The recurring problem with sputter deposited electrodes was abnormal dielectric losses, typically in the range of $tan\delta = 10^{-2}$ to 10^{-3} and sometimes with major loss peaks in the 10 Hz to 10^6 Hz range, neither of which were realistic as the loss tangent of capacitor-grade BOPP is a decade less, in the range of 10^{-4} over a wide frequency span[16, 22, 35, 63, 130]. These abnormalities are exemplified in Figure 3.4. Unless stated otherwise the permittivity measurements presented were done at room temperature using Novocontrol Alpha Analyzer and BDS1200 sample cell, typically at 1 V to 3 V, and sample capacitance was such that $tan\delta$ accuracy of 10^{-4} or better was attainable [131] in the the frequency range of interest, typically between 10 Hz to 10^5 Hz. Problems with the measurement device itself were ruled out on multiple occasions using low-loss reference fixtures.

It was recognized that by increasing the amount/thickness of the sputtered metal realistic values for real permittivity between 2.2 and 2.3 could be obtained. Also, the measured $tan\delta$ decreased, but the losses settled at abnormally high range around $tan\delta = 10^{-3}$. Visible heat-induced film deformation could be eliminated by decreasing the process current or increasing the throw distance. In general, longer and continuous deposition yielded the lowest dielectric losses. It was hypothesized that because of the negligible heat capacity of the sample, thermal damage and associated deformation would occur almost instantly if critical energy flux is exceeded, and intermittent sputtering e.g. in 30 second intervals would not redeem the situation.

In one test trial increasing the thickness of the electrodes brought the $tan\delta$ values down the the realistic range below 1.8×10^{-4}. These samples were dried in vacuum for 24 hours before measurement, after which the sample with the thickest electrodes displayed increasing losses with decreasing frequency below 100 Hz, typical behavior of a material whose dielectric behavior is governed by slow mobile charge carriers [122]. This effect disappeared after the sample had been stored for a few days at room temperature and it was hypothesized that the low-frequency behavior of thin film samples is easily influenced by charge injected during metallization. These results are demonstrated in Figure 3.5. The sputter coater used in this test trial broke, and the result could not be reproduced after repairs. In 2016 a M.Sc. thesis [132] was done about using sputter deposition for electrode preparation, but despite the significant amount of work-hours contributed to the topic concerns about the reproducibility of the method persisted.

While the studies on the sputter deposition still continued, research on using electron beam “E-Beam” evaporation for sample preparation was initiated by the

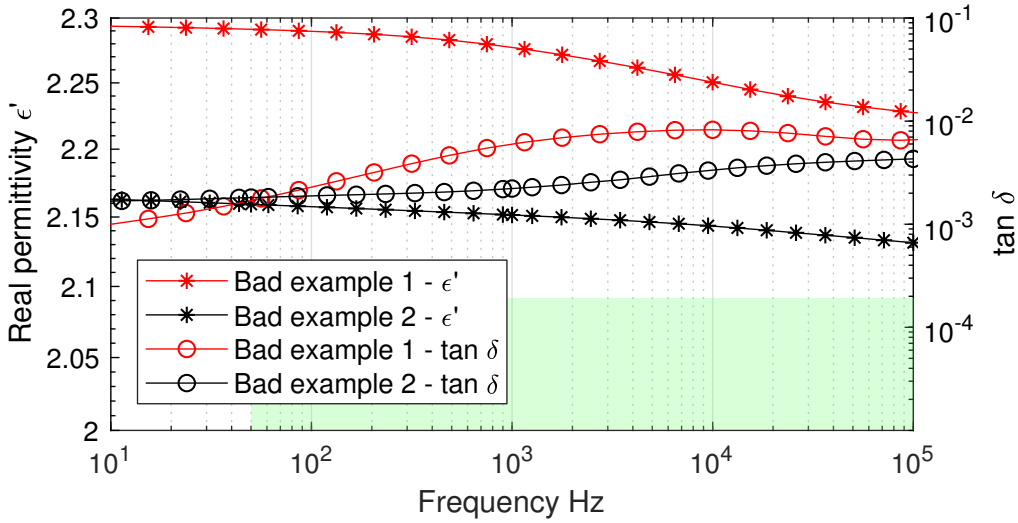

Figure 3.4: Gross errors in the measured permittivity of a 14.4 µm BOPP film caused by failed sample preparation. By manufacturer specification the $tan\delta$ values should lie in the shaded green region.

author. The Leybold L560E E-Beam evaporator used is significantly more complex and the deposition is done in a higher vacuum compared with the sputter coaters, the latter improves the purity of the deposited metal but the required pumping makes the process more time-consuming. Additional advantage compared to the sputter coaters used was the high level of automation, which improves reproducibility as all process parameters can be set numerically. In the available sputter coaters e.g. the throw distance had to be adjusted by hand. In the first test trial aluminum electrodes with a diameter of 12 mm and thickness of 100 nm were deposited on a 14.4 µm hazy BOPP film; gold sputtered samples of this type of film had displayed the realistic $tan\delta$ values of 1.8×10^{-4} once. Two parallel samples prepared displayed stable $tan\delta$ values of 4×10^{-4} over a broad frequency range, which were significantly less compared to what was normally obtainable using sputter deposited electrodes. Since the value was still above the manufacturer specification, in the following trial golden electrodes were evaporated on samples of same film. Gold is more expensive but does not oxidize in air, and should therefore provide a better electrical contact [130]. Electrode thicknesses of 50 nm and 100 nm and the effects of pre-drying in vacuum at moderate temperatures of 30 °C or 50 °C were evaluated. The samples with golden electrodes displayed dielectric losses in the range of $tan\delta = 2 \times 10^{-4}$ to 4×10^{-4}, that is on average lower compared to samples with aluminum electrodes. There was some variation between individual samples and the advantages of pre-drying were not clear.

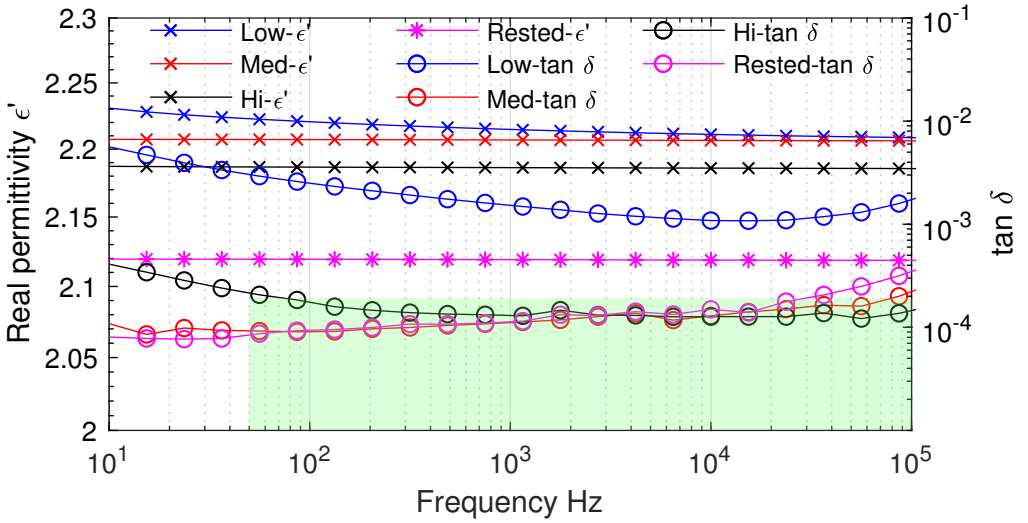

Figure 3.5: The dielectric losses measured from BOPP film samples settle in the manufacturer-specified region below $tan\delta$ 1.8×10^{-4} (shaded green) as the electrode thickness is increased (low→med→hi). Charge injected during metallization may affect the low frequency behavior of the sample with thickest electrodes, but the effect disappeared with time as seen from the "rested" sample.

Immediately before deposition, the samples were washed in 2-propanol and fixed to a sample holder in a clean room environment. The sample holders were laser cut from thin sheet metal. The samples were not annealed before dielectric measurement as such process is claimed to remove an increase of losses with increasing frequency [130] but in our measurement no such effect was seen. Dielectric spectra of samples prepared with Leybold L560E evaporator are illustrated in Figure 3.6.

Evaporating golden electrodes with a diameter of 12 mm and thickness of 50 nm was the first sample preparation method to yield repeatable results falling close to the range of the manufacturer's specification. The $tan\delta$ accuracy of this method was estimated to be 2×10^{-4}, e.g. loss levels below it could not be measured as they are masked behind the additional losses induced by the sample preparation. Nevertheless this accuracy is enough to detect major changes e.g. notable water absorption [133] in hydrophilic nanocomposites. This approach also enabled mass production of up to 36 samples at a time, but was not suitable for very thin (a few µm) samples; the attempt resulted in short circuited electrodes. It was used to study the effects of electro-thermal ageing, compounder screw speed and antioxidant loading of laboratory-scale BOPP films. The first two did not affect the loss levels markedly but reducing the antioxidant loading decreased the losses, as expected from

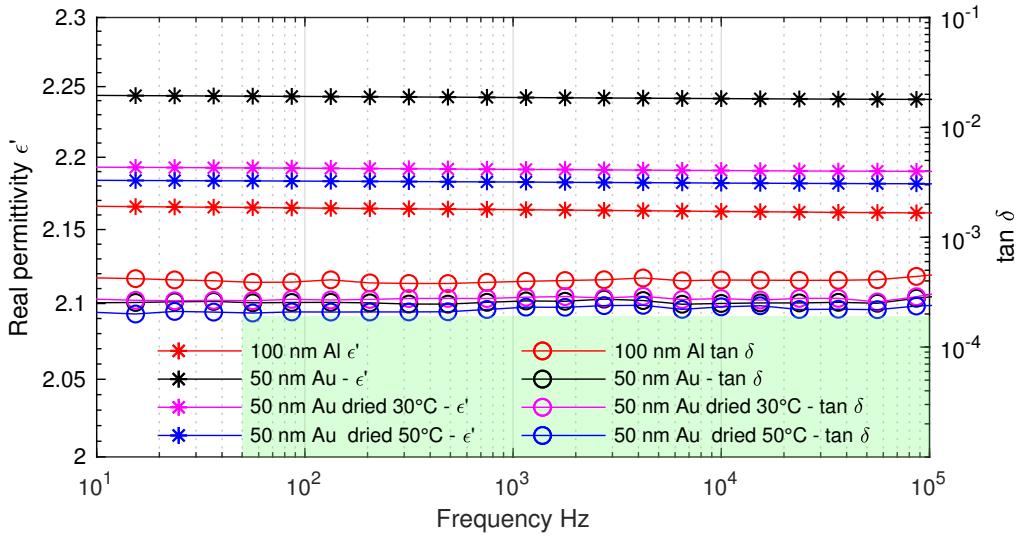

Figure 3.6: Results from early evaporation test trials, the dielectric loss tangent is slightly above manufacturer specification (shaded green area).

literature [23]. The losses of the materials were slightly higher than the estimated accuracy, which suggests that the results stem from the properties of the films itself and not the sample preparation. These results were published in [P4].

Test trials continued with an Instrumentti-Mattila E-beam evaporator in attempt to reach $tan\delta$ accuracy in the range of 1×10^{-5}, that is the loss level of modern high-crystallinity polypropylene film [16]. The Instrumentti-Mattila evaporator is located in ISO 14644-1 class 6 clean room facility and operates in higher vacuum (P<10^{-6} mbar) compared to the Leybold L560E used earlier. First tests were carried out on with a hazy 10 µm film that is a currently available commercial product and a substitute for the type of the 14.4 µm film used earlier. No pretreatments were done as their benefits could not be ascertained with earlier evaporation test trials.

The first test trial with the 10 µm film and 100 nm silver electrodes with a diameter of 22 mm yielded ultra-low loss tangent values in the 10^{-5} range, that is below the manufacturer-reported maximum. These measurements were done immediately after metallization. Similar sample preparation was repeated with a smooth 10 µm metallized BOPP film, an electrode was also evaporated on the side with Zn-Al metallization. The losses were slightly higher, in accordance with the publicly available datasheets and in the range specified by the manufacturer below $tan\delta$ =3×10^{-4}. Two samples each were tested and the result were similar. The variations in real permittivity were probably influenced by the use of average

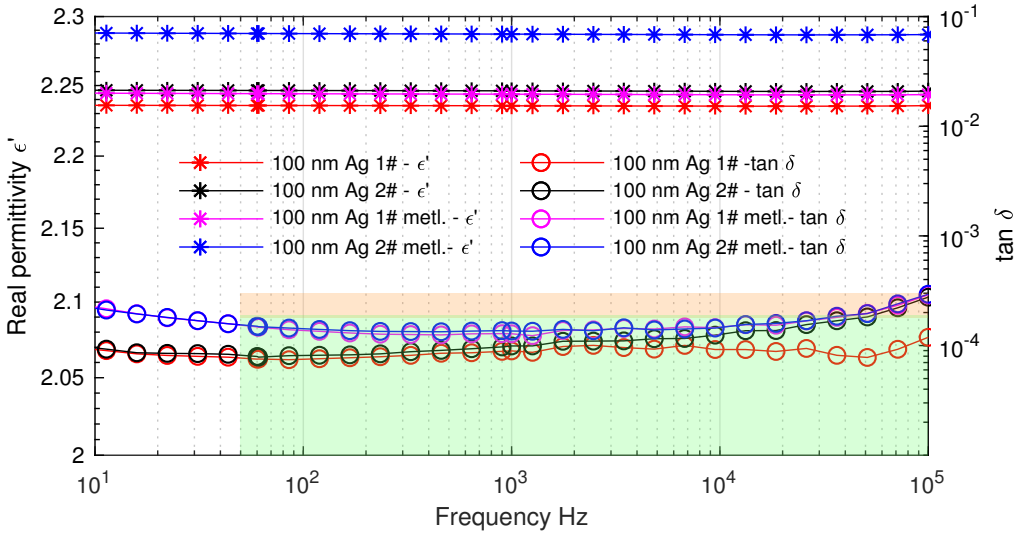

Figure 3.7: Hazy film samples with silver evaporated electrodes displayed ultralow dielectric loss tangent in the $tan\delta$ $=10^{-5}$ range. The shaded green area is the manufacturer specification. The losses in pre-metallized film were higher in accordance with product specifications (shaded orange area)

manufacturer-reported thickness of 10 µm in attempt to avoid extra handling. The results are presented in Figure 3.7

Based on expert advice it was decided to test a two-layer metallization consisting of 10 nm bonding layer of nickel and 100 nm of gold on top. Otherwise, the process was similar. The layers were deposited without breaking the vacuum in between. Two parallel samples were prepared and their permittivity results were the same as with the silver-evaporated samples, as demonstrated in Figure 3.8. Finally, two test trials were conducted with pure gold (100 nm) electrodes ($\varnothing = 22$ mm), the first with the "original" 14.4 µm hazy film and the second with the 10 µm "substitute" film. Gold metallized samples of both films exhibited realistic low losses, the $tan\delta$ was in the 10^{-5} range over a broad frequency range. Slight decrease of the dielectric losses in the $\lessapprox 10$ Hz frequency range was evident in measurements done on the days after metallization, supporting the hypothesis of charge being injected in the film during metallization. Interestingly the losses in this frequency range decreased even in samples that were not stored short-circuited. The conclusion of these test trials is that the choice of metal appears not to be critical for successful sample preparation.

In this thesis work a reproducible method to prepare BOPP thin film samples for dielectric spectroscopy was found: high accuracy $tan\delta$ measurement was enabled by using an Instrumentti-Mattila E-Beam evaporator. During the thesis work various

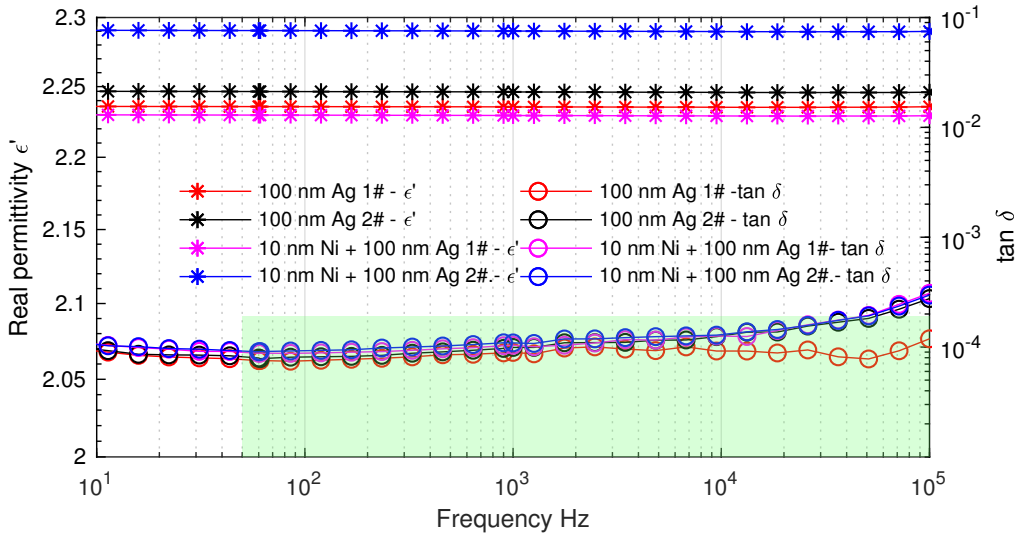

Figure 3.8: Similar ultra-low loss values were measured from samples with either nickel-gold or silver evaporated electrodes. Shaded green area represents the manufacturer specification.

reasons were proposed to explain the high loss levels in samples with sputter deposited electrodes, including but not limited to thermal damage, the low vacuum characteristic of sputtering process and water absorbed in the film. Nevertheless the lone success with sputter deposited gold electrodes appears to counter any claims related to inherent unsuitability of sputter deposition process, and the low losses measured from evaporated samples without any pre- or post-treatments virtually eliminates the possibility of absorbed water. Knowledge of one suitable method is of great aid during material development, but in the end further work is still needed to unravel the true factors behind successful sample preparation.

Summary: Dielectric Permittivity Measurement

Section 3.1.2 recounted the work done to measure the complex dielectric permittivity of capacitor films with extremely low intrinsic losses. Primary purpose of these measurements is to screen capacitor dielectrics based on their capability to recoverable store electrical energy. Such screening is required when developing materials for high energy density capacitors. Realistic results were repeatably achieved with electrodes fabricated by electron beam evaporation in high vacuum, such as those depicted in Figure 3.9. This thesis work shrank the research gap in the preparation of low loss thin film sample; measurements itself can be conducted using commercially available

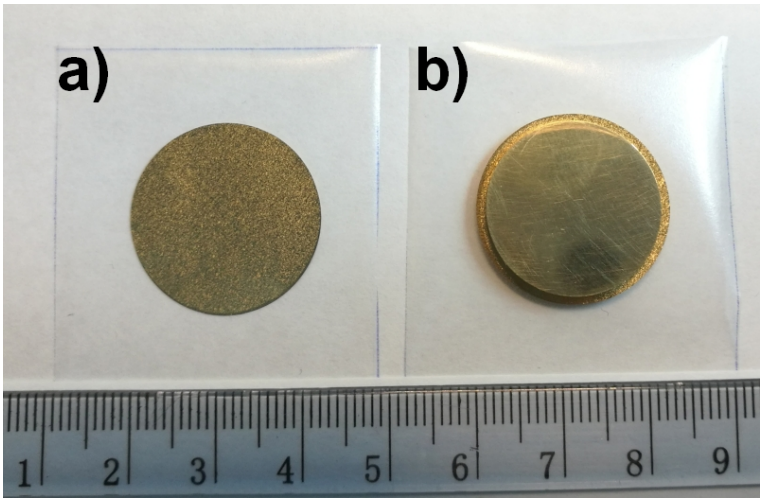

Figure 3.9: **a)** "Hazy" 14.4 µm BOPP film sample used in a dielectric permittivity measurement. **b)** BOPP film sample in a typical electrode arrangement: sandwiched between two $\varnothing = 20\,\text{mm}$ electrodes. This arrangement is then fastened to a sample holder. A "wave washer" can be placed in between to stabilize the sample pressure during large temperature variations in attempt to reduce the risk of puncture. These electrodes are gold.

off-the-shelf hardware and analysis is supported by an extensive body of literature.

One recognized limitation of the metallization method presented is that using it, no feasible method to prepare guard rings could be devised. While the effect of not having guard rings in a permittivity measurement was not quantified, the results aligning well with literature suggests it was not significant at least under the low electric fields involved. Owing to the extremely low intrinsic losses of capacitor-grade BOPP films, the accuracy of the measurement device used has marked contribution to the error in the results, which is amplified towards lower frequencies. To provide an general idea, with top-of-the-line devices, $tan\delta$ accuracy of at least 1×10^{-4} can be expected in the "power electronic" frequency range of $10^1\,\text{Hz}$ to $10^5\,\text{Hz}$ [131]. Only minor variation in the complex permittivity was detected between duplicate samples of same film or with samples metallized in different batches – one measurement may be enough for a baseline characterization. Especially in high field measurement involving DC voltage the effects of charge trapping should be considered because of the tendency of BOPP films to store charge, see Section 3.2.2 for more information.

3.2 High Field Properties

3.2.1 Voltage Endurance Evaluation

When an insulation system is subjected to an electric field and it does not break down instantly, a breakdown may still occur after some time has passed. If during every voltage cycle the insulation is subjected to an electric field corresponding to a finite, non-zero breakdown probability, the probability of insulation failure accumulates as the amount of cycles experienced increases [67]. The insulation may also age, that is, suffer irreversible changes that eventually decrease the breakdown field sufficiently to cause a breakdown [92], same principles apply regardless of the voltage waveform [134]. The times to breakdown t are typically widely scattered, and a Weibull distribution $F(t)$ can be used to model the behavior [92, 134]:

$$F(t) = 1 - \exp\left[-\left(\frac{t}{\alpha}\right)^{\beta}\right] \tag{3.2}$$

where α is the characteristic life corresponding to 63.2 % probability of failure, and β is the shape parameter, which defines the scatter and relates to the failure rate [92, 135]:

- if $0 < \beta < 1$ the failure rate decreases with time,
- if $\beta = 1$ the failure rate is constant and the failures are random,
- if $\beta > 1$ the failure rate increases with time and reliability approaches zero due to progressive degradation [1].

These three regimes model the bathtub curve of reliability: failures caused by major defects etc. tend to occur early and thus the failure rate decreases initially, remaining constant during the service life, only to begin increasing again later as ageing begins to compromise the insulation integrity [92, 135]. A β value of > 1 in a relatively short voltage endurance test indicates unfavorable conditions the insulation system cannot withstand.

The time to breakdown increases from seconds to years as the electric field stress is decreased, this relationship between insulation life L and electric field E can be modeled using the inverse power law (IPL) [92, 134]:

$$L = c \times E^{-n} \tag{3.3}$$

where and c and n are model parameters. Parameter n, also known as the voltage endurance coefficient VEC, determines how rapidly the insulation life increases as

stress level is decreased, thus a high VEC is preferable in applications requiring long service life. VEC can vary with temperature [92], increase at high fields or approach infinity at low fields if a threshold field for electrical ageing exists. In such cases, or if long- and short-term breakdowns are caused by different phenomena (e.g. PD in short-term testing), long-term endurance cannot be extrapolated from high field, short-term test results, indeed the relevant standard IEC 61251 calls for voltage endurance tests with duration of at least 1000 h[134, 136]. Within its scope of validity however the inverse power model is a valuable tool often used in insulation system design [92].

It is thus established that the figures of merit for voltage endurance are a high value of VEC and a failure rate decreasing with time, $\beta < 1$. These parameters are determinable either using times-to-breakdown tests at several constant voltages or with progressive stress tests at multiple ramp rates. The latter can be analyzed using a methodology detailed in IEC 61251 [134] or methods developed by Dissado & Hill [118]. The IEC 61251 recommended testing procedure is to evaluate the high field behavior first using quick ramp tests, and then move to more time-consuming tests at pre-determined constant voltage levels. Times to breakdown in ramp tests t_r can be converted to equivalent lifetimes at constant voltage t_c if the IPL exponent n is known and constant in the relevant range [134]:

$$t_c = \frac{t_r}{n+1} \tag{3.4}$$

Censored Weibull analysis is required if all samples do not break down during testing [135] or if specimens are removed during measurement [137], these statistical methods are beyond the scope of this thesis.

Modern capacitor-grade BOPP film exhibits excellent DC voltage endurance at room temperature, n being in the range of 20 to 30 [109]: for XLPE at room temperature values of 15 to 20 are possible [138]; and for solid insulation under AC values between 8 to 15 are typical [134]. Earlier in 1989 Cygan et al. had determined the DC voltage endurance of a 25.4 µm BOPP film in transformer oil, and found IPL to fit the data well, giving the power law exponent n an value of 14.11 at 23 °C, decreasing to 11.07 at 90 °C [57]. This and any other older BOPP film life data should be evaluated carefully as possible impurities are known to affect the breakdown performance of BOPP films especially above 50 °C [24].

Voltage endurance testing is required in the development of new dielectrics because having a high breakdown strength does not necessarily correlate with good voltage endurance [1, 109, 134]. The importance of voltage endurance evaluation in capacitor film development has been demonstrated in [109], where the DC volt-

age endurance of 4.5 wt.% SiO_2 -BOPP nanocomposite film was studied at room temperature. This film had similar short-term breakdown strength of 700 V/µm compared to the otherwise similar non-filled reference, but voltage endurance testing with multiple ramp rates reveled that the nanocomposite film had lower VEC and its failure rate increased with time, equaling to shorter insulation life. These results were explained with "highly altered charge dynamics" [109], but it must be emphasized that these measurements were done at electric fields stresses far above realistic operational fields, and film performance at operating conditions cannot be predicted from such data. This non-extrapolatability is discussed later in this chapter. Besides, it would be interesting to know the role of nanoparticle agglomeration in such thin ≈16 µm samples. Similar results: a good, in their case improved, short-term DC breakdown strength but decreased DC voltage endurance and an increasing failure rate have been reported also for XLPE - 1 wt.% compatibilized SiO_2 nanocomposite between 20 and 60 °C [1, 139]. Nanocomposite materials can exhibit better partial discharge- and thus AC voltage endurance in presence of PD [75], but these benefits are not relevant in PD-free applications, such as hermetically sealed capacitors — the performance under DC field cannot be inferred from AC experiments. Thus DC voltage endurance testing is established as a recommended approach to evalute capacitor film performance.

In this thesis the large-area multiple breakdown measurement methodology, already featured in several journal articles [3, 117, P4] and theses [2, 4], was adapted to DC times-to-breakdown measurements [P7, P8]. These measurements are suitable for voltage endurance evaluation. The measurement procedure is presented in Figure 3.10, the test setup in Figure 3.1 and the data analysis workflow in Figure 3.11. With this method the DC high-field voltage endurance of a smooth commercial 10 µm BOPP film at 60 °C, 80 °C and 100 °C was determined. In these measurements, DC field and/or gentle physical swiping were used to push out air bubbles from between the metallized film electrodes and the sample film in advance of the application of the full test voltage. Following equation 3.3 the insulation life is highly dependent on magnitude of the electric field and thus the effect of the 50 V/s to 200 V/s voltage ramps and any pre-stressing at lower electric fields could be ignored. The strong field-dependency however necessitated the use of a closed-loop controller to maintain the field stress constant. The adjustments were required to compensate for the varying voltage drop across the series resistances.

Excluding non-breakdown discharges and non-independent breakdowns with a data qualification procedure is the first analysis step of a multiple breakdown

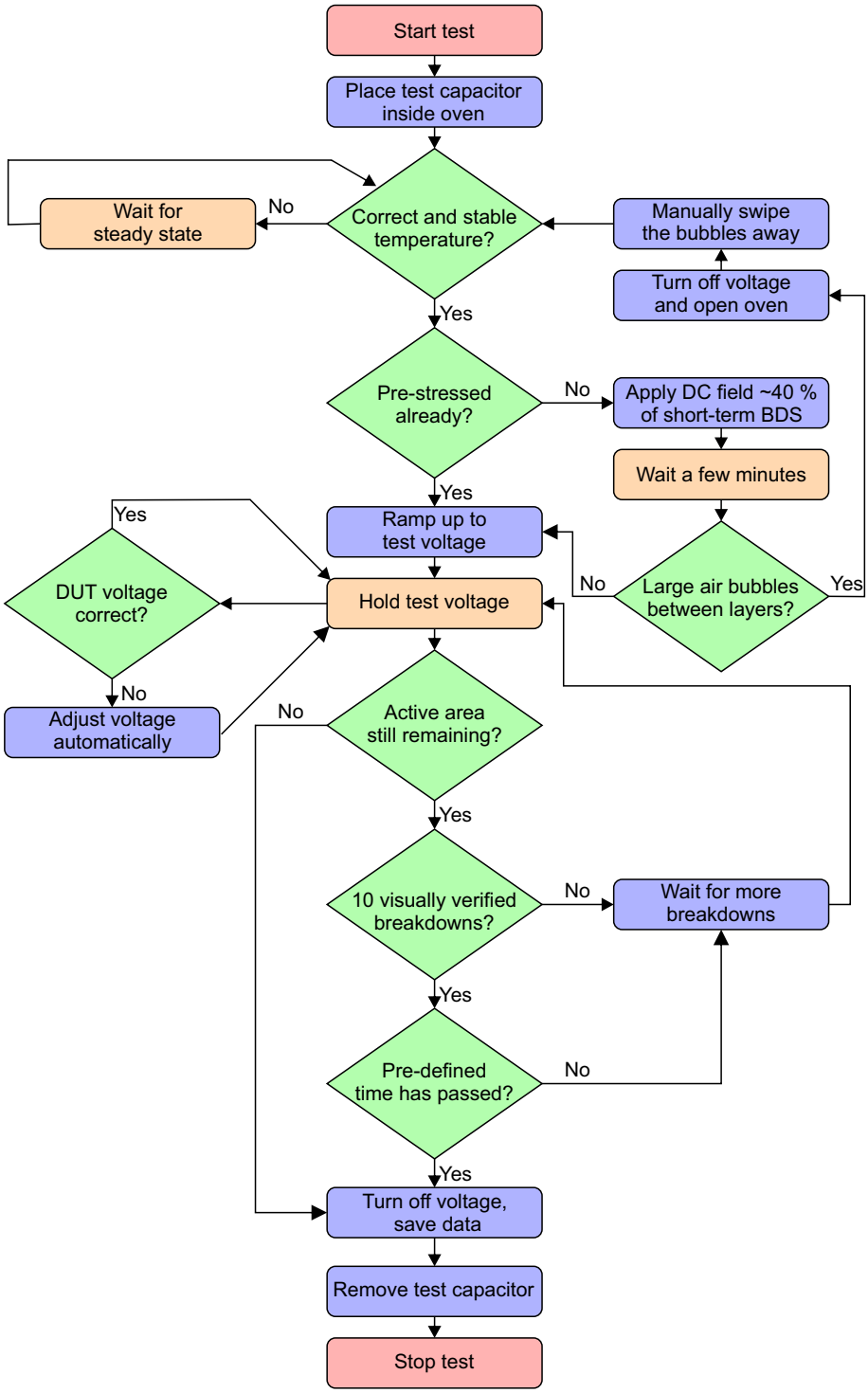

Figure 3.10: DC voltage endurance test process.

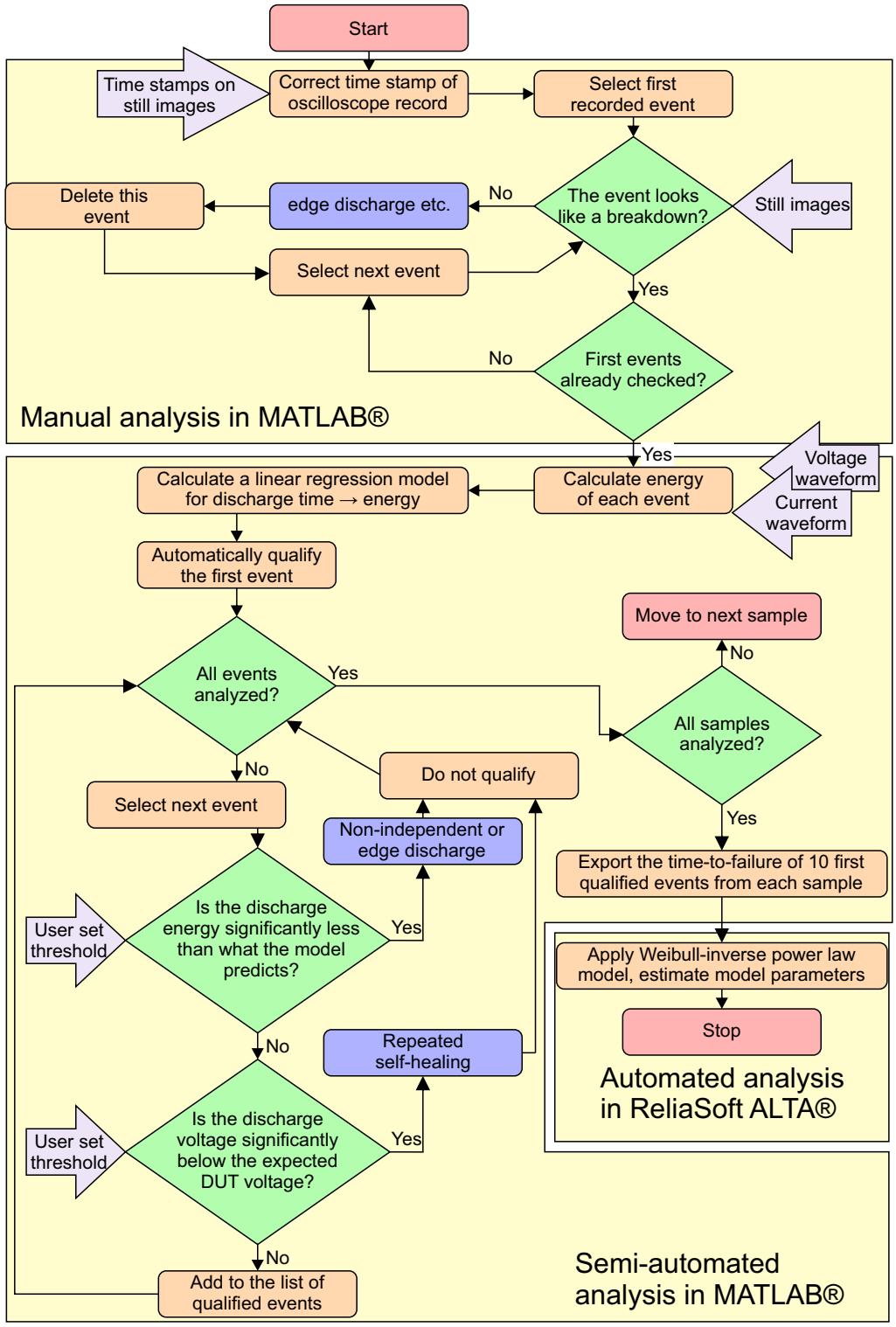

Figure 3.11: Simplified workflow for analyzing DC large-area multiple breakdown voltage endurance test data.

measurement. Similarly to the progressive stress tests, an oscilloscope recorded the current and voltage waveform of all discharges energetic enough to cause a major voltage drop. The apparent self-healing energies of each discharge were integrated from these records, and the data qualification was based on the dependency of the self-healing energy E_{sh} on the breakdown voltage U_{bd} and capacitance C partaking in the self-healing [140]:

$$E_{sh} = a \times C \times U_{bd}^{b} \tag{3.5}$$

where a and b can be regarded as constants in a constant voltage and –temperature measurement. The self-healing energies should follow a slowly decreasing trend as the active area and with it the capacitance C reduces. All discharges whose calculated energy deviated significantly from this trend were excluded, as were those occurring at lower voltage, this indicating a rapid successive self-healing. The first events were also reviewed manually using photographs and any discharges at sample edges were expunged. To harmonize the results only 10 first qualified events from each sample were used in further analyzes. 4 parallel samples were measured in each conditions, yielding 40 data points total. A two-parameter Weibull distribution of Equation 3.2 was fitted to the qualified data points, and the inverse power law of Equation 3.3 was fitted to the Weibull α/characteristic life values. The results are presented in Figure 3.12, also presented are results from small-area ("SA") DC breakdown measurements conducted in room temperature oil using brass electrodes and large-area breakdown measurements at 100 °C. Both were done at four ramp rates and the results were converted to equivalent times-to-breakdown at constant voltage using equation 3.4. Power law exponent n was calculated using the Dissado & Hill methodology [118] used also in [109].

The VEC decreased with with temperature, as seen from Figure 3.12, but the failure rate was increasing with time in all high temperature constant stress measurements as seen from the Weibull $\beta > 1$ in the confidence contour plot of the Weibull parameters presented in Figure 3.13 A and B. The insulation life at 400 V/µm and 60 °C was significantly longer than in other, more severe, test conditions. Therefore, for the sake of clarity the life contours of this experiment are presented in part B of the figure. The rest of the data is presented in part A. This progressive degradation indicates these high-field conditions were unsuitable for the film, indeed in a typical voltage endurance test the sample experienced breakdowns until no active area was left. Due to time constraints the longest tests were sometimes interrupted after ten proper breakdowns were recorded, but due to the increasing failure rate, given time these would have resulted in total elimination of active area as well. As

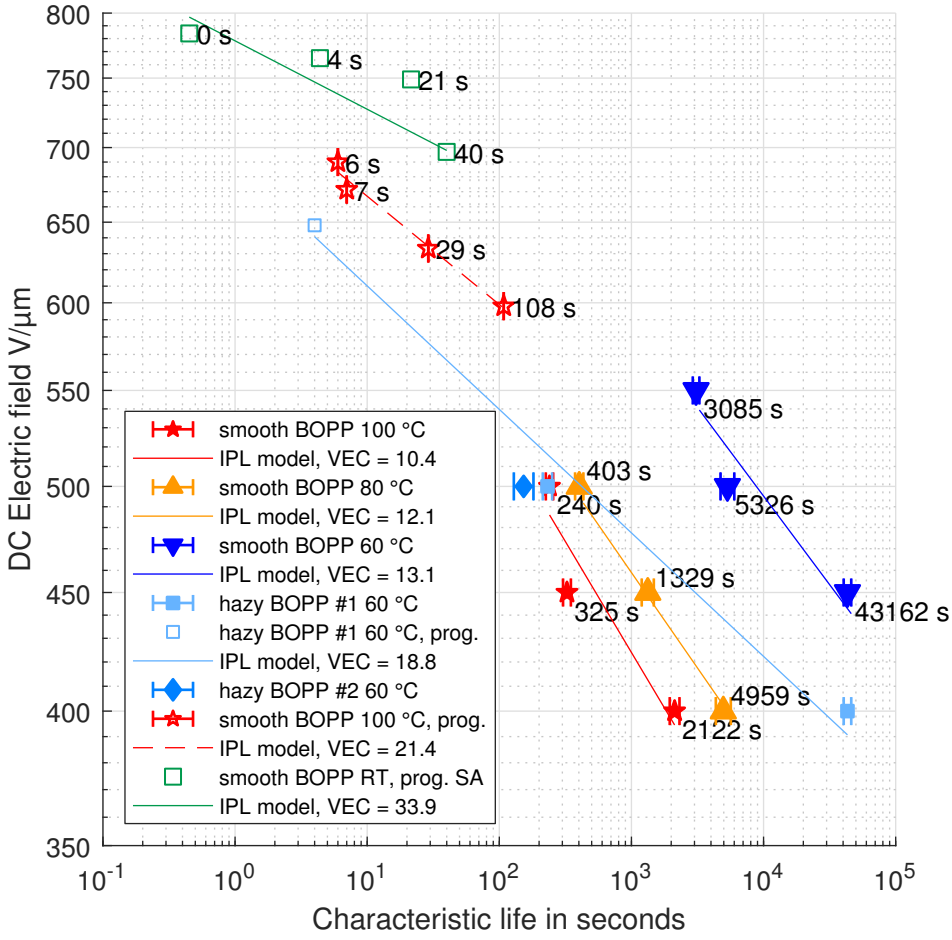

Figure 3.12: DC voltage endurance of three BOPP films, from constant and progressive (prog.) stress tests. The lifetime of all three depended significantly on the applied voltage, this dependency decreased with temperature. Smooth BOPP film appears to have a longer life than hazy variants, but the results are not comparable as Hazy film is designed to operate in an oil-film insulation system.

the operating temperature of BOPP film capacitors extend (slightly) above the range studied [9], temperature itself hardly caused the degradation, but rather the primary cause was the electric field significantly above the highest reported design fields of 240 V/µm in applications requiring reliability [33], pulsed power aside.

The Weibull β and thus the failure rate decreased with decreasing DC electric field stress and temperature in measurements lasting from minutes to hours, but increased again in the longest measurement at 450 V/µm at 60 °C. It was hypothesized that at this point the antioxidants were depleted and oxidation had began to degrade the film. This alone would limit the usefulness of DC voltage endurance measurements

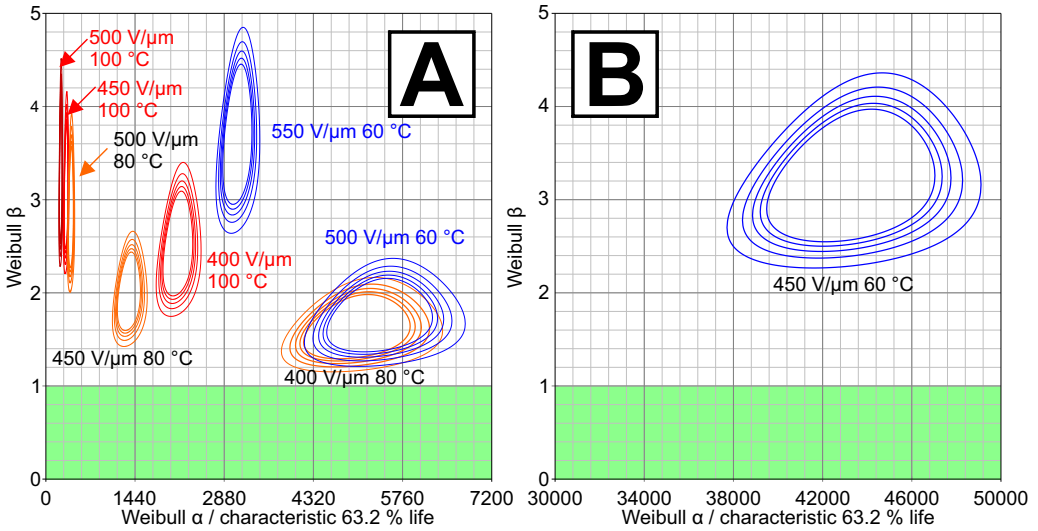

Figure 3.13: 75 % to 95 % confidence contours of Weibull parameters, in 5 % increments. To improve clarity, the data from the longest life tests at 400 V/µm and 60 °C is presented in part B; data from other test conditions is presented in part A of the figure. Notice the different horizontal scale.

in ambient air to the time range from minutes to hours, as oxidation would not be representative of the phenomena in hermetically sealed capacitors, as explained in Chapter 2. Longer measurements should be conducted in inert conditions, such as nitrogen or degassed dielectric oil.

The lifetimes extrapolated from high field data were over a decade less than the several hundred thousand hours [33] what is expected from film capacitors — life at real operating conditions 225 V/µm [13] – 240 V/µm [33] is not extrapolatable from the high-field data. The lifetime was correlated with arbitrarily chosen required reliabilities of 90 % and 95 %, but similar conclusion can be drawn regardless of the percentile chosen. The results are tabulated in Table 3.1. This non-extrapolatability means a non-constant VEC, a possibility mentioned in IEC 61251 [134], that increases at lower electric fields. In the measurement conditions high field degradation is taking place. This phenomenon is explained in [66, 141] as superlinearly increasing conductivity and formation of space charge limited field: at high fields traps no longer hinder the movement of charge carriers; from ageing point of view the excess energy inside the material can accelerate thermal degradation by decreasing its activation energy [92]. The threshold for this high field ageing in “typical polymeric dielectrics” is around 285 V/µm and in the range of 500 V/µm for BOPP [66], these thresholds decrease with temperature [141], thus high field ageing is plausible in

the test conditions used. Worth mentioning is that apart from microscopic stress enhancements the high-field phenomena is nonexistent in AC endurance testing as it would lead to thermal runaway and rapid breakdown [141], these aspects explain why the IEC 61251 standard, that is primarily for AC voltage endurance evaluation [134] does not explicitly mention such increase of VEC when transitioning from high to medium fields.

Table 3.1: Insulation life in hours, extrapolated from high-field voltage endurance data, with 90 % one-sided confidence bounds.

	Use field: 240 V/µm DC:					
	95 % reliability			90 % reliability		
	upper CB	est.	lower CB	upper CB	est.	lower CB
60 °C	13194	8089	4959	18770	11644	7223
80 °C	266	165	103	377	237	149
100 °C	39	27	19	54	38	26

	Use field: 225 V/µm DC:					
	95 % reliability			90 % reliability		
	upper CB	est.	lower CB	upper CB	est.	lower CB
60 °C	31883	18823	11113	45393	27096	16174
80 °C	608	362	216	862	520	313
100 °C	79	53	35	109	74	50

Another fundamental consideration is whether the high field degradation observed in the short time range of hours in the presence of oxygen is representative of degradation phenomena in capacitors where oxygen is eliminated altogether or its ingress is inhibited by slow diffusion through encapsulation. If not, voltage endurance testing in air does not provide useful feedback for R&D process, as the means to improve the voltage endurance in oxidizing environments (e.g. increasing antioxidant loading) would not be beneficial, and might even have negative effects in capacitors [142]. On the other hand, if the degradation phenomena remains the same, but is just accelerated, voltage endurance testing in air proves itself as an relatively easy and quick tool to compare different films. From AC point of view it has been proposed in 1993 [143] that aging accelerated in oxygen-saturated oil would be representative for ageing of high voltage capacitors but further research on this topic from DC point of view and using modern BOPP films is warranted.

It is proposed that an upper threshold for tolerable electric field, as a function of temperature, is determinable with voltage endurance tests by extrapolation to the field corresponding to constant failure rate, that corresponds to Weibull β of 1 in

Figure 3.13 [144]. Using this threshold to guide material development is advocated, as an improvement would indicate that the material being developed should be capable of sustaining higher electric fields. It is not claimed that below this field electrical ageing is negligible, as the very concept of such thresholds is debated [92], but as dictated by Weibull statictics [144] above this threshold the dielectric is in inherently unstable condition that is bound to lead a dielectric breakdown. It is anticipated that below this field the insulation life is significantly lengthened, and thus voltage endurance testing may become unfeasible. Nevertheless the threshold should be verifiable by ageing tests slightly below the extrapolated value— if the threshold is valid one should observe the first two regimes of the bathtub curve of reliability: some "weak points" breaking down in the beginning followed by a long stable time period with a possibility of a few "random failure" breakdowns. Determining the duration of this stable period before the onset of end-of-life degradation, as a function of electric field and temperature, can be envisioned as a way to rationally engineer the service life of a capacitor dielectric.

DC conductivity measurements are advocated to cross-check the threshold for high-field ageing, but inert conditions [41] and/or sophistical measurement methods [145] may be necessary to mitigate the effects of breakdowns at high fields. Worth emphasizing is that the sample preparation procedure described in Section 3.1.2 is also suitable for DC conductivity measurement, indeed such measurements have already been conducted and reported in [146] and are also a prominent in [P8]. The DC conductivity of the same type of film as used in endurance testing was in the range of 10^{-14} S/m to 10^{-17} S/m which is in line with commercial BOPP film specifications [35] and the long-term conductivity decrease observed is also recognized in literature [147]. The film did not exhibit field-dependent conductivity in the measurement conditions extending to 250 V/µm at 30 °C and 200 V/µm at 100 °C [146], this result is in agreement with the thresholds stated earlier in this chapter. Work is being done to enable measurement at higher fields by preventing partial discharging in the sample cell .

In this thesis work a large-area multiple breakdown constant voltage times-to-breakdown measurement was developed and used to evaluate the DC voltage endurance of a 10 µm smooth commercial capacitor-grade BOPP film. A method to determine the upper limits for design electric field is proposed, this threshold was associated with the threshold of progressive high-field degradation. It was also recognized that this high field degradation prevents extrapolation of the insulation life at design field from high field experiments. Before the role of oxygen during short

measurement times is verified, further voltage endurance evaluation is recommended to be done in non-oxidative environments representative of a sealed capacitor.

Summary: Multiple breakdown voltage endurance measurement

The focus of Section 3.2.1 was in a large-area multiple breakdown method for voltage endurance measurements. These measurements are used to determine the distribution of breakdown times when a capacitor film is subjected to electro-thermal stresses less than what would cause a (nigh) instantaneous insulation failure. They can also be used to determine the thresholds for the onset of rapid high field ageing and to screen materials based on their voltage endurance. Known and adequate voltage endurance is a requirement for the capacitor dielectrics used in applications where the service life is tens of years. The times-to-breakdown are inherently scattered, and the multiple breakdown approach expedites the acquisition of statistically significant amount of data points compared to the well-established "one sample – one breakdown" approaches.

The measurement resembles the progressive stress multiple breakdown tests recounted in Section 3.1.1 and depicted in Figure 3.1: both utilize similar 81 cm^2 self-clearing electrodes and take advantage of highly automated discharge energy- and voltage-based data analysis. The main differences are in the data analysis and sample configuration: in endurance tests scissored electrode edges were folded and interlayer air was removed meticulously. Use of square 110 mm$\times$ 110 mm samples enables both measurements to be capitalized starting from early laboratory-scale phases of film development. Consistent results were achieved with four samples.

The main limitation with the voltage endurance tests was that the insulation life at service conditions could not be extrapolated from high field data, presumably due to rapid high field degradation. Additional complication with this type of tests is that at least measurement longer than a few tens of minutes should be done in inert conditions to prevent oxidative degradation not representative of capacitor application. Sophisticated sample handling procedures are also needed to limit the amount of foreign particles between film layers. These aspects are now being actively researched by the research group.

3.2.2 Space Charge in Thin Films

In the context of this thesis space charge refers to electrical charge inside a solid dielectric. Space charge may distort the internal electric field and may greatly reduce insulation life: in plastic insulation it is typically undesired. Space charge

accumulates above a temperature-dependent threshold electric field at interfaces formed by inhomogeneity and field-dependent conductivity. This threshold is why space charge on large scale is a phenomenon unique to DC excitation: apart from microscopic defect regions AC fields sufficiently high to cause charge injection in the bulk would lead to thermal runaway. [91, 97] Space charge and DC conduction are fundamentally related, and these measurements supplement each other: the threshold field for space charge accumulation is in the region where the external conduction current transitions from linear to exponential with regard to the applied electric field [97]. Repetitive packet-like charge injection can also be observed as peaks in conduction current. With multiplexing, both measurements can be carried out near-simultaneously [148].

Space charge measurement can be regarded as well-established technology: in 2006 by Cigré published a comprehensive guide from building a measurement system to analyzing the results [149], in 2017 IEEE published a standard for the space charge characterization of extruded HVDC cables [5], and at least one commercial measurement system for cable and sheet samples is available [150].

There is plenty of literature on space charge in plaque and cable samples that are (at least) several hundred micrometers thick; the measurement systems for such thick specimens do not require the micrometer-scale spatial resolution necessary to characterize the internal charge distribution in capacitor films. Nevertheless, at least one high resolution (a few µm) pulsed electro-acoustic (PEA) space charge measurement system is described in literature. It has been used to visualize space charge at the interfaces of a three layer, 25 µm Kapton®-composite film [148]. The requirements for high spatial resolution are short excitation pulses (<1 ns pulse width), a thin ($\lessapprox 1$ µm) piezoelectric sensor and an analog signal path and analog-to-digital converter (ADC) whose bandwidth extend up to several GHz; the sample capacitance must also be minimized. Proper microwave engineering is needed in the sample cell design to preserve the pulse waveform from the generator to the film under test, and to ensure the high frequency components of the PEA signal are not lost in the analog signal path from piezoelectric sensor to the ADC. The high frequency components are required to reach the high resolution, and they can be distorted by attenuation, reflections at impedance discontinuities and variations in group delay. The author would endorse 3D electromagnetic simulation in the design of $\lessapprox 1$ µm spatial resolution PEA system to characterize modern, $\lessapprox 10$ µm capacitor films. The development of such system is currently hampered by the scarcity of commercially available sub-µm piezoelectric polyvinylidene fluoride (PVDF) films;

elaborately hand-made film or other type of transducer is required. The three other piezoelectrics listed in the comprehensive Cigré manual, SiO_2, $LiNbO_3$ and PZT-4 are brittle single crystals or polycrystalline materials. This brittleness might not be a problem in industrial manufacturing, but using brittle sub-micron wafers in a custom-built system is challenging. At present, the absence of high resolution commercial solutions necessitates unique, individually-built systems. [148, 149, 151]

The electrode material has a strong effect on the apparent DC conductivity of BOPP films [146] and based on their interrelation [97] an effect on space charge behavior would also be expected. Also in HVDC cable insulation systems the insulator-semiconductor interface has a significant effect on space charge accumulation [93]. Thus it would be beneficial if space charge measurements on capacitor films were done using an electrode system similar to what is used in the real capacitors, instead of the combinations of bulk metal and semiconductive layers that would represent HVDC cables. Depending on the application a representative electrode system for capacitor films is either evaporated metal or aluminum foil with the impregnating liquid used in the relevant capacitor design. Preferable the hazy films designed for impregnated film/foil designs should be measured only after proper impregnation. For metallization the prodecure described in Section 3.1.2 would provide solid grounds to begin with, but to the authors best knowledge no attempts to directly measure space charge in metallized capacitor films have been published.

In this thesis work PEA method was used to characterize space charge accumulation in thin capacitor films [P6, P8]. In [P6] a nanostructured biaxially oriented film and its otherwise similar non-filled reference film were studied at high DC fields up to 400 V/µm at room temperature, 40 °C and 60 °C. The thicknesses of the films were approximately 15 µm. In [P8] a commercial BOPP film manufactured from classic isotactic polypropylene homopolymer was measured in largely similar high field conditions and temperatures but up to 500 V/µm at room temperature. This smooth and non-metallized film had a nominal thickess of 10 µm. All measurements consisted of 30 min polarization ("Volt-On") followed by 10 min of depolarization ("Volt-Off"). The high voltage electrodes were discs cut from a semiconducting material and the ground electrode was a polished aluminum block. The piezoelectric was a 9 µm PVDF film. The resolution of this system did not allow direct observation of the internal charge profile, but an increasing intensity of the PEA signal was associated with charge accumulation and a stable signal with the lack of it.

All three films films were space charge free at room temperature up the highest measurement field (400 V/µm and 500 V/µm respectively) but with increasing tem-

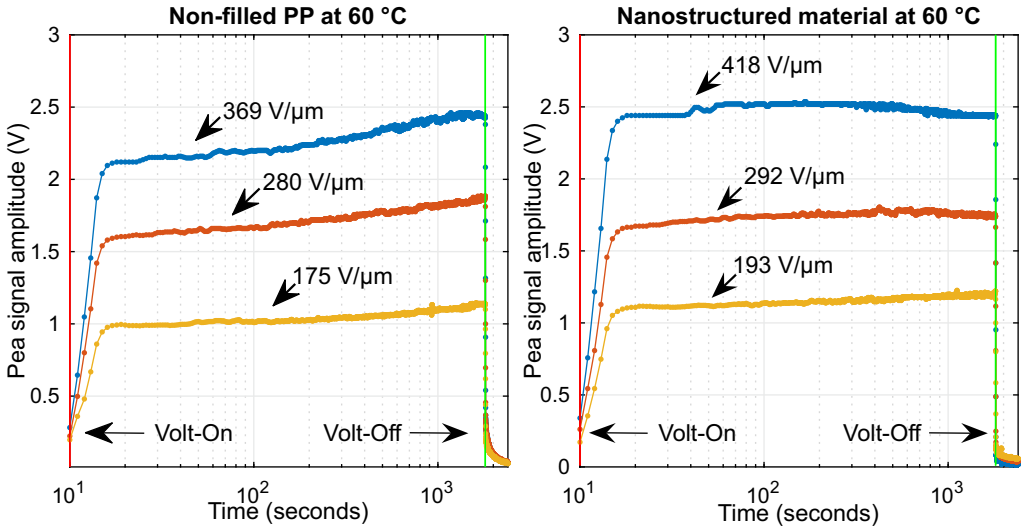

Figure 3.14: Polarization in thin film PEA measurements. An increasing PEA signal intensity marks an increasing amount of space charge inside non-filled PP material, especially at higher fields the nanostructured material appears to reach a stable state within minutes.

perature space charge accumulation was evident in both the non-filled reference film and the commercial 10 µm film while less charge accumulated in the nanostructured film. In [P6] similar reduction in the accumulated charge was also measured in ≈0.5 mm cast film samples of similar constitution at lower $\leqslant 50$ V/µm DC fields at 60 °C. Examples of the behavior of the thin films studied in [P6] during measurements at 60 °C are presented in Figure 3.14. Albeit preliminary, these results suggested that:

1. Nanostructuration can increase the threshold for space charge injection in capacitor films.

2. Similar effect is observed in non-oriented cast films of same composition.

Correlation does not imply causality, but if it can be verified that the space charge properties of oriented films at high fields can be determined by measuring their precursor cast films at medium fields, this knowledge would support material development because

1. materials could be screened early, without the need for time-consuming bi-axial orientation, and

2. space charge characterization is greatly simplified. Measurements on cast films have the benefit of not needing an elaborate high resolution measurement system, which would be needed for direct measurement on oriented films.

The improvement in space charge performance of the nanostructured material was associated with an increasing number of shallow charge traps resulting in increased trap-controlled apparent mobility. The effect is more prominent with increasing temperature. The increased charge mobility in both oriented and cast films was apparent in PEA measurement during depolarization: the injected charge (in cast films) and the signal intensity (in oriented films) decreased more rapidly compared to the corresponding non-filled reference materials. In fact, the charge mobility in non-filled PP was so low that it was found nearly impossible to reuse the cast film samples as space charge was detected in them even after the sample had been short-circuited overnight at 60 °C; this persistent charge can be explained by deep trapping.

Recent thermally stimulated depolarization current (TSDC) measurements conducted within the research group [152] have confirmed that there is significant deep trapping in non-filled BOPP and heavily attenuated deep trapping together with a higher presence of shallow traps in a nanostructured PP-based biaxially oriented film. The calculated trap depth depends on the analysis method, but in general the deep traps are in the range of 1.08 eV to 1.1 eV and the shallow traps lie in the range of 0.75 eV to 0.9 eV. The DC conductivity of these nanostructured materials was lower than their non-filled but otherwise similar references. Additionally, the charge decay was accelerated by the inclusion of nanoparticles. Together with the results presented in [P6], it is affirmed that similar benefits can be achieved by nanostructuring capacitor films that has been achieved in cable insulation. For details on the latter, please see Section 2.3. Worth emphasizing that the materials used in [152] were newer and of different constitution and processing than the ones used in PEA measurements in [P6].

Summary: thin film space charge measurement

In Section 3.2.2 a pulsed electro-acoustic (PEA) method to observed charge accumulation in thin capacitor films was described. Space charge measurements are used for a wide range of purposes, one of them is the screening of materials based on their capability to resist charge injection and -accumulation under DC voltage. Charge injection and accumulated “space charge” have negative connotations and are often associated with ageing and degradation. There are still major research gaps related

to space charge phenomena in thin films, nevertheless this thesis work contributed to that research with results that suggest that nanostructuration may increase the threshold for space charge injection in capacitor films and cast precursor films alike. The principal limitation with thin film PEA measurements is that achieving the spatial resolution required to quantify the internal charge profile requires extremely sophisticated measurement system specifically tailored for 10 µm -scale films.

3.3 Long-Term Reliability

One approach to the ageing of electrical insulation was presented by Fothergill in ICSD 2007 [153], that is to define three phenomena with different time constants: (1) ageing, that is a continuous process occurring during insulation life and may lead to degradation, (2) degradation, that leads to breakdown in less than the required service life and (3) breakdown, which is rapid and often catastrophic loss of the insulation resistance. While for many insulation systems Fothergill's statement that well-designed insulation systems should not breakdown or degrade is true, clearly it does not apply to metallized film capacitors which tolerate numerous breakdowns without a loss of functionality, or to large film-foil capacitor banks which may be designed to have element- and component-level fault tolerance. Localized degradation occurs in capacitors, which results in breakdowns. Excessive ageing would of course necessitate costly refurbishment. The factors that determine the ageing rate of capacitors at component-level were briefly reviewed in Chapter 2, this section centers on the DC electro-thermal ageing of BOPP film insulation in $\geqslant 1000$ h time range.

In this thesis work, the DC ageing of dry BOPP film insulation systems was studied from a phenomenological point of view. This thesis concentrates on the film itself: what happens in it when subjected to electric and thermal stresses comparable to capacitor design, far below what should be required to cause the rapid failure of the insulation system, apart from a few isolated breakdowns that are acceptable in metallized film capacitor designs. Using the term "insulation system" is warranted as the film is always used as part of one, in contact with electrodes, impregnant, etc.; the interactions between PP and oil and the oil quality may affect the ageing behavior [154]. It was of interest to determine whether ageing could be hindered by varying film manufacturing parameters and/or the base material constitution, or if these changes would change the ageing phenomena entirely. Worth mentioning is that polymeric materials can also "age positively", that is, their properties may improve with time. This behavior originates from a slow reorganization of polymer

chains in the solidified state [155]. Indeed, an increase in the breakdown strength of BOPP films after thermal conditioning was demonstrated earlier in the authors M.Sc. thesis [4].

A broad range of dielectric and material measurements were evaluated to identify those most suitable for detecting and evaluating the degree of electro-thermal and thermal ageing in BOPP films. In literature, the ageing of BOPP film insulation systems has been associated with changes in breakdown behavior [154, 156], morphological properties [157], molecular weight distribution [158] and crystallinity [159]. Typically this 20 to 30 year-old research has been conducted using BOPP films and impregnating liquids which may not represent the current state of capacitor film technology, as the capacitor BOPP industry has evolved since then: recently one film producer launched a new product with claims of significantly improved electrical performance [160] and an improvement in the purity of the base PP is evident from improved breakdown performance at high temperatures, see Section 3.1.1. The older literature is also often about the ageing of oil-impregnated, not dry, film systems. Thus as background for this thesis it is argued that when the thesis work began, there was no up-to-date consensus in the published scientific literature about the ageing phenomena in BOPP films used in dry BOPP film insulation systems. Thus there were no recommended practices to evaluate them.

A large-area DC electro-thermal ageing system was developed and using it two 1000 h DC electro-thermal ageing tests were conducted. The method and results from the first experiment have been published in [P4] and results from the second experiment have been published in [P5]. These ageing tests were done using self-healing metallized film electrodes and inert N_2 atmosphere to represent conditions in sealed capacitors by preventing oxidative degradation (see Section 2.1.1 for the background).

The purpose of the first ageing experiment was to determine whether ageing could be hindered by varying a process parameter (compounder screw speed) or base material constitution (antioxidant loading, the addition of hydrophobic SiO_2 nanoparticles, base PP type), or if these changes would change the ageing phenomena entirely. To identify the effects of ageing the experiment was preceded and followed by the characterization of the large-area DC breakdown behavior at room temperature, complex dielectric permittivity (see Section 3.1.2), antioxidant contents and degree of crystallinity, the latter two using gel permeation chromatography (GPC) and differential scanning calorimetry (DSC) [P4]. Eight different PP-based biaxially oriented films were aged at ≈100 V/µm DC at 75 °C for 1000 h. Based on temperature logger

data the target temperature was maintained within 0.5 °C, but due to differences in the film thicknesses the average field stress varied between 95 V/µm to 108 V/µm. The materials were:

- Series 1: PP1-ref and PP2-ref: the references, made from different grades of isotactic PP provided by Borealis Polymers Oy
- Series 2: PP1-sil and PP2-sil: two nanostructured films from the same PP grades compounded with 0.9 wt.% hydrophobic fumed silica Aerosil®R 812 S
- Series 3: PP1-LoAO and PP1-HiAO: the antioxidant series, one film with less (0.20 wt.%) and another with more (0.60 wt.%) antioxidant
- Series 4: PP1-LoSS and PP1-HiSS: the screw speed series, two nanostructured films similar to PP1-sil but compounded with lower (200 rpm) or higher (350 rpm) screw speed.

Apart from their corresponding test series the nominal additive loading was 0.35 wt.% of Irganox 1010 and 0.0075 wt.% of calcium stearate, the nominal compounder screw speed was 300 rpm. The raw materials were dried at 70 °C and vacuum treated and processed in a way that they shared the same thermal history. A detailed description of the material processing is available in [P4].

Large-area DC breakdown behavior was found to be the most sensitive indicator of BOPP film ageing: with ageing the overall breakdown strength decreased and electrically weak points appeared, the latter corresponded to low-field breakdowns deviating from the main Weibull distribution. Electrically weak points appeared also in a commercial 14.4 µm hazy BOPP film aged simultaneously for 1000 h at 66 V/µm DC and 75 °C. Weak points with low breakdown strength in aged films have been reported at least also by Umemura and Akiyama in 1987 [156]. The bulk material properties of different compounds were not affected by the ageing but varied between materials, most notably with PP1-HiSS demonstrating a lower degree of crystallinity and melting point and the PP1-LoAO having the lowest dielectric losses at 50 Hz. Systematic or significant change with ageing was seen neither in crystallinity, molecular weight, antioxidant contents or dielectric permittivity, the absence of antioxidant conversion however confirms that major oxidative degradation did not occur. As the changes in DC breakdown characteristics were the most informative indicator on ageing progression the relevant results are presented in Figures 3.15 and 3.16. The key points to observe are:

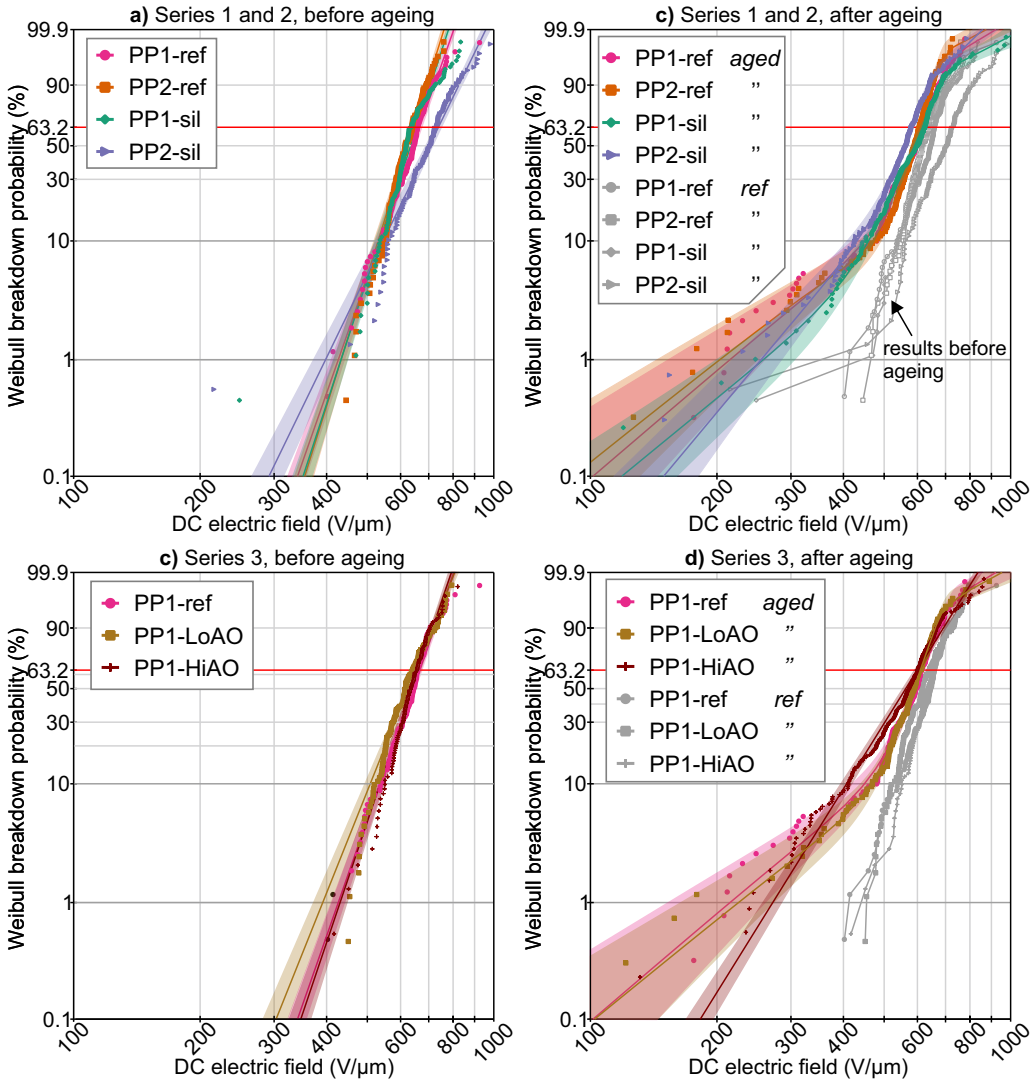

Figure 3.15: DC breakdown characteristics of new and aged PP-based biaxially oriented films from series 1-3 at room temperature.

- In series 1 and 2 the characteristic (63.2 %) breakdown strength of PP2-sil was the highest before ageing, but it decreased the most with DC electro-thermal ageing.
- The DC breakdown behavior of PP-1 and its nanostructured variant PP1-sil were similar before and after ageing.
- Of series 3 aged PP1-HiAO had slightly lower breakdown strength in the medium probability region, but higher breakdown strength in the low probability region.

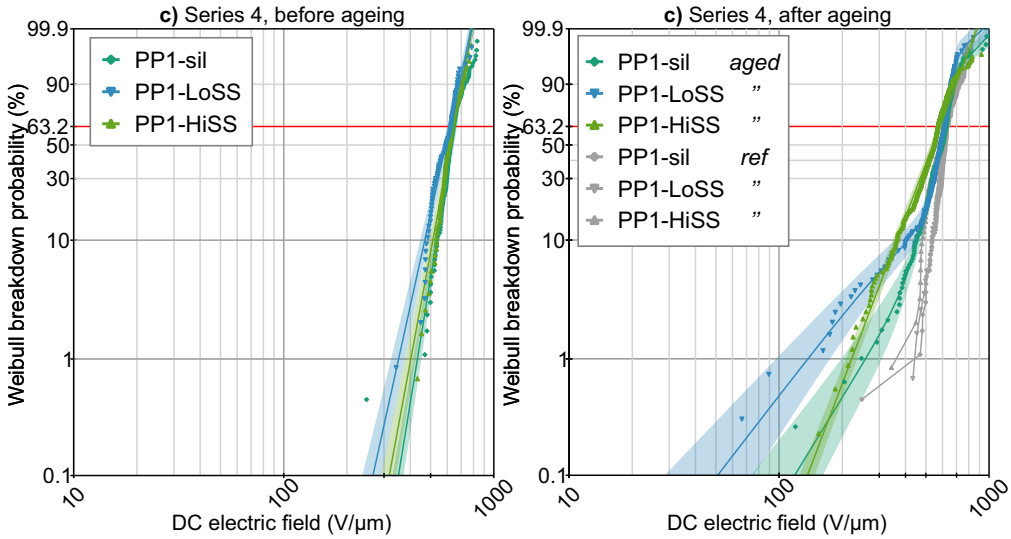

Figure 3.16: DC breakdown characteristics of new and aged PP-based biaxially oriented films from series 4 at room temperature. Please mind the different horizontal scale than in 3.15.

- With electro-thermal ageing weak points deviating from the main Weibull distribution formed in all materials except PP1-HiAo and PP1-HiSS

Joint conclusions will be presented after the results from the second ageing experiment.

In the second ageing test two 5.6 µm BOPP films based on highly isotactic polypropylene grades with different molecular weights were evaluated. These films were provided as film rolls. The methods and results are published in [P5], and the high temperature breakdown performance of these films was discussed in Section 3.1.1. The ageing test duration and target temperature were 1000 h and 100 °C, in this experiment three different stresses were evaluated:

- Thermal stress only
- Thermal stress + 100 V/µm DC
- Thermal stress + 200 V/µm DC

All samples subjected to 200 V/µm DC were destroyed by discharge activity during the first days of the test. This was surprising considering the electric field stress was below the current design fields of 225 V/µm to 240 V/µm. However since the breakdown strength of these films decreased more between room temperature and 100 °C than the 11 % achievable with commercial films (please see Section 3.1.1),

it can be speculated that there is room for improvement in the high temperature performance of these two films. Further analysis is hindered as not much is known of the constitution and film processing these films. Out of the films aged at 100 V/µm DC the breakdown strength of both films decreased, and the relative decrease was greater in the film which had shown superior performance at 100 °C. Electrically weak points (low-field breakdowns) had formed in both thermally and electro-thermally aged films. Additionally the crystallinity (determined with DSC and WAXS) of the films had increased after ageing regardless of the presence of electric field. These films were probably not heat-treated after orientation and being subjected to 100 °C caused secondary crystallization.

Based on these observations from the two ageing tests the following is proposed:

- The formation of weak points is associated with localized DC electro-thermal and thermal ageing of BOPP.
- Improvement in short-term breakdown performance does not mean improved long-term properties.
- The nanostructured PP which had comparable short-term DC breakdown performance before ageing maintained this quality after electro-thermal ageing.
- Base material constitution (antioxidant loading, the addition of hydrophobic SiO_2 nanoparticles, base PP molecular type and weight) and process parameters (compounder screw speed) all affect the DC electro-thermal ageing behavior.
- By varying antioxidant content and compounder screw speed the formation of weak points can be suppressed.

Especially interesting would be to examine whether the absence of weak points in nanostructured PP1-HiSS holds true and did not result from the statistical nature of breakdown phenomena. If verified, it means that proper nanostructuration in combination with optimized film processing can suppress the formation of weak points which is the dominant ageing mechanism at least under DC, and thus suppress the ageing of capacitor insulation.

The efficiency of the large-area DC breakdown measurement in detecting ageing-related changes originates from its “bottom-up” approach, as during such measurement a large area (typically 81 cm^2) is probed continuously, and the degraded regions, no matter how small, break at lower voltages than their non-aged counterparts. This method has been similarly successful in characterizing e.g. the effects of interlayer pressure and film processing related aspects [2, 3, 161]. Material and permittivity

measurements on the other hand evaluate the "bulk" properties from a large volume, and if the degradation that had occurred was only minor and very localized the changes would be swamped or "averaged out" by the majority of volume that is still intact (or even improved if positive ageing had occurred), and/or hidden behind the inherent measurement (in)accuracy that was present due to the limited amount of aged material available for analysis. Scarcity of aged material is expected during early capacitor film development when films are producted only in laboratory scale.

Summary: Ageing Test Method Used in the 1000 h tests

In Section 3.3 a large-area ageing test method was described. Imagery can be found in the appended publications. One advantage of this measurement approach is the use of self-clearing metallized film electrodes that allow the test to continue beyond the first breakdowns. Another advantage is that the required amount of film for thorough material characterization can be aged simultaneously, and a planar geometry makes it applicable already prior to large-scale film manufacturing. Nevertheless, this brings forth its main limitation: without an external source of compressive force or electrodes metallized directly on the sample film surface this approach is not suitable for AC ageing. Similarly to the voltage endurance tests strict procedures are needed to exclude foreign particles from between the lm layers.

One key difference between the ageing test and the breakdown measurements described in sections 3.1.1 and 3.2.1 is that instead of breakdown statistics, the objective of the ageing tests is to detect and quantify the changes in the film induced by prolonged exposure to moderate-low electro-thermal stresses. Such testing is called for because knowing how a dielectric material ages is fundamental before it can be considered suitable for use in high reliability applications. The ageing test is preceded and followed by extensive material characterization, and the stress levels used should be selected in a way that the films are not severely degraded. Results published in [P4, P5] suggest that especially large-area breakdown measurements should be included in the material characterization. A typical test capacitor has an active area of several hundred cm^2, the number of test capacitors made of each type of film can be selected in a way that even after few isolated breakdowns at least four intact 110 mm × 110 mm samples could be prepared afterwards for large-area multiple breakdown tests.

3.4 Using Dielectric Measurements to Steer Film Development

In this last section, an approach to applying the methods presented earlier in Chapter 3 to the research & development of capacitor dielectric films is proposed. An overview of this approach is presented in Figure 3.17. This section focuses on this testing scheme and not on the implementations of individual tests, as these were discussed earlier in this chapter. Nevertheless, some practical issues encountered during the thesis work are highlighted. For some measurements the lack of comprehensive guide is a recognized issue but providing such is not within the scope of this thesis.

Capacitor films must exhibit several features to be suitable for the application, out of which adequate breakdown strength in the operating temperature range is a rather fundamental one [41]. As discussed in Section 3.1.1, the breakdown strength of BOPP decreases with temperature, thus to prevent immediate failure it is necessary to verify the breakdown strength at the maximum operating (or overload) temperature. This equals to a range of 60 °C to 85 °C for many applications[9, 10] extending up to 125 °C in some [162, 163] (e.g. automotive), plus the temperature rise caused by self-heating. To keep self-heating at acceptable levels and to prevent thermal runaway low DC conductivity and dielectric loss factor are required, both tend to increase with temperature and field and should therefore be measured at the maximum expected electro-thermal stress levels. These measurements may compliment each other, e.g. an unexpectedly high reduction in the DC breakdown strength at high temperature may be explained by abnormally high DC conductivity. Compared to typical laboratory setups heat dissipation in real capacitors is more constricted and the overall thermodynamics are different, thus a high breakdown strength in a laboratory test does not guarantee adequate performance of capacitors. If heat is be easily dissipated from the film to a thermally well-conductive surrounding media (e.g. oil or metal), even a lossy (under AC) or conductive (under DC) material might exhibit a decent breakdown strength. To verify this is not affecting the results breakdown measurements should be paired with DC conductivity and dielectric loss measurements.

The required absolute values depend on the target application, knowing it is thus especially beneficial when valuing the individual qualities. Films intended for DC applications where the design fields are typically high should have excellent DC resistivity and breakdown strength. Films for AC applications should on the other hand display low dielectric loss factor, especially if used with foil electrodes.

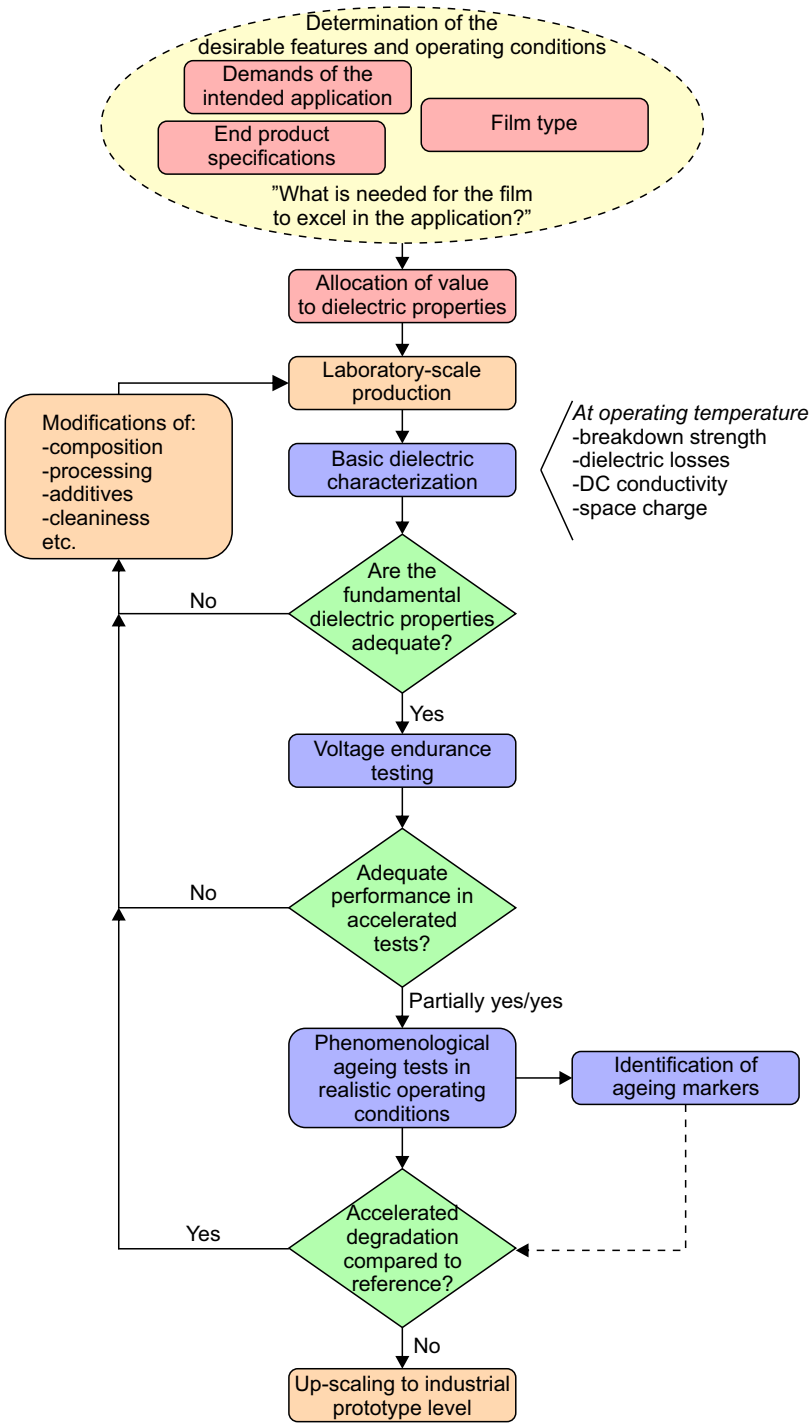

Figure 3.17: Measurement program for laboratory-scale development of capacitor films. Features needed for a film to excel in its application are defined first.

With clean DC capacitors would not be required, thus even "DC capacitors" are subjected to, and must perform well under AC voltage and current ripple. This ripple causes self-heating and is one major design factor. The waveform and intensity of the ripple depend on the application, examples can be found in e.g. [9]. Without prior specification of the intended application, as might be the case in basic research it is helpful to compare the film performance to existing and commercial BOPP films of similar type. Smooth films should not be compared with hazy films since the intended insulation systems are drastically different. The comparative approach described here is of course applicable to any of the longer measurements described later.

In addition to comparing the prototype films to commercial products, it is advisable to produce reference materials of known good composition. For example in a study of nanoadditives [P4], (among other things), PP with only the usual additive package was also produced, and the experimental films were compared against it. Unless comparison between different equipment is the research aim, these references should be produced with similar equipment than the prototype materials. By evaluating the performance of these references against "known good" commercial references, film processing can be optimized until similar (or better) film properties are achieved. The electrical performance of BOPP film is heavily dependent on the film processing [3], and several iterations of optimization may be required. Additionally, the cleanliness of the compounds can be studied and improved if needed. If the film processing and cleanliness are not optimized before commencing with actual test trials using "new technologies", there is a substantial risk that any improvements achieved are masked behind defects caused by improper processing. It is worth emphasizing that case-specific fine-tuning of the film processing might be needed to reach optimal performance. That is, because the processing parameters optimal for "traditional BOPP" might not yield the best achievable performance in films of experimental nature. One such case is reported in [P4]: the DC breakdown strength of two experimental compounds was abnormally low, and this was traced to excessive melting during orientation. These compounds had lower melting points, and orienting them at a 4 °C lower temperature solved the problem.

When a development stage film demonstrates high breakdown strength at maximum expected overload temperatures and has low dielectric losses and DC conductivity at maximum operating temperature and field, it has "passed" the short-term testing phase. Testing should then continue to the verification of voltage endurance. Since endurance and ageing testing is time- and resource consuming compared

to short-term characterization, it should be attempted only after the short-term dielectric properties at operating conditions are at the required level.

Space charge measurement falls somewhere between short- and long-term measurements. Their capability of predicting long-term reliability using a relatively short measurement makes them extremely lucrative, albeit only for DC. Its two challenges are the lack of equipment with a sub-micrometer resolution to visualize internal charge in $\lessapprox 10\,\mu m$ capacitor films, and that the measurement area is small, in the range of one square centimeter. The lack of commercial high-resolution space charge measurement equipment necessitates custom-built, highly experimental devices, and the miniscule measurement areas may limit their usefulness in measuring localized degradation that is prominent of BOPP films, as was presented in Section 3.3. There is still work to be done both in the metrology and the analysis of the results, but preliminary results in this thesis hint that space charge behavior in thin film may correlate with space charge properties of thick cast films that are easily measured using readily available equipment. However, this claim needs to be explored further and this approach is of course unsuitable for evaluating ageing phenomena in capacitor films. If suitable equipment for thin film measurement is available, it should be employed early and often, and material development should be steered toward films which display less space charge in operating conditions, as this may correlate with better voltage endurance.

Voltage endurance testing is advocated to be done using the methodology described in Section 3.2.1 and general principles stated in IEC 61251 [134]. It is done to determine the electric field – insulation life relationship, which is required since good breakdown strength may not correlate with good long-term properties [1]. First hints of voltage endurance may already have been seen if progressive stress breakdown strength tests had been done using multiple ramp rates but also in DC conduction and space charge measurements. The DC conductivity of a material can be determined only after the charging current is small compared to the leakage current [111], and reaching this stable state may take hours with highly resistive materials such as BOPP. This corresponds to DC excitation of at least several hours under temperature and a film with poor voltage endurance may break down already during this period. In progressive stress breakdown tests at multiple ramp rates, the breakdown strength of a film with poor voltage endurance decreases relatively more in slow rate-of-rise measurements. However, the possibility of oxidative degradation in all measurement longer than a few minutes should be evaluated thoroughly. Even in the absence of oxidation the long-term behavior may not be predictable from these

these measurements, especially if done using electrode configuration significantly different from the intended final application or above design fields, at high fields where high field degradation may occur. Indeed, it was shown in Section 3.2.1 that the life at realistic operating conditions was not extrapolatable from high-field data.

Going for lower fields necessitates longer measurement times, but this necessitates inert measuring conditions to inhibit oxidative degradation. The importance of a representative and PD-free electrode arrangement is also emphasized. The onset time of oxidative degradation depends on the antioxidants [164, 165], and thus should be determined individually for each material. Alternative and simple approach is to conduct all tests longer than a few minutes in inert conditions. With reducing stress levels one is expected to pass from a high-field region of hazard rate increasing with time to a region where hazard rate decreases at first. This corresponds to the initial clearing of electrical weak points. After the weak points are cleared, the hazard rate should remain constant, and any breakdowns are isolated random failures. After some time, the failure rate begins to increase again signifying the end of life. [P7]. The latter is the third part of the well-known bathtub curve of reliability. Thus under moderate stresses it is expected that after the initial clearing of electrically weak points nothing major happens for a long time, decades even. Recognizing the onset of the end is necessary as after it breakdowns occur at increasing rate. Voltage endurance testing should be done until the following quantities have been determined:

- the threshold stresses for Weibull hazard rate to begin decreasing with time, reaching a constant value and remaining there long enough to be determined
- the time of constant failure rate as a function of stress, this is the insulation life.

By measuring this insulation life as the function of electric field and temperature one can eventually gather a large enough dataset to reliably evaluate the life at operating conditions, and long before that comparison with existing commercial products is feasible. Nevertheless, the determination of an adequate voltage endurance is a demanding task requiring extensive up-scaling up to component and system level.

Voltage endurance testing yields statistical information but is time-consuming and does not necessarily shed light in the ageing phenomena. Thus when the voltage endurance is deemed "promising", phenomenological electro-thermal ageing testing of 1000 h or more should be initiated. This test must be done in inert conditions to inhibit oxidation. In all possible aspects the ageing environment should represent the application, if known, otherwise a general guideline is to age smooth

and metallized film in an inert atmosphere, in a liquid that does not react with or swell the metallized film or encapsulated in a suitable solid resin. Nitrogen, purified and degassed vegetable oil and polyurethane are some valid options. Hazy film should be aged in an impregnating liquid intended for film/foil capacitors (Jarylec / SAS-60E for example). These oils, but also general mineral and "transformer oil" react with and swell the PP. Metallized BOPP film electrodes cannot be used as the physical deformation causes the metal to flake off. Aluminum foil can be used and has the benefit of being representative of the application but is not self-healing. If self-healing functionality is desired, the foil can be substituted with a non-swelling metallized film such as polyester.

The choice between ageing under DC, AC and arbitrary waveforms should be based on the intended application. Films for DC capacitors should be aged either under DC for a purely phenomenological approach that is relatively simple to analyze or under DC with AC ripple for a more applied study of performance in an real application. Similarly films for AC capacitors should be aged under pure AC or AC with harmonics. If the R&D goal is a capacitor for a specific application with extraordinary stresses, those shall be determined by simulation or measurement and used in ageing. In this thesis only pure DC ageing was considered, but the methodology presented in Section 3.3 is regarded suitable also for ageing under DC with AC ripple. Whenever AC is involved, the PDIV should be determined and any longer tests should be conducted below it for ageing phenomena to remain representative of real application. However, the system is unsuitable for AC ageing as it relies on the electrostatic compressive force in keeping the electrodes attached to the film. AC ageing stress would require means to apply external force, such as a mechanical press or a spring arrangement. In a planar geometry it might be challenging to apply the pressure evenly. Directly metallized electrodes as was done in [P3] is another plausible approach.

The effects of ageing can be analyzed and prominent ageing phenomena can be identified by measuring changes in physical and electrical material properties before and after ageing. This was done in [P4, P5]. Even better would be to remove and characterize some material at specific intervals (e.g. every 200 h), by doing so non-linear behavior and annealing effects can be detected. For example some property may improve first due to secondary crystallization and then begin to decrease due to progressive degradation. It was shown in this thesis that DC large-area breakdown strength is a sensitive indicator of the DC electro-thermal ageing of BOPP and also BOPP-based nanocomposite films. Ageing causes electrically weak points to

appear and large measurement areas are needed to detect them. Thus testing of aged samples should at minimum include large-area breakdown strength tests, but a much wider set of characterization is preferred since the ageing phenomena and the best methods may depend on the nature of the material studied. Another promising approach might be to determine also the mechanical characteristics, as they may enable fitting recently published physics-based ageing model by Montanari et. al. [166, 167]. Fitting the ageing system with a times-to-breakdown recording device is advocated as then it can double as the one long 1000 h endurance test recommended by the relevant IEC standard 61251.

A film can be considered as a success if after ageing under realistic operating stresses its electrical properties remain adequate and nothing indicates progressive degradation more severe than the in similar commercial and/or reference films. At this point production should be up-scaled and testing can continue with wound capacitors. Final reliability evaluation is done using real capacitors and according to the relevant standards.

Chapter 4

Conclusions and Contributions

4.1 Main Conclusions, Scientific Contributions, and Future Work

The thesis objective of a test approach for dielectric measurements on laboratory-scale capacitor films was attained by implementing the required key measurements and advancing the current state of the art where needed. These were large-area high temperature breakdown measurement, voltage endurance test, long-term ageing test, and space charge and complex permittivity measurement. These methods and example results of their usefulness were the topic of Chapter 3. The contributions of this thesis to the breakdown strength metrology are the application of the large-area multi-breakdown methodology from [2] to measurements at elevated temperature and to AC voltages. It was shown that progressive stress tests with a duration of tens of minutes can be done in air, and that when immersed in oil and free of partial discharges, the DC and AC peak short-term breakdown strength of a commercial BOPP film is the same. It was also demonstrated that with commercial capacitor-grade BOPP films a decrease in the large-area breakdown strength of as little as ≈11 % between room temperature and 100 °C is achievable. The relative decrease of 11–20 % is comparable to the reduction of small-area breakdown strength presented in literature, e.g. [66], this builds confidence in the large-area multiple breakdown measurement approach. Results suggesting that the relative decrease correlates with long-term voltage endurance were presented, but further work is needed to confirm this connection. The similarity of DC and AC breakdown strengths is a recognized phenomenon [114], but given the high surface/volume ratio of thin films it would be interesting to verify the effect of heat dissipation to surrounding oil. The high

temperature, large-area multiple breakdown measurement is now used by the High Voltage Engineering research group of TUT for its advantages of expediting routine measurements and being closer to real operating conditions than room temperature measurements. High temperature measurement capabilities also continue to attract the industry working to answer the increasing demand for films suitable for high temperature capacitors.

The thesis objective of developing a repeatable method to prepare capacitor films for the measurement of dielectric permittivity was achieved by identifying the metallization process as the key factor. Electron beam "E-beam" evaporation in high vacuum was identified as the recommended method to fabricate metal electrodes, and it was established that with an optimized metallization procedure no additional sample treatments (prewashing, pre-drying, annealing, etc.) are needed to ensure realistic complex permittivity results in the broad frequency range of 10^1 Hz to 10^5 Hz. Capacitor films are thin ($\approx$10 µm) and have very low dielectric losses, the research challenge was that various methods suitable for thick (millimeter-scale) samples were unsatisfactory as the samples prepared accordingly yielded incorrect results in permittivity measurements. E-beam evaporation is featured in literature, e.g. in [16], but arguably less often than sputter deposition, e.g. [113] which was deemed unsuitable for low loss thin films. The redundancy of post-metallization annealing conflicts with literature [16], but this is interpreted as a result from the use of different equipment and process parameters. In order to avoid damaging samples the degree of freedom in the process the samples appears to be quite narrow, as our experiments with a different E-beam evaporator yielded slightly, but noticeably higher losses.

Nevertheless, knowledge of one reproducible and reliable method to fabricate electrodes on capacitor films is a contribution to the field of fundamental dielectric metrology and supports our research group (and others) by enabling the measurement of dielectric permittivity and DC conductivity. Notable example of the potential of dielectric permittivity measurements was the verification of negligible water absorption in biaxially oriented hydrophobic silica – PP nanocomposite films. The availability of a sample preparation method also led to the rapid implementation of thermally stimulated depolarization current (TSDC) measurement system within the research group. The results from these measurements are presented in [146] and in [P8] along with a discussion about the relationship between the charge trap structure and behavior under DC electric field. There is still work to be done in this field to identify the remaining key factors responsible for increased dielectric losses in samples with sputtered electrodes or evaporated using a different device.

A prominent part and contribution of this thesis was the development of a large-area multi-breakdown constant stress measurement system and associated data analysis tools. The major advantage of this approach over traditional single-breakdown tests is that it greatly expedites the acquisition of a statistically significant number of data points from a times-to-breakdown test that exhibits a high inherent scatter compared with progressive stress breakdown tests. So far this system has been used to prove that life at operating conditions is not extrapolatable from high-field measurements done in air. While this is a valuable piece of information, the system has the appreciably greater potential to determine the insulation life as a function of stress and enable optimized design using new materials. The required measurements at lower fields would require a vacuum oven necessary to attain inert test conditions rapidly. Oxidation must be inhibited for the test conditions to be representative of high performance, state of the art capacitors.

Work was also done to enable space charge measurements on biaxially oriented thin ($\lessapprox 20\,\mu m$) films and preliminary results from total charge measurements were presented. The results suggest that nanostructuration inhibits space charge accumulation and expedites charge dissipation both in polypropylene-based thin and non-oriented thick cast films. Space charge phenomena in thin films are recognized as one of the topics where significant research efforts are still needed before it can become well-established. These efforts should be motivated by promises of a measurement capable of predicting long-term properties using a fast measurement of a few hours maximum.

Developing methods to conduct DC electro-thermal ageing tests on capacitor films was one of the major objectives of this thesis. A suitable test setup was planned, fabricated and used to conduct 1000 h ageing tests. This setup enables the ageing phenomena of novel materials to be studied early in film development when only laboratory-produced biaxially oriented films are available. At this point standardized testing cannot be conducted due the unavailability of wound capacitors or capacitor elements. Early ageing studies are advisable as the long-term properties should determine the film performance in its application, and resources have been wasted if unfit long-term properties are detected only after film R&D has advanced to industrial pilot-scale production.

Identifying methods to measure the ageing of capacitor films was a major objective of this thesis. Large-area DC multi-breakdown strength measurement was identified as the preferred method because of its exceptional capability to detect the formation of electrically weak points that was in turn determined to be the

predominant result of ageing of both commercial and laboratory-scale BOPP films. This conclusion was reached by conducting two 1000 h DC electro-thermal ageing tests and by comparing the dielectric and physical properties of aged and pristine materials. The only significant change in the physical properties was an increase in the degree of crystallinity, that was interpreted as a thermally activated annealing effect and not true "ageing". Also the dielectric loss levels remained unchanged. This bulk of evidence supports the literature concept of localized degradation [25]: the majority of bulk material remains unaffected while aging progresses in a limited volume. Thus the physical measurements that measure the average of large volumes are inherently insensitive to detect the early stages of degradation, and changes are easily hidden under measurement inaccuracy. On the other hand electricity will find the weakest individual degraded regions in a large-area measurement. Nevertheless, an extensive material characterization is advocated in future ageing experiments on novel materials since the ageing phenomena may vary with film processing and composition.

4.2 Closing words

This thesis presents an approach for dielectric characterization, but to be suitable for capacitor winding a much wider set of film properties is needed. No development project should solely rely on dielectric measurements, no matter how broad. Indeed, during the last few years the TUT high voltage engineering research group has distinguished itself in physical characterization, with DSC measurements, profilometry and SEM imaging being done on a regular basis. Exploring the totality of required film properties was the objective of [P8], but only the dielectric measurements were included in this thesis to keep it concise. An observant reader has noticed that nothing was presented about the GRIDABLE materials, another decision to maintain focus. The first promising results were recently published in [152].

References

[1] W. Lei, L. A. Dissado, S. J. Dodd, N. M. Chalashkanov, J. C. Fothergill, Y. Cheng, and X. Zheng, "DC breakdown voltage tests may not be a good indicator of long-term ageing behaviour: A study of silica — XLPE nanocomposites," in *2017 International Symposium on Electrical Insulating Materials (ISEIM)*. IEEE, sep 2017, pp. 425–428.

[2] I. Rytöluoto, "Large-Area Multi-Breakdown Characterization of Polymer Films: A New Approach for Establishing Structure–Processing–Breakdown Relationships in Capacitor Dielectrics," Doctor of Science thesis, Tampere University of Technology, 2016. [Online]. Available: http://urn.fi/URN:ISBN:978-952-15-3663-2

[3] I. Rytöluoto, A. Gitsas, S. Pasanen, and K. Lahti, "Effect of film structure and morphology on the dielectric breakdown characteristics of cast and biaxially oriented polypropylene films," *European Polymer Journal*, vol. 95, no. September, pp. 606–624, oct 2017.

[4] M. Ritamäki, "Effects Of Thermal Aging On Polymer Thin Film Insulations For Capacitor Applications," Master of Science thesis, Tampere University of Technology, 2014. [Online]. Available: http://urn.fi/URN:NBN:fi:tty-201412011554

[5] G. Mazzanti, "Space charge measurements in high voltage DC extruded cables in IEEE Standard 1732," *IEEE Electrical Insulation Magazine*, vol. 33, no. 4, pp. 9–15, jul 2017.

[6] R. Bartnikas and R. Eichhorn, Eds., *Engineering Dielectrics Volume IIA Electrical Properties of Solid Insulating Materials: Molecular Structure and Electrical Behavior*. 100 Barr Harbor Drive, PO Box C700, West Conshohocken, PA 19428-2959: ASTM International, 1983.

[7] L. Hill, M. Maringer, and A. Barlow, "Possible Mechanism of Microvoid

Formation in Polyethlene Insulated High Voltage Cables," *IEEE Transactions on Power Apparatus and Systems*, vol. PAS-102, no. 7, pp. 1921–1926, jul 1983.

[8] S. Nawaz, P. Nordell, H. Hillborg, and U. Gedde, "Antioxidant activity in aluminium oxide – poly(ethylene-co-butyl acrylate) nanocomposites," *Polymer Degradation and Stability*, vol. 97, no. 6, pp. 1017–1025, jun 2012.

[9] EPCOS AG, "Film Capacitors for Industrial Applications," 2012. [Online]. Available: https://en.tdk.eu/download/173546/fc030f0de8e3c68b1d9fe2719d353130/film-capacitors-for-industrial-applications-pp.pdf

[10] EPCOS AG, "Power Factor Correction Power Quality Solutions," 2017. [Online]. Available: https://en.tdk.eu/download/174004/fb6fb19fae2445f847108cde7a10068d/pfc-katalog-pp.pdf

[11] A. Cavallini, D. Fabiani, and G. Montanari, "Power Electronics and Electrical Insulation Systems – Part 1: Phenomenology Overview," *IEEE Electrical Insulation Magazine*, vol. 26, no. 3, pp. 7–15, may 2010.

[12] ABB AB, "HVDC Light® It's time to connect," Ludvika, Sweden, 2013. [Online]. Available: http://new.abb.com/systems/hvdc/hvdc-light

[13] A. Hjert, "Multiscale Modelling of a Metallized Film Capacitor for HVDC Applications," Master's Thesis, Chalmers University of Technology, 2017. [Online]. Available: http://studentarbeten.chalmers.se/publication/251333-multiscale-modelling-of-a-metallized-film-capacitor-for-hvdc-applications

[14] N. Mohan, T. M. Underland, and W. P. Robbins, *Power Electronics: Converters, Applications, and Design, second edition.* John Wiley & Sons, Inc., 1995.

[15] ABB, "ABB review, Special Report High-voltage products," Tech. Rep., 2015. [Online]. Available: http://new.abb.com/high-voltage/capacitors/hv

[16] A. Kahouli, O. Gallot-Lavallée, P. Rain, O. Lesaint, C. Guillermin, and J.-M. Lupin, "Dielectric features of two grades of bi-oriented isotactic polypropylene," *Journal of Applied Polymer Science*, vol. 132, no. 28, jul 2015.

[17] J. Franciscus and B. Guido, "Polypropylene film structure," WO Patent Application WO2 016 174 034A1, 2015. [Online]. Available: https://patents.google.com/patent/WO2016174034A1

[18] P. Denifl, P. Jaaskelainen, T. Leinonen, B. Malm, A. E. Nymark, and T. Vestberg, "Process for the manufacture of a capacitor film," U.S. Patent Application US20 140 220 236A1, 2011. [Online]. Available: https://patents.google.com/patent/US20140220236A1/en

[19] M. Stadlbauer, E. Ernst, L. Huhtanen, Y. Daniels, and F. Jacobs, U.S. Patent.

[20] Borealis, "Polypropylene Borclean™ HC300BF product data sheet," Vienna, Austria, 2016. [Online]. Available: https://www.borealisgroup.com/product/borclean-hc300bf/data-sheets

[21] Borealis, "Polypropylene Borclean™ HB311BF product data sheet," Vienna, Austria, 2016. [Online]. Available: https://www.borealisgroup.com/product/borclean-hb311bf/

[22] J. L. Nash, "Biaxially oriented polypropylene film in power capacitors," *Polymer Engineering and Science*, vol. 28, no. 13, pp. 862–870, jul 1988.

[23] T. Umemura, T. Suzuki, and T. Kashiwazaki, "Impurity Effect of the Dielectric Properties of Isotactic Polypropylene," *IEEE Transactions on Electrical Insulation*, vol. EI-17, no. 4, pp. 300–305, aug 1982.

[24] A. Schneuwly, P. Groning, L. Schlapbach, C. Irrgang, and J. Vogt, "Breakdown behavior of oil-impregnated polypropylene as dielectric in film capacitors," *IEEE Transactions on Dielectrics and Electrical Insulation*, vol. 5, no. 6, pp. 862–868, 1998.

[25] G. W. Ehrenstein and S. Pongratz, *Resistance and Stability of Polymers*. München: Carl Hanser Verlag GmbH & Co. KG, oct 2013.

[26] D. Gloger and J. Paavilainen, "New way to produce polypropylene grade in a sequential process." WO Patent Application WO2 011 080 152A1, 2011. [Online]. Available: https://patents.google.com/patent/WO2011080152A1/

[27] J. Franciscus, "Polypropylene with specific calcium stearate content for special capacitors," WO Patent Application WO2 011 141 380A1, 2011. [Online]. Available: https://patents.google.com/patent/WO2011141380A1

[28] A. Gitsas, D. Gloger, F. Jacobs, H. Braun, and J. Wolfschwenger, "Polypropylene composition for capacitor film," WO Patent Application WO2 016 038 092A1, 2014. [Online]. Available: https://patents.google.com/patent/WO2016038092A1/

[29] D. Busch, T. Mohr, J. Fiebig, F. Jacobs, and Y. Daniels, "Biaxially oriented electrical insulating film," WO Patent Application WO2 008 025 796A1, 2006. [Online]. Available: https://patents.google.com/patent/WO2008025796A1/en

[30] J. Breil, *Film Processing Advances - Chapter 7 - Biaxial Oriented Film Technology*, T. Kanai and G. A. Campbell, Eds. München: Carl Hanser Verlag GmbH & Co. KG, jul 2014.

[31] Zongze Li, H. Uehara, R. Ramprasad, S. Boggs, and Yang Cao, "Pre-breakdown conduction in polymeric films," in *2015 IEEE Conference on Electrical Insulation and Dielectric Phenomena (CEIDP)*, vol. 2015-Decem. IEEE, oct 2015, pp. 872–875.

[32] S. Qin, J. Ho, M. Rabuffi, G. Borelli, and T. Jow, "Implications of the anisotropic thermal conductivity of capacitor windings," *IEEE Electrical Insulation Magazine*, vol. 27, no. 1, pp. 7–13, jan 2011.

[33] EPCOS AG, "Power capacitors for traction converters - on the fast track," Tech. Rep., 2011. [Online]. Available: https://en.tdk.eu/ , Accessed on: February 22, 2018.

[34] Treofan Group, "Treofan Press Release - Treofan wins European Plastics Innovation Award for ultra-thin film Developed jointly with Borealis, the film boosts capacitor efficiency by 30 percent," , Accessed on: February 23, 2018., 2016. [Online]. Available: https://www.treofan.com/en/news/2016/treofan-wins-european-plastics-innovation-award-for-ultra-thin-film.php

[35] Tervakoski Films Group, "Tervakoski Film ECT," Svit, Slovakia, Tech. Rep., 2016. [Online]. Available: http://tervakoskifilm.com/applications/downloads/

[36] Tervakoski Films Group, "Tervakoski Film TZC," Svit, Slovakia. [Online]. Available: http://tervakoskifilm.com/applications/downloads/

[37] Tervakoski Films Group, "Tervakoski film TBX," Svit, Slovakia. [Online]. Available: http://tervakoskifilm.com/applications/downloads/

[38] Tervakoski Films Group, "Tervakoski Film TSC," Svit, Slovakia. [Online]. Available: http://tervakoskifilm.com/applications/downloads/

[39] S. Boggs, J. Ho, and T. Jow, "Overview of laminar dielectric capacitors," *IEEE Electrical Insulation Magazine*, vol. 26, no. 2, pp. 7–13, mar 2010.

[40] D. Shaw, S. Cichanowski, and A. Yializis, "A Changing Capacitor Technology - Failure Mechanisms and Design Innovations," *IEEE Transactions on Electrical Insulation*, vol. EI-16, no. 5, pp. 399–413, oct 1981.

[41] T. D. Huan, S. Boggs, G. Teyssedre, C. Laurent, M. Cakmak, S. Kumar, and R. Ramprasad, "Advanced polymeric dielectrics for high energy density applications," *Progress in Materials Science*, vol. 83, pp. 236–269, oct 2016.

[42] Xiaoguang Qi and S. Boggs, "Analysis of the effects of end connection quality on the dielectric loss of metallized film capacitors," *IEEE Transactions on Dielectrics and Electrical Insulation*, vol. 11, no. 6, pp. 990–994, dec 2004.

[43] X. Qi and S. Boggs, "Electrothermal failure of metallized film capacitor end connections–computation of temperature rise at connection spots," *Journal of Applied Physics*, vol. 94, no. 7, pp. 4449–4456, oct 2003.

[44] Schneider Electric, "Reactive Energy Management, low voltage components, catalogue 2014," 2014. [Online]. Available: http://schneider-electric.com/

[45] R. P. Deshpande, *Capacitors*. McGraw-Hill Education, 2014.

[46] R. Gallay, "Metallized Film Capacitor Lifetime Evaluation and Failure Mode Analysis," CERN, Geneva, Tech. Rep., 2014.

[47] ABB AB, "DryDCap," Ludvika, Sweden, 2014. [Online]. Available: https://new.abb.com/high-voltage/capacitors/mv/capacitor-units/dc-dry-type-capacitors-drydcap

[48] V. O. Belko and O. A. Emelyanov, "Self-healing in segmented metallized film capacitors: Experimental and theoretical investigations for engineering design," *Journal of Applied Physics*, vol. 119, no. 2, p. 024509, jan 2016.

[49] Cigré Working Group D1.43, *Insulation Degradation Under Fast , Repetitive Voltage Pulses Insulation Degradation Under Fast , Repetitive Voltage Pulses*. Cigré, 2017.

[50] A. Cavallini, V. Krotov, G. C. Montanari, P. H. F. Morshuis, and L. E. Mariut, "The role of supply frequency in the evaluation of partial discharge inception voltage in XLPE-embedded cavities," in *2012 Annual Report Conference on Electrical Insulation and Dielectric Phenomena*, no. 1. IEEE, oct 2012, pp. 487–490.

[51] S. Qin and S. a. Boggs, "Limits to the performance and design of high voltage metalized film capacitors," *IEEE Transactions on Dielectrics and Electrical Insulation*, vol. 17, no. 4, pp. 1298–1306, aug 2010.

[52] D. Fabiani and G. Montanari, "The effect of voltage distortion on ageing acceleration of insulation systems under partial discharge activity," *IEEE Electrical Insulation Magazine*, vol. 17, no. 3, pp. 24–33, may 2001.

[53] A. Cavallini, D. Fabiani, and G. C. Montanari, "Power electronics and electrical insulation systems - Part 3: Diagnostic properties," *IEEE Electrical Insulation Magazine*, vol. 26, no. 5, pp. 30–40, sep 2010.

[54] R. Thomas, "Moisture, Myths, and Microcircuits," *IEEE Transactions on Parts, Hybrids, and Packaging*, vol. 12, no. 3, pp. 167–171, sep 1976.

[55] R. Brown, "Linking Corrosion and Catastrophic Failure in Low-Power

Metallized Polypropylene Capacitors," *IEEE Transactions on Device and Materials Reliability*, vol. 6, no. 2, pp. 326–333, jun 2006.

[56] TJ Green Associates LLC, "A Practical Guide to TM 1014 (Seal)," Tech. Rep., 2016. [Online]. Available: https://www.tjgreenllc.com/2016/09/29/a-practical-guide-to-tm-1014-seal/

[57] P. Cygan, B. Krishnakumar, and J. Laghari, "Lifetimes of polypropylene films under combined high electric fields and thermal stresses," *IEEE Transactions on Electrical Insulation*, vol. 24, no. 4, pp. 619–625, 1989.

[58] V. Belko, D. Glivenko, O. Emelyanov, I. Ivanov, and A. Plotnikov, "Current Pulse Polarity Effect on Metallized Film Capacitors Failure," *IEEE Transactions on Plasma Science*, vol. 45, no. 6, pp. 1020–1025, jun 2017.

[59] ARKEMA, "JARYLEC® Dielectric Liquid For High Voltage Electrical Equipments." [Online]. Available: http://www.arkema.com/en/products/product-finder/range-viewer/Jarylec-dielectric-fluids/3/

[60] C. Guillermin and S. Fontana, "Breakdown strength of impregnated capacitor elements," in *2016 IEEE International Conference on Dielectrics (ICD)*. Montpellier: IEEE, jul 2016, pp. 634–637.

[61] A. T. Vu Thi, "Propriétés diélectriques de matériaux isolants sous contraintes impulsionelle répétitive. Application aux modules de commutation en électronique de puissance," Ph.D. dissertation, Université Joseph Fourier Grenoble I, 2011. [Online]. Available: www.theses.fr/2011GRENT042.pdf

[62] DuPont Teijin Films, "Innovative Polyester Films Capacitors," 2014. [Online]. Available: http://europe.dupontteijinfilms.com/markets-applications/capacitors/

[63] Tervakoski Films, "Tervakoski Films RERT," 2016. [Online]. Available: http://tervakoskifilm.com/applications/downloads/

[64] Tervakoski Films, "Tervakoski Film RERS," 2008.

[65] Shin-Etsu Film, "Polypropylene Capacitor Film - Shin-Etsu PP Films," Tokyo, 2016. [Online]. Available: http://www.shinetsu-film.co.jp/e/products/

[66] J. Ho and T. R. Jow, "High field conduction in biaxially oriented polypropylene at elevated temperature," *IEEE Transactions on Dielectrics and Electrical Insulation*, vol. 19, no. 3, pp. 990–995, jun 2012.

[67] L. A. Dissado and J. C. Fothergill, *Electrical Degradation and Breakdown in Polymers*. The Institution of Engineering and Technology, Michael Faraday

House, Six Hills Way, Stevenage SG1 2AY, UK: IET, jan 1992.

[68] G. Chen, J. Zhao, S. Li, and L. Zhong, "Origin of thickness dependent dc electrical breakdown in dielectrics," *Applied Physics Letters*, vol. 100, no. 22, p. 222904, may 2012.

[69] S. Diaham, M. Bechara, M.-L. Locatelli, R. Khazaka, C. Tenailleau, and R. Kumar, "Dielectric strength of parylene HT," *Journal of Applied Physics*, vol. 115, no. 5, p. 054102, feb 2014.

[70] W. Hauschild and W. Mosch, *Statistical Techniques for High-Voltage Engineering*. The Institution of Engineering and Technology, Michael Faraday House, Six Hills Way, Stevenage SG1 2AY, UK: IET, jan 1992.

[71] J. K. Nelson, *Dielectric Polymer Nanocomposites*, J. K. Nelson, Ed. Boston, MA: Springer US, 2010.

[72] S. K. Kumar, B. C. Benicewicz, R. A. Vaia, and K. I. Winey, "50th Anniversary Perspective : Are Polymer Nanocomposites Practical for Applications?" *Macromolecules*, vol. 50, no. 3, pp. 714–731, feb 2017.

[73] K. Y. Lau, A. S. Vaughan, and G. Chen, "Nanodielectrics: opportunities and challenges," *IEEE Electrical Insulation Magazine*, vol. 31, no. 4, pp. 45–54, jul 2015.

[74] T. Ozaki, T. Imai, F. Sawa, T. Shimizu, and F. Kanemitsu, "Partial discharge resistant enameled wire," in *Proceedings of 2005 International Symposium on Electrical Insulating Materials, 2005. (ISEIM 2005).* IEEE, 2005, pp. 184–187 Vol. 1.

[75] H. Kikuchi and H. Hanawa, "Inverter surge resistant enameled wire with nanocomposite insulating material," *IEEE Transactions on Dielectrics and Electrical Insulation*, vol. 19, no. 1, pp. 99–106, feb 2012.

[76] G. Alexis and L. Schosseler, "Plastic film having a high voltage breakdown," U.S. Patent Application US8 804 308B2, 2008. [Online]. Available: https://patents.google.com/patent/US20150221439A1/en

[77] S. Diaham, T. Lebey, M.-L. Locatelli, and F. Saysouk, "Electrically insulating composite material, method for producing such a material and use thereof as en electrical insulant," WO Patent Application WO2 015 004 115A1, 2014. [Online]. Available: https://patents.google.com/patent/WO2015004115A1/en

[78] S. Diaham, F. Saysouk, M.-L. Locatelli, and T. Lebey, "Huge improvements of electrical conduction and dielectric breakdown in polyimide/BN nanocomposites," *IEEE Transactions on Dielectrics and Electrical Insulation*,

vol. 23, no. 5, pp. 2795–2803, oct 2016.

[79] 胡忠胜, 华玲萍, and 吴良军, "Capacitor thin film with high performance," Chinese Patent Application CN106 543 656A, 2016. [Online]. Available: https://patents.google.com/patent/CN106543656A/en

[80] Y. Sun, S. A. Boggs, and R. Ramprasad, "The intrinsic electrical breakdown strength of insulators from first principles," *Applied Physics Letters*, vol. 101, no. 13, p. 132906, sep 2012.

[81] G. M. Treich, M. Tefferi, S. Nasreen, A. Mannodi-Kanakkithodi, Z. Li, R. Ramprasad, G. A. Sotzing, and Y. Cao, "A rational co-design approach to the creation of new dielectric polymers with high energy density," *IEEE Transactions on Dielectrics and Electrical Insulation*, vol. 24, no. 2, pp. 732–743, apr 2017.

[82] L. W. Nagel and D. O. Pederson, "SPICE (Simulation Program with Integrated Circuit Emphasis)," EECS Department, University of California, Berkeley, Tech. Rep. UCB/ERL M382, 1973.

[83] R. Brown, "Distributed Circuit Modeling of Multilayer Capacitor Parameters Related to the Metal Film Layer," *IEEE Transactions on Components and Packaging Technologies*, vol. 30, no. 4, pp. 764–773, dec 2007.

[84] Cigré Working group D1.24, "Polymer Nanocomposites - Fundamentals and possible applications to power sectors," Cigré, Tech. Rep., 2011.

[85] T. Hanley, R. Burford, R. Fleming, and K. Barber, "A general review of polymeric insulation for use in HVDC cables," *IEEE Electrical Insulation Magazine*, vol. 19, no. 1, pp. 13–24, jan 2003.

[86] M. Salah Khalil, "International research and development trends and problems of HVDC cables with polymeric insulation," *IEEE Electrical Insulation Magazine*, vol. 13, no. 6, pp. 35–47, nov 1997.

[87] C. W. Reed, "An assessment of material selection for high voltage DC extruded polymer cables," *IEEE Electrical Insulation Magazine*, vol. 33, no. 4, pp. 22–26, jul 2017.

[88] M. Roy, J. Nelson, R. MacCrone, L. Schadler, C. Reed, R. Keefe, and W. Zenger, "Polymer nanocomposite dielectrics - the role of the interface," *IEEE Transactions on Dielectrics and Electrical Insulation*, vol. 12, no. 4, pp. 629–643, aug 2005.

[89] T. Tanaka, A. Bulinski, J. Castellon, M. Frechette, S. Gubanski, J. Kindersberger, G. Montanari, M. Nagao, P. Morshuis, Y. Tanaka, S. Pelissou,

A. Vaughan, Y. Ohki, C. Reed, S. Sutton, and S. Han, "Dielectric properties of XLPE/Sio2 nanocomposites based on CIGRE WG D1.24 cooperative test results," *IEEE Transactions on Dielectrics and Electrical Insulation*, vol. 18, no. 5, pp. 1482–1517, oct 2011.

[90] Y. Murata and M. Kanaoka, "Development History of HVDC Extruded Cable with Nanocomposite Material," in *2006 IEEE 8th International Conference on Properties and applications of Dielectric Materials*. IEEE, jun 2006, pp. 460–463.

[91] G. Montanari, "Bringing an insulation to failure: the role of space charge," *IEEE Transactions on Dielectrics and Electrical Insulation*, vol. 18, no. 2, pp. 339–364, apr 2011.

[92] G. C. Montanari, "Notes on theoretical and practical aspects of polymeric insulation aging," *IEEE Electrical Insulation Magazine*, vol. 29, no. 4, pp. 34–44, 2013.

[93] D. Fabiani, G. Montanari, C. Laurent, G. Teyssedre, P. Morshuis, R. Bodega, L. Dissado, A. Campus, and U. Nilsson, "Polymeric HVDC Cable Design and Space Charge Accumulation. Part 1: Insulation/Semicon Interface," *IEEE Electrical Insulation Magazine*, vol. 23, no. 6, pp. 11–19, nov 2007.

[94] S. Maruyama, N. Ishii, M. Shimada, S. Kojima, H. Tanaka, M. Asano, T. Yamanaka, and S. Kawakami, "Development of a 500-kV DC XLPE cable system," *Furukawa Review*, no. 25, pp. 47–52, 2004.

[95] "GRID Innovation Online Technology Database," Accessed on: September 9, 2018. [Online]. Available: http://www.gridinnovation-on-line.eu/technology-database/

[96] G. Mazzanti and M. Marzinotto, Eds., *Extruded Cables For High-Voltage Direct-Current Transmission*. Hoboken, New Jersey: John Wiley & Sons, Inc., jul 2013.

[97] S. Boggs, "A rational consideration of space charge," *IEEE Electrical Insulation Magazine*, vol. 20, no. 4, pp. 22–27, jul 2004.

[98] P. Morshuis, G. C. Montanari, G. C. Stevens, A. S. Vaughan, and P. Seri, "Assessing the feasibility of insulation materials for UHVDC cable systems," in *2018 12th International Conference on the Properties and Applications of Dielectric Materials (ICPADM)*. IEEE, may 2018, pp. 389–392.

[99] B. Dang, J. He, J. Hu, and Y. Zhou, "Tailored sPP/Silica Nanocomposite for Ecofriendly Insulation of Extruded HVDC Cable," *Journal of Nanomaterials*,

vol. 2015, pp. 1–9, 2015.

[100] T. Tanaka, "Dielectric nanocomposites with insulating properties," *IEEE Transactions on Dielectrics and Electrical Insulation*, vol. 12, no. 5, pp. 914–928, oct 2005.

[101] G. Montanari, A. Cavallini, F. Guastavino, G. Coletti, R. Schifani, M. di Lorenzo del Casale, G. Camino, and F. Deorsola, "Microscopic and nanoscopic EVA composite investigation: electrical properties and effect of purification treatment," in *The 17th Annual Meeting of the IEEE Lasers and Electro-Optics Society, 2004. LEOS 2004.* IEEE, 2004, pp. 318–321.

[102] J. K. Nelson, W. Zenger, R. John Keefe, and L. S. S. Feist, "Nanostructured dielectric composite materials," U.S. Patent Grant US7 884 149B2, 2005. [Online]. Available: https://patents.google.com/patent/US7884149B2/en

[103] K. Yoon-Jin, N. Jin-Ho, C. Ho-Souk, P. Young-Ho, and H. Son Tung, "Dc power cable with space charge reducing effect," U.S. Patent Application US20 120 012 362A1, 2010. [Online]. Available: https://patents.google.com/patent/US20120012362A1/en

[104] 何金良, 胡军, 党斌, 周垚, 郭宝华, 曾嵘, and 余占清, "Method for preparing inhibiting space charge HVDC cable recyclable materials," Chinese Patent Application CN104 448 553B, 2014. [Online]. Available: https://patents.google.com/patent/CN104448553B/en

[105] 何金良, 胡军, 党斌, 周垚, 郭宝华, 曾嵘, and 余占清, "Preparation method of recyclable high-voltage direct-current cable material with space charge restraining capability," Chinese Patent Application CN106 009 253A, 2016. [Online]. Available: https://patents.google.com/patent/CN106009253A/en

[106] G. Perego, A. Bareggi, and B. Sergio, "Energy cable," WO Patent Application WO2 009 000 326A1, 2010. [Online]. Available: https://patents.google.com/patent/WO2009000326A1

[107] H. Ranta, "Long-term electrical properties of polypropylene nanocomposites for high voltage capacitor applications," Master of Science Thesis, Tampere University of Technology, 2008. [Online]. Available: http://urn.fi/URN:NBN:fi:tty-200910206973

[108] S. A. Boggs, B. Li, and S. Zhang, "Approach to measure in-plane thermal conductivity of thin polymer films," in *2017 IEEE Conference on Electrical Insulation and Dielectric Phenomenon (CEIDP).* IEEE, oct 2017, pp. 274–277.

[109] I. Rytöluoto, M. Ritamäki, K. Lahti, and M. Karttunen, "DC ramp rate effect

on the breakdown response of SiO2-BOPP nanocomposites," in *2015 IEEE 11th International Conference on the Properties and Applications of Dielectric Materials (ICPADM)*. Sydney, Australia: IEEE, jul 2015, pp. 496–499.

[110] EPCOS AG, "Film Capacitors General technical information," 2015. [Online]. Available: https://en.tdk.eu/download/530754/bb7f3c742f09af6f8ef473fd34f6000e/pdf-generaltechnicalinformation.pdf

[111] R. Bartnikas, Ed., *Engineering Dielectrics Volume IIB Electrical Properties of Solid Insulating Materials: Measurement Techniques*. 100 Barr Harbor Drive, PO Box C700, West Conshohocken, PA 19428-2959: ASTM International, jan 1987.

[112] S. Laihonen, U. Gafvert, T. Schutte, and U. Gedde, "DC breakdown strength of polypropylene films: area dependence and statistical behavior," *IEEE Transactions on Dielectrics and Electrical Insulation*, vol. 14, no. 2, pp. 275–286, apr 2007.

[113] J. Ho and R. Jow, "Characterization of High Temperature Polymer Thin Films for Power Conditioning Capacitors," Army Research Laboratory, Adelphi, MD 20783-1197, Tech. Rep., 2009.

[114] S. Chniba and R. Tobazeon, "Long term breakdown of polypropylene films," in *Proceedings of First International Conference on Conduction and Breakdown in Solid Dielectrics*. IEEE, jul 1983, pp. 433–438.

[115] W. Khachen and J. Laghari, "Polypropylene for high voltage high frequency airborne applications," in *IEEE International Symposium on Electrical Insulation*. IEEE, 1990, pp. 80–83.

[116] B. Sanden and E. Iidstad, "DC electrical and mechanical characterisation of polypropylene film," in *ICSD'98. Proceedings of the 1998 IEEE 6th International Conference on Conduction and Breakdown in Solid Dielectrics (Cat. No.98CH36132)*. IEEE, 1998, pp. 210–213.

[117] I. Rytöluoto, K. Lahti, M. Karttunen, and M. Koponen, "Large-area dielectric breakdown performance of polymer films – Part I: Measurement method evaluation and statistical considerations on area-dependence," *IEEE Transactions on Dielectrics and Electrical Insulation*, vol. 22, no. 2, pp. 689–700, apr 2015.

[118] R. M. Hill and L. A. Dissado, "Examination of the statistics of dielectric breakdown," *Journal of Physics C: Solid State Physics*, vol. 16, no. 22, pp. 4447–4468, aug 1983.

[119] S. J. Laihonen, "Polypropylene: Morphology, Defects and Electrical Breakdown," D. Sc. Thesis, Kungliga Tekniska Högskolan, 2005.

[120] A. Schneuwly, P. Gröning, L. Schlapbach, P. Brüesch, M. Carlen, and R. Gallay, "Temperature-dependent dielectric breakdown strength of oil impregnated polypropylene foils," *Materials Science and Engineering: B*, vol. 54, no. 3, pp. 182–188, jun 1998.

[121] F. Kremer and S. Andreas, *Broadband Dielectric Spectroscopy*, F. Kremer and A. Schönhals, Eds. Berlin, Heidelberg: Springer Berlin Heidelberg, 2003.

[122] A. K. Jonscher, "Dielectric relaxation in solids," *Journal of Physics D: Applied Physics*, vol. 32, no. 14, pp. R57–R70, jul 1999.

[123] "Novocontrol Technologies." [Online]. Available: https://www.novocontrol.de/php/index.php

[124] Keysight Technologies, "LCR Meters, Impedance Analyzers and Test Fixtures," 2017. [Online]. Available: http://literature.cdn.keysight.com/litweb/pdf/5952-1430E.pdf

[125] A. Schönhals, "Dielectric Spectroscopy on the Dynamics of Amorphous Polymeric Systems," Berlin, 1998. [Online]. Available: https://www.novocontrol.de/php/info_app_notes.php

[126] Keysight Technologies, "Impedance Measurement Handbook," 2016. [Online]. Available: http://literature.cdn.keysight.com/litweb/pdf/5950-3000.pdf

[127] R. Kriegler and R. Bartnikas, "Dielectric loss and current—Voltage measurements in sodium-contaminated Si—SiO 2 —Cr structures," *IEEE Transactions on Electron Devices*, vol. 20, no. 8, pp. 722–731, aug 1973.

[128] A. A. Tracton, Ed., *Coatings Technology Handbook*, 3rd ed. Boca Raton: CRC Press, 2005.

[129] B. Sanden and E. Ildstad, "DC conduction current and voltage endurance of polypropylene film," in *1998 Annual Report Conference on Electrical Insulation and Dielectric Phenomena (Cat. No.98CH36257)*, vol. 1. IEEE, 1998, pp. 304–307.

[130] A. Kahouli, O. Gallot-Lavallée, P. Rain, O. Lesaint, L. Heux, C. Guillermin, and J.-M. Lupin, "Structure effect of thin film polypropylene view by dielectric spectroscopy and X-ray diffraction: Application to dry type power capacitors," *Journal of Applied Polymer Science*, vol. 132, no. 39, oct 2015.

[131] Novocontrol Technologies GmbH & Co. KG, "Alpha-A Dielectric, Conductivity,

Impedance and Gain Phase Modular Measurement System Technical Specification Alpha-A Mainframe ZGS, ZG4 and ZG2 Test Interfaces," 2010. [Online]. Available: https://www.novocontrol.de/php/ana_alpha.php

[132] N. Riaz, "Dielectric characterization of bi-axially oriented polypropylene insulations," Master's thesis, Tampere University of Technology, 2016. [Online]. Available: https://dspace.cc.tut.fi/dpub/handle/123456789/24450

[133] I. L. Hosier, M. Praeger, A. F. Holt, A. S. Vaughan, and S. G. Swingler, "On the effect of functionalizer chain length and water content in polyethylene/silica nanocomposites: Part I — Dielectric properties and breakdown strength," *IEEE Transactions on Dielectrics and Electrical Insulation*, vol. 24, no. 3, pp. 1698–1707, jun 2017.

[134] "IEC 61251:2015 Electrical insulating materials and systems - AC voltage endurance evaluation Edition 1.0," p. 42, 2015.

[135] ReliaSoft Corporation, "Life Data Analysis Reference Book." [Online]. Available: http://reliawiki.org/

[136] A. Cavallini, D. Fabiani, and G. Montanari, "Power electronics and electrical insulation systems - Part 2: life modeling for insulation design," *IEEE Electrical Insulation Magazine*, vol. 26, no. 4, pp. 33–39, jul 2010.

[137] G. C. Montanari and M. Cacciari, "Progressively-Censored Aging Tests on XLPE-Insulated Cable Models," *IEEE Transactions on Electrical Insulation*, vol. 23, no. 3, pp. 365–372, 1988.

[138] G. Montanari, J. Ghinello, F. Peruzzotti, and M. Albertini, "Endurance characteristics of XLPE compounds under DC voltage," in *ICSD'98. Proceedings of the 1998 IEEE 6th International Conference on Conduction and Breakdown in Solid Dielectrics (Cat. No.98CH36132)*. IEEE, 1997, pp. 439–442.

[139] Y. Wang, Z. Lv, X. Wang, K. Wu, C. Zhang, W. Li, and L. A. Dissado, "Estimating the inverse power law aging exponent for the DC aging of XLPE and its nanocomposites at different temperatures," *IEEE Transactions on Dielectrics and Electrical Insulation*, vol. 23, no. 6, pp. 3504–3513, dec 2016.

[140] Y. Chen, H. Li, F. Lin, F. Lv, M. Zhang, Z. Li, and D. Liu, "Study on Self-Healing and Lifetime Characteristics of Metallized-Film Capacitor Under High Electric Field," *IEEE Transactions on Plasma Science*, vol. 40, no. 8, pp. 2014–2019, aug 2012.

[141] S. Boggs, "Very high field phenomena in dielectrics," *IEEE Transactions on*

Dielectrics and Electrical Insulation, vol. 12, no. 5, pp. 929–938, oct 2005.

[142] J. Ho, R. Ramprasad, and S. Boggs, "Effect of Alteration of Antioxidant by UV Treatment on the Dielectric Strength of BOPP Capacitor Film," *IEEE Transactions on Dielectrics and Electrical Insulation*, vol. 14, no. 5, pp. 1295–1301, oct 2007.

[143] A. Gadoum, B. Gosse, and J. Gosse, "AC Aging of Impregnated Polypropylene Films: Effect of Oxygen," in *Proceedings of 1993 IEEE 11th International Conference on Conduction and Breakdown in Dielectric Liquids (ICDL '93)*. IEEE, 1993, pp. 461–466.

[144] ReliaSoft Corporation, "Accelerated Life Testing Data Analysis Reference," 2014. [Online]. Available: http://reliawiki.org/

[145] Chunchuan Xu and S. Boggs, "Measurement of Resistive and Absorption Currents in Capacitor Films up to Breakdown," in *Conference Record of the 2006 IEEE International Symposium on Electrical Insulation.* IEEE, 2006, pp. 249–252.

[146] I. Rytoluoto, M. Ritamaki, and K. Lahti, "Short-term dielectric performance assessment of BOPP capacitor films: A baseline study," in *2018 12th International Conference on the Properties and Applications of Dielectric Materials (ICPADM).* IEEE, may 2018, pp. 289–292.

[147] H. Ghorbani, T. Christen, M. Carlen, E. Logakis, L. Herrmann, H. Hillborg, L. Petersson, and J. Viertel, "Long-term conductivity decrease of polyethylene and polypropylene insulation materials," *IEEE Transactions on Dielectrics and Electrical Insulation*, vol. 24, no. 3, pp. 1485–1493, jun 2017.

[148] Y. Tanaka, "Recent various space charge measurements using PEA method," Workshop of the 2018 12th International Conference on the Properties and Applications of Dielectric Materials (ICPADM): Space Charge and Degradation Research of Dielectric Materials in HV Power Cable, Xi'an China, 2018.

[149] Cigré Task Force D1.12.01, "Space charge measurement in dielectrics and insulating materials," p. 51, 2006.

[150] TECHIMP, "Space Charge Measuring Equipment - PEA," 2018. [Online]. Available: http://www.techimp.com/products/laboratory-equipment/item/82-pea-cable-cell.html

[151] K. Kumaoka, T. Kato, H. Miyake, and Y. Tanaka, "Development of space charge measurement system with high positionalal resolution using pulsed electro acoustic method," in *Proceedings of 2014 International Symposium on*

Electrical Insulating Materials. IEEE, jun 2014, pp. 389–392.

[152] I. Rytöluoto, M. Ritamäki, K. Lahti, M. Paajanen, M. Karttunen, G. C. Montanari, P. Seri, and H. Naderiallaf, "Compounding, Structure and Dielectric Properties of Silica-BOPP Nanocomposite Films," in *2018 IEEE International Conference on Dielectrics (ICD)*, 2018.

[153] J. C. Fothergill, "Ageing, Space Charge and Nanodielectrics: Ten Things We Don't Know About Dielectrics," in *2007 IEEE International Conference on Solid Dielectrics*. Winchester: IEEE, jul 2007, pp. 1–10.

[154] E. Sebillotte, S. Theoleyre, S. Said, B. Gosse, and J. Gosse, "Ac Degradation of Impregnated Polypropylene Films," *IEEE Transactions on Electrical Insulation*, vol. 27, no. 3, pp. 557–565, jun 1992.

[155] T. Lewis, "Ageing—A Perspective," *IEEE Electrical Insulation Magazine*, vol. 17, no. 4, pp. 6–16, jul 2001.

[156] T. Umemura and K. Akiyama, "Accelerated-Life Testing of Power Capacitor Dielectric Systems," *IEEE Transactions on Electrical Insulation*, vol. EI-22, no. 3, pp. 309–316, jun 1987.

[157] Y. Yoshida and M. Nishimatsu, "Power Capacitors," *IEEE Transactions on Electrical Insulation*, vol. EI-21, no. 6, pp. 963–973, dec 1986.

[158] T. Umemura, K. Abe, K. Akiyama, and D. Couderc, "Thermal-Aging Behavior of Bo-Pp Films," *IEEE Transactions on Electrical Insulation*, vol. EI-22, no. 6, pp. 735–743, dec 1987.

[159] M. Ratra, H. Nagamani, and S. Ganga, "Ageing of impregnated polypropylene film for capacitor application under combined electrical and thermal stress," in *Annual Conference on Electrical Insulation and Dielectric Phenomena*. IEEE, 1990, pp. 295–300.

[160] Tervakoski Films Group White Paper, "Tervakoski Film ECT - Superior BOPP Capacitor Base Film For Dry AC/DC Capacitors," Tervakoski Films Group, Tech. Rep., 2017. [Online]. Available: http://tervakoskifilm.com/blog/tervakoski-film-ect-vs-ec/

[161] I. Rytöluoto and K. Lahti, "Effect of inter-layer pressure on dielectric breakdown characteristics of metallized polymer films for capacitor applications," in *2013 IEEE International Conference on Solid Dielectrics (ICSD)*. Bologna: IEEE, jun 2013, pp. 682–687.

[162] KEMET Electronics Corporation, "Polypropylene Pulse/High Frequency Capacitors R74 125°C Single Metallized Polypropylene Film, Radial, AC

Applications (Automotive Grade)," Greenville, 2017. [Online]. Available: http://www.kemet.com/Film_Capacitors

[163] EPCOS AG, "Metallized Polypropylene Film Capacitors (MKP), Series/Type: B32774P ... B32778P," 2017. [Online]. Available: https://www.tdk-electronics.tdk.com

[164] G. Zhang, C. Nam, T. C. M. Chung, L. Petersson, and H. Hillborg, "Polypropylene Copolymer Containing Cross-Linkable Antioxidant Moieties with Long-Term Stability under Elevated Temperature Conditions," *Macromolecules*, vol. 50, no. 18, pp. 7041–7051, sep 2017.

[165] G. Zhang, C. Nam, L. Petersson, J. Jämbeck, H. Hillborg, and T. C. M. Chung, "Increasing Polypropylene High Temperature Stability by Blending Polypropylene-Bonded Hindered Phenol Antioxidant," *Macromolecules*, p. acs.macromol.7b02720, feb 2018.

[166] G. C. Montanari and P. Seri, "Life models under DC field," Workshop of the 2018 12th International Conference on the Properties and Applications of Dielectric Materials (ICPADM): Space Charge and Degradation Research of Dielectric Materials in HV Power Cable, Xi'an China, 2018.

[167] G. C. Montanari, "A contribution to unravel the mysteries of electrical aging under DC electrical stress: where we are and where we would need to go," in *2018 IEEE 2nd International Conference on Dielectrics (ICD)*. Budapest, Hungary: IEEE, jul 2018, pp. 1–15.

Publications

Publication I

M. Ritamäki, I. Rytöluoto, K. Lahti, and M. Karttunen, "Effects of thermal aging on the characteristic breakdown behavior of Nano-SiO_2-BOPP and BOPP films," in *2015 IEEE 11th International Conference on the Properties and Applications of Dielectric Materials (ICPADM)*, pp. 400–403, 2015.

DOI: 10.1109/ICPADM.2015.7295293

Effects of Thermal Aging on the Characteristic Breakdown Behavior of Nano-SiO_2-BOPP and BOPP Films

M. Ritamäki, I. Rytöluoto, K. Lahti
Department of Electrical Engineering
Tampere University of Technology (TUT)
Tampere, Finland

M. Karttunen
Technical Research Centre of Finland (VTT)
Tampere, Finland

***Abstract*—The effects of thermal stress on the breakdown behavior of biaxially oriented polypropylene (BOPP)-silica nanocomposite thin film and commercial BOPP film was evaluated with a step stress experiment in the temperature range of 50…110 °C. Weak spots were measured in thermally aged un-filled BOPP films but not in the PP-silica, which in turn displayed increasing scatter of the breakdown voltages and the scattering seemingly settled to a certain level. No weak spots were measured in un-filled BOPP films removed after highest temperatures. The behavior of un-filled films is speculated to result from either actual polymer aging in addition to the statistical nature of breakdown phenomena or from thermally-activated processes possibly involving antioxidants. The different behavior in the nanocomposite was speculated to result from polymer-nanoparticle interactions possibly countering the effects of antioxidants and hindering weak spot formation. The results demonstrate the different behavior of polymer-nanocomposites and traditional BOPP films under thermal stress and highlight the importance of evaluating the aging behavior of new materials.**

Keywords—BOPP; silica; nanocomposite; breakdown; Weibull; aging; thermal stress

I. Introduction

Aging of capacitor dielectrics is influenced by thermal and electric stresses. Aging alters their dielectric properties, one of the most essential factors being the dielectric breakdown strength. [1] Thermoelectric aging of biaxially oriented capacitor-grade polypropylene films has been researched by Umemura et al. in [2], in which thermoelectric stress resulted in the formation of scarce weak points in the low probability region. These points diverted from the trend set by the large majority of breakdowns and simultaneously the "intrinsic" breakdown strength was measured to increase, for which unspecified morphological changes were proposed as an explanation. Thermal stresses has been shown to result in structural reorganization and selective degradation in the amorphous phase of BOPP films in [3], but their correspondence with the dielectric breakdown behavior is left uncertain.

Recently, dielectric polymer nanocomposites have been evaluated as means to develop next-generation capacitors with improved properties [4]. Short-term measurements on PP-silica nanocomposites demonstrate the possibility for advances such as increased dielectric breakdown strength and improved partial discharge resistance [5]. There is however a limited amount of information regarding their long-term properties, and given their properties are influenced by the polymer-nanoparticle interface spanning throughout the insulating medium [6], their aging behavior may be exceedingly different from traditional polymer materials.

In this paper a step stress experiment is described in which the effects of thermal aging on the characteristic breakdown behavior of un-filled BOPP films are compared with a polypropylene nanocomposite incorporating 4.5 wt-% of nano-silica. A large-area multi-breakdown measurement detailed in [7], [8] was utilized as means to detect changes in the breakdown distribution. Large measurement areas would allow measuring a statistically significant amount of breakdowns even from the low-probability regions.

II. Experimental

A. Material details

One SiO_2-BOPP nanocomposite, its reference and one commercial BOPP film were evaluated in the experiment. The SiO_2-BOPP was manufactured from unstabilized polypropylene HC318BF by compounding it with 4.5 wt-% of Aerosil R812 S hydrophobic fumed silica. Irganox 1010 (0.47 %) and Irgafos 168 (0.35 wt-%) were used as process stabilizers. The reference-BOPP film was the same with the exception of the added silica. Pilot-scale films were compounded at VTT Technical Research Centre of Finland and manufactured at Brückner pilot line in Denmark. The manufacturing and orientation processes and process parameters of the pilot-scale films has been reported in [9]. A capacitor-grade BOPP film made by Tervakoski Films Group was used as a commercial reference.

B. Aging setup

The aging was conducted in a test oven, in which 15 film sheets were fastened vertically using metal clips. The oven temperature was controlled with a Toho TTM-04SP PID controller operated in self-tuning mode, and after initial

978-1-4799-8903-4/15/$31.00 ©2015 IEEE

stabilization temperature fluctuations less than 0.1 °C and a temperature gradient in the range of +0…+3 °C from the set value were measured at 70 °C. In addition to natural convection a cross-flow fan was used to promote gas circulation, and to inhibit fluttering and film curling at higher temperatures metal clips were attached to the lower edges of the film. To limit the oxidative effects of ambient oxygen a constant flow estimated to be in the range of 10…100 ml/min of inert nitrogen was provided via a precision flow regulator into the otherwise gas tight ageing chamber.

The aging cycle consisted of seven 144-hour steps in ten degree increments from 50 °C to 110 °C. After each step the oven was opened and a portion of the test films was removed for sample preparation. Opening the oven resulted in the loss of the inert atmosphere, but given the maximum exposure duration of 1…2 hours and the rapid cooling as the heaters were disabled for this duration this was regarded as insignificant when compared to the 1008-hour duration of the test cycle. After each closure the oven was flooded with N_2 for 5…10 minutes with the flooding volume estimated to be in the range of 200…300 liters.

C. *Sample preparation and large-area multi-breakdown measurement*

Six 110×110 mm film samples of each film were prepared from portions removed after each temperature step. Both the reference-BOPP and SiO_2-BOPP films had thickness profile in transverse direction and their thicknesses were measured from 25 points inside a 100×100 mm square using a LE-1000-1 precision thickness gauge (accuracy of 0.1 μm). The measured thicknesses and standard deviations are presented in Table I. Additionally these pilot-scale films displayed a few presumably manufacturing-originated physical defects such as dents and scratches and the film samples were prepared from seemingly unaffected regions. Despite this the further visual examination revealed scratches in one ref-BOPP, one cap-BOPP and in two of the SiO_2-BOPP films removed after 50 °C and in one SiO_2-BOPP film removed after 60 °C. These films were used in the measurement, but as the first breakdowns occurred near or at the damaged areas the breakdowns were considered non-independent and the measurement data was excluded from further analysis.

A large-area multi-breakdown measurement described in [7], [8] was utilized to measure the breakdown behavior. A film stack was constructed starting with the film sample. The electrode arrangement consisted of two 90 mm wide metallized BOPP films (main metallization body resistivity 5-12 Ω/□), metallized side towards the sample, placed on each side of the film specimen. With a margin of 10 mm an active area of 81 cm^2 was realized. The outer layers of the stack consisted of two polyester films providing mechanical support. The film stack was attached to a test fixture and submerged in dielectric oil (Shell Diala Oil DX) in order to reduce partial discharges and surface flashovers. Loosely according to IEC-60243-1 slow rate-of-rise test [10] the measurement consisted of a fast voltage ramp-up at 400 V/s up to 4 kV followed by a slow ramp-up at 30 V/s. Breakdowns were measured during the slow ramp which was continued until no more discharges were measured or when the capture buffer limit of 500 breakdown events was reached. Applied voltage and circuit current were monitored real-time using a Tektronix P6015 high voltage probe and a 1.0330 Ω low inductance resistor. Discharge current and voltage waveforms were captured by a LeCroy HRO 66Zi oscilloscope set to trigger at the positive edge of the discharge current pulse.

TABLE I. FILM THICKNESSES AND STANDARD DEVIATIONS

Code	REF		50 °C		60 °C		70 °C	
	Mean	SD	Mean	SD	Mean	SD	Mean	SD
Cap-BOPP	14.46	0.57						
Ref-BOPP	16.24	1.68	16.27	2.16	15.59	1.86	15.03	0.94
SiO_2-BOPP	15.30	1.01	15.82	1.52	16.08	1.04	15.05	0.93
	80 °C		90 °C		100 °C		110 °C	
	Mean	SD	Mean	SD	Mean	SD	Mean	SD
Ref-BOPP	15.36	1.48	16.02	1.99	15.89	2.07	15.40	1.69
SiO_2-BOPP	15.32	1.21	15.44	1.15	15.78	1.08	15.69	0.89

In addition to independent self-healing breakdowns the recorded data included non-breakdown discharges such as surface flashovers and non-independent breakdown activity such as rapid self-healings and breakdowns influenced by previously cleared areas. Therefore a two-criterion breakdown qualification procedure detailed in [8] was carried out. Also to uniform the results any discharges beyond the initial 50 were omitted from further analysis.

Breakdown fields were calculated using the average thickness of the sample, for pilot-scale films the average of the 25 measurement points was used while for capacitor-grade BOPP the 14.4 μm thickness given by the manufacturer was used. The use of averaged thickness has been shown to result in small errors [8], but for the purpose of this research they were considered negligible. Additional 25-point thickness measurements were carried out on individual cap-BOPP film samples removed after 80 °C and beyond to evaluate possible shrinkage, but the average thicknesses were within the standard deviation of reference thickness measurements conducted on 30 unaged film samples.

D. *Analysis of the large-area multiple breakdown data*

Weibull statistical analysis was applied to the selected breakdown data which was fitted with two-parameter Weibull distributions to reach a visually and mathematically adequate fit. Loosely following IEC 62539 single distributions were preferred [11] but in case noticeable deviation from the calculated probability line was observed additively mixed two-subpopulation Weibull distributions were applied instead [12]. Given the nature of the multiple breakdown measurement unequal number of breakdowns was recorded for each step and material. The distribution parameters were calculated either with maximum likelihood estimation (MLE) or non-linear rank regression (NLRR) methods using Weibull++ 9 software.

III. RESULTS AND DISCUSSION

The amount of selected breakdowns and distribution parameters are presented in Table II. Distributions and data points from samples removed after 50 °C, 80° C and 110 °C together with the unaged reference are plotted in Fig. 1.

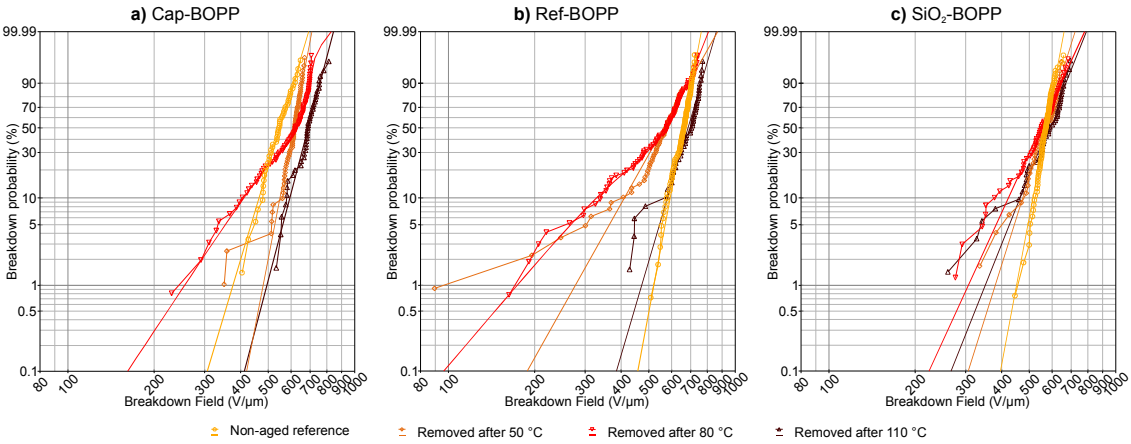

Fig. 1. Large-area multiple breakdown measurement results of **a)** Capacitor-grade BOPP film, **b)** Reference pilot-scale BOPP film, **c)** Pilot-scale silica-PP nanocomposite film on Weibull probability scale.

Considering the development of the measured dielectric breakdown behavior as a function of temperature and accumulated stress three distinct changes can identified:

- Low field breakdowns or "weak spots" were measured in cap-BOPP film after 70 °C and in reference BOPP after 50 °C.
- No low field breakdowns were measured after temperature step of 110 °C (cap-BOPP) or 80 °C (ref-BOPP).
- Increasing scatter and the absence of a distinct "weak spot" population in aged SiO_2-BOPP film samples.

The reference-BOPP film was seen to exhibit machine direction stripes presumably related to manufacturing-originating issues, which were considered as a possible cause for some of the weak spots. However following their appearance weak spots were always measured in more than one of the six film samples. Together with the similar weak spot formation in capacitor-grade BOPP film this reinforces the presumption of them being influenced by the accumulating thermal stress. The scarcity of the weak points suggests towards selective degradation, but the nature and mechanisms of degradation remains unknown. The degradation was regarded as permanent since the samples were measured at room temperature after several hours from their removal, having had time to settle.

In related literature thermoelectric aging of BOPP films has been reported to result in defect formation with simultaneously increasing Weibull-α [2] and in a decrease of breakdown voltages in the < 10 % probability region [13]. Given that similar weak spot formation was measured in film subjected to thermal stress alone it is suggested thermal stress alone resulted in polymer aging, which manifested as defect formation.

In the un-filled BOPP samples removed after the highest temperatures an increase of the 63.2 % dielectric breakdown strength compared to the unaged reference was noted in addition to the absence of distinct weak spot subpopulation. In related literature both Arrhenius [14] and multiple-process models [15] have been used to model polymer aging, but neither of the aforementioned models predicts this kind of increase. An alternative explanation for the observed behavior

TABLE II. WEIBULL PARAMETERS

Cap-BOPP	reference	50 °C	60 °C	70 °C	80 °C	90 °C	100 °C	110 °C
Number of points	49	67	65	73	85	75	65	43
Weibull β_1	11.22	17.44	21.30	5.78	5.06	5.55	2.72	12.76
Weibull α_1	567	624	635	581	543	584	680	709
Weibull β_2				46.28	21.92	34.84	15.81	
Weibull α_2				672	677	684	688	
Ref-BOPP	reference	50 °C	60 °C	70 °C	80 °C	90 °C	100 °C	110 °C
Number of points	96	75	118	55	89	55	50	45
Weibull β_1	17.93	5.97	5.56	3.28	3.94	12.33	8.53	11.36
Weibull α_1	673	599	547	633	385	721	692	707
Weibull β_2			21.84	15.08	8.77			
Weibull α_2			631	687	629			
SiO2-BOPP	reference	50 °C	60 °C	70 °C	80 °C	90 °C	100 °C	110 °C
Number of points	91	41	65	61	56	55	64	48
Weibull β_1	17.82	10.63	15.81	5.88	7.31	8.45	8.54	8.39
Weibull α_1	584	586	568	575	575	609	580	607

would be thermally activated processes, which while progressing would result in localized "weak spots", but after completion the measured response would be at higher fields that of the unaged film. In case such processes existed they should be regarded as heat treatment rather than thermal aging. Antioxidant conversion by thermally activated or accelerated reactions is seen as one possible explanation for the changes in un-filled BOPP films, largely based on studies by Ho et al. [16] in which UV-facilitated conversion of Irganox 1010 in capacitor-grade BOPP film has been proposed to result in increased dielectric breakdown strength. However the statistical nature of the breakdown phenomena is seen as an alternative explanation for the disappearance of the weak spots.

Thermal stress resulted in increasing scatter (decreasing Weibull-β) of breakdown voltages in SiO_2-BOPP film. Scatter increased until after 70 °C a slight decrease was noted. The changes diminished with increasing temperature and after 90°C the breakdown distributions displayed similarly increased scatter together with a slight increase of the 63.2 % breakdown strength when compared to the unaged reference. The breakdown voltages followed a single Weibull distribution and no weak spot subpopulation was measured. Scatter in the low probability region was attributed to the use of average thickness in breakdown field determination and to the statistical nature of breakdown phenomena.

The absence of weak spots in SiO_2-BOPP suggest towards changes occurring throughout the material. The diminishing variations or "stabilization" towards higher temperatures may be attributed to thermally activated processes which alter the material permanently but whose effects diminish with time. In this case the processes should be regarded as heat treatment rather than thermal aging. If the antioxidant depletion-approach is considered, it is regarded possible that either the measured changes are combined effects of antioxidant conversion and another silica-influenced processes, or that the different nano-scale structure in nanocomposites alters the progression of antioxidant conversion reactions.

It has been suggested by Nawaz et al. in [17] that in aluminum oxide – poly(ethylene-*co*-butyl acrylate) nanocomposite the nanoparticle surfaces adsorb and then slowly release Irganox 1010 antioxidant. Similar behavior is seen as one possible explanation for the changes in SiO_2-BOPP film, but thorough material characterization would be needed to identify the exact changes. For material evaluation the knowledge on such processes would be valuable as changes were measured immediately after 50°C, well within the typical operating temperature range for capacitor dielectrics.

IV. Conclusions

Distinct defect population was measured in un-filled PP materials after being subjected to 50…70 °C, whereas in silica-PP nanocomposites thermal stress resulted in increasing scatter of the measured breakdown voltages. No defect population was measured in un-filled PP samples removed after 100 °C and 110 °C, and the 63.2 % breakdown strength of said samples was in slightly higher than that of the unaged reference. Alternative explanations were given to the weak point population and its disappearance: localized degradation and the statistical nature of breakdown phenomena and thermally activated processes involving additives. For the polymer-silica-nanocomposite the increasing scatter was speculated to result from thermally activated changes in the polymer-nanoparticle interface, but additional research is needed to clarify the issue. The results demonstrate the different thermal aging behavior of un-filled PP and silica-PP nanocomposite and exemplify the importance of large sample areas to measure statistically significant amount of breakdowns from the possible defect populations.

References

[1] L. Dissado and J. C. Fothergill, *Electrical degradation and breakdown in polymers*. Peter Peregrinus Ltd., 1992.

[2] T. Umemura and K. Akiyama, "Accelerated-life testing of power capacitor dielectric systems," *Electr. Insul. IEEE Trans.*, vol. EL-22, no. 3, 1987.

[3] T. Umemura, K. Abe, K. Akiyama, and D. Couderc, "Thermal-aging behavior of Bo-Pp films," *Electr. Insul. IEEE Trans.*, vol. EI-22, no. 6, pp. 735–743, 1987.

[4] J. K. Nelson, *Dielectric polymer nanocomposites*. Springer US, 2010.

[5] M. Takala, H. Ranta, P. Nevalainen, P. Pakonen, J. Pelto, M. Karttunen, S. Virtanen, V. Koivu, M. Pettersson, B. Sonerud, and K. Kannus, "Dielectric properties and partial discharge endurance of polypropylene-silica nanocomposite," *Dielectr. Electr. Insul. IEEE Trans.*, vol. 17, no. 4, pp. 1259–1267, 2010.

[6] T. Tanaka, M. Kozako, N. Fuse, and Y. Ohki, "Proposal of a multi-core model for polymer nanocomposite dielectrics," *Dielectr. Electr. Insul. IEEE Trans.*, vol. 12, no. 4, pp. 669–681, 2005.

[7] I. Rytoluoto and K. Lahti, "New approach to evaluate area-dependent breakdown characteristics of dielectric polymer films," *Dielectr. Electr. Insul. IEEE Trans.*, vol. 20, no. 3, pp. 937–946, 2013.

[8] I. Rytöluoto, K. Lahti, M. Karttunen, and M. Koponen, "Large-area dielectric breakdown performance of polymer films – Part I: measurement method evaluation and statistical considerations on area-dependence," *Dielectr. Electr. Insul. IEEE Trans.*, vol. 22, no. 2, pp. 689–700, 2015.

[9] I. Rytöluoto, K. Lahti, M. Karttunen, and M. Koponen, "Large-area dielectric breakdown performance of polymer films – Part II: interdependence of filler content, processing and breakdown performance in polypropylene-silica nanocomposites," *Dielectr. Electr. Insul. IEEE Trans.,* In press.

[10] IEC, "International standard IEC 60243-1, Part 1: Tests at power frequencies. Edition 3.0." 2013.

[11] "IEC/IEEE Guide for the statistical analysis of electrical insulation breakdown data (Adoption of IEEE Std 930-2004)," *IEC 62539 First Edition 2007-07 IEEE 930*. 2007.

[12] W. Hauschild and W. Moss, *Statistical techniques for high voltage engineering*. London: Peter Peregrinus Ltd., 1992.

[13] B. Gosse, J. P. Gosse, S. Saïd, A. Gadoum, and M. Nemamcha, "Electrical degradation of polypropylene: A study by FTIR microspectroscopy," *J. Appl. Polym. Sci.*, vol. 46, no. 6, pp. 1121–1124, Oct. 1992.

[14] L. W. McKeen, *Effect of temperature and other factors on plastics and elastomers*. Norwich, NY: William Andrew Publishing, 2008.

[15] M. Celina, K. T. Gillen, and R. A. Assink, "Accelerated aging and lifetime prediction: Review of non-Arrhenius behaviour due to two competing processes," *Polym. Degrad. Stab.*, vol. 90, no. 3, pp. 395–404, Dec. 2005.

[16] J. Ho, R. Ramprasad, and S. Boggs, "Effect of alteration of antioxidant by UV treatment on the dielectric strength of BOPP capacitor film," *Dielectr. Electr. Insul. IEEE Trans.*, vol. 14, no. 5, pp. 1295–1301, 2007.

[17] S. Nawaz, P. Nordell, H. Hillborg, and U. W. Gedde, "Antioxidant activity in aluminium oxide – poly(ethylene-co-butyl acrylate) nanocomposites," *Polym. Degrad. Stab.*, vol. 97, no. 6, pp. 1017–1025, Jun. 2012.

Publication II

M. Ritamäki, I. Rytöluoto and K. Lahti, "Temperature Effect on Breakdown Performance of Insulating Polymer Thin Films," in *24th Nordic Insulation Symposium on Materials, Components and Diagnostics (NORD-IS 15)*, pp. 75–79, 2015.

Temperature Effect on Breakdown Performance of Insulating Polymer Thin Films

M. Ritamäki, I. Rytöluoto, K. Lahti
Department of Electrical Engineering
Tampere University of Technology, Tampere, Finland

Abstract

The effect of temperature on the breakdown performance of metallized capacitor-grade BOPP film was characterized using a large-area multi-breakdown measurement method. The measurements conducted in the temperature range from room temperature to 100 °C revealed a linearly decreasing trend in the characteristic 63.2 % breakdown probability after 60 °C and the presence of a smaller weak spot subpopulation. The weak spots remained relatively unaffected by temperature, and first breakdowns occurred in a seemingly statistical manner. The brief exposure to elevated temperature was considered as one explanation behind the variations in the number of weak points, but fluctuations in film quality and Weibull dynamics were seen are more probable explanations. The results demonstrate the possibility of multiple breakdown mechanisms and their different temperature-dependency, and demonstrate the high short-term breakdown strength of BOPP film even at high temperatures.

1. Introduction

Recently there has been a growing demand for capacitor dielectrics for high-temperature applications. Biaxially oriented polypropylene (BOPP) has been used in high power density capacitors, with metallized electrodes providing self-healing capabilities and graceful aging behavior [1]. When compared to traditional temperature-resistant plastics such as polytetrafluoroethylene (PTFE), poly(phenylene sulfide) (PPS) or polyimides polypropylene offers high dielectric breakdown strength, good self-healing capabilities and polypropylene films can be manufactured to thicknesses in the range of few µm, facilitating its use in low and medium-voltage applications [2]. Polypropylene melts in the region of 165–170 °C, but its operating temperature has been limited to 85 °C, or with voltage deration to about 105 °C. [2]

The maximum operating temperature of polymer dielectrics is largely determined by the increasing losses and decreasing dielectric breakdown strength at higher temperatures. In [3] and [4] the effect of temperature on the breakdown strength of polymer materials has been divided in low and high temperature regions. In the low temperature region the dielectric breakdown strength is relatively independent of the temperature, whereas in the high temperature region the breakdown strength decreases with temperature. For polar polymers a "critical temperature" may exist, above which the breakdown strength falls rapidly. In [3] a decreasing electric strength with increasing temperature has been reported for isotactic polypropylene. Owing to its nonpolar nature there is no critical temperature. Contradicting views are presented in [5] in which it is presented that the dielectric breakdown strength of polymers is unaffected by temperature.

Capacitor-grade films differ from traditional polymer materials, especially in terms of the biaxial orientation and the purity of the base polymer. In this paper the effect of temperature on the breakdown behavior of commercial capacitor-grade Zn/Al –metallized PP film is evaluated from room temperature to 100 °C. A large-area multi-breakdown measurement method detailed in [6], [7] was utilized. By taking advantage of the self-healing capabilities of metallized PP film total sample areas up to 350 cm^2 were measured at each temperature step. Large measurement areas allow measuring statistically significant amount of breakdowns even from the lower-probability regions.

2. Experimental

2.1 Material and sample details

A commercial zinc/aluminum alloy metallized capacitor-grade BOPP film manufactured by Tervakoski Films Group was used in the experiment. The film had a manufacturer-reported thickness of 6 µm and the one-sided metallization had a main body surface resistance of 5–12 Ω/□ and a reinforced edge with a surface resistance of 2–4 Ω/□. The 72.5 mm wide film had a free margin 2.5 mm. Six 110 mm samples plus an additional six reference samples were prepared for each temperature, with the exception of the room temperature measurement for which no reference samples were needed.

2.2 Measurement setup

Measurements at elevated temperature were conducted in atmospheric air by utilizing a test oven detailed in [8]. The oven temperature was controlled by a self-tuning PID controller and a cross-flow fan was utilized to promote air circulation. The test fixture was placed in the oven and its temperature was let to stabilize for 10–15 minutes. Both the air and fixture temperatures were

monitored during this stabilization period, with the fixture temperature monitored by a K-type thermocouple placed between the bench edge and the top plate. The oven was opened to remove the thermocouple before the multi-breakdown measurements. Between the removal of the thermocouple and the actual measurement the system was let to stabilize for approximately 1–2 minutes.

To determine the reversibility of the measured changes for each high temperature measurement one reference sample in a paper envelope was placed in the upper section of the oven. The reference sample was removed after the multi-breakdown measurement and measured after a few days, having had time to settle at room temperature.

Six film samples were measured at room temperature and at temperatures of 60, 80 and 100 °C. Excessive film curling resulted in the loss of one reference sample for each temperature; therefore the reference measurements consisted of five samples each.

2.3 Large-area multi-breakdown measurement

A large area multi-breakdown measurement detailed in [6], [7] was applied to determine changes in the breakdown behavior. The self-healing test capacitors were manufactured by placing two 90 mm wide 12 µm Zn/Al metallized BOPP films (main body metallization resistivity 5–12 Ω/□) on both sides of the test sample. The one-sided metallization of the test sample functioned as the lower electrode and the 12 µm film was used to make electrical contact between it and the test fixture. The upper 12 µm film functioned as the other electrode. This arrangement resulted in an active area of approximately 58 cm^2, with six samples equaling to a total measured area of approximately 350 cm^2. To provide mechanical support two 100 µm thick polyester films were placed on both sides of the film stack. The film stack was attached to a test fixture consisting of a Bakelite baseboard and two glass plates. The 12 µm metallized films were clamped between two aluminum plates on opposing edges of the fixture, to which the electrical connections were made. The test capacitor arrangement is illustrated in Figure 1.

Loosely according to IEC-60243-1 slow rate-of-rise test [9] the measurement consisted of a fast voltage ramp up at 400 V/s to 1800 V, corresponding to a field of 300 V/µm, followed by a slow ramp at 30 V/s. Breakdowns were measured during the slow ramp which was continued until no more discharges were detected.

Based on an equation presented in [10] the 2.5 mm free margin was presumed to exhibit flashovers above 4–5 kV. The inception voltage for repeating flashovers was determined using an otherwise similar 9 µm metallized film, in which rapid flashovers were measured at DC voltages above 5.5–6 kV. For the 6 µm film flashovers across the free margin were not seen as a limiting issue since the test voltage rarely exceeded 5 kV.

The measurement used a Spellman SL1200 DC high voltage supply, controlled and monitored using a resistive Spellman 1:10 000 voltage divider, National Instruments PCI-6221 DAQ card and a LabVIEW-based program. Test capacitor voltage and circuit current were monitored real-time using one AC and one DC coupled Tektronix P6015 high voltage probe and a 1.0330 Ω impulse current measurement resistor. Discharge current and voltage waveforms were captured by a LeCroy HRO 66Zi oscilloscope set to trigger at the falling edge of the AC coupled voltage channel. Compared to the current triggering method in [6], [7] the voltage drop – based trigger enabled detection of discharges with substantially lower energies. An USB-camera was used to provide a video feed from above the test fixture which was monitored to verify the absence of repeating flashovers at the sample edges.

A two-criterion breakdown selection procedure detailed in [6] was used to exclude non-independent breakdowns and non-breakdown discharges from the measurement data. These included phenomena such as multiple sequential self-healings occurring rapidly in one spot, breakdowns at previously cleared areas, surface flashovers and other non-breakdown discharges. To uniform the results and due to the increased probability of surface flashovers at the free margin near the end of the measurements for each sample any discharges beyond the initial 50 were omitted from further analysis.

2.4 Statistical analysis

Weibull statistical analysis was used to fit the breakdown data with suitable distributions to reach a visually and mathematically adequate fit. In every measurement deviation from a single 2-parameter Weibull distribution was evident and additively mixed two-subpopulations were used [6], [7], [11]:

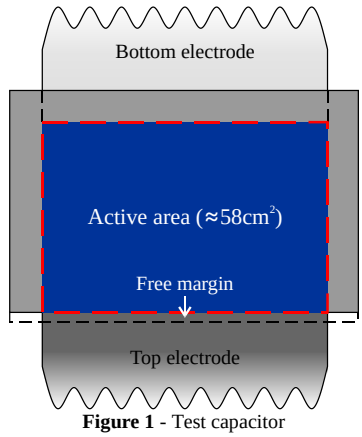

Figure 1 - Test capacitor

Table 1 – Weibull parameters

	RT	60 °C	80 °C	100 °C	REF-60 °C	REF-80 °C	REF-100 °C
Number of points	90	119	93	88	79	104	97
Weibull β_1	2.51	3.67	5.86	5.71	4.04	4.69	7.14
Weibull α_1 (V/µm)	507	468	527	506	516	570	601
N_1/N	0.08	0.12	0.19	0.24	0.25	0.29	0.41
Weibull β_2	23.72	16.69	19.76	20.48	24.94	27.88	23.80
Weibull α_2 (V/µm)	686	665	644	610	686	694	698
N_1/N	0.92	0.88	0.81	0.76	0.75	0.71	0.59

$$F(x)=\frac{N_1}{N}\left[1-\exp\left\{-\left(\frac{x}{\alpha_1}\right)^{\beta_1}\right\}\right]+\ldots \\ \ldots\frac{N_2}{N}\left[1-\exp\left\{-\left(\frac{x}{\alpha_2}\right)^{\beta_2}\right\}\right] \quad (1)$$

In (1) $F(x)$ is the 2-parameter two-subpopulation Weibull distribution, N_1/N and N_2/N are the relative portions of and β and α are the Weibull scale and shape parameters of the two subpopulations. The scale parameter α represents the $1\text{-}e^{-1} \approx 63.2$ % breakdown probability and the shape parameter β depicts the homogeneity of the data points, being analogous to the inverse of the standard deviation of Gaussian distributions. The first subpopulation primarily accounts for the low field breakdowns whereas the second one represents the intrinsic behavior, which in this paper refers to the region of recurring breakdowns. The distribution parameters were estimated with maximum likelihood estimation (MLE) or non-linear rank regression (NLRR) methods. One-sided 90 % confidence bounds were calculated using Fisher Matrix (FM) –based method. Calculations were done using Weibull++ 9 software.

Given the nature of the multi-breakdown measurement unequal number of breakdowns was recorded in every measurement. Despite this the amount of selected breakdowns was around 90 for each temperature step, and more importantly the trend in the amount of selected points does not correlate with the changes observed in the breakdown behavior. Therefore the error caused by the variation between the numbers of points was seen insignificant at least in the > 10% probability region. The increasing uncertainty in the low probability region is evident from the broadening confidence bounds.

3. Results and discussion

The distribution parameters and the number of selected breakdowns are presented in Table 1. Data points and Weibull distributions from measurements at elevated temperature are presented in Figure 2a together with percentiles corresponding to 5 %, 30 % and 63.2 % breakdown probabilities. Both are presented with one-sided 90 % confidence bounds. Data points and distributions from corresponding reference measurements at room temperature are presented in Figure 2b. Looking at the results it can be summarized that:

- the characteristic 63.2 % breakdown strength

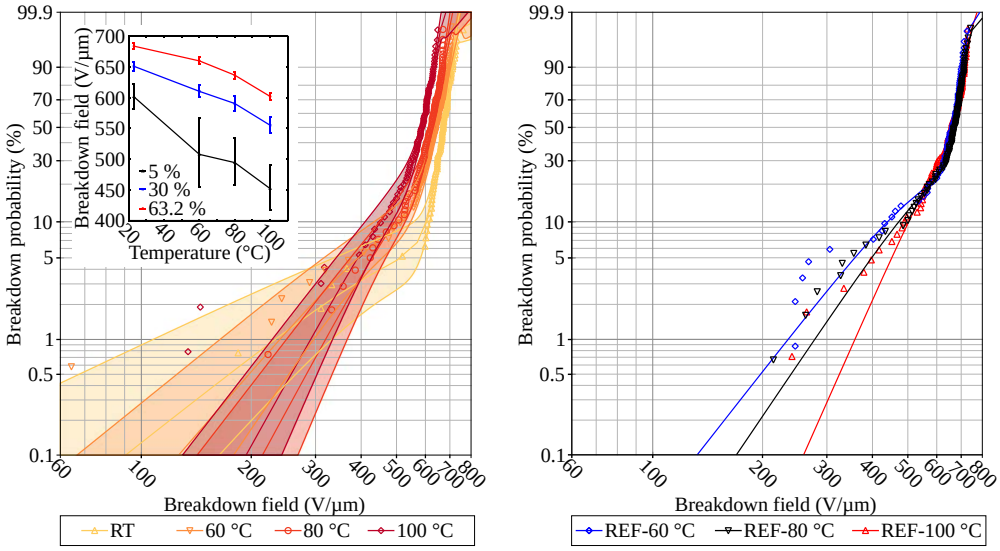

Figure 2 – a) Breakdown behavior at room temperature, 60, 80 and 100 °C together with calculated 5 %, 30 % and 63.2 % percentiles **b)** Reference measurements at room temperature

decreased from 684 V/µm at room temperature to 602 V/µm at 100 °C
- the decrease can be considered as reversible, since the reference samples displayed similar behavior at room temperature
- two subpopulations were distinguishable in all measurements
- the effect of temperature was most significant in the second Weibull subpopulation
- the weak spot subpopulation was not heavily influenced by the elevated temperature

In [7] similar multi-breakdown measurement was used to characterize areas up to 1950 cm^2 of same brand of film from different roll at room temperatures. The distinct weak spot subpopulation and the intrinsic region reported here correspond to the first two portions of the S-shape [7], and the absence of the third subpopulation can be explained by the omission of any breakdowns beyond the initial 50. Additionally the Weibull parameters of the first two subpopulations are fully in line with presented in Table 1. This supports the repeatability of the measurement method.

The shape of the Weibull distribution remains relatively unchanged with temperature. Moreover based on [6] it is presumed that the variations in Weibull β_2 are at least partially due to the use of average thicknesses for breakdown field determination.

Given the minor variations in the distribution shape the decreasing trends in the 30 % and 63.2 % percentiles and in the Weibull α_2 are similar. Although a similar trend is also observed in the 5 % percentiles, the statistical uncertainty, as evident in the large error bars, limits the usability of the data. The visually discernible inverse linear trend in data after 60 °C–100 °C is in line with the results presented for isotactic polypropylene in [3], in which a similar decrease is reported approximately after 50–60 °C. The room temperature measurements are omitted and based on the data from 60–100 °C an inverse linear relationship between the Weibull α_2 and the temperature T is formulated as:

$$\alpha_2 = kT + b\,, \tag{2}$$

where *k* and *b* are constants with values of -1.38 and 749.9 V/µm respectively. The fit was calculated using MATLAB software and has a R-square value of 0.9843. Based on charts presented in [3] the relationship is presumed hold from 60°C up to 130 °C, but additional research is needed to confirm validity especially above 100 °C.

For practical applications however the presence of a distinct weak spot subpopulation is of more importance than the changes in the high field behavior. Given typical operating fields below 100 V/µm even for high energy density metallized film designs, the temperature of 100 °C does not result in the operating field exceeding the intrinsic breakdown strength.

The presence of two subpopulations may indicate the presence of two breakdown mechanisms [5], out of which the mechanism responsible for low field breakdowns is not heavily affected by temperature. Accurate determination of its temperature-dependency is made impossible by the scarcity of data points in the low probability region. However the nature of the two proposed breakdown mechanisms cannot be determined using the available data.

In addition to the large-area multi-breakdown results published for same brand of film in [7], in related literature similar two-subpopulation breakdown behavior has been reported as fingerprint-like in unaged PP film [12] and as a result from thermoelectric [13] and thermal aging [8] of PP film having previously displayed single population breakdown behavior. The aging cycles after which diverging weak spots were measured spanned from 20 hours of thermoelectric aging [13] to 144 hours of thermal aging [8]. Even though in this study the films were exposed to elevated temperature for a relatively short period of 10–20 minutes fewer low field breakdowns were measured in room temperature measurement. It is therefore presented that

- at least a portion of the low field breakdowns are a part of the characteristic “fingerprint” of the film
- the exposure to elevated temperature may have caused material degradation leading to more low field breakdowns.

In the reference films the relative portion of the first subpopulation increased from 0.25 after 60 °C to 0.41 after 100 °C, but this increase was simultaneous with increasing Weibull α_1, suggesting that the increase is related to Weibull dynamics rather than actual breakdown phenomena. Additionally the distributions in Figure 2b are in line with each other. Therefore it is considered more probable that the low field breakdowns were solely an intrinsic film property, and that the variations were a result from the statistical nature of breakdown phenomena and fluctuations in film quality rather than from rapid heat-induced degradation. If the low field breakdowns are regarded solely as an intrinsic material property is should be noted the first few breakdowns occurred in a seemingly statistical manner independent of temperature.

Given the lack of temperature dependency in the low probability region, based on [2] dielectric losses are established as the main limiting factor for use at higher temperatures, requiring voltage deration. In addition to intolerable power loss rapidly increasing losses may lead to thermal runaway-type breakdown phenomena. Nevertheless in the multi-breakdown measurement self-healing phenomena worked successfully up to 100 °C, and no permanent insulation failures were observed. It is however worth noting that the measurement duration of few minutes is not long enough to rule out the possibility of breakdown and degradation mechanisms acting in time scales from minutes to hours. If such mechanisms exist they may also limit the usability of high temperatures. Therefore broad characterization of dielectric and aging properties is needed before any materi-

als can be regarded sufficiently stable for long-term use at elevated temperatures.

4. Conclusions

Large-area multi-breakdown measurements using metallized capacitor-grade BOPP film revealed the presence of temperature-independent weak spots, and two-subpopulation Weibull distributions were applied to reach a visually and mathematically good fit. An inverse power law relationship between temperature and Weibull α_2 was determined between 60–100 °C. Similar trend was also evident in 30 % and in the characteristic 63.2 % breakdown strengths.

Diminishing differences were measured in reference samples measured at room temperature after equivalent thermal stresses, based on which the changes in the intrinsic behavior were regarded as a reversible effect of temperature rather than heat-induced degradation. Compared to the room temperature reference the relative portion of the weak spot subpopulation increased in all films subjected to elevated temperature. For this heat-induced degradation and fluctuations in film quality were proposed as complementary explanations, out of which the latter was considered more probable.

5. References

[1] W. J. Sarjeant, "Capacitor fundamentals," in *Electrical Electronics Insulation Conference, 1989. Chicago '89 EEIC/ICWA Exposition., Proceedings of the 19th*, 1989, pp. 1–51.

[2] J. Ho and R. Jow, "Characterization of High Temperature Polymer Thin Films for Power Conditioning Capacitors," Adelphi, MD 20783-1197, 2009.

[3] M. Ieda, "Dielectric Breakdown Process of Polymers," *Electr. Insul. IEEE Trans.*, vol. EI-15, no. 3, pp. 206–224, 1980.

[4] A. K. Jonscher and R. Lacoste, "On a Cumulative Model of Dielectric Breakdown in Solids," *Electr. Insul. IEEE Trans.*, vol. EI-19, no. 6, pp. 567–577, 1984.

[5] L. Dissado and J. C. Fothergill, *Electrical degradation and breakdown in polymers*. Peter Peregrinus Ltd., 1992.

[6] I. Rytöluoto, K. Lahti, M. Karttunen, and M. Koponen, "Large-Area Dielectric Breakdown Performance of Polymer Films – Part I : Measurement Method Evaluation and Statistical Considerations on Area-dependence," IEEE Trans. Dielectr. Electr. Insul., vol. 22, no. 2, pp. 689–700, 2015.

[7] I. Rytoluoto and K. Lahti, "New approach to evaluate area-dependent breakdown characteristics of dielectric polymer films," *Dielectr. Electr. Insul. IEEE Trans.*, vol. 20, no. 3, pp. 937–946, 2013.

[8] M. Ritamäki, "Effects of Thermal Aging on Polymer Thin Film Insulations for Capacitor Applications," Tampere University of Technology, 2014.

[9] IEC, "International standard IEC 60243-1, Part 1: Tests at power frequencies. Edition 3.0." 2013.

[10] V. Belko, O. Emelyanov, and M. Shemet, "A study of nanosecond arcsurface flashover in metallized polymer films," in *Electrical Insulation and Dielectric Phenomena (CEIDP), 2013 IEEE Conference on*, 2013, pp. 476–477.

[11] W. Hauschild and W. Moss, *Statistic Techniques for High Voltage Engineering*. London: Peter Peregrinus Ltd., 1992.

[12] S. J. Laihonen, "Polypropylene : Morphology, defects and electrical breakdown," Kungliga Tekniska Högskolan, 2005.

[13] B. Gosse, J. P. Gosse, S. Saïd, A. Gadoum, and M. Nemamcha, "Electrical degradation of polypropylene: A study by FTIR microspectroscopy," *J. Appl. Polym. Sci.*, vol. 46, no. 6, pp. 1121–1124, Oct. 1992.

Publication III

M. Ritamäki, I. Rytöluoto, M. Niittymäki and K. Lahti, "Differences in AC and DC large-area breakdown behavior of polymer thin film," in *2016 IEEE International Conference on Dielectrics (ICD)*, pp. 1011–1014, 2016.

DOI: 10.1109/ICD.2016.7547789

The following paper is the final version accepted for publication in the 2016 IEEE International Conference on Dielectrics. The published version of this paper is available at IEEE Xplore.

Differences in AC and DC large-area breakdown behavior of polymer thin films

M. Ritamäki, I. Rytöluoto, M. Niittymäki, K. Lahti
Department of Electrical Engineering
Tampere University of Technology (TUT)
Tampere, Finland

M. Karttunen
Technical Research Centre of Finland (VTT)
Tampere, Finland

***Abstract*—A large-area multiple breakdown measurement using self-healing gold sputtered electrodes was evaluated in determining the AC breakdown characteristics of insulating biaxially oriented polypropylene (BOPP) and BOPP-silica nanocomposite thin films. Results were compared with conventional small area measurements and it is shown that the large-area approach could be extended into AC measurements as long as good quality film-electrode interface in ensured. Special electrode arrangements are needed due to the absence of electrostatic force. AC small-area breakdown strength of pilot-scale films was ramp rate dependent but no such effect was clearly noticed for a commercial product. Conventional DC small-area breakdown measurements were also conducted and the results were compared to previously published large-area multiple breakdown data. The consistent results support the dependency between ramp rate and DC breakdown strength in the studied BOPP-silica nanocomposite.**

Keywords— polymer films; dielectric measurement; Weibull distribution; electric breakdown; AC; DC

I. INTRODUCTION

A self-healing multiple breakdown measurement methodology, originally utilized for studying e.g. thin MOS capacitors [1], has recently been developed and utilized for studying large-area breakdown characteristics of thin polymeric capacitor films in TUT/DEE [2]. As examples the effects temperature [3], interlayer pressure [4] and thermal ageing [5] on DC breakdown strength and its ramp-rate dependency [6] have been studied together with several thin film processing related aspects [7]. Large measurement areas have enabled detecting weak points and slight changes with high statistical accuracy, which otherwise would have required an extensive amount of time-consuming conventional small-area single-breakdown measurements. However, from a practical viewpoint both DC and AC breakdown characteristics are of utmost importance. Our earliest attempts to extend the large-area approach to AC breakdown measurements using various test capacitors with metallized film electrodes were problematic, as contrary to DC measurements no electrostatic compressive force was pushing oil and gas bubbles from between the film layers. In many cases excessive discharging was observed and breakdown voltages were anomalously low, which was associated with partial discharging in an air gap in the electrode-film interface. Some experimental structures using separate metallized electrodes gave convincing results, but they were rejected as it could not be verified that the results reflected the properties of the film, and not an oil-film-oil multilayer insulation or the measurement system itself.

The purpose of this paper is to report on our recent efforts to use sputtered electrodes to enable AC large-area multi-breakdown characterization of biaxially oriented polypropylene (BOPP) films. This approach was evaluated by comparing the large-area results with conventional breakdown measurements using both AC and DC voltages at different ramp rates.

II. EXPERIMENTAL

A. Material details

One pilot-scale SiO_2-BOPP nanocomposite 'SiO_2-BOPP', its un-filled reference 'Ref-BOPP' and one commercial capacitor grade BOPP film 'Cap-BOPP' were used in the experiments. The films were similar as studied in [5]–[8]. The SiO_2-BOPP was manufactured by compounding unstabilized polypropylene HC318BF with 4.5 wt-% of Aerosil R812 S hydrophobic fumed silica. To stabilize the material 0.47 wt-% of Irganox 1010 and 0.35 wt-% of Irgafos 168 (0.35 wt-%) were added. The pilot-scale materials were compounded at VTT Technical Research Center of Finland and bi-axially oriented films were produced in a Brückner pilot tenter line in Denmark. Detailed manufacturing parameters have been reported in [7]. The smooth pilot-scale films had a few presumably manufacturing-related deformations and samples were prepared from visually intact regions. A commercial hazy capacitor-grade BOPP film with a nominal thickness of 14.4 µm from Tervakoski Films Group was used as a reference. Sample thicknesses were measured with LE-1000-1 precision thickness gauge (accuracy of 0.1 µm). Average values are presented in Table 1.

B. AC and DC small-area single-breakdown measurements

Twenty 30×30 mm film samples were prepared for each small-area single-breakdown test. Breakdown measurements were conducted using a test setup depicted in [9] which is roughly in accordance with IEC-60243 standard. The sample was fastened between two Ø = 11 mm graphite pads and then immersed in dielectric oil. The graphite pads were polished

TABLE 1. MATERIAL THICKNESSES

	Average thickness (µm)	SD
Cap-BOPP	13.8	0.56
Ref-BOPP	16.0	1.02
SiO_2-BOPP	14.6	0.52

after each measurement and replaced every 40 measurements.

AC breakdown measurements were conducted for all three films using one slow and one fast AC ramp. Average ramp rates were 450 V/s and 55.9 V/s. AC voltage was supplied by an Elgar SmartWave SW 5250A switching amplifier driving a 3000 VA 220:50000 transformer. A 7.5 MΩ series resistor was used to limit damage to the electrodes. Circuit voltage and current were measured with Tektronix P6015 high voltage probe and a 1.0330 Ω low inductance resistor. Discharge current and voltage waveforms were recorded by a LeCroy HRO 66Zi oscilloscope. Test voltage was also measured with a North Star High Voltage PVM-1 1:2000 probe together with National Instruments PCI-6221 DAQ-card and a LabView-based program. Both the voltage tens of nanoseconds before breakdown, later *actual voltage*, and the IEC-60241 [10] recommended peak voltage reached before breakdown were determined.

DC small-area single-breakdown measurements were conducted for Ref-BOPP and SiO_2-BOPP films at two ramp rates: 50 V/s and 400 V/s using Spellman SL 1200 high voltage DC source. Series resistance of 100 kΩ was used; otherwise the measurement methods were similar to the AC case.

C. Sample preparation and AC large-area multiple breakdown measurement

In large-area multiple breakdown measurements a number of key features can be identified:

- The electrodes must be self-healing to continue the measurement beyond the first breakdowns.
- The circuit should have sufficient damping to prevent voltage spikes during discharges.
- The cleared areas should be small compared to the total sample surface to measure multiple breakdowns from one sample.
- The results must stem from the properties of the film tested, not from the test system or sample preparation used.

Gold electrodes were sputtered on 65 × 40 film samples using Quorum SC7620 magnetron sputter coater. Easily removable tape was used as sputter masks and samples were cleaned with isopropanol afterwards. To prevent thermal damage sputtering was done in 30 seconds intervals with 30 second pauses between at a throw distance of 45 mm, with the process current manually adjusted to 25 mA. Each sample was cleaned with a nitrogen spray gun before sputtering. Test capacitors depicted in Fig. 1a had an active area of 9 cm^2. Samples were sputtered for 5 × 30 seconds resulting in roughly 44 nm metallization thickness according to the manufacturer's documentation. To realize electrical connections with the metallized electrodes stranded copper wires were attached to the side tabs using high purity silver paint (SPI-paint). The test capacitor was then immersed in dielectric oil (Shell Oil Diala) and a 50 Hz AC voltage ramp at 50 V/s was applied to it until discharge activity had ceased. Images of actual samples before and after measurement are presented in Fig. 1 b and c.

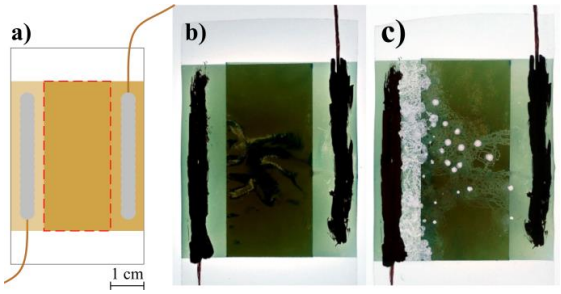

Fig. 1. AC large-area multiple breakdown test capacitor with metallized gold electrodes. **a)** Basic structure, active area circled in red. Actual test capacitor before **b)** and after **c)** measurement.

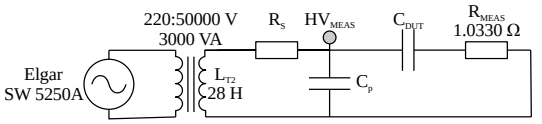

Fig. 2 AC large-area multiple breakdown measurement circuit. Same setup without parallel capacitance C_P was used for small-area single breakdown measurement.

The measurement circuit is depicted in Fig. 2. Series resistor R_S of 300 kΩ and a parallel capacitor C_P of 1 nF was chosen based on circuit modeling to overdamp the circuit, thus resulting in no observable voltage overshoots in the LabView record. In Fig. 2 C_{DUT} is the sample capacitance, R_{MEAS} is the current measurement resistor and L_{T2} represents the inductance of the transformers secondary at 50 Hz. LeCroy HRO 66Zi oscilloscope recorded discharge current and voltage waveforms. The measurement system was similar as used in the small-area single breakdown measurements.

Six samples of Cap-BOPP and two samples of Ref-BOPP and SiO_2-BOPP were measured at room temperature. The electrodes self-healed and no permanent shorts occurred. The de-metallized areas were small compared to DC large-area measurements in a similar voltage range using separate sheets of metallized electrode film as presented in e.g. [5], [11]. The measurements ended as a rapid high-intensity discharge evaporated the metallization near the wire contacts isolating the remaining intact active areas, as seen in Fig. 1c. This may be a result from electric field surpassing the breakdown strength in a large portion of the film, causing numerous nearly simultaneous self-healings. The excessive power draw and high inrush current would have heated and vaporized the electrodes.

D. Data qualification and statistical analysis

A slightly modified version of the discharge energy and breakdown voltage -based data qualification process detailed in e.g. [2], [11] was used to validate each event recorded during the large-area measurements. Breakdown fields were determined based on average sample thicknesses. The qualified events from large-area measurements and the single breakdown measurement results were fitted with two-parameter Weibull-distributions of the form [12]:

$$F(E) = 1 - \exp\left\{-\left(\frac{E}{\alpha}\right)^{\beta}\right\} \quad (1)$$

In Eq. (1) $F(E)$ is the 2-parameter Weibull distribution for breakdown field E, and α and β are the scale and shape

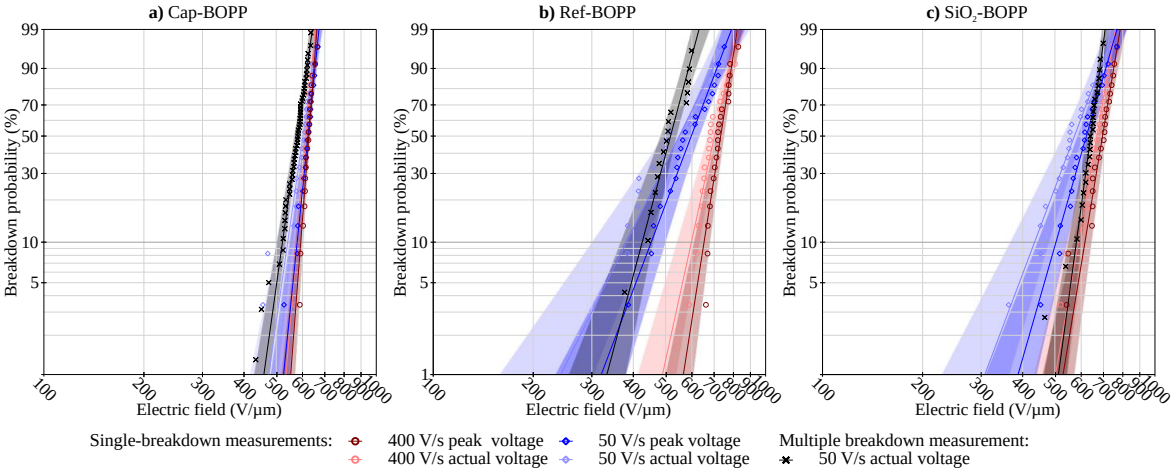

Fig. 3: Weibull plots of AC small area single-breakdown and AC large-area multiple breakdown measurement results for **a)** Capacitor-grade BOPP film **b)** Reference pilot-scale BOPP film and **c)** Pilot-scale silica-PP nanocomposite film. Shaded area represents one-sided 90 % confidence bounds.

parameters estimated using maximum likelihood estimation or rank regression techniques. One-sided 90 % confidence bounds were calculated using Fisher Matrix –based method. Statistical analysis was done using Weibull++ software.

III. Results and Discussion

A. AC measurements

The results from AC large-area multiple breakdown and conventional small-area single-breakdown measurements at two ramp rates are presented in Fig. 3 and Table 2.

The AC large-area multiple breakdowns results of Cap-BOPP (Fig. 3a) were in line with the small area AC measurements. The slight decrease in the characteristic breakdown strength (α) was linked with area dependency [12], [13]. While thermal [5] or thermo-electrical [14] damage on BOPP films may result in the formation of weak points, the absence of low-field breakdowns suggest that the electrode sputtering did not deteriorate the breakdown strength of the film. As seen from Fig. 3a Cap-BOPP displayed extreme distribution homogeneity and its small-area AC breakdown strength was rather independent of the ramp rate. This seems to indicate that in the times from seconds to minutes its AC breakdown was a voltage-driven phenomenon. This is also supported by the breakdowns occurring near or at the voltage peaks as highlighted by the minimal difference between the actual and peak values. The slight differences between the ramp rates may result from the statistical nature of breakdown phenomena and more importantly from the small number of data points. [15]

For Ref-BOPP and SiO_2-BOPP (Fig. 3b–c) the characteristic AC breakdown strength (α) and the distribution homogeneity (β) decreased at slower AC ramps. Breakdowns tended to occur at the falling or rising edges of the voltage waveform, and their apparent breakdown strength increased if peak voltages were considered. This seems to indicate their breakdown phenomena may have an inception-like component, and that in this setting AC breakdown was both time- and voltage driven, in stark contrast to the Cap-BOPP film. [15] For Ref-BOPP and SiO_2-BOPP films the AC large-area multiple breakdown measurements were more in line with the actual breakdown fields of the AC 50 V/s small-area curve. However as only two samples of each film were measured further analysis was not conducted.

B. DC measurements

The results from the conventional small-area DC measurements at two ramp rates are presented in Figure 4 and Table 2. For comparison additionally shown are:

TABLE 2 WEIBULL PARAMETERS

		AC			DC			
		Slow (actual values)	***Fast (actual values)***	***Large-area (slow)***	***Slow***	***Fast***	***Large-area[a] (slow rate-of-rise)***	***Large-area[a] (fast)***
Cap-BOPP	Points	20	20	53	N/A	60[a]	793	N/A
	α	615	622	591		689[a]	638	
	β	17.8	30.4	18.2		31.3[a]	10.6	
REF-BOPP	Points	20	20	16	20	20	124	124
	α	590	724	537	751	752	701	756
	β	5.2	11.7	9.6	16.6	14.9	13.1	8.5
SiO2-BOPP	Points	20	20	25	20	20	121	86
	α	604	686	653	749	835	609	733
	β	6.8	14.8	18.9	19.8	19.5	18.1	9.2

[a.] Single two-parameter Weibull distributions were calculated for previously published data from [5], [7], [8], [11]

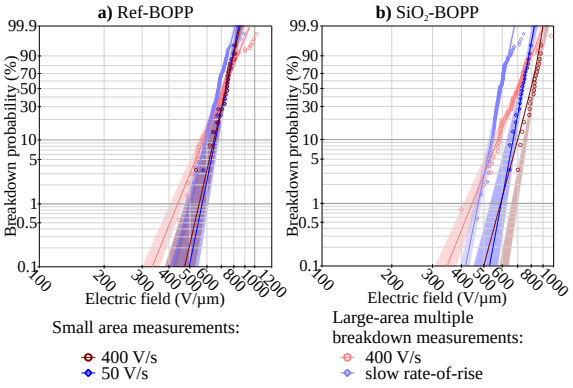

Figure 4. DC large-area multiple breakdown and small area single breakdown results on a Weibull probability scale. Large-area multiple breakdown measurement data previously published in [7].

- large-area breakdown results for Cap-BOPP and SiO_2-BOPP previously published in [7]. Measurements were conducted using a fast 400 V/s ramp and a slow rate-of-rise profile; data was fitted with two-parameter Weibull distributions.
- previously published large-area [5], [8] and conventional small area [11] breakdown measurement results for Cap-BOPP, fitted with Weibull distributions

The decrease of Weibull α for SiO_2-BOPP at slower DC ramp rates is in agreement with large-area results presented in [6]. However in AC small area measurements the decrease in the characteristic breakdown strength in SiO_2-BOPP with slower ramp was 6.7 percentage points lower than in ref-BOPP. This indicates that the DC ramp-rate dependency may be caused by space charge effects and/or altered charge dynamics of polymer–silica interface [16], considering that such effects should not be as pronounced under AC voltage stresses [17]. The lack of DC ramp rate dependency in Ref-BOPP also suggests that the AC ramp rate dependency of breakdown strength may have originated from time rather than purely voltage-dependent rapid high-field degradation.

IV. Conclusions

The preliminary results presented suggest that the large-area multiple breakdown approach could be extended into AC measurements. A gas bubble and oil-free polymer-electrode interface has an important role, as it inhibits discharging and ensures the measurements do not stem from an oil-polymer-oil multilayer insulation. An AC ramp rate dependency of breakdown strength was noticed in Ref-BOPP and SiO_2-BOPP films, and breakdowns tended to occur at the rising or falling edges of the AC waveform. Based on [15] this was suspected to indicate that in this setting their AC breakdown phenomena were both time and field-driven. No such effect was clearly noticed for Cap-BOPP, as in this time interval its AC breakdown was seen almost exclusively voltage-driven. The conventional DC measurements seem to support the DC ramp-rate dependency of breakdown voltages in silica-BOPP nanocomposites [6] and the contrast with AC measurement may indicate it originates from space charge effects.

References

[1] R. M. Hill and L. A. Dissado, “Examination of the statistics of dielectric breakdown,” *J. Phys. C Solid State Phys.*, vol. 16, no. 22, pp. 4447–4468, Aug. 1983.

[2] I. Rytöluoto, “Large-Area Multi-Breakdown Characterization of Polymer Films: A New Approach for Establishing Structure–Processing–Breakdown Relationships in Capacitor Dielectrics,” Doctor of Science thesis, Tampere University of Technology, 2016.

[3] M. Ritamäki, I. Rytöluoto, and K. Lahti, “Temperature Effect on Breakdown Performance of Insulating Polymer Thin Films,” in *24th Nordic Insulation Symposium on Materials, Components and Diagnostics (NORD-IS)*, 2015, pp. 75–79.

[4] I. Rytoluoto and K. Lahti, “Effect of inter-layer pressure on dielectric breakdown characteristics of metallized polymer films for capacitor applications,” in *2013 IEEE International Conference on Solid Dielectrics (ICSD)*, 2013, pp. 682–687.

[5] M. Ritamäki, “Effects Of Thermal Aging On Polymer Thin Film Insulations For Capacitor Applications,” Master of Science thesis, Tampere University of Technology, 2014.

[6] I. Rytoluoto, M. Ritamaki, K. Lahti, and M. Karttunen, “DC ramp rate effect on the breakdown response of SiO2-BOPP nanocomposites,” in *2015 IEEE 11th International Conference on the Properties and Applications of Dielectric Materials (ICPADM)*, 2015, pp. 496–499.

[7] I. Rytoluoto, K. Lahti, M. Karttunen, M. Koponen, S. Virtanen, and M. Pettersson, “Large-area dielectric breakdown performance of polymer films – Part II: Interdependence of filler content, processing and breakdown performance in polypropylene-silica nanocomposites,” *IEEE Trans. Dielectr. Electr. Insul.*, vol. 22, no. 4, pp. 2196–2206, Aug. 2015.

[8] M. Ritamaki, I. Rytoluoto, K. Lahti, and M. Karttunen, “Effects of thermal aging on the characteristic breakdown behavior of Nano-SiO2-BOPP and BOPP films,” in *2015 IEEE 11th International Conference on the Properties and Applications of Dielectric Materials (ICPADM)*, 2015, pp. 400–403.

[9] M. Takala, H. Ranta, P. Nevalainen, P. Pakonen, J. Pelto, M. Karttunen, S. Virtanen, V. Koivu, M. Pettersson, B. Sonerud, and K. Kannus, “Dielectric properties and partial discharge endurance of polypropylene-silica nanocomposite,” *IEEE Trans. Dielectr. Electr. Insul.*, vol. 17, no. 4, pp. 1259–1267, Aug. 2010.

[10] IEC, “International standard IEC 60243-1, Part 1: Tests at power frequencies. Edition 3.0.” 2013.

[11] I. Rytoluoto, K. Lahti, M. Karttunen, and M. Koponen, “Large-area dielectric breakdown performance of polymer films - part i: measurement method evaluation and statistical considerations on area-dependence,” *IEEE Trans. Dielectr. Electr. Insul.*, vol. 22, no. 2, pp. 689–700, Apr. 2015.

[12] W. Hauschild and W. Mosch, *Statistical Techniques for High-Voltage Engineering*. The Institution of Engineering and Technology, Michael Faraday House, Six Hills Way, Stevenage SG1 2AY, UK: IET, 1992.

[13] S. Laihonen, U. Gafvert, T. Schutte, and U. Gedde, “DC breakdown strength of polypropylene films: area dependence and statistical behavior,” *IEEE Trans. Dielectr. Electr. Insul.*, vol. 14, no. 2, pp. 275–286, Apr. 2007.

[14] T. Umemura and K. Akiyama, “Accelerated-Life Testing of Power Capacitor Dielectric Systems,” *IEEE Trans. Electr. Insul.*, vol. EI-22, no. 3, pp. 309–316, Jun. 1987.

[15] L. A. Dissado and J. C. Fothergill, *Electrical Degradation and Breakdown in Polymers*. The Institution of Engineering and Technology, Michael Faraday House, Six Hills Way, Stevenage SG1 2AY, UK: IET, 1992.

[16] K. Lau, A. Vaughan, G. Chen, I. Hosier, A. Holt, and K. Ching, “On the space charge and DC breakdown behavior of polyethylene/silica nanocomposites,” *IEEE Trans. Dielectr. Electr. Insul.*, vol. 21, no. 1, pp. 340–351, Feb. 2014.

[17] T. Blythe and D. Bloor, *Electrical Properties of Polymers*. New York: Cambridge University Press, 2005.

Publication IV

M. Ritamäki, I. Rytöluoto, K. Lahti, T. Vestberg, S. Pasanen, and T. Flyktman, "Large-area Approach to Evaluate DC Electro-thermal Ageing Behavior of BOPP Thin Films for Capacitor Insulation Systems," in *IEEE Transactions on Dielectrics and Electrical Insulation*, vol. 24, no. 2, pp. 826–836, 2018.

DOI: 10.1109/TDEI.2017.006405

The following paper is the final version accepted for publication in IEEE Transactions on Dielectrics and Electrical Insulation. The published version of this paper is available at IEEE Xplore.

Large-area Approach to Evaluate DC Electro-thermal Ageing Behavior of BOPP Thin Films for Capacitor Insulation Systems

Mikael Ritamäki, Ilkka Rytöluoto, Kari Lahti
Tampere University of Technology
Department of Electrical Engineering
P.O. Box 692
FI-33101 Tampere, Finland

Torvald Vestberg
Borealis Polymers Oy
P.O. Box 330,
FI-06101 Porvoo, Finland

Satu Pasanen and **Timo Flyktman**
VTT Technical Research Centre of Finland Ltd
P.O. Box 1300
FI-33101 Tampere, Finland

ABSTRACT

A large-area electro-thermal ageing test setup was developed and utilized to age several laboratory-scale biaxially oriented polypropylene (BOPP)–hydrophobic silica nanocomposite films. The films were aged in test capacitors with self-healing metallized film electrodes, which enabled the ageing test to continue beyond the first breakdowns. Eight different films were aged for 1000 hours under 100 V/µm DC stress at 75 °C, and large-area DC breakdown measurements, dielectric spectroscopy, gel permeation chromatography (GPC), differential scanning calorimetry (DSC) and dielectric spectroscopy were used to detect localized and bulk degradation after the ageing period. The effects of antioxidant contents, different PP grades and compounder screw speed were evaluated. Material characterization indicates no bulk degradation had occurred during ageing, which was associated with moderate temperature stress and inert nitrogen atmosphere. On the other hand, low-field breakdowns (weak points) were observed in all but two of the aged materials, indicating that ageing was dominated by localized degradation which may have introduced new breakdown mechanisms. Weak points were also measured in a similarly aged commercial capacitor-grade BOPP film aged at a lower field, supporting this conclusion. The importance of long-term characterization in material development is demonstrated, and it is shown that long-term properties of the evaluated nanocomposites were at least on the same level compared to neat BOPP films.

Index Terms — **Aging, films, polymers, electric breakdown, nanocomposites, dielectric measurement, dielectric spectroscopy, thermal analysis, molecular weight.**

1 INTRODUCTION

AGEING of electrical insulation, as presented by Fothergill in [1] is a continuous process taking place throughout insulation during its service life. Ageing may lead to degradation, which in turn can lead to electric breakdown during service life, and so the three are mutually linked. In addition to changes in breakdown behavior [2], [3] ageing of polymeric capacitor insulation systems has been associated with chemical and physical changes, examples of which include oxidation and changing morphological properties, elongation [4, 5], molecular-weight distribution and crystallinity [6, 7]. Another important factor is space charge accumulation, which can be seen both as a result and a cause of ageing [8]. For power capacitors individual breakdowns of the film dielectrics are not always fatal, as the insulations can be made defect-tolerant by the use of self-healing metallized electrodes [9], [10]. However the causal link between ageing and breakdown makes it possible to use changes in breakdown behavior as an indicator of ageing progression. In

Manuscript received 19 October 2016, in final form 3 January 2017, accepted 1 February 2017. Corresponding author: M. Ritamäki.

[11] it has been reported that in general the breakdown strength of insulation remains rather unchanged, only to decrease drastically in the final moments before breakdown. More specifically for capacitor dielectric films increasing or decreasing overall breakdown strengths and weak point formation have been reported in [5]. While the breakdown strength of insulation tends to follow the Weibull distribution [12], weak point formation justifying the use of multiple Weibull subpopulations indicates ageing may introduce new breakdown mechanisms [13].

Appearance of low-probability low-field breakdowns or 'weak points' in AC electrothermally aged polypropylene (PP) film capacitor elements has been demonsrated in the recent work of Guillermin et al [14]. In their work this was associated with partial discharging (PD) at the film edges above an electric field threshold due to field enhancement effects. In general accelerated ageing experiments should be conducted using stress levels which do not introduce new ageing mechanisms, such as PD, which has been reported to be the fastest ageing mechanism of polymeric insulation [15, 16]. Appearance of weak points in PP film combined with an increase in its characteristic breakdown strength has been reported by Umemura et al [5] for films aged in PP/kraft paper (KP)/PP multilayer model capacitors for 370 days at 1.4× nominal voltage and 90 °C, in which the weak points were associated with a non–specified morphological change. On the other hand Sebillotte et al [2] report no significant changes in the breakdown behavior of PP sheets AC aged in pure impregnating liquids for 1800 hours at 80 °C. Presence of oxygen and/or additives however decreased the breakdown strength depending on the the liquid used. The effect of impregnation on the ageing beeohavior of PP films is hardly suprising, since physical interactions such as swelling and dissolution between impregnating liquid and PP have been reported in literature [4, 9, 17]. For low and medium voltage capacitors thin metallized electrodes are often used [10]. This provides defect-tolerancy via electrode self-healing, but degradation, principally corrosion of this thin metallization has been reported [10, 18, 19] as one of the dominant ageing phenomena in such capacitors. Because of different ageing phenomena in different types of capacitors, and also due to the effects of capacitor manufacturing, the ageing of film insulation systems cannot be determined solely by the film property, necessitating endurance testing of finalized capacitor products, as outlined in IEC 60871-2 [20].

At present at least two unknows have been introduced in the field of ageing in polymeric capacitor insulations: new insulating materials [21], such as polymer nanocomposites (PNCs) [22] and nonsinusoidal waveforms, such as DC and repeating voltage transients [16]. Research on polymer nanocomposite systems [23, 24] have shown different ageing behavior compared to neat materials and the (nano)particle interfaces may introduce new degradation mechanisms [25, 26]. Ongoing research [27] at TUT has also revealed differences in the DC voltage endurance coefficient of BOPP-hydrophobic silica nanocomposites compared to neat materials. PNCs have also shown improved electrical properties, viz. enhanced partial discharge resistance [28, 29]. Improved partial discharge resistance is especially beneficial as electrical insulations, capacitors included, are nowadays utilized in applications where repetitive voltage transients from power electronics are present, which have been associated with non-conventional and highly accelerated ageing behavior [15], [16, 30].

Material development would benefit from a practical way to evaluate the long-term properties of laboratory scale materials before expensive and time-consuming pilot-line production. Accurate evaluation of the long-term properties of a polymer-based film is however complicated, requiring knowledge of which type of capacitor it will be used in and also to what kind of stresses it will be subjected to. During material development these are rarely feasible. Properly wound up model capacitors would also require more film than can be produced using laboratory-scale film stretchers. The use of traditional metal foil is also problematic, as ageing tests cannot usually continue beyond the first permanent breakdowns.

The need to evaluate the long-term properties of laboratory-scale materials has led to the development of an ageing test system using stacked plate-type capacitors with self-healing metallized film electrodes. The system was used to age several BOPP-silica nanocomposites under 100 V/µm DC stress at 75 °C for 1000 hours, followed by extensive material characterization to detect ageing-induced changes. Two types of isotactic PP were compounded with hydrophobic fumed silica, and for one PP type compounder screw speed and antioxidant contents were varied.

2 EXPERIMENTAL DETAILS

2.1 MATERIAL DETAILS

The laboratory scale materials were produced at VTT Technical Research Centre of Finland Ltd. Two grades of isotactic polypropylene provided by Borealis Polymers Oy, PP1 and PP2, were used as the base materials. 0.9 wt% of hydrophobic fumed silica Aerosil® R 812 S was added in the nano-silica compounds. Aerosil® R 812 S is a fumed silica aftertreated with hexamethyldisilazane (HMDS). 0.35 wt% of Irganox 1010 powder antioxidant and 0.0075 wt% of calcium stearate was added to all compounds. In antioxidant series the effects of low (0.20 wt%, PP1-LoAO) and high (0.60 wt%, PP1-HiAO) antioxidant contents were evaluated. The raw materials were dried at 70 °C and vacuum treated before processing. All the materials were compounded similarly with a Berstorff ZE 25/48D twin-screw compounder using a highly mixing screw configuration and same processing parameters, therefore the materials share the same thermal history. In one of the trials, the compounder screw speed was varied from the nominal 300 1/min, resulting in the low (PP1-LoSS, 200 1/min) and high (PP1-HiSS, 350 1/min) screw speed variants. The materials details and processing parameters are summarized in Table 1.

The compounder strands were cooled, pelletized and dried and thereafter extruded into cast films with a Brabender Plasticorder extruder using a flat die. To prevent contamination, compounding and cast film extrusion were done in a clean room environment and the machines were cleaned before processing. All the cast films were similar in appearance. Cast films were biaxially oriented (stretching ratio of 5.8 × 5.8) with a Brückner KARO IV biaxial stretcher

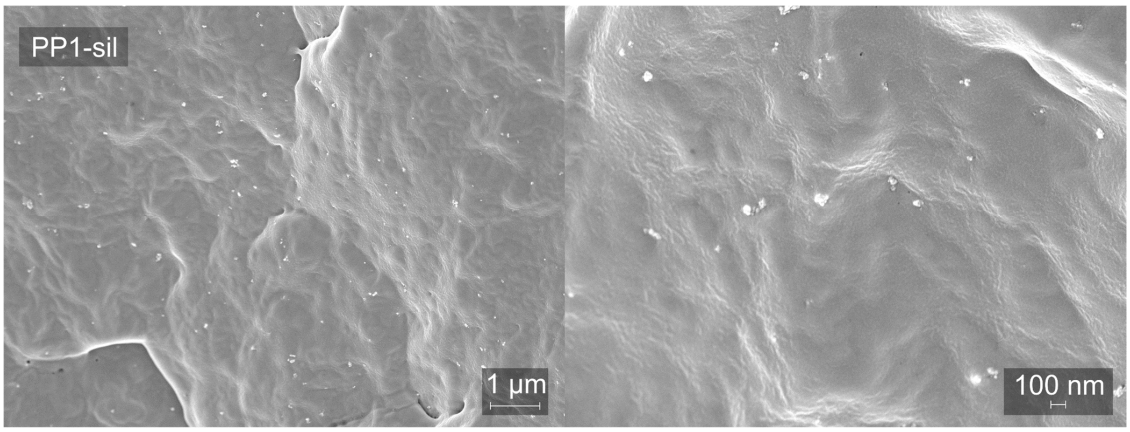

Figure 1. Cross-sectional SEM images of cryofractured PP1-sil (0.9 wt% silica) cast film at two zoom levels, taken at VTT Technical Research Centre of Finland Ltd. These images were representative of the nanoparticle distribution and dispersion in all of the evaluated nanocomposites. The effects of screw speed variation were not clear. Nanoparticle distribution and dispersion were adequate and similar to what has been measured in our earlier nanocomposite research projects using the same hydrophobic fumed silica.

at the set temperature of 161°C, except films PP1-HiSS and PP2-LoSS, which were oriented at the set temperature of 157°C. PP1-HiSS oriented at 161 °C had a significantly decreased large-area breakdown strength and it was decided to re-do PP1-LoSS at 157 °C as well for reference purposes. This was associated with excessive melting during orientation, which had also manifested in significantly decreased stretching forces. Material details are presented in Table 1. The average thicknesses of the reference samples demonstrate that the target thickness of ≤ 10 µm was reached. Cast film samples of the nanocomposite materials were cryofractured in liquid nitrogen and the nanoparticle dispersions were evaluated by cross-sectional imaging of the samples by Zeiss® Merlin-42-63 field-emission scanning electron microscope (FE-SEM). There were no clear differences between the materials, and the overall dispersion was considered adequate and in line with our previous results [31] using the same hydrophobic silica. Representative SEM images of PP1-sil are presented in Figure 1.

In addition to the laboratory-scale films, a commercial 14.4 µm capacitor-grade BOPP film was aged both thermally and electro-thermally. This film is the same used in our earlier thermal ageing experiments in [32], [33]. Film rolls were stored under normal room temperature conditions.

2.2 SAMPLE PREPARATION AND TEST CAPACITORS

Film samples were prepared for use as dielectrics in test capacitors. The test capacitor dielectric was either four 110 mm × 145 mm samples from laboratory-scale films or a 300 mm × 400 mm sheet of the commercial capacitor-grade film. Four 380 mm × 90 mm sheets of commercial Zn-Al metallized capacitor-grade 12 µm BOPP film were used as electrodes, the self-healing capability of which enabled the test capacitors to tolerate breakdowns during ageing [3, 34]. The film arrangement resulted in an active area of approximately 400 cm^2. This also left an at least 10 mm free margin around the film samples. The test capacitors were sandwiched between two 3 mm thick 400 mm × 400 mm glass plates. In preliminary high temperature tests in ambient air the metallized BOPP electrode film adhered to the glass plates. To prevent this, A4-sized 100 µm polyester sheets were placed between test capacitor and the glass plates. The ageing test capacitor structure is depicted in Figure 2a.

20 test capacitors were produced; 16 using laboratory-scale materials and 4 using the commercial capacitor-grade film. The test capacitors were loaded into two custom-made test racks and the protruding metalized film edges were sandwiched between two flat aluminum bars. To evaluate the effects of thermal stress only, additional sheets of the commercial capacitor-grade film were placed on top of the test rack assembly in paper envelopes.

2.3 AGEING SETUP

The ageing test circuit, illustrated Figure 2b, was designed to minimize the demetallized area during self-healings which is related to the inverse of self-healing energy, which in turn is inversely proportional to the capacitance partaking in the self-healing process [3]. This capacitance was decreased by connecting the high voltage bar electrodes to a common feedthrough via 10 kΩ low inductance thick film resistors. Test voltage was supplied via Keithley 2290E-5 high voltage

Table 1. Specifications of the laboratory-scale materials evaluated. All the materials were produced at VTT Technical Research Centre of Finland Ltd.

Material	Nanosilica (wt%)	Antioxidant (wt%)	Screw speed	Bi-axial stretching ratio	Bi-axial orientation set temperature (°C)	Film thickness (µm) Mean	SD
PP1-ref	-	0.35	normal	5.8 × 5.8	161	9.97	1.01
PP2-ref	-	0.35	normal	5.8 × 5.8	161	10.24	0.87
PP1-sil	0.9	0.35	normal	5.8 × 5.8	161	8.47	0.79
PP2-sil	0.9	0.35	normal	5.8 × 5.8	161	9.49	0.78
PP1-LoAO	-	0.2	normal	5.8 × 5.8	161	8.96	0.99
PP1-HiAO	-	0.6	normal	5.8 × 5.8	161	10.31	0.84
PP1-LoSS	0.9	0.35	low	5.8 × 5.8	157	9.59	0.76
PP1-HiSS	0.9	0.35	high	5.8 × 5.8	157	9.16	0.65

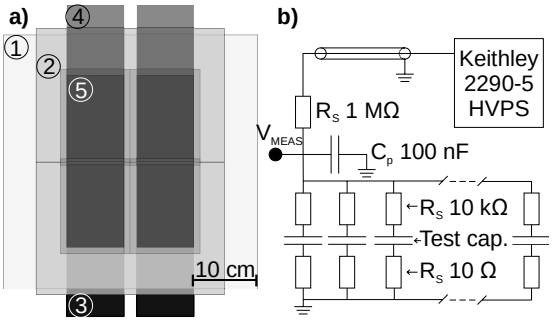

Figure 2. Ageing experiment test capacitor **(a)** and circuit **(b)**. Parts: (1) glass plates (2) polyester support films, two on each side (3) bottom electrode BOPP films (4) top electrode films (5) four film samples. For commercial capacitor-grade film four samples were replaced with one large sheet. Voltage was measured from V_{MEAS}.

power supply (HVPS) having a manufacturer reported maximum output ripple of 0.1 V_{RMS}. An external RC-filter was used to smooth out transients. Test voltage was ramped up in 50 V increments, giving the HVPS current, monitored via the HVPS current meter (resolution of 0.001 mA), time to stabilize after each step. This was done to limit the inrush current to the highly capacitive load and to prevent degradation of the metallized electrode film – aluminum electrode interface caused by Joule heating in the resistive aluminum oxide layers.

The test capacitor racks were placed in a gas-tight environmental chamber or 'oven' detailed in [33], and a constant nitrogen flow of approximately 40 ml/min was fed into the oven through an Aalborg flowmeter to prevent ambient oxygen and moisture from seeping in. During the first 72 hours over 500 liters of nitrogen was fed into the oven to displace air inside. To push air out from between the film layers a voltage of 340 V was applied to the test capacitors during this period, which in preliminary tests had been deemed sufficient to remove visible air bubbles from between film layers. Temperature was maintained with two 400 W heaters and a cross-flow fan, the latter being necessary in reducing the temperature gradient [33]. The ageing setup is illustrated in Figure 3.

After ageing the capacitances of the individual test capacitors were measured (at 1 kHz and 2 V_{AC}) with GW Instek LCR-8101G LCR meter. The results are reported in Table 2. The measured capacitances were in line with the film thicknesses, which is interpreted to indicate proper adhesion of electrode and sample films. The series resistance of the test capacitors varied considerably not only between samples but also between consecutive measurements on the same test capacitors. This is presumed to result from contact issues caused by aluminum oxidation.

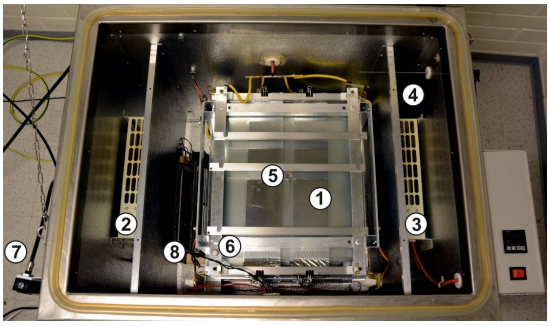

Figure 3. Ageing test setup, parts shown: (1) test racks; (2 & 3) heaters; (4) controller PT100 sensor; (5 & 6) temperature loggers placed on top; (7) nitrogen regulator and flowmeter; (8) cross-flow fan.

2.4 ELECTRO-THERMAL STRESS LEVELS

Target electro-thermal stress levels were 100 V/µm for laboratory-scale films and 75 °C. Oven temperatures were recorded from bottom, middle and top of the test racks with iButton temperature loggers every three hours. Based on these measurements the temperature accuracy was estimated to be better than 0.5 °C and temperature variations after initial stabilization were minimal.

The test voltage of 950 V was determined based on the average thickness (9.52 µm) of the reference laboratory-scale samples, as the thickness of aged samples was determined after ageing. This was done to avoid any extra film handling before the ageing experiment. Voltage was measured with a North Star High Voltage PVM-1 1:2000 probe and a Fluke 179 multimeter, which after stabilization indicated a voltage of 948.6 V. Realized electric field stress levels were determined from the 81 cm^2 samples to be measured using the large-area breakdown measurement [35–37], more detailed in subsection 2.6. LE1000-1 high-precision thickness gauge with a manufacturer-reported accuracy of 0.1 µm and a ball-point measurement tip was used for all the thickness measurements, and only the thicknesses from areas with breakdowns during the breakdown measurement were used for the calculation of mean thickness. The material-specific electric field stress levels are reported in Figure 4.

2.5 AGEING TEST PROGRESSION

The test duration of 1000 hours at the target stress levels was loosely based on IEC TS 60871-2 [20]. The initial 72-hour gas exchange period took place at room temperature, after which the heating was turned on together with the full test voltage. Temperature logs indicate that the oven temperature stabilized to 75 °C after 5 hours. The PID controller had been tuned beforehand and thus no significant overshoot was expected.

After 1000 hours the supply side of the RC filter was grounded and the oven was let to cool for several days. Grounding was done via its 1 MΩ resistance to give space charge time to dissipate as based on literature rapid grounding of energized XLPE cables has been associated with electrical

Table 2. Features of test capacitors after ageing: number of self-healing breakdowns and series capacitances and -resistances. Electrical parameters were measured at 1 kHz and 2 V_{AC}. Resistive component varied between measurements, which is interpreted to indicate imperfect contact at the bar electrode – metallization interface.

Cap.	Material	BDs	C_S (nF)	R_S (Ω)	Cap.	Material	BDs	C_S (nF)	R_S (Ω)
1	PP1-ref	0	95	212	11	PP1-HiAO	0	93	93
2	PP1-ref	0	88	73	12	PP1-HiAO	0	98	165
3	PP2-ref	1	84	173	13	PP1-LoSS	1	98	75
4	PP2-ref	0	82	133	14	PP1-LoSS	2	92	86
5	PP1-sil	5	107	40	15	PP1-HiSS	1	90	23
6	PP1-sil	0	110	89	16	PP1-HiSS	1	92	73
7	PP2-sil	0	89	386	17	cap-BOPP	0	67	86
8	PP2-sil	0	92	47	18	cap-BOPP	0	64	122
9	PP1-LoAO	2	92	185	19	cap-BOPP	0	66	130
10	PP1-LoAO	2	100	50	20	cap-BOPP	0	63	76

degradation (treeing) [38]. Nitrogen flow remained on until room temperature was reached. Logs indicate that the gas temperature had dropped below 30 °C in 20 hours

The test capacitors were visually inspected for breakdowns. Laboratory-scale materials had a total of 15 breakdowns and the commercial capacitor-grade film had none. The breakdowns were located seemingly randomly on the film surface, with no breakdowns at electrode edges. The amount of breakdowns in each test capacitor has been presented in Table 2.

The test circuit was fitted with discharge logging system capable of measuring µs-scale current pulses in individual test capacitors. As a discharge or a breakdown took place, the dissipated energy would be replaced by a fast current pulse. These pulses would be detected by actively comparing the voltage difference across the 10 Ω low-inductance resistors to an adjustable voltage reference. The 20-channel measurement circuit consisted of peak hold rectifiers, comparators and a FPGA-based detector. Based on initial testing this setup would be capable of detecting pulses with amplitude of approximately 100 mA.

Analysis of the recorded data indicated excessive discharging in test capacitors 2 (80 events) and 4 (105 events). Visual inspection of these aged samples however revealed that neither of these samples had any breakdown holes. This discrepancy indicated that discharging may have taken place in the aluminum bar – metallized film electrode. This was further supported by discernible demetallization in the film-bar interface regions.

2.6 MATERIAL CHARACTERIZATION

Large-area DC breakdown behavior of all the materials and the complex dielectric permittivity of the laboratory-scale materials was measured before and after ageing. Additionally, differential scanning calorimetry (DSC) and gel permeation chromatography (GPC) measurements were conducted for all the PP1-based materials.

Breakdown measurements were conducted using large-area multiple breakdown methodology detailed in e.g. [35]–[37]. 12 µm metallized BOPP film was used as electrodes and measurements were conducted in dielectric oil (Shell Oil Diala). A fast voltage ramp-up of 400 V/s up to 2 kV followed by a slower ramp at 30 V/s was used, and measurement was continued until no breakdowns were detected.

A self-healing discharge energy and breakdown voltage –based data qualification procedure detailed in e.g. [37] was used to validate each recorded event. For laboratory-scale films the breakdown fields were determined manually by combining the 25-point thickness data with a video recording of the measurement. To reach a both statistically and visually adequate fit the qualified events were fitted to either single two-parameter or additively mixed two-subpopulation Weibull-distributions [13]. For a few materials individual outliers were excluded from Weibull parameter estimation to reach an adequate fit with the large majority of data points.

The complex dielectric permittivity of reference and aged laboratory scale films was measured using Novocontrol Alpha A –analyzer. Measurements were done using a shielded sample cell BDS 1200 with a test voltage of 1 V_{RMS}, the sample being sandwiched between gold-plated 40 mm Ø bottom and 10 mm Ø top electrodes. Golden electrodes (d=50 nm) with a diameter of 12 mm were evaporated on two approximately 32 × 32 mm film samples using Leybold L560E E-Beam evaporator. Before evaporation the samples were dried overnight in a vacuum flask at 35 °C, then washed twice in 2-propanol and fastened to a metal sample holder, with the latter two steps conducted in a clean room to prevent contamination by airborne particles. For accurate determination of the relative permittivity, the thicknesses of the samples were measured from four points around the evaporated electrode.

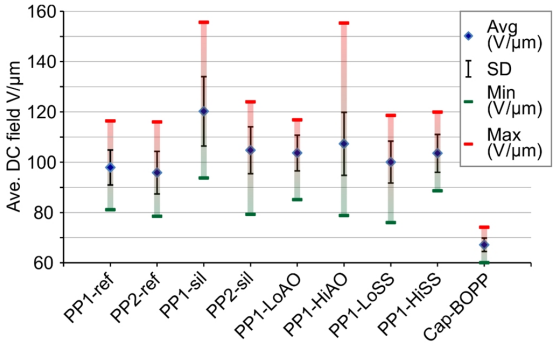

Figure 4. Electric field stresses for different material, with averages, extreme values and standard deviations. Target field for laboratory-scale materials was 100 V/µm.

To evaluate the repeatability of the measurement two samples of each film were prepared and measured twice. The average and standard deviation of these four measurements 50 Hz are reported. For some materials one of the two samples had a hole, recognized by indentures and loss characteristics typical of surface conduction [39] (other sample displaying rather flat loss levels in the measured frequency range). The measurement data from the broken samples was not used in any of the analyses.

3 RESULTS

3.1 LAB-SCALE MATERIALS

The Weibull distributions of the large-area multiple breakdown measurement results of laboratory-scale materials are presented in Figure 5 and their distribution parameters are given in Table 4. The absolute values of relative permittivity and the loss tangent (tan δ) at 50 Hz together with the results from DSC and GPC measurements on PP1 materials are presented in Table 3. Of the DSC measurement melting T_m and crystallization T_{cr} temperatures and the calculated degree of crystallinity X_c are presented. Of the GPC results the number- M_n, weight- M_w, z- M_z and viscocity- M_v averaged molar masses, the polydispersity PD and antioxidant contents in ppm are reported.

3.2 COMMERCIAL BOPP FILM

The Weibull distributions from large-area multiple breakdown measurements on reference, electro-thermally aged and also thermally aged commercial capacitor-grade film are presented in Figure 6 and the Weibull distribution parameters are shown in Table 5. The reference measurements consist of 30 samples while the thermal and electro-thermally aged results are from 12 and 11 samples respectively. Due to the uniform thickness profile in the

commercial capacitor-grade films no manual thickness correction was used. The reference measurement results have been previously presented in [32], [33].

4 DISCUSSION

4.1 LABORATORY-SCALE MATERIALS

The large-area DC breakdown strength of the neat PP and the nanocomposite films was in line with our earlier studies [31, 37] using the same hydrophobic silica. The overall large-area breakdown strength was also in line with the commercial BOPP film, and also largely in line with what is reported for eight non-metallized BOPP films in [37]. The breakdown behavior of all materials was homogeneous, despite the one statistically insignificant outlying low-field breakdown in PP1-sil and PP2-sil references. Of the nanosilica series (Figure 5a) PP2-sil had the highest breakdown characteristic strength, yet this apparent improvement was accompanied with a decreased distribution homogeneity compared to the other materials of the series. From the antioxidant series the low antioxidant variant had slightly decreased breakdown strength, but more interestingly the breakdown strength of the high-AO variant was in line with the reference. This was also the case in the screw speed series, where the low variant was slightly lower. All in all the overall differences between the materials were considered small compared to for example the effects of increasing silica content beyond 1 % [31].

The small amount (0.9 wt%) of silica was chosen since increasing nanosilica filler loading has been associated with decreasing characteristic breakdown strength in BOPP-silica nanocomposite films [31] and also in polyethylene matrices [40]. The hydrophobicity of the silica limits water absorption, recognized as one of the main challenges in nanodielectrics research and which has been associated with deteriorating dielectric properties [25] and sources therein. A commercial product available in large quantities was used for its suitability for pilot and industrial-scale manufacturing. The compounder screw speed trial was based on our earlier studies with 4.5 wt% hydrophobic silica BOPP-nanocomposites [41], where decreased screw speed resulted in significantly higher overall breakdown strength. In this study however no such clear effect was observed, which may be associated with lower silica loading.

The complex dieletric permittivity of the silica- and screw speed series reference materials was similar, indicating that neither the addition of 0.9 wt% nano-silica nor the screw speed markedly affect the loss levels. However PP1-LoAO from the antioxidant series, both reference and aged, had the lowest dielectric loss levels in the frequency range of 0.1–100k Hz. The decrease in the loss levels with a lighter antioxidant loading was in line with the study of Umemura *et al.* [42], based on which more pronounced differences could be expected if measurements were repeated at elevated temperature.

Notable differences can be seen in the DSC-results of the screw speed series, with both variants, but especially PP1-HiSS displaying a lower degree of crystallinity accompanied with lower melting and crystallization temperatures. This explains the difficulties in successfully bi-axially orienting these films at 161 °C (Subsection 2.2). Worth mentioning is also that a similar, albeit slighter, decrease was measurable between PP1-ref and PP1-sil. The degree of crystallinity does not however correlate with the dielectric loss levels or the DC large-area dielectric breakdown strength, contrary to [43] where lower dielectric loss levels are reported for a high crystallinity BOPP film. The GPC results however do not indicate significant changes in the averaged molecular weights, which may indicate that the differences in DSC results originate from morphological changes. It is therefore postulated, that in future the orientation parameters should be optimized individually for each material to obtain the best and most representative dielectric performance for each material.

4.2 EFFECTS OF AGEING

Distinct differences in the DC large-area breakdown behavior were seen between the electro-thermally aged and the reference films. The characteristic 63.2 % breakdown strength of all the materials had decreased after electro-thermal ageing, and all of them except PP1-HiAO and PP1-HiSS displayed curvature towards lower fields in the low probability region. The two aforementioned materials in turn displayed increased scatter in breakdown voltages, and thus significantly decreased Weibull β. For capacitor applications

Table 3. Physical and electrical properties of the laboratory-scale films: melting and crystallization temperatures and total crystallinity from DSC measurements; molar masses, polydispersity and amount of antioxidants from on GPC measurements and complex dielectric permittivity at 50 Hz. Electro-thermal DC ageing did not significantly affect these bulk material properties. **) only one sample was measured.*

Not aged	T_m °C	T_{cr} °C	X_c %	*Mn /1000*	*Mw /1000*	*Mz /1000*	*Mv /1000*	*PD*	*Antioxidants (ppm)*	$\lvert\varepsilon_r\rvert$ *(50 Hz)*	*SD*	$\tan\delta$ *(×10⁻⁴) (50 Hz)*	*SD (×10⁻⁴)*
PP1-ref	159.9	115.5	48	56.4	257	600	223	4.57	2350	2.10	*-	7.0	0.1
PP2-ref										2.13	0.04	5.8	0.7
PP1-sil	159.6	114.6	47	58.3	256	596	221	4.39	2140	2.11	*-	5.9	0.1
PP2-sil										2.12	0.01	4.5	0.3
PP1-LoAO	159.0	116.3	47	47.0	232	509	202	4.93	840	2.15	0.01	3.6	0.2
PP1-HiAO	158.9	114.2	45	59.6	260	608	224	4.36	3430	2.18	0.01	6.6	0.2
PP1-LoSS	156.3	113.1	44	55.1	263	646	226	4.78	2910	2.11	0.00	5.0	0.2
PP1-HiSS	156.7	112.6	41	53.5	234	551	202	4.36	3600	2.06	0.02	7.4	0.1
Aged													
PP1-ref	160.6	115.6	44	57.9	259	596	221	4.47	2340	2.15	0.03	6.0	0.7
PP2-ref										2.18	0.02	4.3	0.9
PP1-sil	160.8	114.6	44	59.6	260	595	225	4.35	2320	2.19	0.03	5.6	0.5
PP2-sil										2.16	0.01	4.5	0.1
PP1-LoAO	158.6	116.9	48	58.3	239	529	209	4.09	1180	2.18	0.01	4.2	0.3
PP1-HiAO	158.3	114.7	45	61.8	268	642	231	4.33	4130	2.20	0.01	5.6	0.1
PP1-LoSS	157.7	113.4	43	54.6	272	697	232	4.98	3040	2.16	0.02	4.7	0.3
PP1-HiSS	155.0	113.4	41	53.8	229	528	198	4.26	2950	2.18	0.00	5.4	0.6

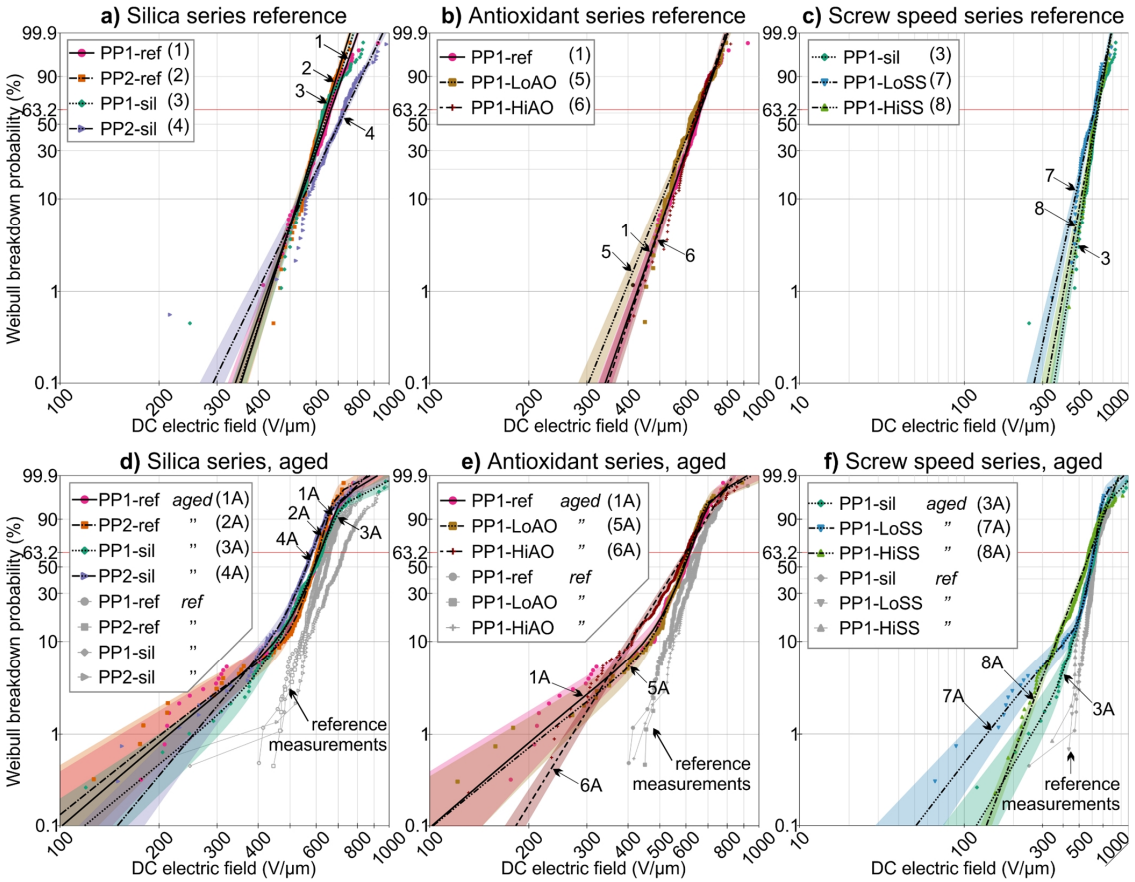

Figure 5. Large-area DC multi-breakdown performance of aged and reference films. a & d) The effects of two grades of PP base polymer and 0.9 wt-% of hydrophobic nano-silica. Low-field weak points are seen in all four aged material, and in comparison with the other three the characteristic breakdown strength of PP2-sil decreased rather notably. b & e) The effects of high and low antioxidant contents and c & f) the effects of high and low compounder screw speed.

the weak points are the most interesting, albeit difficult to measure in statistically significant quantities using traditional small-area single-breakdown methods. However, the large-area measurement method used is capable of detecting these statistically rare events. Similar 'weak point' formation has been reported in neat BOPP films thermally aged using a 1000 hour step stress from 50 to 110 °C [32, 33], in which however weak points were not measured after the highest stresses, raising questions whether the changes were 'ageing' or thermal conditioning or if they were related to varying film quality.

It is remarkable that the PP1 based nanocomposites displayed similar breakdown behavior compared to its un-filled reference, even though referring to Figure 4 PP1-sil was aged in a higher mean electric field. This may indicate that PP1-silica is more resistant to ageing compared to its un-filled reference. One possible explanation could be improved partial discharge (PD) resistance in silica-filled material [29], but this cannot be verified since the PD levels in the test capacitors were not measured, and since although silica filler has been associated with improved PD resistance, it is not known if this benefit remains with small (0.9 wt%) amounts of silica. On the contrary the breakdown strength of the aged PP2-sil film was slightly lower than its un-filled reference, in comparison with reference measurements in which PP2-sil demonstrated highest breakdown strength. This illustrates the importance of both long-term testing and evaluating different PP grades when preparing nanocomposites.

No changes in the bulk material properties were detected in the aged film samples, as demonstrated by the essentially unchanged GPC and DSC measurement results. GPC measurements would have indicated if the average molecular weight had changed, which would have indicated that chain scission or crosslinking had occurred. However, based on the results in Table 3 it is evident that neither of the aforementioned had occurred in significant quantity. The variations seen may as well result from measurement uncertainty, caused by a limited quantity of aged film used in the analyses. This is also suspected to be the prime reason behind the apparent *increase* of antioxidant contents in the majority of the aged materials. Nevertheless, it is clear that non-significant antioxidant consumption took place during electro-thermal ageing. The DSC measurements indicate that the degree of crystallinity was not affected by electro-thermal DC ageing.

The complex dielectric permittivity over a broad frequency range (~0.1–100 kHz) of the laboratory-scale materials remained unchanged, and was essentially the same for all the materials apart from PP1-LoAo which displayed lower

Table 4. Weibull distribution parameters for large-area DC breakdown measurements on the laboratory-scale films.

Material	*Reference*			*Electro-thermally aged*						
	Points	*α*	*β*	*Points*	*Portion*	*α₁*	*β₁*	*Portion*	*α₂*	*β₂*
PP1-ref	143	666	10.3	217	0.18	542	3.1	0.82	622	11.0
PP2-ref	154	644	11.6	215	0.14	504	2.9	0.86	612	14.4
PP1-sil	154	655	11.1	265	0.14	623	3.0	0.86	617	9.3
PP2-sil	124	738	7.4	227	0.34	572	4.3	0.66	585	12.5
PP1-LoAO	149	652	9.0	228	0.15	554	3.0	0.85	612	11.6
PP1-HiAO	128	662	10.7	302		599	5.8			
PP1-LoSS	102	645	9.8	228	0.18	465	2.4	0.82	620	12.8
PP1-HiSS	82	617	8.2	304		583	4.8			

overall loss levels. The differences between the two measurements on individual samples were minimal, but the differences between the two samples measured were in many occasion in the same scale as the differences between materials. As such it can be concluded that with the possible exception of the antioxidant contents neither of the process variations had major effect on the real permittivity or dielectric loss levels. This confirms that ageing, at least within this scope, does not markedly affect the dielectric loss levels. Nevertheless, together the aforementioned results assert that the ageing had no significant effect on the bulk material. In comparison significant morphological changes have been reported [6] in BOPP films thermally aged for 60 days at 150 °C in SF_6 gas. These changes were detected using DSC and GPC measurements and were also associated with changed dielectric response. This confirms that such changes *can* be measured using the methods used, but also that 75 °C was probably not high enough to induce such changes.

None of these measurements can however provide information on any localized degradation which has been associated with polymer ageing [3, 32]. Limited and localized degradation could explain the 'weak points' measured in the aged films, but on the other hand the decrease of the characteristic breakdown strength, which could indicate changing intrinsic properties, remains unaccounted for.

Low-probability low voltage breakdowns or 'weak points' were also measured in the electro-thermally aged commercial BOPP film. This suggests that localized degradation similar

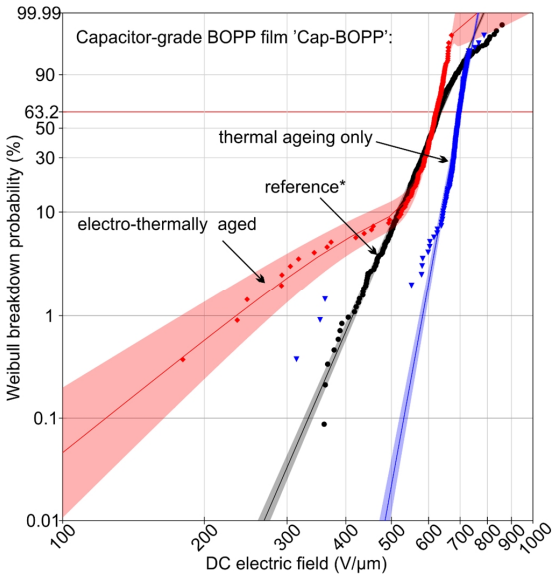

Figure 6. Large-area breakdown behavior of a commercial BOPP film: breakdown strength increased with thermal ageing while electro-thermal ageing resulted in weak point formation. Reference results are from [32], [33].

to the laboratory-scale films had taken place. On the other hand, the thermally only aged commercial film samples displayed an increase in overall breakdown strength, similar behavior has been reported for one thermally aged commercial BOPP film in [33]. Worth mentioning is also that the film thickness was not affected by the thermal stressing, indicating that no shrinkage had occurred. This behavior may however be related to annealing effects rather than true 'ageing', especially considering the relatively short duration of 1000 hours when compared to capacitor service lives, often measured in decades.

4.3 AGEING TEST

The function of the ageing test system used was not to perfectly imitate conditions found in real capacitors, but to subject several different films to similar stresses for a prolonged period, and to use the differences in material properties after ageing as a guideline in further material development. The ageing test system fulfilled these purposes, since the differences in the breakdown behavior between aged and reference samples, especially the weak point formation clearly indicate measurable ageing had occurred, despite no changes in bulk material property were measured in DSC and GPC. The next step is to apply the methodology to AC ageing, although care is needed to prevent partial discharging whose deleterious effects on BOPP films have been demonstrated recently at TUT [44] and also in related literature [45].

One possible source of uncertainty in the ageing system used is the success in removing the ambient air. Atmospheric air containing oxygen and moisture may have been 'trapped' between the metalized electrode films and the dielectrics. The presence of oxygen has been linked with accelerated degradation and the appearance of low-field weak points [2], [46]. In the latter degradation has been associated with radical-oxidation reactions progressing non uniformly, resulting in localized degradation and the weak points. Worth mentioning is also that in [47] it has been proposed that ageing of polymeric insulation in air would be representative (albeit accelerated) of ageing in oxygen-free environments. However in [46] oxygen-accelerated reactions have been also associated with *notably* lower mean molecular weight due to chain scissions, contrary to what was measured in this study. This, combined with the result that no antioxidant depletion had occurred seem to indicate the air removal was indeed

Table 5. Weibull distribution parameters for Cap-BOPP:

	Points	*Portion*	*α₁*	*β₁*	*Portion*	*α₂*	*β₂*
Reference	793		-		1	638	10.6
Electro-thermally aged	185	0.11	448	3.7	0.89	627	23.5
Thermally aged	183		-		1	700	25.1

successful. Based on [46] FTIR measurements would however be useful in confirming this further.

5 CONCLUSIONS

A new type of large-area electro-thermal ageing test system for polymer thin films was designed, assembled and evaluated successfully. Self-healing metallized electrodes enabled the ageing test to continue beyond the first breakdowns, and in principle would have enabled collection of times-to-breakdown data, although in practice this was hampered by possible non-breakdown discharging elsewhere in the system.

The ageing test system was used in a long-term DC ageing test, the results of which suggest that localized degradation in BOPP and BOPP-silica nanocomposite films during ageing results in the formation of low-field breakdowns or "weak points". No changes in bulk material properties were measured with DSC, GPC and dielectric spectroscopy, as such the large-area breakdown methodology from [31, [35–37] was proven especially suitable in evaluating the effects of thin film ageing.

Eight laboratory-scale films were stressed for 1000 hours at 75 °C and 100 V/µm. In multiple cases the relative order of goodness of the films reversed after ageing, demonstrating the importance of long-term characterization during material development. The effect of two PP grades, the addition of 0.9 wt% of hydrophobic nano-silica, compounder screw speed and antioxidant contents were evaluated. Slight differences were detected between materials, and more importantly it was proven that it was possible to reproduce the results from earlier projects, in which laboratory-scale BOPP-nanocomposites having large-area DC breakdown strength comparable to neat BOPP films and commercial capacitor-grade products were produced successfully. Moreover, the oriented nanocomposite films had similar dielectric loss levels to the neat PP materials. Together these results suggest that BOPP-silica nanocomposites may have long-term properties comparable to neat BOPP films.

ACKNOWLEDGMENT

The authors gratefully acknowledge financial support from Borealis and the approval to publish this research.

REFERENCES

[1] J. C. Fothergill, "Ageing, Space Charge and Nanodielectrics: Ten Things We Don't Know About Dielectrics," IEEE Int'l. Conf. Solid Dielectr., pp. 1–10, 2007.

[2] E. Sebillotte, S. Theoleyre, S. Said, B. Gosse, and J. P. Gosse, "AC degradation of impregnated polypropylene films," IEEE Trans. Electr. Insul., Vol. 27, No. 3, pp. 557–565, 1992.

[3] C. W. Reed and S. W. Cichanowskil, "The fundamentals of aging in HV polymer-film capacitors," IEEE Trans. Dielectr. Electr. Insul., Vol. 1, No. 5, pp. 904–922, 1994.

[4] Y. Yoshida and M. Nishimatsu, "Power Capacitors," IEEE Trans. Electr. Insul., Vol. 21, No. 6, pp. 963–973, 1986.

[5] T. Umemura and K. Akiyama, "Accelerated-Life Testing of Power Capacitor Dielectric Systems," IEEE Trans. Electr. Insul., Vol. 22, No. 3, pp. 309–316, 1987.

[6] T. Umemura, K. Abe, K. Akiyama, and D. Couderc, "Thermal-Aging Behavior of Bo-Pp Films," IEEE Trans. Electr. Insul., Vol. 22, No. 6, pp. 735–743, 1987.

[7] M. C. Ratra, H. N. Nagamani, and S. Ganga, "Ageing of impregnated polypropylene film for capacitor application under combined electrical and thermal stress," IEEE Conf. Electr. Insul. Dielectr. Phenomena, pp. 295–300, 1990.

[8] G. Mazzanti, G. C. Montanari, and L. A. Dissado, "Electrical aging and life models: the role of space charge," IEEE Trans. Dielectr. Electr. Insul., Vol. 12, No. 5, pp. 876–890, 2005.

[9] A. Schneuwly, P. Groning, L. Schlapbach, C. Irrgang, and J. Vogt, "Breakdown behavior of oil-impregnated polypropylene as dielectric in film capacitors," IEEE Trans. Dielectr. Electr. Insul., Vol. 5, No. 6, pp. 862–868, 1998.

[10] D. Shaw, S. Cichanowski, and A. Yializis, "A Changing Capacitor Technology - Failure Mechanisms and Design Innovations," IEEE Trans. Electr. Insul., Vol. 16, No. 5, pp. 399–413, 1981.

[11] G. C. Montanari, G. Mazzanti, and L. Simoni, "Progress in electrothermal life modeling of electrical insulation during the last decades," IEEE Trans. Dielectr. Electr. Insul., Vol. 9, No. 5, pp. 730–745, 2002.

[12] "IEC/IEEE Guide for the Statistical Analysis of Electrical Insulation Breakdown Data (Adoption of IEEE Std 930-2004)," IEC 62539 First Edition 2007-07 IEEE 930. 2007.

[13] W. Hauschild and W. Mosch, *Statistical Techniques for High-Voltage Engineering*, The Institution of Engineering and Technology, Michael Faraday House, Six Hills Way, Stevenage SG1 2AY, UK: IET, 1992.

[14] C. Guillermin and S. Fontana, "Breakdown strength of impregnated capacitor elements," IEEE 1st Int'l. Conf. Dielectr., pp. 634–637, 2016.

[15] A. Cavallini, D. Fabiani, and G. Montanari, "Power electronics and electrical insulation systems - Part 2: life modeling for insulation design," IEEE Electr. Insul. Mag., Vol. 26, No. 4, pp. 33–39, 2010.

[16] G. C. Montanari, D. Fabiani, P. Morshuis, and L. Dissado, "Why residual life estimation and maintenance strategies for electrical insulation systems have to rely upon condition monitoring," IEEE Trans. Dielectr. Electr. Insul., Vol. 23, No. 3, pp. 1375–1385, 2016.

[17] A. M. Andreyev, N. M. Zhuravleva, and M. Yevtich, "Degradation of the impregnated polypropylene insulation of power capacitors under operating conditions," Electr. Technol. Russ., Issue 3, pp. 96–106, 2002.

[18] R. W. Brown, "Modeling of Capacitor Parameters Related to the Metal Film Layer With Partial Edge Disconnection," IEEE Trans. Components Packag. Technol., Vol. 30, No. 4, pp. 774–780, 2007.

[19] R. W. Brown, "Linking Corrosion and Catastrophic Failure in Low-Power Metallized Polypropylene Capacitors," IEEE Trans. Device Mater. Reliab., Vol. 6, No. 2, pp. 326–333, 2006.

[20] IEC, "CEI IEC TS 60871-2 Technical Specification,Shunt capacitors for a.c. power systems having a rated voltage above 1 000 V – Part 2: Endurance testing." 1999.

[21] T. D. Huan, S. Boggs, G. Teyssedre, C. Laurent, M. Cakmak, S. Kumar, and R. Ramprasad, "Advanced polymeric dielectrics for high energy density applications," Prog. Mater. Sci., Vol. 83, pp. 236–269, 2016.

[22] J. K. Nelson, *Dielectric Polymer Nanocomposites*, Boston, MA: Springer, USA, 2010.

[23] P. Preetha, M. Thomas, and R. Ranjan, "Electrothermal ageing of epoxy nanocomposites," IEEE Trans. Dielectr. Electr. Insul., Vol. 19, No. 6, pp. 2081–2089, Dec. 2012.

[24] P. Preetha and M. J. Thomas, "Life estimation of electrothermally stressed epoxy nanocomposites," IEEE Trans. Dielectr. Electr. Insul., Vol. 21, No. 3, pp. 1154–1160, 2014.

[25] K. Y. Lau, A. S. Vaughan, and G. Chen, "Nanodielectrics: opportunities and challenges," IEEE Electr. Insul. Mag., Vol. 31, No. 4, pp. 45–54, 2015.

[26] S. W. Rowe, "Electrical Ageing of Composites: An Industrial Perspective," IEEE Int'l. Conf. Solid Dielectr., pp. 401–406, 2007.

[27] I. Rytöluoto, M. Ritamäki, K. Lahti, and M. Karttunen, "DC ramp rate effect on the breakdown response of SiO_2-BOPP nanocomposites," IEEE 11th Int'l. Conf. Properties Applications Dielectr. Materials (ICPADM), pp. 496–499, 2015.

[28] T. Tanaka, Y. Ohki, M. Ochi, M. Harada, and T. Imai, "Enhanced partial discharge resistance of epoxy/clay nanocomposite prepared by newly developed organic modification and solubilization methods," IEEE Trans. Dielectr. Electr. Insul., Vol. 15, No. 1, pp. 81–89, 2008.

[29] M. Takala, H. Ranta, P. Nevalainen, P. Pakonen, J. Pelto, M. Karttunen, S. Virtanen, V. Koivu, M. Pettersson, B. Sonerud, and K. Kannus, "Dielectric properties and partial discharge endurance of polypropylene-silica nanocomposite," IEEE Trans. Dielectr. Electr. Insul., Vol. 17, No. 4, pp. 1259–1267, 2010.

[30] A. Cavallini, D. Fabiani, and G. Montanari, "Power electronics and electrical insulation systems - Part 1: Phenomenology overview," IEEE Electr. Insul. Mag., Vol. 26, No. 3, pp. 7–15, 2010.

[31] I. Rytöluoto, K. Lahti, M. Karttunen, M. Koponen, S. Virtanen, and M. Pettersson, "Large-area dielectric breakdown performance of

polymer films – Part II: Interdependence of filler content, processing and breakdown performance in polypropylene-silica nanocomposites," IEEE Trans. Dielectr. Electr. Insul., Vol. 22, No. 4, pp. 2196–2206, 2015.
[32] M. Ritamäki, I. Rytöluoto, K. Lahti, and M. Karttunen, "Effects of thermal aging on the characteristic breakdown behavior of Nano-SiO_2-BOPP and BOPP films," IEEE 11th Int'l. Conf. Properties Applications Dielectr. Materials (ICPADM), pp. 400–403, 2015.
[33] M. Ritamäki, *Effects Of Thermal Aging On Polymer Thin Film Insulations For Capacitor Applications*, M.Sc. thesis, Tampere University of Technology, 2014.
[34] M. Rabuffi and G. Picci, "Status quo and future prospects for metallized polypropylene energy storage capacitors," IEEE Trans. Plasma Sci., Vol. 30, No. 5, pp. 1939–1942, 2002.
[35] I. Rytöluoto, K. Lahti, M. Karttunen, and M. Koponen, "Large-area dielectric breakdown performance of polymer films – Part I: Measurement method evaluation and statistical considerations on area-dependence," IEEE Trans. Dielectr. Electr. Insul., Vol. 22, No. 2, pp. 689–700, 2015.
[36] I. Rytöluoto and K. Lahti, "New approach to evaluate area-dependent breakdown characteristics of dielectric polymer films," IEEE Trans. Dielectr. Electr. Insul., Vol. 20, No. 3, pp. 937–946, 2013.
[37] I. Rytöluoto, *Large-Area Multi-Breakdown Characterization of Polymer Films: A New Approach for Establishing Structure–Processing–Breakdown Relationships in Capacitor Dielectrics*, Ph.D. thesis, Tampere University of Technology, 2016.
[38] L. A. Dissado and J. C. Fothergill, Electrical Degradation and Breakdown in Polymers. The Institution of Engineering and Technology, Michael Faraday House, Six Hills Way, Stevenage SG1 2AY, UK: IET, 1992.
[39] L. Frenkel, "On the Measurement of Dielectric Losses and Surface Conductivity of Dielectrics in Parallel Plane Test Capacitors," J. Res. Natl. Bur. Stand. - A. Phys. Chem., Vol. 68A, No. 2, pp. 185–188, 1964.
[40] K. Y. Lau, *Structure and Electrical Properties of Silica-based Polyethylene Nanocomposites*, Ph.D. thesis, University of Southampton, UK, 2013.
[41] I. Rytöluoto, K. Lahti, M. Ritamäki, and M. Karttunen, "The Role of Film Processing in the Large-Area Dielectric Breakdown Performance of Nano-Silica-BOPP Films," in 24th Nordic Insulation Sympos. Materials, Components and Diagnostics (NORD-IS), pp. 63–68, 2015.
[42] T. Umemura, T. Suzuki, and T. Kashiwazaki, "Impurity Effect of the Dielectric Properties of Isotactic Polypropylene," IEEE Trans. Electr. Insul., Vol. 17, No. 4, pp. 300–305, 1982.
[43] A. Kahouli, O. Gallot-Lavallee, P. Rain, O. Lesaint, C. Guillermin, and J.-M. Lupin, "A comparison of electric and dielectric properties of standard and high-crystallinity polypropylene films," IEEE Int'l. Conf. Solid Dielectrics (ICSD), pp. 23–26, 2013.
[44] M. Ritamäki, I. Rytöluoto, M. Niittymäki, K. Lahti, and M. Karttunen, "Differences in AC and DC large-area breakdown behavior of polymer thin films," IEEE Int'l. Conf. Dielectr. (ICD), pp. 1011–1014, 2016.
[45] S. Chniba and R. Tobazeon, "Long term breakdown of polypropylene films," IEEE First Int'l. Conf. Conduction Breakdown Solid Dielectr., pp. 433–438, 1983.
[46] B. Gosse, J. P. Gosse, S. Saïd, A. Gadoum, and M. Nemamcha, "Electrical degradation of polypropylene: A study by FTIR microspectroscopy," J. Appl. Polym. Sci., Vol. 46, No. 6, pp. 1121–1124, 1992.
[47] A. Gadoum, B. Gosse, and J. P. Gosse, "AC aging of impregnated polypropylene films: Effect of oxygen," IEEE 11th Int'l. Conf. Conduction Breakdown Dielectr. Liquids (ICDL), pp. 461–466, 1993.

Mikael Ritamäki (S'15) was born in Tampere, Finland in 1990. He received the M.Sc. (Tech.) degree in electrical engineering from Tampere University of Technology, Tampere, Finland in 2014. Since 2015 he has been working as a Researcher in the high voltage research group of the Department of Electrical Engineering at TUT, with aim towards the D.Sc. (Tech.) degree. His current research interests include electro-thermal ageing of polymeric insulations and dielectric characterization of thin films.

Ilkka Rytöluoto (S'13-M'16) was born in Tampere, Finland on 17 April 1985. He received the M.Sc. (Tech.) and Doctoral degrees in electrical engineering from Tampere University of Technology (TUT), Tampere, Finland in 2011 and 2016, respectively. Since 2011 he has been working at the Department of Electrical Engineering at TUT, currently as a post-doctoral researcher. His main research interests are in the field of high voltage and insulation material engineering, including e.g. dielectric characterization of polymeric thin films and establishing processing–structure–dielectric property relationships in polymer nanocomposite- and capacitor films.

Kari Lahti (M'01) was born in Hämeenlinna, Finland in 1968. He received the M.Sc. and Doctoral degrees in electrical engineering from Tampere University of Technology in 1994 and 2003, respectively. Since then he has worked at the Department of Electrical Engineering at TUT, currently as a Research Manager and Adjunct Professor. He is the head of TUT's research group on high voltage insulation systems. He has also been responsible for the high voltage laboratory services at TUT since 2002. His research interests are in the area of high voltage engineering including surge arresters, nanocomposite insulation systems, environmental testing of high voltage materials and apparatus, high voltage testing methods and dielectric characterization of insulating materials.

Torvald Vestberg was born Petalax, Finland in 1957. He received the M.Sc degree in chemical engineering and Doctoral degree in polymer technology from Åbo Akademi University in 1983 and 2013, respectively. He has been working with Borealis the last 20 years where he holds a group expert position. His area of interest is Ziegler-Natta catalysed polymerisation of propylene as well as effect of polymerization conditions on polymer structure and properties.

Satu Pasanen was born in Tampere, Finland in 1977. She received the B.Sc. (Tech.) in chemical engineering from the Tampere University of Applied Sciences, Tampere, Finland in 2001 and M.Sc. (Tech.) in Plastic and elastomer technology (including biomaterials) from Tampere University of Technology (TUT), Tampere, Finland in 2010. Since 2001 she has worked at VTT first as a Research Engineer and later as a Research Scientist. Her main research interests are nanocomposites, functional polymer composites, polymer film applications, electrical applications and recycling & reuse of waste materials.

Timo Flyktman was born in Tampere, Finland in 1977. He received the B.Sc. (Tech.) degree in electrical engineering from Tampere University of Applied Sciences, Tampere, Finland in 2003. Since 2002 he has been working as a Research Engineer at VTT. His main research interests are plastic processing, plastic film applications, sensor technology and electrical applications.

Publication V

M. Ritamäki, I. Rytöluoto and K. Lahti, "High Temperature and Ageing Test Methods to Characterize the Dielectric Properties of BOPP Capacitor Films," in *2017 IEEE Conference on Electrical Insulation and Dielectric Phenomenon (CEIDP)*, pp. 266–269, 2017.

DOI: 10.1109/CEIDP.2017.8257518

The following paper is the final version accepted for publication in the proceedings of 2017 IEEE Conference on Electrical Insulation and Dielectric Phenomenon (CEIDP). The published version of this paper is available at IEEE Xplore.

High Temperature and Ageing Test Methods to Characterize the Dielectric Properties of BOPP Capacitor Films

Mikael Ritamäki, Ilkka Rytöluoto, Kari Lahti
Tampere University of Technology
Electrical Energy Engineering
P.O. Box 692
FI-33101 Tampere, Finland

***Abstract*- A large-area high temperature breakdown measurement and an ageing test method are presented. These methods facilitate the development of reliable higher energy density film capacitors by exploiting large measurement areas to provide information on weak point formation and subtle changes in breakdown behavior after electro-thermal or thermal ageing. The test methods were used to characterize two types of highly isotactic biaxially oriented polypropylene capacitor films, which had similar breakdown behavior at room temperature, but different breakdown properties at high temperature and out of which one was more susceptible to electro-thermal DC ageing.**

I. INTRODUCTION

Large-area breakdown tests and electro-thermal ageing tests during material development are used to evaluate effects, which limit the energy density of assembled capacitors far below any theoretical values calculated from small-area breakdown strength and permittivity. These mechanisms include the decrease of breakdown strength when insulation area [1], temperature [2] or duration of applied voltage [3] is increased.

Today state-of-the-art power capacitors utilize biaxially oriented isotactic polypropylene (BOPP) as the main insulation. By using high purity base materials a low dielectric loss factor ($\tan\delta \sim 10^{-4}$) [4] and with optimized film processing [5] a small-area breakdown strength above 700 V/µm are achieved. Moreover, the capacitance of BOPP capacitors remains constant over a wide temperature range. These convincing dielectric properties however come at a cost of larger physical size, as the available energy density is constricted by the relatively low dielectric constant of BOPP (2.22–2.25) [6].

There is a continuing effort to manufacture higher energy density capacitors demanded for high energy- and power density applications, such as voltage source converters (VSCs) in wind turbines and offshore AC/DC converter stations. Energy density can be increased either by developing materials which can withstand higher electric fields during operation or by using higher permittivity dielectrics [7]. Increasing the operating field improves the energy density in a power of two, while for increased permittivity the increase is only linear. Moreover, a look at a list of common dielectric plastics reveals that higher permittivity often comes at a cost of increased dielectric losses, which limits the energy density through the limited service temperature [8].

This paper presents our recent progress in developing and evaluating suitable and reproducible test methods to rank the dielectric performance of different capacitors films. In this study, two BOPP films from highly isotactic PP grades were evaluated, yet similar methods could also be used to characterize other dielectric films with self-healing capability. Properties of the films were determined using room- and high temperature large-area multiple breakdown measurements and DC electro-thermal and thermal ageing tests. The high temperature test method is further developed from [9] and the ageing test methodology is featured in a recent TDEI article [10]. The effects of ageing were characterized with wide-angle x-ray scattering (WAXS), differential scanning calorimetry (DSC) and large-area multiple breakdown measurements.

II. EXPERIMENTAL DETAILS

A. Capacitor materials tested

Two industrially produced BOPP films based on highly isotactic polypropylene grades with different molecular weights were characterized. The films were provided as film rolls and later on referred as PP-1 and PP-2. The average thicknesses of the both film were approximately 5.6 µm with a standard deviation of 0.1 µm.

B. Large-Area Multiple Breakdown Measurement

The large-area DC breakdown strength of the films was measured at room temperature and 100 °C using methodology detailed in e.g. [5]. Similar measurements at room temperature were also done on intact portions of electro-thermally and thermally aged films, as changes in breakdown behavior is an indicator of insulation ageing [11], with large measured areas revealing possible weak point formation or localized degradation. All breakdown measurements were done in ambient air.

Reference and high-temperature breakdown measurements were done on 12 samples and 6 samples of aged materials were measured. Each sample had an active area of 81 cm^2. A commercial 12-µm Zn-Al metallized BOPP film was used as

electrodes and a voltage ramp of 30 V/s was applied to the "test capacitor" until no more discharges were detected.

Proper and independent breakdowns were selected from all recorded discharge events using a self-healing energy and voltage –based data qualification procedure [5]. Breakdown fields were calculated using the average thickness of the film samples and fitted with either single two-parameter or additively mixed two-subpopulation Weibull distributions. The first breakdowns from the reference measurements were also reviewed using video recordings and any possible non-breakdown discharges were manually removed in order to ensure highest reliability BDS results.

C. High Temperature Breakdown Measurement

Breakdown strength measurements at 100 °C were conducted in a 0.125 m^3 test chamber, heated with 800 W PID-controlled heaters. As an improvement to our earlier high temperature large-area measurements [9], the temperature accuracy was improved by using an 800 W hot plate to heat the test fixture. The temperature of the test fixture was monitored in real time, and temperatures on top of the hotplate and test fixture were used to evaluate temperature gradient. The temperature accuracy was estimated to be better than ± 1.5 °C. The warm-up period before measurements was approximately 15 minutes.

C. DC Electro-Thermal Ageing Test

The ageing test was designed to simulate real capacitors where thermal and electrical stresses are present and the exposure to oxygen and moisture is limited. Oxidative degradation has been linked to decreasing breakdown strength of BOPP films [12], [13], against which capacitors are protected with vacuum impregnated oil or epoxy encapsulation. Based on IEC 60871-2 [14] the ageing test duration was 1000 hours (41 ⅔ days), and target stress levels were 100 °C and 100 V/µm for half and 100 °C and 200 V/µm for the rest of the samples. These were in the range of operating fields of metallized film PP capacitors [15] and in the < 1% probability range in 100 °C breakdown measurements. At the same time sheets of film were also aged thermally in the oven.

Eight parallel-plate test capacitors, as depicted in Fig 1a, were constructed from both materials. Metallized polyethylene naphthalate (PEN) films (1) were used as electrodes and the assembly was supported by 100 µm polyester films (2). The capacitors were sandwiched between two 3 mm × 400 mm × 400 mm glass plates and installed in test racks. The connections to Keithley 2290-5 power supplies and ground were realized by clamping the protruding edges of the electrode films between two aluminum bars (3).

An initial preconditioning step was done to expunge air from between the film layers. This consisted of energizing at 40 V_{DC}/µm for 24 hours during which the chamber was flooded with inert nitrogen gas. A nitrogen flow was maintained during ageing to retain overpressure and prevent air from leaking in. Nevertheless, the presence of trace air cannot be ruled out, as some air may have been left between the supporting polyester and glass layers. However, a limited supply of air and moisture may be trapped between the layers of dry-type film capacitors during winding [16].

The test voltages of 561 and 1122 V_{DC} were applied after preconditioning and the chamber was heated to 100 °C. Temperature recorders inside the chamber indicated that the temperature stabilized to 96–100 °C after 8 hours, but after a cross-flow fan inside the oven broke at 600 hours the temperatures dropped to 90–94 °C. After ageing the capacitors were short-circuited and let to cool for a several days before further characterization.

III. Results and Discussion

The Weibull distributions from large-area DC multiple breakdown measurements at room temperature (RT) and 100 °C (HT) measurements are displayed in Fig. 2a with results from thermo-electrically and thermally aged films displayed in Fig. 2b. Only films aged at 100 V/µm could characterized, as those aged under 200 V/µm were destroyed by discharge activity, and no samples could be prepared from them. In the first days of the measurement, relentless self-healing activity in 200 V/µm capacitors was suspected since the supply current remained unstable for the first days of measurement, after which occasion current spikes were detected. Visual post-ageing inspection confirmed separation of active electrode areas caused by extensive demetallization, which was probably followed by occasional DC corona discharges. The damage is illustrated in Fig 1b The results was rather surprising, since the 200 V/µm is still below those encountered in high energy density PP capacitors [15].

The materials had high initial crystallinity, which increased further due to thermally induced secondary crystallization [17] as evident in WAXS and DSC measurements summarized in Table I. The increased degree of crystallinity is also reflected in increasing melt peak temperatures, but presumably due to dominating ageing mechanism did not result in increasing breakdown strength. WAXS verified that the BOPP films contained only monoclinic α-form, as expected since β-form crystallinity in cast films, if any, transforms to α-form during biaxial orientation process [18].

Both non-aged films had similar breakdown behavior at room temperature and their characteristic 63.2% breakdown strength of 792–794 V/µm was high compared to other commercial and pilot-scale films measured using similar techniques, reported in e.g. [5]. Single Weibull distributions fit the RT data well, which suggest that one breakdown mechanism was operating [19].

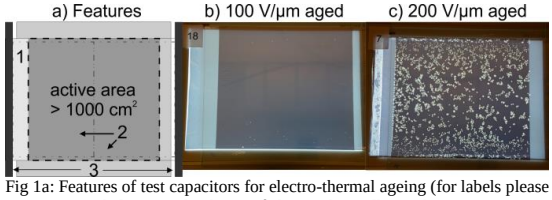

Fig 1a: Features of test capacitors for electro-thermal ageing (for labels please see text) and 1b: example photos of electro-thermally aged test capacitors. Capacitors aged at 200 V/µm were destroyed by self-healing breakdowns while those aged at 100 V/µm had a few isolated clearing.

TABLE I
THERMAL, MORPHOLOGICAL AND DIELECTRICAL FEATURES OF CAPACITOR INSULATION FILMS TESTED

	Melt onset °C	Melt peak °C	Crystallinity X_C (DSC)%	Crystallinity X_C (WAXS)%	63.2% breakdown strength (V/µm)	Breakdown points
PP-1 reference RT	154.5	166.6	60.3%	67.5%	792	277
PP-1 100 °C					633	351
PP-1 thermal	168.0	168.5	71.5%	76.3%	747	153
PP-1 thermo-electrical 100 V/µm	165.8	168.0	69.1%	73.7%	677	234
PP-2 reference RT	157.0	166.2	60.3%	65.5%	794	325
PP-2 100 °C					607	504
PP-2 thermal	167.4	169.0	66.8%	74.7%	721	126
PP-2 thermo-electrical 100 V/µm	169.6	170.0	68.8%	73.1%	718	245

At 100 °C the characteristic breakdown strength of both films decreased by approx. 18%, and differences between the films became evident, with PP-2 demonstrating lower breakdown fields in the 5–50% probability range. Nevertheless, both films still displayed similar breakdown behavior in the few percent probability region that may be the most interesting for practical capacitor applications.

The ~18% decrease in characteristic breakdown strength from RT to 100 °C is high compared to literature value of 11% presented in [2] or in our earlier studies [9]. This does not seem be related to the degree of crystallinity as the relative degrees of crystallinity, both from DSC and WAXS measurements is close to the 61% reported in [20]. The DSC-based crystallinity is also high compared to 53% reported for high crystallinity BOPP film in [21]. In this sense, the relationship between crystallinity and high temperature breakdown strength seems to differ from HDPE, as reported in [22] and summarized in [17], lower crystallinity HDPE demonstrated higher breakdown strength at room temperature decreasing rapidly with increasing temperature and eventually falling below that of higher crystallinity materials.

Both electro-thermally aged materials had decreased characteristic breakdown strength compared to room temperature reference measurements and even more interestingly the Weibull distribution was curved, suggesting that ageing had introduced a second defect-dominated breakdown mechanism [17], [19]. A similar phenomenon had occurred in thermally aged PP-2, and possibly also in PP-1, but the scarcity of data points in the low probability regions makes statistical analysis unreliable. These findings are in line with our earlier electro-thermal ageing tests, where a defect subpopulation appeared in laboratory-scale BOPP and nanosilica materials aged for 1000 hours at 80 °C and 100 V/µm [10]. Similar weak point formation has been reported for thermally aged BOPP films in [23], and for capacitor-grade films aged under AC voltages in oxygen-statured oils [24]. Thus, degradation accelerated by trace oxygen cannot be ruled out.

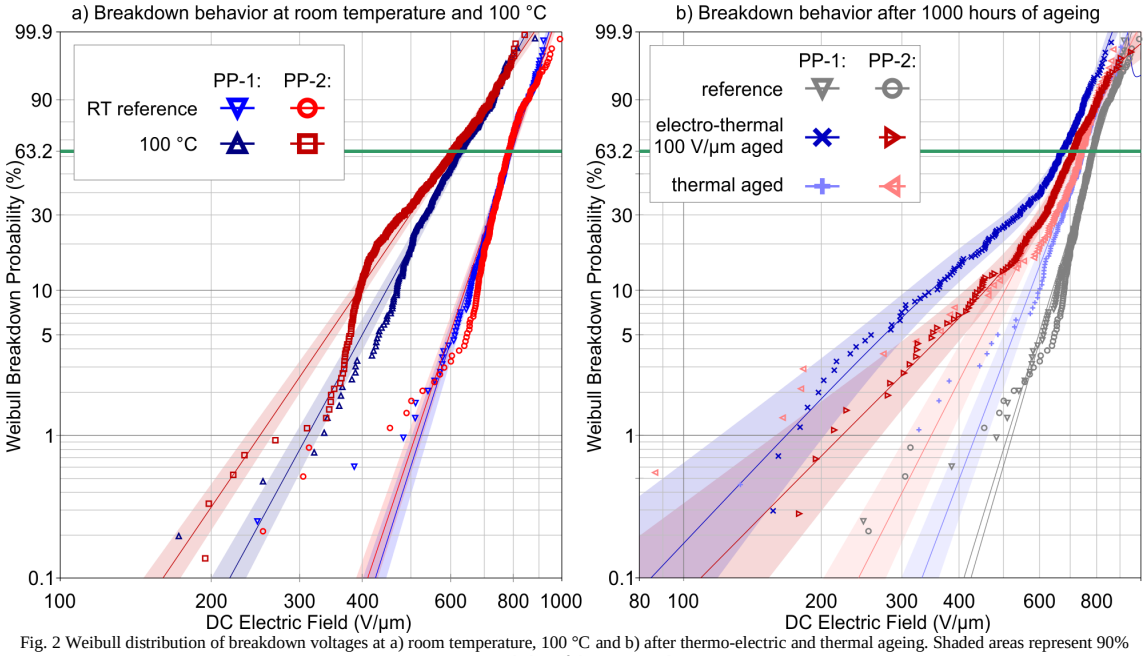

Fig. 2 Weibull distribution of breakdown voltages at a) room temperature, 100 °C and b) after thermo-electric and thermal ageing. Shaded areas represent 90% two-sided confidence intervals.

TABLE II
CAPACITANCES AND NUMBER OF BREAKDOWNS IN AGED CAPACITORS

		Capacitance (nF)	BD holes
Capacitors PP-1	1	293	53
	2	309	10
	3	294	9
	4	314	8
Capacitors PP-2	1	273	28
	2	289	26
	3	288	10
	4	286	22

The degree of ageing, as indicated by the number of self-healing breakdowns during long-term test was heavily dependent on the electric field stress: the 100 V/µm capacitors had relatively few breakdowns while the 200 V/µm units were destroyed by them. In literature [25] voltage stresses have also been shown to have a more negative effect on insulation life than temperature. The breakdowns were distributed rather evenly on the active areas, which calls into question major field enhancements at electrode edges. The number of breakdowns and capacitances in 100 V/µm test capacitors are reported in Table II. The capacitances were line in with the film thicknesses and active areas, from which it was deducted that no air gap existed between the film under test and electrodes. The capacitances were measured several days after voltage was turned off, revealing that the electrodes had adhered to the BOPP films. Lastly, no change in film thicknesses after ageing was detected in measurements with a precision thickness gauge (accuracy of 0.1 µm).

IV. CONCLUSIONS

BOPP films from highly isotactic base PP grades were compared. Breakdown measurements at high temperature and both thermal and thermo-electrical ageing tests brought forward differences in two BOPP films which displayed similar breakdown performance at room temperature. In breakdown measurements at 100 °C PP-1 film demonstrated slightly higher breakdown voltages but in thermo-electric ageing tests this "order of goodness" reversed, with aged samples of PP-2 material having higher breakdown strength. This highlights the importance of both high temperature and ageing tests during material research and development.

REFERENCES

[1] S. J. Laihonen, "Polypropylene: Morphology, Defects and Electrical Breakdown," D.Sc. Thesis, Kungliga Tekniska Högskolan, 2005.

[2] J. Ho and T. R. Jow, "High Field Conduction in Biaxially Oriented Polypropylene at Elevated Temperature," *IEEE Trans. Dielectr. Electr. Insul.*, vol. 19, no. 3, pp. 990–995, Jun. 2012.

[3] IEC 61251:2015 Electrical Insulating Materials and Systems - AC Voltage Endurance Evaluation, Edition 1.0. IEC standard, 2015.

[4] J. L. Nash, "Biaxially Oriented Polypropylene Film in Power Capacitors," *Polym. Eng. Sci.*, vol. 28, no. 13, pp. 862–870, Jul. 1988.

[5] I. Rytöluoto, "Large-Area Multi-Breakdown Characterization of Polymer Films: A New Approach for Establishing Structure–Processing–Breakdown Relationships in Capacitor Dielectrics," D.Sc. Thesis, Tampere University of Technology, 2016.

[6] R. P. Deshpande, *Capacitors*. McGraw-Hill Education, 2014.

[7] T. D. Huan, S. Boggs, G. Teyssedre, C. Laurent, M. Cakmak, S. Kumar, and R. Ramprasad, "Advanced polymeric dielectrics for high energy density applications," *Prog. Mater. Sci.*, vol. 83, pp. 236–269, Oct. 2016.

[8] M. Biron, Ed., *Material Selection for Thermoplastic Parts - Practical and Advanced Information for Plastics Engineers*. Elsevier, 2016.

[9] M. Ritamäki, I. Rytöluoto, and K. Lahti, "Temperature Effect on Breakdown Performance of Insulating Polymer Thin Films," in *24th Nordic Insulation Symposium on Materials, Components and Diagnostics (NORD-IS)*, 2015, pp. 75–79.

[10] M. Ritamäki, I. Rytöluoto, K. Lahti, T. Vestberg, S. Pasanen, and T. Flyktman, "Large-area Approach to Evaluate DC Electro-thermal Ageing Behavior of BOPP Thin Films for Capacitor Insulation Systems," *IEEE Trans. Dielectr. Electr. Insul.*, vol. 24, no. 2, pp. 826–836, Apr. 2017.

[11] C. W. Reed and S. W. Cichanowskil, "The Fundamentals of Aging in HV Polymer-film Capacitors," *IEEE Trans. Dielectr. Electr. Insul.*, vol. 1, no. 5, pp. 904–922, 1994.

[12] B. Gosse, J. P. Gosse, S. Saïd, A. Gadoum, and M. Nemamcha, "Electrical Degradation of Polypropylene: A Study by FTIR Microspectroscopy," *J. Appl. Polym. Sci.*, vol. 46, no. 6, pp. 1121–1124, Oct. 1992.

[13] A. Gadoum, B. Gosse, and J. P. Gosse, "AC Aging of Impregnated Polypropylene Films: Effect of Oxygen," in *Proceedings of 1993 IEEE 11th International Conference on Conduction and Breakdown in Dielectric Liquids (ICDL '93)*, 1993, pp. 461–466.

[14] CEI IEC TS 60871-2 Technical Specification, Shunt capacitors for a.c. power systems having a rated voltage above 1 000 V – Part 2: Endurance testing." 1999.

[15] R. Gallay, "Metallized Film Capacitor Lifetime Evaluation and Failure Mode Analysis," Geneva, 2014.

[16] Y. Chen, H. Li, F. Lin, F. Lv, Z. Li, and M. Zhang, "Effect of Interlayer Air on Performance of Dry-type Metalized Film Capacitor in DC, AC and Pulsed Applications," *IEEE Trans. Dielectr. Electr. Insul.*, vol. 18, no. 4, pp. 1301–1306, Aug. 2011.

[17] R. Bartnikas and R. Eichhorn, Eds., *Engineering Dielectrics Volume IIA Electrical Properties of Solid Insulating Materials: Molecular Structure and Electrical Behavior*. 100 Barr Harbor Drive, PO Box C700, West Conshohocken, PA 19428-2959: ASTM International, 1983.

[18] M. B. Elias, R. Machado, and S. V. Canevarolo, "Thermal and Dynamic-Mechanical Characterization of Uni- And Biaxially Oriented Polypropylene Films," *J. Therm. Anal. Calorim.*, vol. 59, no. 1/2, pp. 143–155, 2000.

[19] W. Hauschild and W. Mosch, *Statistical Techniques for High-Voltage Engineering*. The Institution of Engineering and Technology, Michael Faraday House, Six Hills Way, Stevenage SG1 2AY, UK: IET, 1992.

[20] J. Ho and R. Jow, "Characterization of High Temperature Polymer Thin Films for Power Conditioning Capacitors," Adelphi, MD 20783-1197, 2009.

[21] A. Kahouli, O. Gallot-Lavallée, P. Rain, O. Lesaint, C. Guillermin, and J. M. Lupin, "Dielectric features of two grades of bi-oriented isotactic polypropylene," *J. Appl. Polym. Sci.*, vol. 132, no. 28, pp. 1–5, 2015.

[22] H. Miyauchi and K. Yahagi, "Electronic Breakdown in Polyethylene Film in Room Temperature Range," *Trans. Inst. Electr. Eng. Japan. A*, vol. 92, no. 1, pp. 36–45, 1972.

[23] M. Ritamäki, "Effects of Thermal Aging on Polymer Thin Film Insulations for Capacitor Applications," M.Sc. thesis, Tampere University of Technology, 2014.

[24] E. Sebillotte, S. Theoleyre, S. Said, B. Gosse, and J. P. Gosse, "AC Degradation of Impregnated Polypropylene Films," *IEEE Trans. Electr. Insul.*, vol. 27, no. 3, pp. 557–565, Jun. 1992.

[25] A. Cavallini, D. Fabiani, and G. Montanari, "Power Electronics and Electrical Insulation Systems – Part 1: Phenomenology Overview," *IEEE Electr. Insul. Mag.*, vol. 26, no. 3, pp. 7–15, May 2010.

Publication VI

G.C. Montanari, P. Seri, M. Ritamäki, K. Lahti, I. Rytöluoto and M. Paajanen, "Performance of Nanoparticles in the Electrical Behavior of DC Capacitor Films," in *2018 IEEE 12th International Conference on the Properties and Applications of Dielectric Materials (ICPADM)*, pp. 41–44, 2018.

DOI: 10.1109/ICPADM.2018.8401024

The following paper is the final version accepted for publication in the proceedings of 2018 IEEE 12th International Conference on the Properties and Applications of Dielectric Materials (ICPADM). The published version of this paper is available at IEEE Xplore.

Performance of Nanoparticles in the Electrical Behavior of DC Capacitor Films

Gian Carlo Montanari[1,2], Paolo Seri[1], Mikael Ritamäki[3], Kari Lahti[3], Ilkka Rytöluoto[3] and Mika Paajanen[4]
[1]DEI, University of Bologna, Italy
[2]Center for Electromechanics, University of Texas, USA
[3]Tampere University of Technology, Electrical Energy Engineering, Tampere, Finland
[4]VTT Technical Research Centre of Finland Ltd., Tampere, Finland

***Abstract*— In this work space charge accumulation characteristics of nanostructured polypropylene films are investigated, providing preliminary results for the basis of the new materials formulations to be developed in the European project GRIDABLE, where novel MV and LV DC capacitor films having enhanced performance with respect to present polypropylene films are being developed. This paper shows that nanostructuration may be beneficial, especially at higher temperature, to improve material performance. Better space charge performance will help in optimizing the dielectric strength, design field and reliability of the insulation system for DC use.**

I. Introduction

As the use of DC technology is increasing in the transfer of electricity over long distances or in relation to integration of the renewable energy sites into the main grid, there are specific challenges with the traditionally used insulating materials. Voltage source converter (VSC) based DC technology is the newest and 'smartest' way for connecting both renewable energy production and stationary energy storage units into AC grids. In addition, VSC is utilized to transmit and distribute electrical energy over long distances or from DC energy sources to users. VSC technology, together with energy storage, improves the power quality, transient and voltage stability, reduces losses and increases power oscillation damping. Furthermore, self-commutation of VSC enables the so called black start, i.e. starting of power injection into a non-energized network, for example from stationary energy storage. This way VSC improves the overall reliability of the grid and VSC technology can also enable an increase in distributed energy source density, since otherwise power quality and stability issues normally limit the amount of distributed production in a network.

The technological and economic potential of voltage source converter based DC transmission technology can be further increased by introducing new advanced materials into these systems, specifically improving the performance of HVDC capacitor films commonly found in VSCs. However, long-term performance of such new nanostructured material needs careful investigation.

Accumulation of space charge can be the main degradation process in DC insulations, since it can distort and enhance the Laplacian electric field distribution inside insulation, thus bring the maximum electric field amplitude to exceed the design field. This would shorten considerably life compared to the requested performance, considering, in particular, that electrical life line of insulation systems can be described by an inverse power law, [1], thus a small variation of electric field translated into large variation of life (e.g. 5% field increase can shorter life of one order of magnitude) [2], [3].

If voltage polarity inversions phenomena are also present, the accumulation of homocharge (that is, charge having the same sign as that of the near electrode) can bring to further abnormal field distribution, which can affect apparatus reliability and life. Any material which has to be used as DC insulation, therefore, has to be characterized to be space charge free at the operating field and temperature. Nanostructuration can help increasing field and/or temperature above which space charge accumulation becomes large enough to accelerate local degradation mechanisms [2]-[7].

In this paper, space charge accumulation characteristics of filled and un-filled cast and BOPP films are compared under different temperatures.

II. Material specifications

The new DC insulation technology characterized in this work had been developed in previous studies [8]. It is a capacitor-grade isotactic polypropylene homopolymer matrix, with 4.5 wt-% of nanoparticles. An antioxidant package was added to prevent thermo-oxidative degradation of the PP-matrix during melt processing. An otherwise similar reference film was made without nanofillers. The thickness of the oriented films, Ref-BOPP and nanofilled BOPP (n-BOPP) are in the range of 15–18 μm. In addition to the oriented films, space charge in thick cast film specimens of similar films was studied. The cast films were from the reference and from two nanofilled PP grades with different screw speeds.

III. Space charge measurements

Space charge measurements were carried out by the Pulsed Electro-Acoustic (PEA) method. In the PEA method, a specimen is subject to the superposition of a DC voltage U0 and a pulsed voltage Up(t). While the application of DC voltage is responsible for the formation of space charge in the material, pulses are necessary to generate a perturbation on the electric field acting on those charges. The resulting electric force pulse on charges causes them to accelerate and interact with the surrounding dielectric material. Such interaction initiates two acoustic pressure waves travelling in opposite directions and parallel to the electric field orientation, through the thickness of the sample. The wave moving towards the ground electrode is transferred through the whole thickness of the electrode itself, finally being acquired by a piezoelectric sensor and translated into a voltage signal. In this method,

several factors limit the spatial resolution achievable. Pulse width, piezoelectric thickness and the bandwidth of the electronics utilized for signal amplification are the main limiting factors.

In this work two PEA systems were used, one for thick cast film samples and another for thin oriented films. Both systems utilize 10 ns pulses with an intensity of 300 V for thin films and 580 V for cast films. The acoustic signal is collected by a 9 μm thick PVDF piezoelectric and amplified by an amplifier cascade. The thin film system amplifier has a -3 dB bandwidth of 200 MHz. These features resulted in a spatial resolution of few tens of micrometers. This is comparable to the thickness of the specimens, therefore information on exact charge density vs. distance is partially lost, but a clear measurement of accumulated space charge during and after a period of polarization can be derived. Other interesting quantities can be extracted from space charge trends in depolarization, that is, apparent charge mobility and trap depth distribution [9]. Those are fundamental parameters for the characterization of insulating materials for DC applications, because the presence of space charge in the insulation can modify substantially the electric field distribution and, hence, the insulation life [1]-[7].

Calibration of the system is made after 10 s from polarization of the sample, through the following equations:

$$E(z) = \frac{\int_0^z \rho(z)dz}{\varepsilon}$$

$$\rho = \varepsilon E_{DC}$$

Where $E(z)$ and $\rho(z)$ are the electric field and the charge density in the thickness of the specimen, ε is the permittivity of the specimens tested and E_{DC} and ρ are the theoretical electric field and surface charge density when no space charge is accumulated in the sample. Stored charge density at a specific field and depolarization time, $q(E,t)$, derived from the space charge profile measurements, as follows:

$$q(E,t) = \frac{1}{L}\int_0^L \left| q_p(E,x,t)\,dx \right|$$

where 0 and L denote the electrodes positions and $q_p(E,x,t)$ is the space charge profile for a given poling field E.

Trap controlled apparent mobility can be roughly evaluated from the q vs t characteristic as [9]:

$$\mu(t) = \frac{\varepsilon}{q^2(t)}\frac{dq(t)}{dt}$$

where $q(t)$ is the charge density that can be calculated at any depolarization time and $dq(t)/dt$ is the slope of the depolarization curve at time t. Once the apparent trap-controlled mobility is known, the trap depth distribution, ΔU, could be estimated, as described in [9], which provides the following equation:

$$\Delta U(t) = KT \ln\left(\mu(t)\frac{h}{eR^2} \right)$$

where K is Boltzman constant, T is temperature, R is the mean distance between localized states, e is the electron charge and h is the Planck's constant. Therefore, the values of the trap depth can be determined from the values previously calculated for $\mu(t)$.

Complex permittivity measurements within our research group suggest that there is negligible water absorption from the atmosphere in these materials, therefore space charge measurements were conducted on cast and oriented films as received. Polarization time (when DC voltage is applied) was 1800 s, followed by 600 seconds of depolarization (when DC voltage is absent). A mechanical switch was used to short the sample in the beginning of the depolarization. Tests were done at room temperature, 40°C and 60°C, in a controlled environment, with fields of 200, 300 and 400 kV/mm, to obtain indications about the threshold conditions for space charge accumulation, as well as accumulation rate as function of field. The test voltages were chosen by assuming a uniform thickness of 16 μm; the thicknesses were measured afterwards the actual fields were determined. The chosen stresses are comparable to operating conditions of DC metallized-film capacitors.

IV. Space Charge Accumulation Performance

Figures 1 and 2 show the signal amplitude from thin film PEA measurements at 40°C, in poling fields from 200 to 400 kV/mm. The PEA signal amplitude originates from the superposition of Laplacian field (voltage at electrodes) and image field (space charge), hence if the measurement the voltage is kept constant any change in the amplitude is caused by space charge density variation. Very little differences were noticed for filled and non-filled materials both during polarization and depolarization periods (Fig. 1 A, B). During polarization (Fig.1), after an initial transient of less than 5 second, PEA signal amplitude remains stable. This is a clear indication that little to no charge is stored in the sample during polarization. When depolarization is started (Fig.3), PEA signals for filled and non-filled materials drop to similarly low asymptotic levels, with comparable time dynamics. This suggests that those two materials are characterized by comparable levels of traps depth distributions. Similar performance was also observed at room temperature. In order to enhance the relevance of this investigation and to approach conditions more similar to real working conditions for such materials, tests were run at the higher temperature of 60°C. The effect of introducing a 4.5%-wt of nanofiller under poling fields of 200 to 400 kV/mm can be now noticed in Figures 2 and 4. During polarization at 60°C the PEA signal amplitude of non-filled material increases, while it stays flat in the filled material. This is an interesting difference, since it is a clear suggestion that while the non-filled material has the tendency to increase the amount of stored charge over time (Fig.4A), this is not true for the filled one (Fig.4B), showing a flat trend of PEA signal during the polarization period.

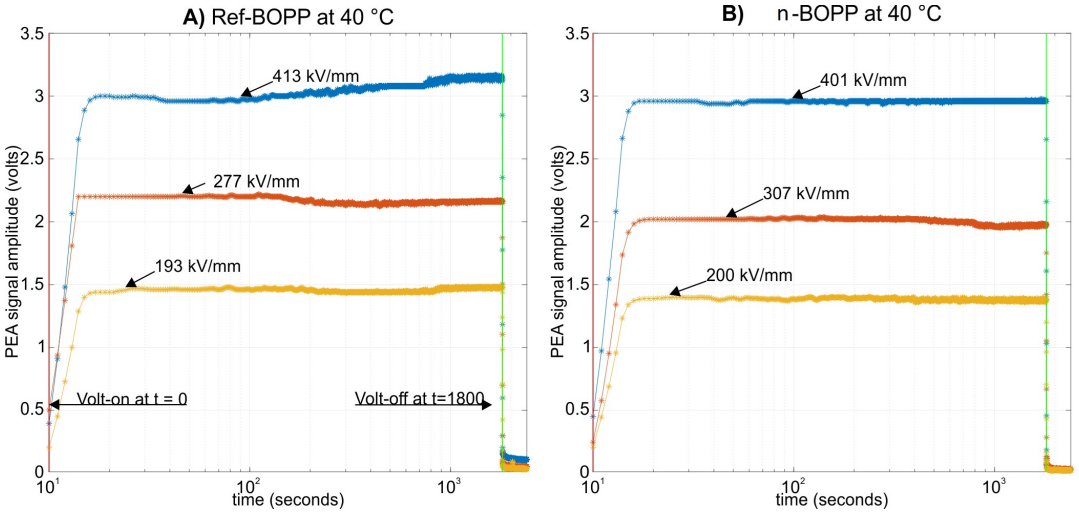

Fig. 1. PEA signal trends at 40°C for non-filled (A) and filled (B) materials. Depolarization period starts in correspondence with the green line.

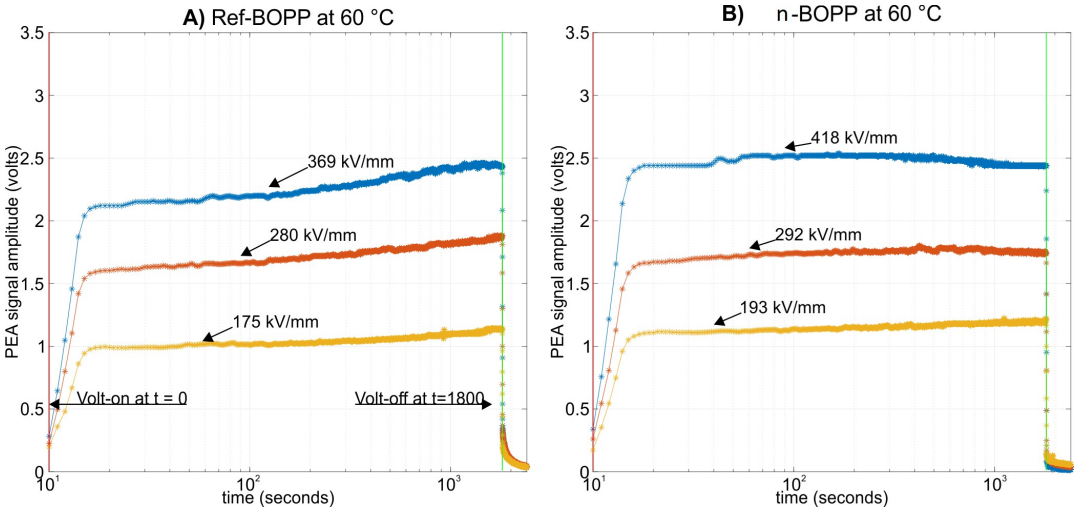

Fig. 2. PEA signal trends at 60°C for non-filled (A) and filled (B) materials. Depolarization period starts in correspondence with the green line.

A second interesting development highlighted by the investigation done at 60°C is the increase of charge dissipation dynamics of bulk space charge when the nanofiller is introduced. In fact, Figure 4 displays a clear modification of the PEA signal behavior over time during the depolarization periods, showing how filled materials have faster dissipation rate of charge over time, when no poling field is applied. To study whether similar performance improvement is seen also in cast films, PEA measurements were done at 60 °C, poling the samples for 10000 seconds at 30 kV/mm. The results, as summarized in Figure 5, were similar to those obtained for oriented films, with filled-PP displaying less charge accumulation. The non-filled PP accumulated more space charge, and the trapped charge decays more slowly than for nanofilled PP. This observation is especially interesting since the thin films were measured at 10 times or higher fields, meaning that space charge measurements have the potential to offer a viable way to "screen" a selection of thin films compositions by a preliminary investigation on thicker cast films, before orientation, despite the technical limits preventing testing at fields close to the typical design conditions for those materials. Calculations for the apparent trap depth distribution are supporting the already discussed indications given by the depolarization trends. Nanofilled materials show higher mobilities and lower trap depth distributions than the reference. This is an important characteristic for HVDC materials, since higher charge mobility or lower trap depth distribution contributes to a quicker stored charge removal, therefore a lower field enhancement in the case of polarity inversion and quicker restoration of the material natural charge neutrality.

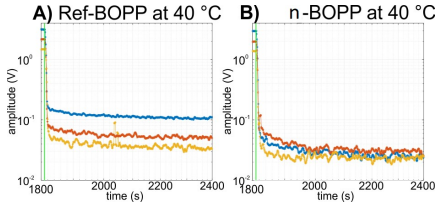

Fig. 1 PEA signal trends during depolarization at 40°C for non-filled and filled materials.

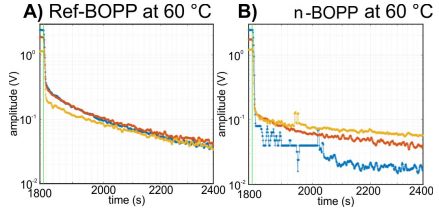

Fig. 2 PEA signal trends during depolarization at 60°C for non-filled and filled materials.

V. Conclusions

The addition of nanoparticles to a bulk of PP has revealed interesting modifications of electrical properties that may affect positively film capacitors design and performance on short term and long term basis. This work shows that the introduction of nanofillers reduce the amount of accumulated charge at medium-high fields. This improvement was seen both in oriented and non-oriented cast films. On the other hand, charge depletion rate increases significantly from base (pure) to filled material, so that charge is released considerably faster for nanocomposites than for base (unfilled) materials. This behavior became prominent with increasing temperature. These results suggest a modification of trap density and trap depth distribution, confirmed by the depolarization space charge characteristics. Trapped charge is released, in fact, (as it could be expected due to the large interaction between nanofiller surface and host material) more rapidly by the nanofilled materials, and the residual charge after long depolarization times is smaller in nanofilled materials than in the base PP. As a consequence, trap-controlled apparent mobility increases significantly for nanofilled materials. Trap depth distribution seems to involve larger density of shallow traps compared to unfilled material (see Figure 5). The reduction of accumulated space charge would indicate that most of these carriers, as well as electrode-injected carriers, crossing insulation through shallow traps are more easily extracted at the electrodes. The results shown in this work set encouraging preliminary results for the GRIDABLE project: PEA measurements on thin and thick samples proved to deliver consistent results, suggesting a fast and viable way to preliminarily select a variety of materials at the early stages of new thin film materials development. Further, long term, investigations are needed to understand the contribution of nanofillers (both their nature and quantity) to the modification of electrical properties.

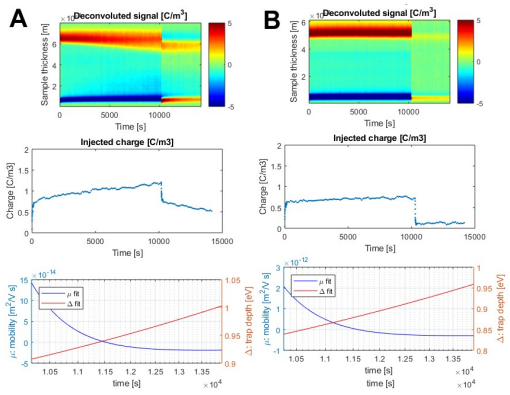

Fig. 3- Apparent charge mobility and trap depth at 60°C for non-filled (A) and filled (B) materials. Results from thick cast film samples.

Acknowledgment

GRIDABLE is an industrially-driven consortium consisting of 3 industrial partners (GE Grid Solutions, Nexans and Terichem Tervakoski), 1 consulting company (InnoEXC), 1 research institute (VTT) and 3 universities (University of Bologna, University of Tampere and University of Twente). This project has received funding from the European Union's Horizon 2020 research and innovation programme under grant agreement No 720858.

References

[1] G.C. Montanari, G. Mazzanti, L. Simoni, "Progress in electrothermal life modeling of electrical insulation during the last decades", IEEE Trans. on Dielectrics and Electrical Insulation, Vol. 9, n. 5, pp. 730-745, October 2002.

[2] G. C. Montanari and G. Pattini, "Thermal Endurance Evaluation of Insulating Materials: A Theoretical and Experimental Analysis," in IEEE Transactions on Electrical Insulation, vol. EI-21, no. 1, pp. 69-77, Feb. 1986 .

[3] Cavallini, D. Fabiani, G. Mazzanti, and G. C. Montanari, "Life model based on space-charge quantities for HVDC polymeric cables subjected to voltage-polarity inversions," IEEE Trans. Dielectr. Electr. Insul., vol. 9, no. 4, pp. 514–523, Aug. 2002.

[4] G. Montanari, "Bringing an insulation to failure: the role of space charge," IEEE Trans. Dielectr. Electr. Insul., vol. 18, no. 2, pp. 339–364, Apr. 2011.

[5] G. C. Montanari, "The electrical degradation threshold of polyethylene investigated by space charge and conduction current measurements," IEEE Trans. Dielectr. Electr. Insul., vol. 7, no. 3, pp. 309–315, Jun. 2000.

[6] G. Mazzanti, G. C. Montanari, and L. A. Dissado, "Electrical aging and life models: the role of space charge," IEEE Trans. Dielectr. Electr. Insul., vol. 12, no. 5, pp. 876–890, Oct. 2005.

[7] G. C. Montanari, "Relation between space charge and polymeric insulation ageing: cause and effect," IEE Proc. - Sci. Meas. Technol., vol. 150, no. 2, pp. 53–57, Mar. 2003.

[8] M. Ritamäki, I. Rytöluoto, K. Lahti, and M. Karttunen, "Effects of thermal aging on the characteristic breakdown behavior of Nano-SiO2-BOPP and BOPP films," in 2015 IEEE 11th International Conference on the Properties and Applications of Dielectric Materials (ICPADM), 2015, pp. 400–403.

[9] G. Mazzanti, G. C. Montanari, and J. M. Alison, "A space-charge based method for the estimation of apparent mobility and trap depth as markers for insulation degradation-theoretical basis and experimental validation," IEEE Trans. Dielectr. Electr. Insul., vol. 10, no. 2, pp. 187–197, Apr. 2003.

Publication VII

M. Ritamäki, I. Rytöluoto and K. Lahti, "DC Voltage Endurance of Capacitor BOPP Films at High Temperature," in *2018 IEEE International Conference on Dielectrics (ICD)*, pp. 1–4, 2018.
DOI: 10.1109/ICD.2018.8514598

The following paper is the final version accepted for publication in the proceedings of 2018 IEEE International Conference on Dielectrics (ICD). The published version of this paper is available at IEEE Xplore.

DC Voltage Endurance of Capacitor BOPP Films at High Temperature

Mikael Ritamäki, Ilkka Rytöluoto, Kari Lahti
Electrical Energy Engineering
Tampere University of Technology
Tampere, Finland
mikael.ritamaki@tut.fi

***Abstract*—A large-area method for determining the voltage endurance of capacitor films is presented. The method was used to characterize the high field – high temperature performance of a commercial biaxially oriented polypropylene film. Following IEC standard 61251, an inverse power law model was fitted to the Weibull-distributed times-to-breakdown data. The insulation life increased rapidly as either field or temperature was decreased. Even at mildest stresses used, the failure rate was still increasing with time, implying that the conditions were above reasonable design limits. Determining the threshold conditions below which the failure rate starts to decrease with time may open up new paths for development of dielectric for higher energy density film capacitors.**

Keywords— Dielectric measurement, materials reliability, capacitors, materials testing, life testing

I. Introduction

High voltage direct current (HVDC) transmission is indispensable in utilizing distant renewable energy sources, such as offshore wind power. Voltage source converters (VSCs) offer a smart, new way to connect HVDC networks to the existing AC power transmission grid. Especially when combined with stationary energy storage both power quality and grid stability are improved. Capacitors are key components in VSC systems, thus ensuring extreme technical performance and uncompromised reliability is of great importance. New high energy density dielectrics could open up paths to improved VSC systems. However, the reliability and long-term properties of any new dielectrics needs to be verified before their use in these often reliability-critical applications. Repeatable and reliable voltage endurance test methods are needed for early screening of novel would-be dielectrics, before expensive industrial scale production, which is the prerequisite for tests using wound capacitor elements.

Biaxially oriented polypropylene (BOPP) is the current state of the art technology for high energy density film capacitors, offering high dielectric breakdown strength, low dielectric losses, and stable capacitance with temperature. The Achilles knee of BOPP is their low permissible operating temperature around 100 °C. The reliable life decreases with increasing temperature, thus for highest reliability their operating temperature is limited. Preliminary measurements on new nanostructured dielectrics have demonstrated improved high temperature characteristics [1], therefore highlighting one possibly way to develop better film capacitors.

Various self-healing multiple breakdown measurement methods have been developed and utilized in TUT high voltage research group to study the DC [2], AC [3] and long-term [4] properties of various oriented capacitor films. These methods utilize self-healing metallized film electrodes to continue the measurement beyond the first breakdowns, enabling rapid gathering of large amounts of data. In [4] it was proposed to extend this methodology to times-to-breakdown "voltage endurance" tests, an implementation of which is reported in this paper. This method is used to evaluate the high field – high temperature endurance of an industrially produced capacitor-grade BOPP film.

II. Experimental

A. Measurement methods

Three types of DC breakdown measurements were conducted: single breakdown ramp tests in oil at room temperature using polished brass electrodes, and large-area multiple breakdown ramp tests and times-to-breakdown measurements in air at various temperatures. The film studied is a smooth commercial 10 µm BOPP film for capacitor applications. A list of test conditions is given in Table 1.

Large-area samples had an active area of 81 cm2, and used a Zn-Al metallized 12 µm BOPP film as the electrodes, similar to as described in e.g. [2]. High temperature tests were done in an oven with forced air circulation. The test fixture had been pre-heated, and the system was given at least 10 minutes to reach thermal equilibrium before test voltage was applied. Temperature stability was around 3 %.

After temperature stabilization, a DC voltage ramp was applied, during which the electrostatic force compressed the

TABLE 1 DC BREAKDOWN TESTS WERE DONE IN THE FOLLOWING CONDITIONS

Temperature (°C)	Constant stress test (kV/mm)	Ramp test (V/s)
ambient		500, 50, 10, 5 (small-area)
80	500, 450, 400	
100	500, 450, 400	50, 10, 2.5 (large-area)

978-1-5386-6389-9/18/$31.00 ©2018 IEEE

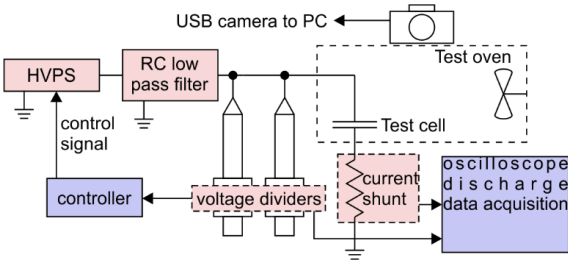

Fig. 1. Large-area breakdown measurement system utilizing a feedback control for voltage stability

film layers, pushing air from between them. Nevertheless sometimes major pockets of air remained initially between the electrodes and the film being tested, in these cases a DC voltage below the intended test voltage was applied for a several seconds, and then a soft cloth was used to swipe the air bubbles out. Despite the sample being not energized during this "swiping" no major air bubbles were seen as the full test voltage was applied afterwards, and any small bubbles disappeared rapidly. Since insulation life is highly dependent on the applied field, the influence of this pre-stressing on the measured times-to-breakdown values was deemed non-significant.

In large-area tests, the voltage ramp was applied until either no discharges were detected (in ramp tests) or until the intended voltage was reached, after which a constant voltage was maintained using closed-loop feedback control. Discharge current and voltage waveforms were recorded using a high-resolution 12-bit oscilloscope, and an USB camera was set up to photograph the sample after each discharge. The measurement system is depicted in Fig. 1.

B. Times to breakdown data qualification

The discharge energy and breakdown voltage –based qualification procedure explained in e.g. [5] was modified for tests at constant voltage, and used in combination with the recorded photos to validate each recorded event. The selection criteria is based on the dependency of the self-healing energy E_{sh} on the breakdown voltage U_{bd} and the capacitance partaking in the self-healing C [6]:

$$E_{sh} = a \times C \times U_{bd}^{b}$$

with a and b being factors that can be assumed remain constant during a measurement at constant voltage. The self-healing energies should follow a (slowly) decreasing trend as other factors remain constant and the capacitance decreases as the active area is reduced. Any discharges were excluded as non-independent or non-breakdown discharges if their energy deviated notably from this trend, or if they occurred at lower voltages, the latter being a sign of rapid successive self-healings. The first events were also reviewed using the photographs to exclude edge discharges, and finally to harmonize the results only the 10 first qualified events for each sample were used in further analyses. Four parallel samples in each condition were measured, yielding 40 data points in total.

C. . Statistical analysis

The breakdown data was fitted with two-parameter Weibull-distributions using maximum likelihood estimation, and confidence bounds were calculated using a Fisher Matrix – based method. The Weibull distribution for breakdown times t (or electric fields) is written as [7]:

$$F(t) = 1 - \exp\left\{-\left(\frac{t}{\alpha}\right)^{\beta}\right\}$$

where $F(t)$ is the Weibull distribution with scale and shape parameters α and β. The scale parameter α is the characteristic life, that is the time (or electric field in progressive stress tests) after which 63.2 % of samples have failed.

An inverse power law (IPL) model, as recommended by IEC 61251 was fitted to the Weibull times-to-breakdown data:

$$L = c \times E^{-n},$$

where L is the characteristic insulation life (Weibull α), E is the electric field stress and c and n are constants. Parameter n is also known as the voltage endurance coefficient (VEC). Of the IPL parameters, the VEC is the most interesting, as it describes how rapidly the insulation life decreases as electric field is increased. [8]

The Weibull electric field and time parameters were extracted from ramp tests results using the statistical methods described by Dissado & Hill in e.g. [9], similarly as in [10]. The time parameter is equivalent to the β in Weibull times-to-breakdown distribution. This enabled the results from ramp tests to be converted to equivalent times-to-breakdowns values using the formula from IEC-61251:

$$t_{\text{equivalent constant voltage}} = \frac{t_{\text{ramp test}}}{n+1}$$

where n is the power law exponent of the IPL model.

III. Results and Discussion

The Weibull parameters and the voltage endurance coefficients are reported in Table 2. The characteristic insulation life (Weibull α) as a function of DC field and temperature is visualized in Fig. 2. The VEC calculated from room temperature ramp tests is extremely high, but the trend

TABLE 2 WEIBULL PARAMETERS.

Ramp tests converted to constant voltage equivalents

Tamp.	RT ~22–24°C				100 °C			
Ramp rate Vs-1µm-1	50	5	1	0.5	5	4.65	1	0.25
α (s)	0.4	4.4	21.5	40.0	6.2	6.5	28.6	108.2
β	0.23	0.31	0.41	0.30	2.84	2.83	2.80	2.78
VEC	34				21			

Tests at constant voltage

Temp.	80 °C			100 °C		
E-field (V/µm)	500	450	400	500	450	400
α (s)	403	1330	4960	240	325	2122
β	2.88	1.99	1.62	3.28	3.10	2.49
VEC	12			10		

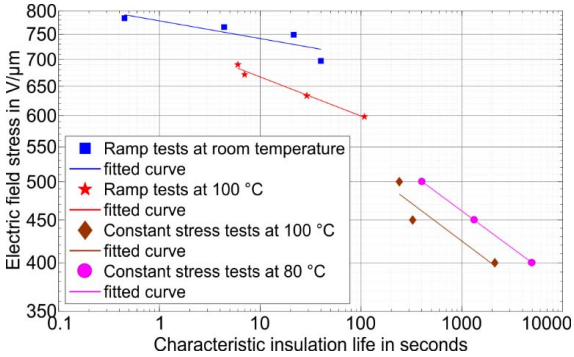

Fig. 2. Characteristic insulation life reduces as either DC electric field or temperature is increased.

appears to decrease towards longer times. This type of behavior is also mentioned in IEC 61251. From a practical point of view, this means that the insulation life at lower fields cannot be extrapolated from high field data, as the predictions would be overly optimistic. Less evident VEC curvature may also be seen between ramp and constant stress tests at 100 °C, but this may originate from differences in data qualification between large-area ramp and constant stress tests. In general, the VEC of 10–12 in constant voltage tests is within the expected range of 8-15 [8] for dielectrics. An interesting observation is also that the VEC appears to increase with decreasing temperature, as explained in [11], based on which values as high as 15–20 might be expected at room temperature for polymeric dielectrics.

It would be extremely beneficial in steering the development of new capacitor dielectrics if the VEC of the film itself could be correlated with life test results done on actual capacitors. Even more if the VEC can be determined using a simple and repeatable method like the one reported in this study. A proper comparison would require capacitors wound from the same type of film, which is, however, not within the scope of this study. In general, care should be taken to distinguish between AC and DC life test results, especially since preliminary measurements indicate space charge accumulation in BOPP thin films in typical operating conditions [1] while DC ageing is dominated by space charge effects [12]. These effects should be negligible under AC excitation. Moreover, it needs to be ensured that accelerated ageing does not bring phenomena uncommon in real capacitors, such as partial discharging at electrode edges.

In Fig. 3, the confidence contours for Weibull parameters are shown in 5 % increments from 75 to 95 %. Weibull β is crucial for understanding the failure characteristics in constant stress tests, as three regimes can be identified [7]:

1. if $\beta < 1$ the failure rate decreases with time, representing early failures

2. if $1 < \beta < 2$, the failure rate increases with time, but at a decreasing rate, representing end of life (EOL) wear out

3. if $\beta > 2$ the failure rate increases at an increasing rate, signifying rapidly approaching EOL.

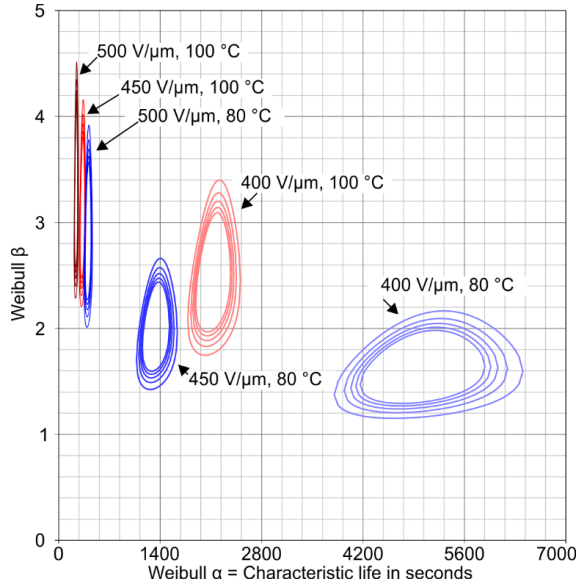

Fig. 3. Weibull parameters visualized using confidence contours, the rate at which the failure rate increases with time decreases with temperature and DC field, approaching constant at β=1.

When combined these three regimes can be used to model the whole bathtub curve of failure rate for capacitors [7], [13]. Obviously, if β is above one in short-term voltage endurance tests such as the ones reported in this study, the film is not reliable in the test conditions. Looking at Fig. 3 Weibull β decreases with decreasing temperature and field, but even with the confidence bounds considered remains above one in all high temperature measurements. However by extrapolating from the available data towards lower fields and the room temperature points in Table 2 where $\beta < 1$, it can be postulated that a threshold exists, below which the failure rate starts decreasing with time. This threshold marks the highest allowed stresses and is a function of temperature and field.

To determine this threshold the large-area constant stress measurement methodology can be extended to longer measurement times, but doing so requires an inert atmosphere to limit oxidation, as was done in e.g. [4]. Capacitors are usually sealed to prevent the ingress of oxygen, as at least their ageing under AC stresses is influenced by the presence of oxygen [14]. Ageing in atmospheric air in may be significantly accelerated due to the presence of oxygen [15], or the phenomena, such as antioxidant conversion [16] may not be representative of those occurring in capacitors during normal operation. However, since the duration of the measurements reported was in the range of hours, oxidation was not considered a major issue. Also for longer measurement times the absence of DC PD shall be ensured.

IV. Conclusions

The large-area multiple breakdown method was extended to DC voltage endurance tests, and then used in high field – high temperature characterization of a capacitor BOPP film. The

large-area approach was beneficial in gathering large amounts of data for improved statistical accuracy. As long as the absence of PD and oxygen is controlled, this test method is also suitable for longer tests.

The failure rate decreased with field and temperature, thus a threshold presumably exists, below which the film is "stable", that is, has a decreasing failure rate. Determination of this threshold may prove beneficial in R&D work aiming to produce better capacitors for high field HVDC applications.

ACKNOWLEDGMENT

This project has received funding from the European Union's Horizon 2020 research and innovation programme under grant agreement No 720858.

REFERENCES

[1] G. C. Montanari, P. Seri, M. Ritamäki, K. Lahti, I. Rytöluoto, and M. Paajanen, "Performance of Nanoparticles in the Electrical Behavior of DC Capacitor Films," in *2018 IEEE 12th International Conference on the Properties and Applications of Dielectric Materials (ICPADM)*, 2018 (*In Press*).

[2] I. Rytöluoto, "Large-Area Multi-Breakdown Characterization of Polymer Films: A New Approach for Establishing Structure–Processing–Breakdown Relationships in Capacitor Dielectrics," D.Sc. thesis, Tampere University of Technology, 2016.

[3] M. Ritamäki, I. Rytöluoto, M. Niittymäki, K. Lahti, and M. Karttunen, "Differences in AC and DC large-area breakdown behavior of polymer thin films," in *2016 IEEE International Conference on Dielectrics (ICD)*, 2016, pp. 1011–1014.

[4] M. Ritamäki, I. Rytöluoto, K. Lahti, T. Vestberg, S. Pasanen, and T. Flyktman, "Large-area Approach to Evaluate DC Electro-thermal Ageing Behavior of BOPP Thin Films for Capacitor Insulation Systems," *IEEE Trans. Dielectr. Electr. Insul.*, vol. 24, no. 2, pp. 826–836, Apr. 2017.

[5] I. Rytöluoto, K. Lahti, M. Karttunen, and M. Koponen, "Large-area dielectric breakdown performance of polymer films – Part I: Measurement method evaluation and statistical considerations on area-dependence," *IEEE Trans. Dielectr. Electr. Insul.*, vol. 22, no. 2, pp. 689–700, Apr. 2015.

[6] Y. Chen, H. Li, F. Lin, F. Lv, M. Zhang, Z. Li, and D. Liu, "Study on Self-Healing and Lifetime Characteristics of Metallized-Film Capacitor Under High Electric Field," *IEEE Trans. Plasma Sci.*, vol. 40, no. 8, pp. 2014–2019, Aug. 2012.

[7] ReliaSoft Corporation, "Life Data Analysis Reference Book." [Online]. Available: http://reliawiki.org/index.php/Life_Data_Analysis_Reference_Book.

[8] "IEC 61251:2015 Electrical insulating materials and systems - AC voltage endurance evaluation Edition 1.0." IEC, 2015.

[9] R. M. Hill and L. A. Dissado, "Examination of the statistics of dielectric breakdown," *J. Phys. C Solid State Phys.*, vol. 16, no. 22, pp. 4447–4468, Aug. 1983.

[10] I. Rytöluoto, M. Ritamäki, K. Lahti, and M. Karttunen, "DC ramp rate effect on the breakdown response of SiO2-BOPP nanocomposites," in *2015 IEEE 11th International Conference on the Properties and Applications of Dielectric Materials (ICPADM)*, 2015, pp. 496–499.

[11] G. C. Montanari, "Notes on theoretical and practical aspects of polymeric insulation aging," *IEEE Electr. Insul. Mag.*, vol. 29, no. 4, pp. 34–44, 2013.

[12] G. C. Montanari, "Relation between space charge and polymeric insulation ageing: cause and effect," *IEE Proc. - Sci. Meas. Technol.*, vol. 150, no. 2, pp. 53–57, Mar. 2003.

[13] R. Gallay, "Metallized Film Capacitor Lifetime Evaluation and Failure Mode Analysis," Proceedings of the CAS-CERN Accelerator School: Power Converters , Geneva, 2014.

[14] B. Gosse, J. P. Gosse, S. Saïd, A. Gadoum, and M. Nemamcha, "Electrical Degradation of Polypropylene: A Study by FTIR Microspectroscopy," *J. Appl. Polym. Sci.*, vol. 46, no. 6, pp. 1121–1124, Oct. 1992.

[15] T. D. Huan, S. Boggs, G. Teyssedre, C. Laurent, M. Cakmak, S. Kumar, and R. Ramprasad, "Advanced polymeric dielectrics for high energy density applications," *Prog. Mater. Sci.*, vol. 83, pp. 236–269, Oct. 2016.

[16] J. Ho, R. Ramprasad, and S. Boggs, "Effect of Alteration of Antioxidant by UV Treatment on the Dielectric Strength of BOPP Capacitor Film," *IEEE Trans. Dielectr. Electr. Insul.*, vol. 14, no. 5, pp. 1295–1301, Oct. 2007.

Publication VIII

M. Ritamäki, I. Rytöluoto and K. Lahti, “Performance Metrics for a Modern BOPP Capacitor Film ,” in *IEEE Transactions on Dielectrics and Electrical Insulation*

DOI: 10.1109/TDEI.2019.007970

The following paper is the final version accepted for publication IEEE Transactions on Dielectrics and Electrical Insulation. The published version of this paper is available at IEEE Xplore.

Performance Metrics for a Modern BOPP Capacitor Film

Mikael Ritamäki, Ilkka Rytöluoto and **Kari Lahti**
Tampere University
Electrical Engineering
P.O. Box 692
FI-33101 Tampere, Finland

ABSTRACT

In this paper, a set of performance metrics for modern biaxially oriented polypropylene (BOPP) capacitor films is established. The fundamental and applied properties of BOPP films required for application in state-of-the-art DC metallized film capacitors are reviewed, highlighting aspects related to high temperature operation, base PP properties and film processing. Commercial BOPP films—both base films and metallized films based on classic isotactic PP—are studied comprehensively, encompassing structural–morphological characterization and short- to medium-term dielectric characterization. Dielectric spectroscopy results demonstrate the negligible dielectric losses of BOPP, being in the range of 10^{-4} or less in the expected operation temperature regime. Thermally stimulated depolarization current (TSDC) measurements indicated a modest density of shallow traps (~0.75 eV) and a high density of deep traps (~1.08 eV) in the 5 µm and 10 µm film variants showing differences presumably arising from film processing. Such an electronic structure was found to be connected with ultra-low conductivity (in the range of 10^{-17}–10^{-16} S/m), high breakdown strength (~700 V/µm) and negligible space charge accumulation up to temperatures of ~70 °C. It is shown that at current design stresses (~200 V/µm at ~60 °C) BOPP is operated close to its fundamental thermal and electrical limitations. Voltage endurance tests at higher fields revealed the onset of high-field degradation and drastically reduced insulation life, and thermal activation of deep traps in the high temperature region (~100 °C) was found to result in reduced dielectric performance.

Index Terms — **polypropylene films, capacitors, energy dissipation, conductivity, materials reliability, Weibull distribution, dielectric breakdown, dielectric losses**

1 INTRODUCTION

POWER electronics utilizing metallized polypropylene film capacitors are ubiquitous. Their applications such as STATCOM, motor drives and MMC-HVDC will benefit if the size, weight or cost of capacitors can be reduced. There is also a demand for capacitors with improved performance at high temperature: capacitors performing reliably above 100 – 150 °C would aid the thermal management in applications with space and weight limitations, such as in electrical vehicles [1]. Film capacitor performance is governed by the dielectric film and metallization end connections. Advances in both are required to increase the energy density that ultimately determines the size and weight. This paper is about biaxially oriented isotactic polypropylene film (BOPP) that forms the main insulation in these capacitors.

In power electronics, the capacitor main insulation must endure both electrical and thermal stresses that can rise above 200 V/µm and up to 125 °C. Such extremes cannot be applied simultaneously; at present operating above ~70–85 °C requires field de-rating. For a capacitor to operate reliably, its insulation materials must exhibit a high breakdown strength, low DC conductivity and low losses under AC. These three are the fundamental film properties. [2] DC conduction and AC losses must be minimized to curtail self-heating – heat dissipation in a wound capacitor is constricted by the poor thermal conductivity of metallized BOPP [3]. Low AC losses in the relevant frequency range is required also in "DC-type" capacitors to limit self-heating caused by AC ripple. The dielectric properties of plastics often deteriorate with temperature; it is thus imperative to determine the film performance at maximum anticipated temperatures.

The capacitor film must also exhibit a wide set of applied properties [2], which have complex correlations with each other and also with the fundamental properties. Owing to these correlations, extensive monitoring of film properties is crucial in the development of dielectric film. With a sufficient testing protocol unforeseen trade-offs are avoided. Notable example of these properties is the surface texture related to the strain-induced transformation of β-form PP crystallites into more stable and dense α-form during biaxial stretching of the extruded film in semi-molten state. Controlled BOPP-film

Manuscript received on 4 December 2018, in final form 5 February 2019, accepted xx Month 20yy. Corresponding author: M. Ritamäki.

surface roughness is mandatory to prevent blocking during capacitor winding, but, unless the skin-core-type morphology of the extruded (precursor) film is carefully controlled, the above transition upon biaxial stretching may also lead to microvoid formation that decreases the breakdown strength. [4] Another example is the relationship between crystallinity, thermal stability and dielectric permittivity: an increase in crystallinity leads to superior properties: increased melting point and real permittivity and attenuated dielectric loss in a broad temperature range, especially in the glass transition region around 0 °C [5]. On the downside, highly crystalline base materials are more difficult to process.

Behavior of BOPP film under DC is a topic that must be considered as a whole – the phenomena are too complex for a single measurement method to provide adequate and truthful picture of film performance. Ideally, the measurements should span in time, measurement area, temperature, and field to cover the operating conditions of capacitors. The intrinsic DC conductivity of BOPP is nil, the observable conductivity originates from physical/ chemical defects, impurities and additives that form localized conduction states (viz. shallow traps) and deep traps. At typical operating fields above 100 V/µm and at elevated temperatures, DC conduction in BOPP is by charge carrier hopping between shallow trap states [6]. Interestingly, also ionic conduction has been proposed recently for high crystallinity BOPP at temperatures above 80 °C [5]. DC conduction in a dielectric correlates with the presence of space charge. Space charge, and thus conductivity, is to be minimized as it increases local electric fields and supplies energy to ageing reactions, which are accelerated further by the temperature rise caused by conduction-induced Joule heating.

There has been a paradigm shift from oil-impregnated film-foil capacitors to dry metallized film designs, catalyzed by environmental aspects and the perceived fire hazard of oils. The insulation systems in these capacitors are different, which makes the bulk of published knowledge on capacitors from 80s and 90s outdated. A broad study of the performance of a modern polypropylene capacitor film is therefore warranted to serve as a baseline for further materials development, and to demonstrate the capability of BOPP films to withstand electrical stresses unrealistic for almost any other type of insulation. This paper is divided into two parts: first, the capacitor film manufacturing technology is briefly outlined, and then, a comprehensive review of a modern capacitor-grade polypropylene film is given.

2 CAPACITOR FILM PROCESSING

Capacitor-grade BOPP film is made of highly isotactic polypropylene. The molecular structure of PP with higher isotacticity is more regular. This enables packing that is more compact during crystallization, and thus enables the production of high crystalline films with reduced losses and conductivity [5]. High isotacticity makes the material more difficult to process. Patent literature mentions using beta nucleating agents to circumvent this problem. According to patent literature the extremely pure capacitor-grade polypropylene is either washed after polymerization or produced using single-site catalysts to mitigate the effects of catalyst residues, and additives are generally avoided as high purity is required for low dielectric losses, low conductivity and high performance at elevated temperature. Hindered phenolic additives such as Irganox® 1010 are nevertheless added in low < 0.5 wt-% quantities to prevent oxidation during melt processing as PP is more susceptible to thermo-oxidative degradation than for example polyethylene because of its tertiary carbon [7]. Calcium stearate can also be added to scavenge acids and to mitigate the effects of catalyst residues.

The stabilized PP is normally sold as granulates to film manufacturers. The granulates are melt-extruded into a thick cast film which is cooled on a chill roll under controlled conditions to achieve the desired cast film morphology. The cast film is then biaxially stretched and optionally heat-treated. The crystallization conditions during cast film extrusion and the temperature profile during biaxial stretching are the main parameters for controlling the BOPP film surface texture. Biaxial stretching can be either sequential tenter or simultaneous process. The first has higher output speed in terms of meters per minute, but the latter is more flexible. [8] Biaxial orientation improves the breakdown strength [4] and thermal conductivity [3], and the current technology enables design fields in excess of 200 V/µm .Typical film thicknesses are in the range of 2–20 µm and there is a trend toward thinner films.

The biaxially oriented film is corona treated and a ~10 nm electrode of zinc, aluminum or their alloy is metallized on the film surface. The thin metallization is self-clearing; should the BOPP film break down the metallization evaporates around the breakdown site, hence isolating it from the remaining active area. The metallization can be tailored for reliability or lower losses and thus uniform, segmented and thickness-profiled variants are available. Ultrathin or segmented metallization reduces the probability and impact of failed self-healing but increase the metallization I^2R losses, which are the main cause of losses in metallized BOPP film capacitors [2, 9].

3 EXPERIMENTAL

3.1 MATERIAL SPECIFICATION

The film studied in this paper is a smooth BOPP film provided by Tervakoski Films. It is manufactured from classic isotactic polypropylene homopolymer by tenter process. As is common with these films, various thicknesses are available and metallization is an optional feature; some capacitor manufacturers prefer in-house metallization. In this paper, 5 µm and 10 µm films were studied both as non-metallized base film and in the factory-metallized form with uniform Zn/Al metallization. These films are labeled as PP5, PP5-met, PP10 and PP10-met, factory-metallized versions being identified with suffix –met. Moreover, a non-stretched (precursor) cast film of similar PP composition, PP250-cast, was included in the morphological analysis.

3.2 FILM STRUCTURE AND MORPHOLOGY

Thermal characteristics, crystalline morphology and surface/cross-sectional structure of the films were analyzed by differential scanning calorimetry (DSC), optical microscopy (OM) and 3D optical profilometry.

The surface textures of the base films PP5 and PP10 were quantified by using a Veeco Wyko® NT1100 optical profiling

system in vertical scanning interferometry (VSI) mode. Table Compared to mechanical stylus profilometers, optical profilometry has the benefit of being contactless and enables 3D imaging. On the downside imaging transparent or translucent BOPP films requires care to identify and eliminate reflections from beyond the film surface. The surface morphology of the base films was also imaged using Meiji Techno ML8530 microscope. Surface profile was characterized on both sides.

Differential scanning calorimetry (DSC) measurements were performed for the non-metallized base films using a TA Instruments Q2000 DSC in the −50 °C to 230 °C temperature range using a dynamic heating rate of 10 °C/min. Degree of crystallinity (X_{DSC}) was calculated assuming a heat of fusion of 209 g/J for completely crystalline α-form polypropylene.

3.3 DIELECTRIC SPECTROSCOPY, THERMALLY STIMULATED DEPOLARIZATION CURRENT (TSDC) AND DC CONDUCTIVITY MEASUREMENT

For dielectric spectroscopy, TSDC and DC conductivity measurements, samples having round electrodes with a diameter of 22 mm were prepared. The electrodes were evaporated on both sides of the samples by electron beam. To ensure good electrical contact, an electrode was also metallized on the already metallized side of factory-metallized films. For most samples, the electrode was 100 nm of gold on top of a 10-nm bonding layer of nickel. Additionally, a number of samples were prepared with 100 nm aluminum electrodes to evaluate the effects of electrode metal. The evaporated samples were stored short-circuited in vacuumed desiccator for a few days prior measurement in an attempt to remove residual charge that may had been injected during the evaporation. Most samples were desiccated this way at room temperature, but some were dried otherwise similarly at 70 °C.

Complex dielectric permittivity was measured as a function of frequency and temperature using Novocontrol Alpha-A dielectric analyzer with BDS-1200 sample cell and Novocool cryosystem. The measurement voltage was 1 V_{RMS}. Isothermal (room temperature) measurements were carried out in a frequency range of 1 Hz – 10 kHz. For the studied samples, the dielectric loss measurement accuracy of the system is ~10^{-4} or better in this frequency range. At lower frequencies the measurement inaccuracy inherent to the Alpha-A and conduction effects prevent accurate determination of the dielectric losses. Temperature dependence of the complex dielectric permittivity was studied in the −60 °C to +120 °C temperature range.

DC conductivity and TSDC measurements were done using BDS-1200 high voltage sample cell and Keithley 6517B electrometer. Voltages below 1 kV were supplied by the electrometer and above by a Keithley 2290E-5 power supply. An overload protection device was used to prevent damage in case of breakdown. Temperature control was realized using Novocool cryosystem or a PID-controlled heater apparatus.

DC conductivity measurements were done at 30, 70 and 100 °C, at electric fields of 30–250 V/μm. The fields was applied stepwise in an ascending order of magnitude. The duration of each step was 20–24 hours, after each the sample was let to discharge under isothermal conditions. Unless specified otherwise, the same sample was then used for the next higher electric field. The TSDC measurement procedure was as described in [10], consisting of isothermal DC poling at 80 °C for 40 minutes, cooling to −50 °C and linear heating at 3 °C/min up to 125 °C under short-circuit conditions.

3.4 DIELECTRIC BREAKDOWN STRENGTH

The DC breakdown strength of all four films was determined using small-area single breakdown “SB” (400 V/s) and large-area multiple breakdown “MB” measurements. The AC breakdown strength was determined using small-area measurements (also 400 V/s). The voltage rise in MB tests was according to IEC-60243-1 slow rate-of-rise test: the discharge events occurred approximately 120–240 s after the voltage ramp initiation. Weibull distributions were fitted to the data points. These measurement methods have been presented in e.g. [11]. The temperatures, measurement areas, total measured areas and sample sizes are presented in Table 1.

Table 1. Breakdown measurement specifications.

Method	Voltage	T (°C)	A (cm^2)	N	A_{tot} (cm^2)
Large-area MB	DC	RT (~23 °C)	81	20	1620
Large-area MB	DC	100 °C	81	6	486
Small-area SB	DC	RT (~23 °C)	1	20	20
Small-area SB	AC	RT (~23 °C)	1	20	20

3.5 VOLTAGE ENDURANCE TESTS

The DC voltage endurance of PP10 was determined with a large-area multiple breakdown measurement done in air. Self-healing electrodes were used and the field was applied until and adequate number of breakdowns had occurred. Non-breakdown discharges were detected and removed from analysis with an algorithm developed at TUT. The measurement and analysis methods were presented in [12]. Both constant stress tests and progressive stress tests at variable ramp rates were done. The results of the latter were converted to constant stress equivalents. A summary of the test conditions and the number of samples is presented in Table 2.

Table 2. Voltage endurance test specifications.

Temperature	Constant stress test (V/μm)	Progressive stress test (V/s)	N
60 °C	550, 500, 450		4 each
80 °C	500, 450, 400		4 each
100 °C	500, 450, 400	50, 10, 2.5 (large-area)	4 each

3.5 QUANTIFICATION OF ACCUMULATED CHARGE

Charge accumulation in PP10 was evaluated in the conditions presented in Table 3. A measurement consisted of isothermal poling for 30 minutes followed by 10 minutes of depolarization. The pulsed electro acoustic measurement method was as presented in [13], with the exception that the measurements at room temperature were done using a pulse generator with fast pulse repetition frequency. A slower one was used in the others. The PEA signal intensity was monitored during the measurement, and a change in it was interpreted as a sign of charge accumulation in the sample.

Table 3. Charge accumulation measurement conditions.

Temperature	Field (V/μm)	Charge accumulation
RT (~23 °C)	100, 200, 300, 400, 500	No
40 °C	300	No
60 °C	300, 400	Yes

4 RESULTS AND DISCUSSION

4.1 MORPHOLOGY AND FILM STRUCTURE

Figure 1 presents a representative cross-polarized light micrograph of a PP250 cast film section. The non-stretched cast PP film was seen to exhibit a skin-core-type morphology gradient comprising of α/β-form spherulites. The existence of a small amount of hexagonal β-form crystallites in the cast film was confirmed in the DSC measurement, with the 1st heating endotherms showing small β-form melting peaks at ~141.1 and ~149.5 °C corresponding to melting–recrystallization–remelting of the β-phase during the DSC heating scan [14]. For the cast film specimens, the major α-form melting peak (1st heating) was observed at ~163.8 °C, indicating a high isotactic content for the base PP. The initial cast film crystallinity was X_{DSC} ~46 %. Glass transition temperature T_g, determined from the 2nd heating scan, was approx. −5.9 °C.

Exemplifying optical microscope images and 3D surface height profiles of the studied biaxially oriented PP5 and PP10 base films are presented in Figure 1b and Figure 1c, respectively. Albeit being smooth films intended for metallization, both PP5 and PP10 exhibited shallow crater-like surface structures as is typical for BOPP. PP5 base film was found to exhibit slightly higher mean area surface roughness in comparison to PP10, with this difference presumably being attributable to different film processing parameters. The BOPP film 1st DSC heating endotherms corresponded to that of a monoclinic α-form crystalline structure, showing melting peak in the 164.3 – 165.0 °C range. No traces of hexagonal β-form were detected in the biaxially stretched films, indicating complete β→α crystal transformation upon biaxial stretching.

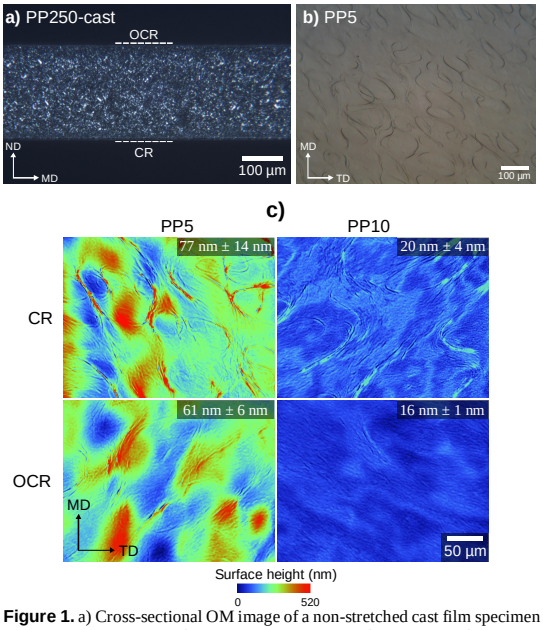

Figure 1. a) Cross-sectional OM image of a non-stretched cast film specimen under cross-polarized reflected light. b) OM surface image of biaxially stretched PP5 base film. c) Optical profilometer height profiles of PP5 and PP10 base BOPP films (both surfaces). The values given in c) are the calculated mean area surface roughness (10 samples). Chill roll side (CR), opposite side of chill roll (OCR), normal direction (ND), machine direction (MD) and transverse direction (TD) are labeled.

4.2 DIELECTRIC SPECTROSCOPY

The real permittivity ε_r of all four films was 2.22 – 2.30 and decreased with temperature. The decrease between −60 to +100 °C was approximately 5 %. The values were typical of BOPP, and similar decrease has been reported by Kahouli *et al* to occur irrespective to the relative crystallinity [5]. The dielectric loss features of all films were similar, representative results of PP10 are presented in Figure 2. The measured dielectric loss in all four films was low in the frequency range of interest between 1 and 10^5 Hz. The loss tangent (tan δ) was 10^{-4} or less, and one broad relaxation peak was seen between −5 and +60 °C. This peak is related to the glass transition and occurs above glass transition temperature T_g that was determined by DSC. The relaxation mechanism is a gradual liberation of polymer chains in the amorphous phase above T_g.

An increase in loss angle was evident below ~1 Hz, as seen in the inset in Figure 2. The measurement accuracy in this frequency range is limited, nevertheless even after it is considered, an increase is present. The decrease of sub-Hz losses after thermal conditioning ascertains its origins in space charge. It is presumably an artifact caused by metallization and thus, it must be differentiated from true AC behavior.

The dielectric losses increased with temperature, the increase was especially strong at low frequencies below 1 Hz. This intensity is presumably caused by a superposition of space charge effects, DC conduction, and the release of charge trapped during evaporation. Intrinsic DC conduction at such low fields can be disputed, but if present, the mechanism is most probably ionic [6].

The dielectric spectroscopy measurements confirmed the relatively low permittivity of BOPP and its negligible losses in a broad frequency range at low fields and moderate temperatures. Negligible losses are mandatory to limit self-heating. The dielectric losses of modern BOPP are low enough

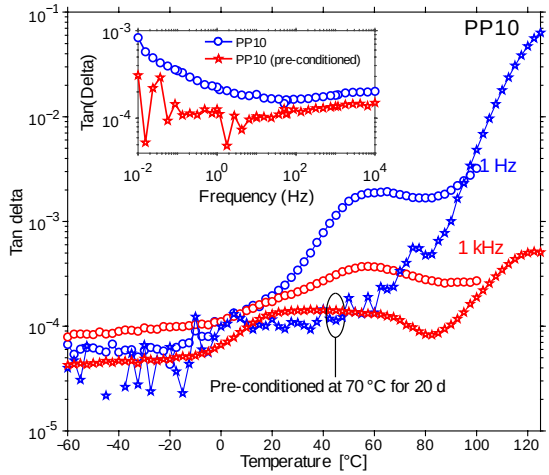

Figure 2. Tan δ behavior of PP10 base-BOPP as a function of temperature at 1 Hz and 1 kHz (Ni/Au evaporated electrodes). Circles: non-conditioned sample. Stars: pre-conditioned sample. Inset: Room temperature tan δ as a function of frequency.

for their effect on the capacitor self-heating to be negligible. The component losses are dominated by the metallization resistance. [2] Behavior at low fields and high temperatures is dominated by DC effects, including the presence of trapped charge. This sub-Hz phenomena is to be seen separately from "true" AC behavior.

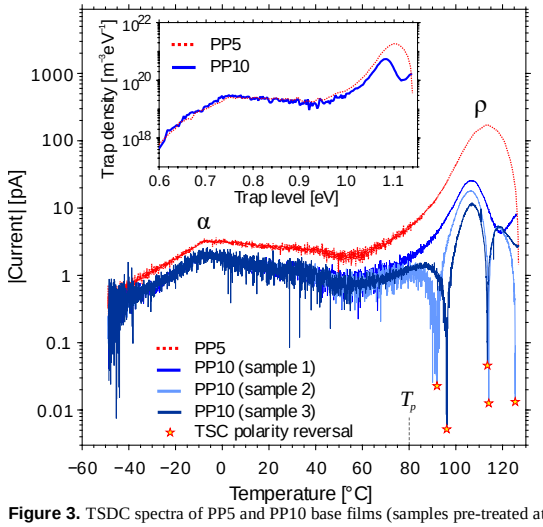

Figure 3. TSDC spectra of PP5 and PP10 base films (samples pre-treated at 70 °C for several days prior to measurements). Three parallel samples of PP10 are shown, demonstrating the TSDC polarity reversal phenomenon observed in the high temperature region. The depolarization current (y-axis) is represented as absolute values in order to use logarithmic scale. The inset shows the calculated trap depth vs. density distribution for PP5 and PP10.

4.3 TSDC

Exemplifying TSDC spectra of PP5 and PP10 samples polarized under 100 V/µm are presented in Figure 3. Due to the largely non-polar nature of BOPP the thermally stimulated currents are mainly attributable to space charge relaxation from shallow and deep traps. The TSDC spectra of PP5 and PP10 exhibited similar characteristics as has been presented in other BOPP-related studies by e.g. Kahouli *et al* [5] and Li *et al* [15]: a broad TSDC peak in the low temperature region (approx. −5 °C) corresponding to the glass transition (α-relaxation) and a major TSDC peak in the high temperature region (>100 °C) corresponding to space charge (ρ-) relaxation from deep traps. Interestingly, as shown in Figure 3, a polarity reversal and anomalous discharge current phenomenon (i.e. current which is flowing in the same direction as charging current) was sometimes observed in the high temperature region (above the polarization temperature T_p of 80 °C). The occurrence of anomalous TSDC for samples poled under high field and high temperature conditions is indeed a direct evidence of injected space charge, and it is known to be influenced by the nature of the electrode–dielectric interface [16, 17].

While TSDC can essentially provide a wealth of information about space charge properties of polymers, evaluation of the trapping parameters from the experimental data is often not straightforward due to several overlapping or (quasi-) continuous distribution of trap bands. Therefore, simple methods assuming single elementary relaxations from a discrete trapping level—such as the initial-rise and peak shape methods—are often inapplicable to complex TSDC data. Assuming negligible retrapping of the thermally released charges (electrons), Tian *et al* recently introduced a numerical method enabling direct determination of arbitrary (continuous) trap distribution from TSDC data, the details of which are presented in [18]. The inset in Figure 3 shows the calculated trap depth vs. density distributions for PP5 and PP10 base films, assuming an attempt-to-escape frequency of 10^{12} s^{-1} and that all the traps were initially filled uniformly into a depth of 3 µm [19] before depolarization. It is noted here that the trap depth and density scales in Figure 3 are dependent on the chosen attempt-to-escape frequency and penetration depth, respectively, and hence the calculated trap parameter values should be taken as approximates only [18]. Both PP5 and PP10 show similar densities of broadly distributed shallow traps around the glass-transition region with the peak density occurring at ~0.75 eV. These traps are likely the localized conduction states responsible for the observed conductivity in the <100 °C range. The high-temperature space charge relaxation corresponds to deep trap peak density occurring in the 1.08–1.1 eV energy range, with PP5 showing a higher density of deep trap states in comparison to PP10. This difference may arise from e.g. morphological differences (crystallinity, crystallite size, orientation) between the 5 µm and 10 µm BOPP films. The above trap depths—being in good agreement with e.g. recent *ab initio* calculations for those originating from carbonyl, conjugated double bond and dienone defects in isotactic PP [20]—may be attributed to impurities and chemical defects present in the studied BOPP films.

4.4 DC CONDUCTIVITY AND ORIGIN OF BEHAVIOR AT SERVICE FIELDS

The behavior of all four PP films under DC excitation was similar; example results on PP10 are presented in Figure 4. The current after 20–24 hours was independent of the applied field (30 – 200/250 V/µm) and still decreasing. The apparent conductivity, calculated from this current was in the range of 10^{-17}–10^{-16} S/m for temperatures of 30 and 70 °C and approx. 10^{-15} S/m at 100 °C. These low values are typical of BOPP. The apparent independency of DC conductivity on temperature up to 70 °C is a desirable feature, as a conductivity increasing with temperature would risk thermal runaway. The lack of field dependency rules out the majority of mechanisms responsible for absorption and conduction currents: electrode polarization, dipolar orientation, tunneling and hopping conduction. Formation of trapped space charge with constricted charge injection may explain the observed behavior [21]. Ghorbani *et al* report similar long-term conductivity decrease in LDPE, XLPE and BOPP [22]. By recognizing that the conductivity decays even in the absence of electric field, they deducted that the behavior is induced by thermally activated physical change. Similar effect could be reproduced in our step-stress measurement: heat-treatment of one sample at 70 °C reduced the current during the initial steps markedly.

Ho *et al* associate the conduction currents in BOPP at fields above >10 V/µm but below the onset of hopping conduction with electron and hole mobility caused by localized conduction states. Many of these states are caused by the physical irregularity of the amorphous region. [6] Thermally activated

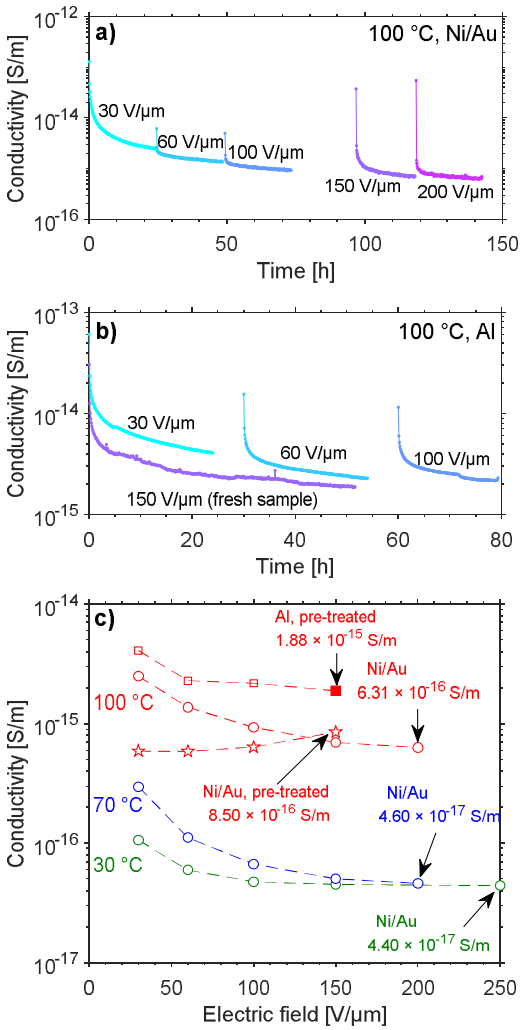

Figure 4. Conductivity vs. time for PP10 base-BOPP film with evaporated a) Ni/Au electrodes and b) Al-electrodes (pre-treated samples) at 100 °C.c) Conductivity at the end of each 20–24 h voltage application period. Additional data from heat-treated samples with either Ni/Au or Al electrodes are also shown. The filled marker at 100 °C (Al-electrodes) corresponds to a fresh sample with no prior electrical stress subjected to 150 V/µm field for ~51 h.

secondary crystallization reduces the volume fraction of amorphous regions, which should reduce the number of localized conduction states and thus the conductivity. This line of though is also supported by the reduced DC conductivity in highly crystalline BOPP grades [5]. Therefore, the observed long-term conductivity decrease may be explained by secondary crystallization.

By measuring a 7 µm tenter-processed BOPP-film at 35 °C and above, Ho *et al* have recognized the onset of hopping DC conduction above 100 V/µm; a decrease in this threshold field with temperature is also reported. [6] Interestingly, no such behavior was evident in our measurements. Absorption currents in PP film at temperatures below 0 °C have been associated with dipolar relaxation with small dipolar moment and a broad distribution of relaxation times; mind that dipolar relaxations in non-polar PP are minimal. A sharp drop in conduction current was seen when a sample was cooled below 0 °C under voltage, as was done during the polarization phase prior to TSDC measurements.

Interestingly, a higher conductivity of ~10^{-15} S/m with no clear field dependency was measured in one sample with aluminum electrodes. This sample had been heat-treated at 70 °C. This dependency of electrode metal is indicative of electrode polarization, tunneling, or charge injection with space charge formation. Out of these three, only charge injection is plausible owing to the lack of field dependency. [21]

Thus in summary, our results indicate that the absorption current in PP10 is a superposition of (1) vacuum polarization, (2) electrode metal -dependent charge injection and associated formation of space charge and (3) intrinsic conductivity in the amorphous region decaying with thermally activated secondary crystallization.

4.5 DIELECTRIC BREAKDOWN STRENGTH

The DC and AC (50 Hz) small-area dielectric breakdown strength of all four BOPP films was in the range of 700 – 800 V/µm that is typical of BOPP. The results are presented in Table 4. The short-term DC and AC peak fields were essentially the same, similarly as in other capacitor-grade BOPP films studied in [11]. This can be traced to the low dielectric loss of BOPP that inhibits thermal runaway at line frequencies. Due to the very similar breakdown behavior the short-term AC and DC breakdown mechanism is likely similar. Ho and Jow have verified that at high fields the breakdown of BOPP is caused by hopping conduction leading to a thermal runaway [6].

The notable feature in the large-area DC breakdown strength results was the presence of a distinct defect subpopulation in both non-metallized films, and conversely the absence of such subpopulation in the metallized films. This is illustrated in Figure 5. The characteristic breakdown 63.2 % strengths were in the same region with the small-area results. This absence of weak points in metallized films is statistically significant observation since 20 large-area samples of each material were measured at room temperature. The reason for the absence could not be ascertained, but the possibility of quality variations along the film roll cannot be ruled out. Between room temperature and 100 °C the 63.2 % breakdown strength decreased 13–20 %, this decrease aligns well with literature [6]. The modesty of this decrease also verifies that the films are free from significant impurities [23].

4.6 REGARDING THE VOLTAGE ENDURANCE

Voltage endurance tests are done to extrapolate the insulation life at operating conditions from accelerated tests at higher stresses. An inverse power law (IPL) model with a voltage endurance coefficient (VEC) is most often used to model the effect of electric field. Voltage endurance tests done on PP10

Table 4. Dielectric breakdown strength.

	Large-area 63.2% (V/µm)		Small-area 63.2% (V/µm)	
	RT	100 °C	DC	AC
PP10	769	671	811	729
PP5	647	545	727	698
PP10-met	743	629	777	668
PP5-met	702	559	773	717

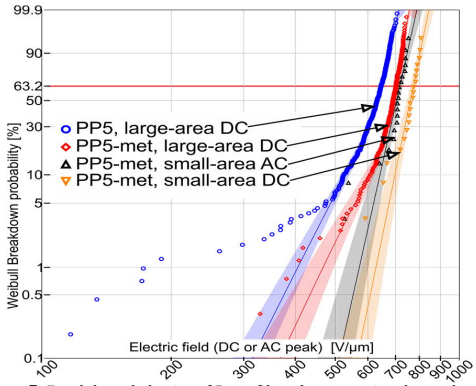

Figure 5. Breakdown behavior of 5 µm films demonstrating the weak points in non-metallized base films, and their absence in its metallized version. Shaded area represents one-sided 90% confidence bounds.

revealed the caveat in applying approach for BOPP films: the phenomena leading to breakdown is different in accelerated high-field tests and in service. Oxidation (if the tests are done in air) and the onset of high field conduction and associated rapid degradation cause the VEC vary with field. An inverse power law model assuming constant VEC is unsuitable to model this type of behavior.

The DC VEC of PP10 was 10–12 and decreased with increasing temperature, that is, the effect of electric field on insulation life was attenuated with increasing temperature. Similar temperature-dependency and VECs have been reported for PP film tested in oil under DC [24]. Ideally, extrapolating the voltage endurance test results would yield the insulation life at operating conditions. On the basis that the lifetime of a metallized film capacitor corresponds to a small, few percent, reduction in capacitance, the lifetime of PP10 was defined as a time with 5 % probability of failure. This percentage was chosen arbitrarily. The lifetimes are tabulated in Table 5.

The lifetimes extrapolated at realistic design stress, 60 °C and 225 V/µm were unlikely short – a whole capacitor bank is expected to perform 20–30 years in these conditions. Moreover, Weibull analysis of the times-to-breakdown data revealed that in all experimental conditions the failure rate increased with time. Increasing failure rate indicates progressive degradation and conditions unsuitable for the film. In the shorter tests, the increase of the failure rate decreased systematically with reducing stress levels. This decrease is interpreted as the diminishing effect of electric field with decreasing field. However, the failure rate had again increased in the longest test with characteristic time of failure of 12 hours. This is interpreted as the onset of severe oxidation. In real service conditions, oxidation is non-existent, or at least slowed by limited diffusion of oxygen through potting.

It is hypothesized that the increased effect of the electric field at higher fields originates from high field conduction, specifically the onset of space charge limited field conditions inside the film. Degradation is greatly accelerated under such conditions. The high field phenomena are characterized by a threshold field. Boggs [25] placed this threshold at 285 V/µm, below the lowest stresses used in the endurance tests. The design fields for capacitors are below this threshold, as verified by the DC conductivity measurement: high field conduction is characterized by an exponential increase in conductivity with field, and no such behavior was seen in the conductivity measurements. The measurement fields of 200–250 V/µm correspond to realistic design stresses. Worth mention is that degradation at high fields is accelerated further in the presence of oxygen. [2, 6, 25]

Table 5. Lifetime based on accelerated tests.

Temperature °C	Life at 225 V/µm	Design field for 30 year life
60	~2 years	184 V/µm
80	12 days	131 V/µm
100	2 days	99 /µm

In summary, IPL model with constant VEC was found unsuitable in extrapolating the lifetimes of BOPP based on high field tests. That is, because the VEC is drastically reduced at high fields due to high field conduction. To estimate the lifetime of BOPP in service conditions one must determine the VEC of BOPP at design fields. For this purpose, tests at fields below the threshold for high field condition and in an inert atmosphere would be needed.

4.7 A NOTE ON SPACE CHARGE

Space charge measurements were done to study high field phenomena at fields where DC conduction measurements are unfeasible because the samples break down before steady state current can be determined. The results are summarized in Table . Measurements done at room temperature up to 500 V/µm revealed no evidence of space charge accumulation, and neither did the measurement at 40 °C 400 V/µm. At 60 °C, however, space charge accumulation was evident both at 300 V/µm and at 400 V/µm. The onset of high field phenomena appears to be strongly dependent on temperature. The general observation of temperature-dependency is in agreement with the high field hopping conduction model proposed in [6]. Obviously, it is a characteristic feature of other models as well. The true yield of the space charge measurements is that the deducted threshold conditions for high field conduction and associated space charge are in agreement with the conduction measurements and the voltage endurance tests. This further supports the analysis presented in the section on endurance tests.

4.8 SUMMARY OF THE FUNDAMENTS

The performance of BOPP in capacitors originates from the demonstrated fundamental dielectric properties: high breakdown strength, low conductivity and low dielectric losses. Equally important is that in the typical operating region the DC conductivity is independent of field and temperature and that the losses are minimal in the broad frequency where power electronics operate. The need to develop better insulation materials for high temperature is clearly visible from the 10-fold increase in conductivity when going from 70 to 100 °C. Indeed, there is a growing interest in materials for high temperature [1].

5 CONCLUSIONS

The four BOPP films studied demonstrated excellent dielectric properties at least up 70 °C – towards 100 °C the conductivity began to increase, marking the upper limit of service temperature. Conductivity, space charge, and voltage endurance measurements indicated that a threshold electric

field for high-field conduction exists. Above this threshold the film is inherently unstable and will fail in times much less than the expected service life. The concept of a threshold field for high field conduction is well supported by literature, as is its value around 300 V/µm, and its observed decrease with temperature [6, 25]. This field would mark the upper limit for design stress. Accurate determination of this threshold field is proposed as a way to quantify the performance of a specific BOPP film, analogously to comparing the threshold fields for space charge accumulation when studying cable insulation materials. However, equally important is to verify all the fundamental properties remain adequate with time.

ACKNOWLEDGMENT

This project has received funding from the European Union's Horizon 2020 research and innovation programme under grant agreement No 720858.

REFERENCES

[1] J. S. Ho, and S. G. Greenbaum, "Polymer Capacitor Dielectrics for High Temperature Applications," ACS Appl. Mater. Interfaces, vol. 10, no. 35, pp. 29189–29218, Sep. 2018.

[2] T. D. Huan *et al*, "Advanced polymeric dielectrics for high energy density applications," Prog. Mater. Sci., vol. 83, pp. 236–269, Oct. 2016.

[3] S. Qin, J. Ho, M. Rabuffi, G. Borelli, and T. Jow, "Implications of the anisotropic thermal conductivity of capacitor windings," IEEE Electr. Insul. Mag., vol. 27, no. 1, pp. 7–13, Jan. 2011.

[4] I. Rytöluoto, A. Gitsas, S. Pasanen, and K. Lahti, "Effect of film structure and morphology on the dielectric breakdown characteristics of cast and biaxially oriented polypropylene films," Eur. Polym. J., vol. 95, no. September, pp. 606–624, Oct. 2017.

[5] A. Kahouli, O. Gallot-Lavallée, P. Rain, O. Lesaint, C. Guillermin, and J.-M. Lupin, "Dielectric features of two grades of bi-oriented isotactic polypropylene," J. Appl. Polym. Sci., vol. 132, no. 28, Jul. 2015.

[6] J. Ho, and T. R. Jow, "High field conduction in biaxially oriented polypropylene at elevated temperature," IEEE Trans. Dielectr. Electr. Insul., vol. 19, no. 3, pp. 990–995, Jun. 2012.

[7] G. W. Ehrenstein, and S. Pongratz, *Resistance and Stability of Polymers*. München: Carl Hanser Verlag GmbH & Co. KG, 2013.

[8] J. Breil, "Biaxial Oriented Film Technology" in *Film Processing Advances*, München: Carl Hanser Verlag GmbH & Co. KG, 2014, pp. 194–229.

[9] A. Hjert, "Multiscale Modelling of a Metallized Film Capacitor for HVDC Applications," Master's thesis, Dept. of Materials and Manufacturing Technology, Chalmers University of Technology, 2017.

[10] I. Rytöluoto, M. Ritamäki, and K. Lahti, "Short-term dielectric performance assessment of BOPP capacitor films: A baseline study," *IEEE Int. Conf. Prop. Appl. Dielectr. Mat. (ICPADM)*, 2018, pp. 289–292.

[11] M. Ritamäki, I. Rytöluoto, M. Niittymäki, K. Lahti, and M. Karttunen, "Differences in AC and DC large-area breakdown behavior of polymer thin films," *IEEE Int. Conf. Dielectr. (ICD)*, 2016, pp. 1011–1014.

[12] M. Ritamaki, I. Rytoluoto, and K. Lahti, "DC Voltage Endurance of Capacitor BOPP Films at High Temperature," *IEEE Int. Conf. Dielectr. (ICD)*, 2018, pp. 1–4.

[13] G. C. Montanari, P. Seri, M. Ritamaki, K. Lahti, I. Rytoluoto, and M. Paajanen, "Performance of nanoparticles in the electrical behavior of DC capacitor films," *IEEE Int. Conf. Prop. Appl. Dielectrl Mat. (ICPADM)*, 2018, pp. 41–44.

[14] I. Rytöluoto, A. Gitsas, S. Pasanen, and K. Lahti, "Effect of film structure and morphology on the dielectric breakdown characteristics of cast and biaxially oriented polypropylene films," Eur. Polym. J., vol. 95, pp. 606–624, Oct. 2017.

[15] H. Li *et al.*, "Study on the impact of space charge on the lifetime of pulsed capacitors," *IEEE Trans. Dielectr. Electr. Insul.*, vol. 24, no. 3, pp. 1870–1877, Jun. 2017.

[16] A. Thielen, J. Niezette, G. Feyder, and J. Vanderschueren, "Thermally stimulated current study of space charge formation and contact effects in metal-polyethylene terephthalate film-metal systems. I. Generalities and theoretical model," J. Phys. Chem. Solids, vol. 57, no. 11, pp. 1567–1580, 1996.

[17] P. K. Khare and S. K. Jain, "Anomalous thermally stimulated currents and space charge in poly(vinyl pyrrolidone)," Polym. Int., vol. 49, no. 3, pp. 265–268, Mar. 2000.

[18] F. Tian, W. Bu, L. Shi, C. Yang, Y. Wang, and Q. Lei, "Theory of modified thermally stimulated current and direct determination of trap level distribution," J. Electrostat., vol. 69, no. 1, pp. 7–10, Feb. 2011.

[19] F. Zheng, Y. Miao, J. Dong, Z. An, Q. Lei, and Y. Zhang, "Space charge characterization in biaxially oriented polypropylene films," IEEE Trans. Dielectr. Electr. Insul., vol. 23, no. 5, pp. 3102–3107, Oct. 2016.

[20] H.-V. Nguyen and T. H. Pham, "Structural and Electronic Properties of Defect-Free and Defect-Containing Polypropylene: A Computational Study by van der Waals Density-Functional Method," Phys. Status Solidi, vol. 1700036, p. 1700036, Oct. 2017.

[21] D. K. Das Gupta and K. Joyner, "On the nature of absorption currents in polyethylene terephthalate (PET)," J. Phys. D. Appl. Phys., vol. 9, no. 5, pp. 829–840, Apr. 1976.

[22] H. Ghorbani *et al.*, "Long-term conductivity decrease of polyethylene and polypropylene insulation materials," IEEE Trans. Dielectr. Electr. Insul., vol. 24, no. 3, pp. 1485–1493, Jun. 2017.

[23] A. Schneuwly, P. Groning, L. Schlapbach, C. Irrgang, and J. Vogt, "Breakdown behavior of oil-impregnated polypropylene as dielectric in film capacitors," IEEE Trans. Dielectr. Electr. Insul., vol. 5, no. 6, pp. 862–868, 1998.

[24] A. N. Stokes, J. L. Suthar, J. R. Laghari, and W. J. Sarjeant, "Lifetime characteristics of electrically and thermally preaged polypropylene films," in *Annu. Rep. Conf. Electr. Insul. Dielect. Phenom. (CEIDP), 1992* pp. 741–746.

[25] S. Boggs, "Very high field phenomena in dielectrics," IEEE Trans. Dielectr. Electr. Insul., vol. 12, no. 5, pp. 929–938, Oct. 2005.

M. Ritamäki (S'15) was born in Tampere, Finland, in 1990. He received the M.Sc. (Tech.) degree in electrical engineering from Tampere University of Technology in 2014. Since 2015 he has been working in the High Voltage Engineering research group at TUT, with aim towards the D.Sc. (Tech.) degree. His research interests are the reliability of electrical insulation and development of performance metrics to quantify it.

I. Rytöluoto (S'13, M'16) was born in Tampere, Finland on 17th April 1985. He received the M.Sc. (Tech.) and Doctoral degrees in electrical engineering from Tampere University of Technology (TUT), Tampere, Finland in 2011 and 2016, respectively. Since 2011 he has been working in the High Voltage Engineering research group at TUT, currently as a post-doctoral researcher. His current research interests include e.g. establishing processing–structure–dielectric property relationships in polymer nanocomposites for HV capacitor and cable applications.

Kari Lahti (M'01) was born in Hämeenlinna, Finland in 1968. He received the M.Sc. and Doctoral degrees in electrical engineering from Tampere University of Technology in 1994 and 2003, respectively, where he currently works as Research Manager and Adjunct Professor. He is the head of TUT's research group on High Voltage Engineering. His research interests include e.g. surge arresters, nanocomposite insulation systems, high voltage and environmental testing and dielectric characterization of insulation materials.